

Department of Neurology  
Faculty 2: Medicine - Clinical Medicine  
Saarland University, Homburg/Saar, Germany

# **Toll-Like Receptor 2 and Partner Receptors in Alzheimer's Disease**

**Dissertation**

*A dissertation submitted in partial fulfillment of the requirements  
for the degree of Doctor rerum naturalium at*

Faculty of Medicine of

**SAARLAND UNIVERSITY**

2011

**Submitted by: Shirong Liu**

Born on: 12 November 1976, in Jiangxi, PR China

Aus dem Bereich: Neurologie  
Klinische Medizin der Medizinischen Fakultät  
der Universität des Saarlandes, Homburg/Saar

# **Die Funktion von Toll-Like Rezeptor 2 und verwandten Rezeptoren in der Pathogenese der Alzheimer Krankheit**

**Dissertation**

*Dissertation zur Erlangung des Grades eines Doktors der  
Naturwissenschaften*

der Medizinischen Fakultät

der UNIVERSITÄT DES SAARLANDES

2011

vorgelegt von: Shirong Liu

geb. am: 12 November 1976, in Jiangxi, VR China

献给我深爱的父母

*To my beloved parents*

*Für meine geliebten Eltern*

# Declaration

I hereby declare that this thesis is my own original work and effort. All experiments, except for those specified, were exclusively performed by me. Except for the publications written by myself listed in the publication list, the data presented here have not been submitted anywhere else for any award. Where other sources of information and help that have been used, they have been indicated and acknowledged.

Homburg, 27.07.11

---

Shirong Liu

## Abbreviations

aa	Amino acid
AA	Arachidonic acid
A $\beta$	Amyloid $\beta$ -peptide
AD	Alzheimer's disease
AIF1	Allograft Inflammatory Factor-1
AP-1	Activating protein-1
APP	Amyloid precursor protein
$\alpha 7$ nAChRs	$\alpha 7$ nicotinic acetylcholine receptors
BDNF	Brain-derived neurotrophic factor
BLAST	Basic local alignment search tool
BM	Bone marrow
BMDM	Bone marrow derived macrophages
bp	Base pair
BSA	Bovine serum albumin
CCL-2 / MCP-1	Chemokine (C-C motif) ligand 2 / monocyte chemotactic protein-1
CD	Cluster of differentiation
cDNA	Complementary deoxyribonucleic acid
CNS	Central nervous system
Ct	Threshold cycle
CT-B	Cholera toxin subunit B
CuBD	Cu-binding domain
Da	Dalton
DC	Dendritic cell
DHA	Docosahexaenoic acid
diH <sub>2</sub> O	Deionized water
DMEM	Dulbecco's Modified Eagle Medium
DMSO	Dimethyl sulfoxide
DNA	Deoxyribonucleic acid
dsDNA	Double-strand deoxyribonucleic acid
dsRNA	Double-stranded RNA
<i>E. coli</i>	<i>Escherichia coli</i>
<i>e.g.</i>	<i>exempli gratia</i> , for example
EDTA	Ethylene diamine tetraacetic acid
EL	Erythrocyte Lysing
ELISA	Enzyme-Linked Immunosorbent Assay
EPA	Eicosapentaenoic acid
ER	Endoplasmic reticulum
ERK/ MAP kinase	Extracellular-signal-regulated kinase/ mitogen-activated protein kinase
<i>etc.</i>	<i>et cetera</i>
FACS	Fluorescence-activated cell sorting
F-actin	Filamentous actin
FADD	FAS-Associated death domain-containing protein
FBS	Fetal bovine serum
FC	Flow cell
FITC	Fluorescein isothiocyanate
g	Gram
<i>g</i>	<i>Gravity</i>
G-actin	globular-actin

GFP	Green fluorescence protein
Gua-HCl	Guanidine chloride buffer
H <sub>2</sub> O <sub>2</sub>	Hydrogen peroxide
HEK-293	Human embryonic kidney 293
HEPES	4-(2-Hydroxyethyl)-1-piperazineethanesulfonic acid
HFIP	1, 1, 1, 3, 3, 3-Hexafluoro-2-propanol
HMGR	hydroxymethylglutaryl-CoA reductase
Iba-1	Ionized calcium-binding adaptor molecule 1
IGF-1R	Insulin-Like Growth Factor 1 receptor
IgG	Immunoglobulin G
IL-8/ CXCL8	Interleukin-8/ Chemokine CXCL8
IL-6	Interleukin-6
IL-10	Interleukin-10
IL-1 $\beta$	Interleukin-1 $\beta$
I- $\kappa$ B	NF-kappa-B inhibitor
IKK	I- $\kappa$ B kinase
IKK-I/ IKK- $\epsilon$	Inducible IKK
iNOS	Inducible nitric oxide synthase
IRAK	Interleukin-1 Receptor-Associated Kinase
IRES	Internal ribosome entry site
IRF	Interferon-Regulatory factor
IP-10	Interferon-Inducible Protein 10, Chemokine CXCL10
JNK	c-JUN N-terminal Kinase
kb	Kilo base pairs
kDa	Kilodalton
KO/ ko	knock out
LAL	Limulus Amebocyte Lysate
LB	Luria-Bertani
LPS	Lipopolysaccharides
LRR	Leucine-rich repeats
LTD	Long-term depression
LTP	Long-term potentiation
L-VGCC	L-type voltage-gated Ca <sup>2+</sup> channels
M	Molar
MAL	MyD88-adaptor-like
MAPKs	Mitogen Activated Protein (MAP) kinases
MCS	Multiple cloning site
mFI	Mean fluorescence intensity
min	Minute
MMLV	Moloney Murine Leukemia Virus
MMP	Matrix metalloproteinase
MyD88	Myeloid Differentiation Factor 88
NC	Nitrocellulose
NF- $\kappa$ B	Nuclear Factor kappa B
Ni-NTA	Nickel-nitrilotriacetic acid
NO	Nitric oxide
NSAIDs	Non-steroidal anti-inflammatory drugs
O.D.	Optical density
OPN-i	Intracellular osteopontin
PAMPs	Pathogen-associated molecular patterns
PBS	Phosphate-Buffered Saline

PCR	Polymerase chain reaction
pDCs	Plasmacytoid dendritic cells
PEG	Polyethylene glycol
PFA	Paraformaldehyde
PGE2	Prostaglandin E2
PMSF	Phenylmethylsulfonyl fluoride
pNA	p-nitroaniline
PRRs	Pattern recognition receptors
PSD-95/ DLG4	Postsynaptic density protein-95/ disks large homolog 4
PUFA	Polyunsaturated fatty acid
RAGE	Receptor for advanced glycation end products
RIP1	Receptor-Interacting Protein kinase 1
RNA	Ribonucleic acid
RNase	Ribonuclease
ROS	Reactive oxygen species
rpm	Revolution(s) per minute
RT-PCR	Reverse transcription PCR
RU	Resonance Unit
SD	Standard deviation
SDS-PAGE	Sodium dodecyl sulfate-polyacrylamide gel electrophoresis
sec	Second
SEM	Standard error of the mean
SM	Sphingomylin
SNP	Single nucleotide polymorphisms
SPR	Surface Plasmon Resonance
SR-A	Scavenger Receptors, Class A
TANK	TRAF family member-associated NF- $\kappa$ B activator
Taq	Thermus aquaticus
TBK-1	TANK-Binding Kinase 1
TBS	Tris buffer with salt
TEMED	Tetramethylethylenediamine
TGN	Trans-Golgi network
TIR	Toll, IL-1R, and Resistance protein
TIRAP	TIR-associated protein
TLR	Toll-like receptor
TM	Transmembrane
TNF- $\alpha$	Tumor Necrosis Factor- $\alpha$
TRADD	TNF Receptor type 1-Associated Death Domain protein
TRAF	TNF Receptor-Associated Factor
TRAM	TRIF-related adaptor molecule
TRIF	TIR-domain-containing adaptor inducing IFN- $\beta$
Tris	Tris-(hydroxymethyl)-aminomethane
TSS	Transformation and storage solution for chemical transformation
UV	Ultraviolet
V	Volt
WB	Western blot
WT/wt	Wild type
% (v/v)	Volume/volume percentage solution
% (w/v)	Weight/volume percentage solution

## Content

<b>ABSTRACT</b> .....	<b>1</b>
<b>ZUSAMMENFASSUNG</b> .....	<b>4</b>
<b>PART I. TOLL-LIKE RECEPTOR 2 IS A PRIMARY RECEPTOR FOR A<math>\beta</math> TO TRIGGER ALZHEIMER'S INFLAMMATORY PATHOLOGY</b> .....	<b>7</b>
<b>1 INTRODUCTION</b> .....	<b>8</b>
1.1 ALZHEIMER'S DISEASE: OVERVIEW.....	8
1.2 PATHOLOGY.....	10
1.2.1 Amyloid $\beta$ .....	10
1.2.2 Microglia.....	13
1.2.3 Microglia and A $\beta$ pathogenesis.....	16
1.3 TOLL-LIKE RECEPTOR 2 AND OTHER TOLL-LIKE RECEPTORS.....	18
1.3.1 History.....	19
1.3.2 Structure.....	20
1.3.3 Toll-like receptor signaling.....	24
1.3.4 Toll-like receptor 2: a special TLR.....	26
<b>2 AIM OF THIS WORK</b> .....	<b>28</b>
<b>3 MATERIALS AND METHODS</b> .....	<b>30</b>
3.1 MATERIALS.....	30
3.1.1 Instruments.....	30
3.1.2 Experimental materials.....	32
3.1.3 Experimental kits and systems.....	34
3.1.4 Chemicals, reagents and customized services.....	35
3.1.5 Media.....	36
3.1.6 Enzymes.....	37
3.1.7 Antibodies.....	37
3.1.8 Oligonucleotides.....	37
3.1.9 Organisms.....	40
3.1.10 Mice.....	43
3.2 METHODS.....	44
3.2.1 Primary cell culture.....	44
3.2.2 Preparation of A $\beta$ peptides and quality control.....	45
3.2.3 A $\beta$ 42 challenge and sample collection.....	46
3.2.4 TNF- $\alpha$ , IL-1 $\beta$ and IL-8 level detection with ELISA kits.....	47
3.2.5 Confocal microscopy analysis of TLR2-A $\beta$ 42 co-localization.....	48
3.2.6 Biacore analysis of TLR2-A $\beta$ direct interaction.....	48
3.2.7 Pull-down analysis of TLR2-A $\beta$ 42 direct interaction.....	50
3.2.8 Construction of plasmids and establishment of TLRs-mutated cell lines.....	50
3.2.9 G-actin/F-actin assay in primary macrophages during A $\beta$ 42 phagocytosis.....	62
3.2.10 Flow cytometric analysis of FITC-A $\beta$ 42 phagocytosis in primary macrophages.....	62
3.2.11 Bone marrow transplantation.....	62
3.2.12 Tissue collection.....	63
3.2.13 Immunohistochemistry staining of Iba-1.....	63
3.2.14 Reverse transcription PCR and Real-time PCR analysis of gene transcripts.....	65
3.2.15 Brain homogenates.....	68
3.2.16 Bio-Rad Protein Assay.....	69
3.2.17 A $\beta$ ELISA.....	69
3.2.18 Barnes maze test.....	70
3.2.19 Immunofluorescence staining of NeuN on paraffin brain sections.....	70
3.2.20 Western blot analysis of PSD-95.....	71
3.2.21 Statistics.....	74
<b>4 RESULTS</b> .....	<b>76</b>
4.1 TLR2 IS A PRIMARY RECEPTOR FOR A $\beta$ 42 TO TRIGGER INFLAMMATORY ACTIVATION.....	76

4.1.1	<i>Tlr2-deficiency reduces A<math>\beta</math>42-induced inflammatory activation in microglia and macrophages</i>	76
4.1.2	<i>TLR2 co-localizes with A<math>\beta</math> in A<math>\beta</math>-treated microglia</i>	77
4.1.3	<i>TLR2 directly binds to A<math>\beta</math></i>	77
4.1.4	<i>TLR2 expression enables HEK-293 cells to respond to A<math>\beta</math> challenge</i>	79
4.2	<b>MOLECULAR MECHANISMS OF TLR2 IN A<math>\beta</math>-TRIGGERED INFLAMMATORY SIGNALING</b>	79
4.2.1	<i>TLR1 enhances whereas TLR6 suppresses TLR2-mediated A<math>\beta</math>-triggered inflammatory activation</i>	79
4.2.2	<i>Extra cellular LRR domains on TLR2 are essential for ligand recognition</i>	80
4.2.3	<i>Intracellular domains of TLR1 and TLR6 are involved in the diverse reactions of TLR2/1 and TLR2/6 complexes upon ligand challenge</i>	83
4.2.4	<i>EKKA(741-744) motif at DD-loop of TLR2 is essential for A<math>\beta</math>-triggered inflammatory signaling; the signaling defect due to the motif mutation is restored by TLR1 expression in a tyrosine<sup>737</sup>-dependent manner</i>	87
4.2.5	<i>Lysine<sup>742</sup> is the key residue in TLR2EKKA (741-744) motif for A<math>\beta</math>-triggered inflammatory signaling</i>	89
4.3	<b>TLR2-DEFICIENCY ENHANCES A<math>\beta</math> PHAGOCYTOSIS IN VITRO</b>	90
4.4	<b>TLR2-DEFICIENCY AMELIORATES AD-LIKE PATHOLOGICAL CHANGES IN AD MOUSE MODEL</b>	91
4.4.1	<i>Deficiency of microglial TLR2 decreases neuroinflammation</i>	91
4.4.2	<i>Tlr2-deficiency in myeloid cells decreases the A<math>\beta</math> load in AD mouse brain</i>	93
4.4.3	<i>Tlr2-deficiency in myeloid cells attenuates neuronal damage in the AD mouse brain</i>	94
<b>5</b>	<b>DISCUSSION</b>	<b>97</b>
5.1	<b>TLR2 IS A PRIMARY RECEPTOR FOR A<math>\beta</math></b>	97
5.2	<b>TLR1 AND TLR6 ARE CO-RECEPTORS OF TLR2 MODULATING A<math>\beta</math> INDUCED RESPONSE</b>	98
5.3	<b>TLR2 LYSINE<sup>742</sup> IS ESSENTIAL FOR SIGNALING</b>	99
5.4	<b>A<math>\beta</math>-TRIGGERED PHAGOCYTOSIS AND INFLAMMATORY ACTIVATION ARE MEDIATED THROUGH RELATIVELY INDEPENDENT PATHWAYS</b>	101
5.5	<b>PATHOGENIC ROLE OF TLR2 IN AN AD MOUSE MODEL</b>	101
5.5.1	<i>Tlr2-deficient bone marrow chimeric APP transgenic mice is a feasible model to investigate the pathogenic role of TLR2</i>	101
5.5.2	<i>Reduction of neuroinflammatory activation could improve the cognitive deficits in APP transgenic mice</i>	102
5.5.3	<i>Reduction of A<math>\beta</math> load could be another mechanism to improve neuronal function in APP transgenic mice</i>	104
<b>PART II. OMEGA-3 FATTY ACIDS REDUCE ALZHEIMER'S AMYLOID PEPTIDE-INDUCED PROINFLAMMATORY ACTIVITIES IN MACROPHAGES</b>		<b>106</b>
<b>1</b>	<b>SUMMARY</b>	<b>107</b>
<b>2</b>	<b>INTRODUCTION</b>	<b>108</b>
<b>3</b>	<b>MATERIALS AND METHODS</b>	<b>109</b>
3.1	<b>MATERIALS</b>	109
3.2	<b>METHODS</b>	109
3.2.1	<i>Preparation and characterization of A<math>\beta</math> aggregates</i>	109
3.2.2	<i>Culture of bone marrow-derived macrophages</i>	109
3.2.3	<i>Cell challenge and ELISA analysis of cytokine release</i>	109
3.2.4	<i>Reverse transcription and quantitative PCR for analysis of inflammatory genes and A<math>\beta</math> phagocytosis-related receptors</i>	110
3.2.5	<i>Apoptosis caspase 3 assay</i>	111
3.2.6	<i>LDH toxicity assay</i>	111
3.2.7	<i>Flow cytometric analysis of A<math>\beta</math>42 internalization</i>	112
3.2.8	<i>Statistics</i>	112
<b>4</b>	<b>RESULTS</b>	<b>113</b>
4.1	<b>DHA REDUCES TLR2, 3, 4 AND 9-INITIATED PRO- BUT NOT ANTI-INFLAMMATORY CYTOKINE SECRETION IN MACROPHAGES</b>	113
4.2	<b>DHA SUPPRESSES IFN-<math>\gamma</math> INDUCED IP-10 SECRETION IN MACROPHAGES</b>	114
4.3	<b>DHA REDUCES AGGREGATED A<math>\beta</math>42-INDUCED PRO-INFLAMMATORY CYTOKINE SECRETION IN MACROPHAGES</b>	115
4.4	<b>DHA SUPPRESSES AGGREGATED A<math>\beta</math>-INDUCED PGE2 SECRETION IN MACROPHAGES</b>	117

4.5	DHA DOES NOT AFFECT MACROPHAGE UPTAKE OF A $\beta$ AGGREGATES .....	117
<b>5</b>	<b>DISCUSSION</b> .....	<b>119</b>
	<b>REFERENCES</b> .....	<b>121</b>
	<b>PUBLICATIONS</b> .....	<b>139</b>
	<b>ACKNOWLEDGEMENTS</b> .....	<b>140</b>
	<b>CURRICULUM VITAE</b> .....	<b>142</b>

## Abstract

Alzheimer's disease (AD) is characterized by extracellular deposition of amyloid  $\beta$  peptide ( $A\beta$ ) in the brain and intracellular accumulation of tau filaments (Liu Y *et al.*, 2005). Microglial activation, triggered by  $A\beta$ , acts as a double-edged sword in the pathogenesis of AD: on the one hand it damages neurons by releasing neurotoxic inflammatory mediators while on the other hand it reduces  $A\beta$ -induced neuronal injury by internalizing  $A\beta$  (Walter Lisa *et al.*, 2009; Hao *et al.*, 2011). The innate immune receptors, *e.g.* Toll-like receptors (TLRs), have been shown to be associated with  $A\beta$ -induced microglial inflammatory activation and  $A\beta$  internalization (Fassbender *et al.*, 2004; Liu Y *et al.*, 2005; Tahara *et al.*, 2006; Jana *et al.*, 2008; Richard *et al.*, 2008; Reed-Geaghan *et al.*, 2009; Reed-Geaghan *et al.*, 2010; Hao *et al.*, 2011), but the mechanisms of how TLRs recognize  $A\beta$  and initiate cellular responses remain unclear.

In this thesis study, it was shown that  $A\beta$ -induced inflammatory cytokine secretion in primary cultured *tlr2*-deficient microglia and bone marrow derived macrophages (BMDMs) was much less than that in wild type (WT) cells. Further, the co-localization of TLR2 and  $A\beta$ 42 in microglia was demonstrated through confocal microscopy. Additionally, by utilizing real-time surface plasmon resonance spectroscopy and conventional biochemical pull-down assay, this study showed direct binding between TLR2 and aggregated  $A\beta$ 42. Finally, expression of TLR2 in endogeneously TLR2-deficient human embryo kidney (HEK-293) cells conferred their inflammatory response to an  $A\beta$  challenge. Combined, these data show that TLR2 is a primary receptor of  $A\beta$ 42 in microglial and macrophage inflammation.

TLR2 is known to co-operate with TLR1 and TLR6 in ligand recognition (Medzhitov *et al.*, 1997a; Farhat *et al.*, 2008; Jin *et al.*, 2008a). In this study, in order to tell whether TLR1 or TLR6 is the selective co-receptor for TLR2 in the  $A\beta$ 42 response, TLR2 was co-expressed with TLR1 or TLR6 in HEK-293 cells. It was found that TLR1 co-expression enhances, while TLR6 co-expression decreases the inflammatory response upon  $A\beta$ 42 triggering. Meanwhile, in TLRs endogenously expressing RAW264.7 macrophages, knocking down TLR1 via RNA interference was observed to decrease, while knocking down TLR6 was observed to increase  $A\beta$ -induced inflammatory response. These data suggest that TLR1 is a selective co-receptor of TLR2 for  $A\beta$ 42 recognition.

Furthermore, in order to uncover the detailed TLR2/TLR1 signaling mechanisms, genetically mutated TLR2 and TLR1 were generated and they were either expressed alone or

co-expressed in HEK-293 cells. An EKKA (741-744) motif in TLR2 was identified as a critical cytoplasmic region to transduce inflammatory signals. Interestingly, the signaling dysfunction of TLR2 due to EKKA (741-744)→PQNS motif mutation can be restored by co-expressing WT TLR1 in a TLR1 tyrosine<sup>737</sup> dependent way. The key amino acid residue in the TLR2EKKA motif was localized to the lysine at the position of 742.

More interestingly, even though TLR2-deficiency reduces the A $\beta$ 42-induced inflammation, the internalization of A $\beta$ 42 in *tlr2*-deficient primary macrophages was observed to be increased, which suggests that A $\beta$ 42-triggered inflammation and phagocytosis are mediated through relatively independent pathways.

By constructing bone marrow chimeric Alzheimer's disease amyloid precursor protein transgenic mice, it was confirmed that *tlr2*-deficiency in microglia attenuated neuroinflammation *in vivo*, and that the attenuated neuroinflammation was associated with improved neuronal function. This study demonstrates that TLR2 is a primary receptor for A $\beta$  to trigger neuroinflammatory activation and suggests that inhibition of TLR2 in microglia could be beneficial in AD pathogenesis.

There are epidemiological studies that suggest that diets enriched with omega-3 polyunsaturated fatty acids (PUFAs), *e.g.* docosahexaenoic acid (DHA), reduce risk for AD (Barberger-Gateau *et al.*, 2002; Morris *et al.*, 2003; Schaefer *et al.*, 2006). However, the underlying mechanism remains unclear. In another part of this thesis study, the role of PUFAs in A $\beta$ -triggered macrophage-dominated inflammation and phagocytosis was investigated. It was found that, in cultured BMDMs, DHA inhibits A $\beta$ 42 aggregate-induced production of pro- (*e.g.* TNF- $\alpha$  and IL-6) but not of anti- (*e.g.* IL-10) inflammatory cytokines. In order to elucidate the mechanisms mediating the anti-inflammatory effects of omega-3 PUFAs, the effect of DHA on TLR2, TLR3, TLR4 and TLR9 ligands, as well as interferon- $\gamma$ -induced inflammatory activation was investigated and it was found that DHA suppresses all of these ligands triggered inflammation in protein level. Interestingly, DHA does not reduce the uptake of A $\beta$  aggregates by macrophages.

In summary, this study demonstrates that TLR2 is a primary receptor in A $\beta$ 42-triggered inflammation. TLR1 enhances, while TLR6 suppresses, A $\beta$ 42-induced TLR2 activation. An intracellular EKKA motif, especially lysine<sup>742</sup> of TLR2, is essential for TLR2 signaling; the dysfunction of which can be restored by TLR1. Microglial *tlr2*-deficiency decreases the A $\beta$  pathology and improves cognitive function in AD mice. These findings provide new insight into the regulation of A $\beta$ -triggered activation of TLR2 signaling and provide fundamental knowledge about AD pathogenesis. Furthermore, the finding that Omega-3 PUFAs reduce

A $\beta$ -initiated inflammation (but not reducing phagocytosis in macrophages) provides new evidence on the beneficial role of omega-3 PUFA for the prevention of AD.

## Zusammenfassung

Die Alzheimer-Krankheit (AK, lat. *Morbus Alzheimer*) wird durch extrazelluläre Ablagerung des Amyloid-beta-Peptids (A $\beta$ ) im Gehirn sowie intrazelluläre Akkumulation von Tau-Filamenten charakterisiert (Liu Y *et al.*, 2005). Die durch A $\beta$ -eingeleitete Aktivierung von Mikroglia fungiert als ein zweischneidiges Schwert in der Pathogenese von AK: auf der einen Seite schädigt sie Neuronen, indem neurotoxische Mediatoren der Inflammation freigesetzt werden, während sie auf der anderen Seite die A $\beta$ -induzierten neuronalen Schäden durch Internalisierung des A $\beta$  vermindert (Walter Lisa *et al.*, 2009; Hao *et al.*, 2011). Die Rezeptoren der angeborenen Immunität, z.B. Toll-like Rezeptoren (TLRs), wurden in Verbindung mit der durch A $\beta$ -eingeleitete inflammatorische Aktivierung der Mikroglia und A $\beta$ -Internalisierung gebracht (Fassbender *et al.*, 2004; Liu Y *et al.*, 2005; Tahara *et al.*, 2006; Jana *et al.*, 2008; Richard *et al.*, 2008; Reed-Geaghan *et al.*, 2009; Reed-Geaghan *et al.*, 2010; Hao *et al.*, 2011), wobei die Mechanismen, auf welche Art und Weise TLRs A $\beta$  erkennen und entsprechende zelluläre Antworten einleiten, noch ungeklärt bleiben.

In dieser Studie wurde festgestellt, dass die A $\beta$ -induzierte Sekretion von inflammatorischen Zytokinen in Primärkulturen von *tlr2*-defizienten Mikroglia und Makrophagen aus dem Knochenmark (BMDMs, eng. *bone marrow derived macrophages*) gegenüber Wildtyp (WT)-Zellen deutlich reduziert ist. Weiterhin konnte die Ko-lokalisation von TLR2 und A $\beta$  in Mikroglia mittels konfokaler Mikroskopie gezeigt werden. Zusätzlich wurde die direkte Bindung zwischen TLR2 und A $\beta$ 42-Aggregaten mit Hilfe der Oberflächenplasmonresonanzspektroskopie und des konventionellen *pull-down* Assays nachgewiesen. Schließlich verleiht die Expression von TLR2 menschlichen embryonalen Nierenzellen (HEK-293, eng. *human embryonic kidney*), die endogen TLR2-defizient sind, die Fähigkeit, eine inflammatorische Antwort nach A $\beta$ -Stimulation einzuleiten. Zusammengefasst zeigen diese Ergebnisse, dass TLR2 ein primärer Rezeptor von A $\beta$  in der Immunantwort von Mikroglia und Makrophagen ist.

Bekanntere Interaktionspartner von TLR2 in der Erkennung von Liganden sind TLR1 und TLR6 (Medzhitov *et al.*, 1997a; Farhat *et al.*, 2008; Jin *et al.*, 2008a). Um nachzuweisen, welcher der beiden der selektive Ko-Rezeptor für TLR2 in der A $\beta$ -induzierten Immunantwort ist, wurde TLR2 zusammen mit TLR1 oder TLR6 in HEK-293 exprimiert. Es wurde festgestellt, dass die Ko-Expression von TLR1 die Immunantwort auf A $\beta$  verstärkt während die Ko-Expression von TLR6 sie abschwächt. Außerdem wurde mit Hilfe von RNA-Interferenz-Experimenten beobachtet, dass ein Knock-Down von TLR1 die A $\beta$ -induzierte

Immunantwort in RAW264.7-Makrophagen vermindert, während ein Knock-Down von TLR6 zu einer Erhöhung führt. Diese Daten deuten darauf hin, dass TLR1 der ausgewählte Co-Rezeptor für TLR2 in der Erkennung von A $\beta$  ist.

Zur Entschlüsselung des detaillierten Mechanismus des Signalweges von TLR2/TLR1, wurden genetisch mutierte TLR2/TLR1 generiert und entweder TLRs alleine oder gemeinsam in HEK-293-Zellen exprimiert. Die EKKA (741-744)-Region des TLR2 wurde als eine kritische cytoplasmatische Domäne für die Transduktion des Signals in der Immunantwort identifiziert. Interessanterweise wurde herausgefunden, dass eine durch EKKA (741-744) PQNS Mutation bedingte Fehlfunktion des TLR2 durch Ko-Expression von WT-TLR1 auf einer TLR1 Tyrosin<sup>737</sup> abhängige Art und Weise wiederhergestellt werden kann. Die Schlüsselaminosäure in der TLR2EKKA Domäne ist auf dem Lysin an der Position 742 lokalisiert.

Noch interessanter war die Beobachtung, dass die Internalisierung von A $\beta$  in TLR2-defizienten primären Makrophagen erhöht ist, obwohl TLR2-Defizienz die A $\beta$ -induzierte Immunantwort reduziert ist. Dies deutet darauf hin, dass die A $\beta$ -induzierte Immunantwort und Phagozytose über unterschiedliche Signalwege vermittelt werden.

Mit APP-transgenen Knochenmarkchimären konnte bestätigt werden, dass eine TLR2-Defizienz in murinen Mikroglia die Neuroinflammation *in vivo* vermindert und dass diese Reduktion der Neuroinflammation von verbesserter neuronaler Funktion begleitet wird. Diese Studie weist nach, dass TLR2 ein primärer Rezeptor für A $\beta$  ist, wodurch neuroinflammatorische Aktivierung eingeleitet wird und legt nahe, dass eine Inhibition von TLR2 in Mikroglia sich positiv auf den Krankheitsverlauf der AK auswirken kann.

Epidemiologische Studien weisen darauf hin, dass eine Diät reich an Omega-3-ungesättigten Fettsäuren (PUFAs, eng. *polyunsaturated fatty acids*), z. B. Docosahexaensäure (DHA), das Risiko für AK vermindert (Barberger-Gateau *et al.*, 2002; Morris *et al.*, 2003; Schaefer *et al.*, 2006). Jedoch ist der grundlegende pathophysiologische Mechanismus weiterhin unklar. In einem anderen Teil diese Studie wurde die Rolle von PUFAs in der A $\beta$ -induzierten Immunantwort von Makrophagen und Phagozytose untersucht. Es wurde herausgefunden, dass DHA die A $\beta$ -induzierte Produktion von pro- (z. B. TNF- $\alpha$  und IL-6), jedoch nicht anti-inflammatorischen Zytokinen (z. B. IL-10) in BMDMs inhibiert. Um den Mechanismus der anti-inflammatorischen Effekte durch Omega-3-PUFAs aufzuklären, wurde nachgewiesen, dass DHA eine durch TLR2, TLR3, TLR4, TLR9 sowie Interferon- $\gamma$  eingeleitete Immunantwort unterdrückt. Interessanterweise reduziert DHA die Aufnahme von A $\beta$ -Aggregaten in Makrophagen nicht.

Zusammengefasst wurde gezeigt, dass TLR2 ein primärer Rezeptor in der A $\beta$ -induzierten Immunantwort ist. TLR1 verstärkt und TLR6 vermindert die A $\beta$ -induzierte TLR2-Aktivierung. Eine intrazelluläre EKKK Domäne, besonders das Lysin<sup>742</sup> des TLR2, ist essentiell für die Signalübertragung von TLR2; die Fehlfunktion von TLR2 kann durch TLR1 wiederhergestellt werden. Mikrogliale Defizienz von TLR2 schwächt die A $\beta$ -Pathologie ab und verbessert die kognitive Funktion in AK-Modellmäusen. Diese Ergebnisse liefern neue Einblicke in die Regulation der A $\beta$ -eingeleitete Aktivierung des TLR2-Signalweges und bieten fundamentale Erkenntnisse über die AK-Pathogenese. Weiterhin zeigten die Ergebnisse, dass Omega-3-PUFAs die A $\beta$ -induzierte Immunantwort vermindern und stellen einen neuen Anhaltspunkt für die günstige Rolle der Omega-3-PUFAs bei der Prävention von AK dar.

(Thank Mr. Kan Xie and Miss Manuela Gries for translating the English abstract to German)

**Part I. Toll-Like Receptor 2 is a primary receptor for A $\beta$  to trigger  
Alzheimer's inflammatory pathology**

# 1 Introduction

## 1.1 Alzheimer's disease: overview

Alzheimer's disease (AD) is an irreversible, progressive, brain degenerative disease characterized by the insidious onset of dementia. Impairment of memory, judgement, attention span and problem solving skills is followed by severe apraxias and a global loss of cognitive abilities (Adams *et al.*, 1997). AD primarily occurs after age 60, and is marked pathologically by severe cortical atrophy and the triad of senile plaques, neurofibrillary tangles and neuropil threads (Adams *et al.*, 1997). This disease is named after German psychiatrist and neuropathologist Dr. Alois Alzheimer, who for the first time on November 3rd, 1906 reported in his lecture "Über eine eigenartige Erkrankung der Hirnrinde (A peculiar disease of the cerebral cortex)" at a meeting of psychiatrists in Tübingen (O'Brien, 1996). In that lecture, Alzheimer reported the histopathological findings of many abnormal clumps (amyloid plaques) and tangled bundles of fibers (neurofibrillary tangles) in the brain of one of his female patients named Auguste Deter, who had died of an unusual mental illness (O'Brien, 1996; Maurer *et al.*, 1997; Goedert *et al.*, 2006) (Figure 1.1).

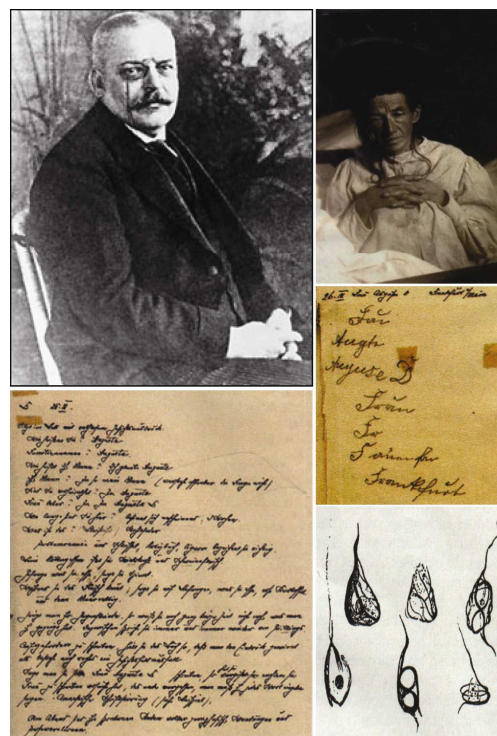


**Figure 1.1. Alzheimer's disease history.** Upper left, a portrait of Dr. Alois Alzheimer (1864-1915) (Goedert *et al.*, 2006); upper right, A 1902 photograph shows Dr. Alzheimer's patient Auguste D's helplessness (O'Brien, 1996; Maurer *et al.*, 1997); middle right, Auguste D's handwriting. She was attempting to write her own name, showing "amnesic writing disorder" (Maurer *et al.*, 1997); lower left, extracts from Alzheimer's notes file of Auguste Deter on Nov 29, 1901. When she was chewing meat and was asked what she was doing, she answered "potatoes and horseradish", suggesting loss of recognition (Maurer *et al.*, 1997); lower right, neurofibrillary tangles drawn by Alzheimer (Alzheimer, 1911; Maurer *et al.*, 1997).

More than a century has passed since Alzheimer's first report of AD. Currently, approximately 10% of people over 65 years old are demented, and about 70% of the demented patients suffer from AD. It is estimated that 13.5 million US citizens and 80 million people worldwide older than 65 years will develop AD in 2050 (about 4% of the whole population) (Szekely *et al.*, 2007; The Lancet, 2010). The rate of AD in those aged 85 and older might reach 50% (Evans *et al.*, 1989; Szekely *et al.*, 2007).

The mortality rate due to AD is also increasing rapidly. The recent WHO data show that AD is the 6<sup>th</sup> leading cause of death in high-income countries (Figure 1.2.) (Table 1.1).

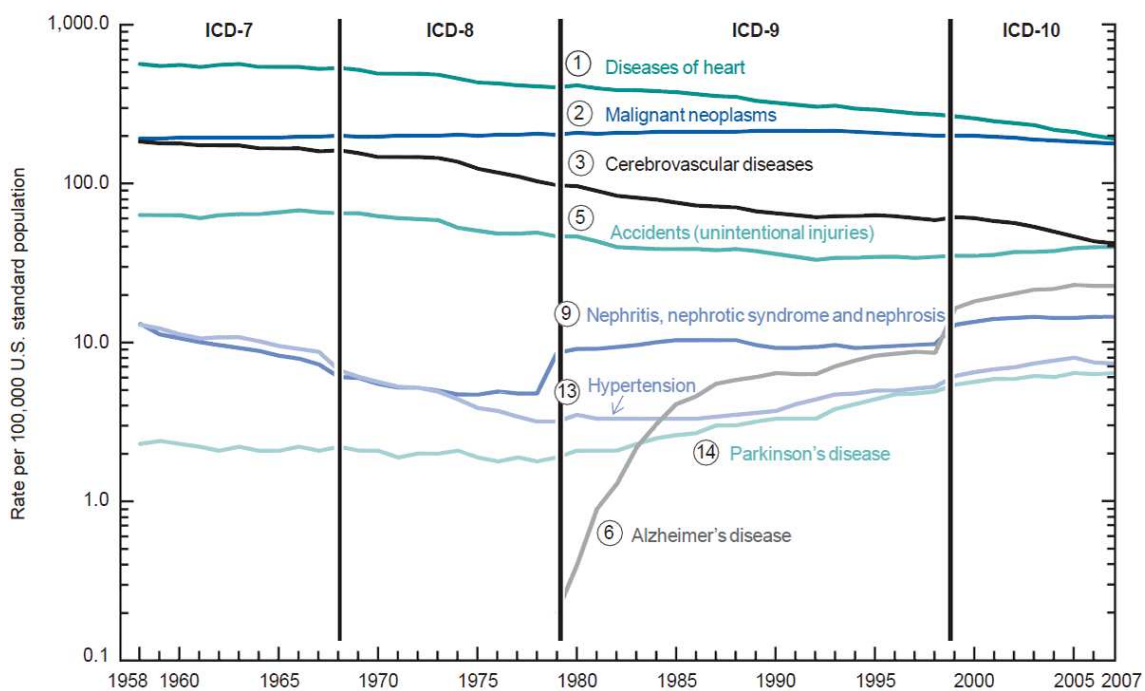


**Figure 1.2. Age-adjusted death rates for selected leading causes of death: United States, 1958-2007 (Xu JQ *et al.*, 2010).** Notes: ICD is the International Classification of Diseases. Circled numbers indicate ranking of conditions as leading causes of death in 2007. Source: CDC/NCHS, National Vital Statistics System, Mortality.

**Table 1.1. The 10 leading causes of death in high-income countries (2004)**

High-income countries	Deaths in millions	% of deaths
Coronary heart disease	1.33	16.3
Stroke and other cerebrovascular diseases	0.76	9.3
Trachea, bronchus, lung cancers	0.48	5.9
Lower respiratory infections	0.31	3.8
Chronic obstructive pulmonary disease	0.29	3.5
Alzheimer and other dementias	0.28	3.4
Colon and rectum cancers	0.27	3.3
Diabetes mellitus	0.22	2.8
Breast cancer	0.16	2.0
Stomach cancer	0.14	1.8

(Source: World Health Organization (WHO) <http://www.who.int/mediacentre/factsheets/fs310/en/index.html>)

However, as yet, no single “magic bullet” is able to prevent or cure AD. On average, patients survive from 8 to 10 years after diagnosis. Current AD medications primarily aim to support mental functions, to improve behavioral symptoms and to delay the disease progression. Moreover, the cost of health care for AD patients is huge and will only continue to increase (Table 1.2) (Alzheimer's-association, 2011). Thus, strategies for effective prevention and treatment of AD are urgently needed.

**Table 1.2. Average per person payments for healthcare and long-term care services, medicare beneficiaries aged  $\geq 65$  years, with and without Alzheimer's disease or other dementia, 2004 medicare current beneficiary survey, 2010 dollars (Alzheimer's-association, 2011).**

Average Per Person Payments	<u>Beneficiaries with no Alzheimer's or Other Dementias</u>	<u>Beneficiaries with Alzheimer's or Other Dementias</u>
Total payments*	\$13,515	\$42,072
Payments from Specified Sources		
Medicare	6720	19,304
Medicaid	915	8419
Private insurance	1869	2354
Other payer	629	662
HMO	897	523
Out-of-pocket	2442	3141
Uncompensated	256	333

\*Payments by source do not equal total payments exactly due to the effect of population weighting.

## 1.2 Pathology

The pathologic hallmarks of AD are extracellular senile plaques composed of deposits of ~4 kDa amyloid- $\beta$  ( $A\beta$ ) and intracellular neurofibrillary tangles formed by the accumulation of abnormally phosphorylated tau filaments in the brain regions that serve memory and cognitive function. A prominent neuroinflammatory activation process has also been observed (Citron, 2010).

### 1.2.1 Amyloid $\beta$

There are two major forms of  $A\beta$ : 40 or 42 amino acids (aa) long ( $A\beta_{40}$  and  $A\beta_{42}$  respectively), which are generated by sequential proteolytic cleavage of the transmembrane amyloid precursor protein (APP) by  $\beta$  and  $\gamma$  secretases (Figure 1.3). The N terminus of  $A\beta$  is located in the extracellular domain of APP, 28aa from the transmembrane region, and its C terminus is in the transmembrane region. A third group of enzymes,  $\alpha$ -secretases, cleave between residues 16 and 17, precluding  $A\beta$  formation (Goedert *et al.*, 2006). In neurons, besides generation on the cell surface, the endoplasmic reticulum (ER) was found to be the site for  $A\beta_{42}$  and the trans-Golgi network (TGN) was found to be the site for  $A\beta_{40}$  generation (Hartmann *et al.*, 1997).  $A\beta_{42}$  is the more amyloidogenic form because of its two

additional hydrophobic amino acids that is thought to be the real culprit for AD (Iwatsubo *et al.*, 1994; Younkin, 1995; Goedert *et al.*, 2006). In the three-dimensional structure of the A $\beta$  fibril, residues 1 to 17 are disordered, and residues 18 to 42 form a  $\beta$ -strand-turn- $\beta$ -strand motif that contains two parallel  $\beta$  sheets formed by residues 18 to 26 and 31 to 42 (Figure. 1.3 and 1.4) (Goedert *et al.*, 2006; Ahmed *et al.*, 2010).

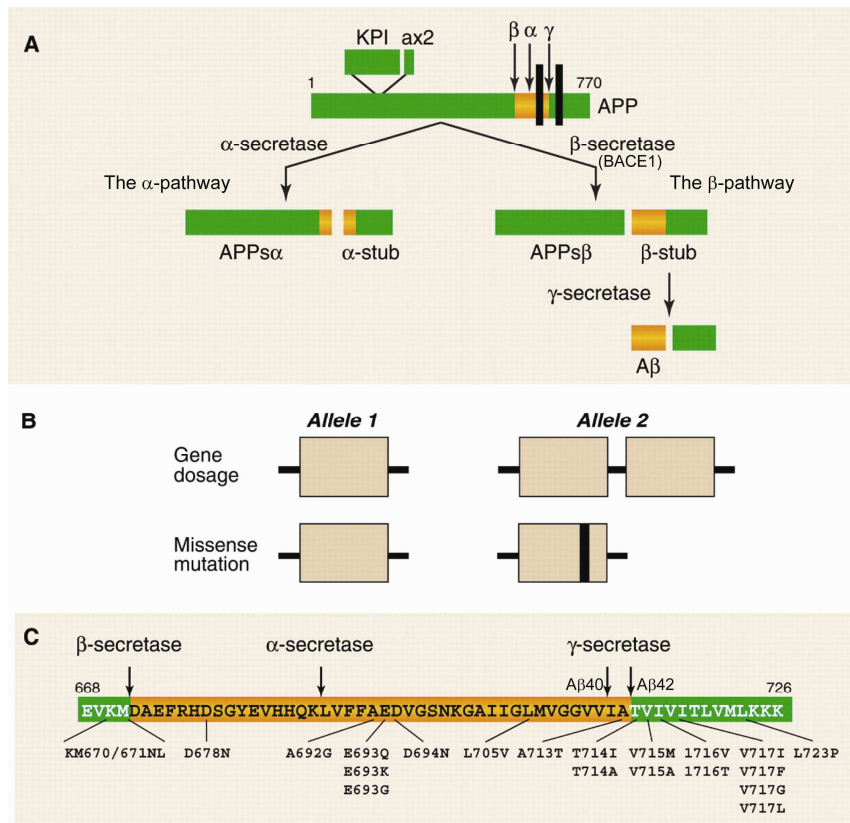


**Figure 1.3. Amyloid- $\beta$  generation (Goedert *et al.*, 2006).** (A) Generation of A $\beta$  from the amyloid precursor protein (APP). Cleavage by  $\beta$ -secretase generates the N terminus and intramembranous cleavage by  $\gamma$ -secretase gives rise to the C terminus of A $\beta$ . Cleavage by  $\alpha$ -secretase precludes A $\beta$  formation. (B) Duplication of the APP gene and missense mutations (black box) in the APP gene cause inherited forms of AD and cerebral amyloid angiopathy. (C) Twenty missense mutations in APP are shown. Single-letter abbreviations for amino acid residues: A, Ala; C, Cys; D, Asp; E, Glu; F, Phe; G, Gly; H, His; I, Ile; K, Lys; L, Leu; M, Met; N, Asn; P, Pro; Q, Gln; R, Arg; S, Ser; T, Thr; V, Val; W, Trp; Y, Tyr (modified from (Goedert *et al.*, 2006) ).

Many factors may influence A $\beta$  generation including the most commonly investigated cholesterol (Puglielli *et al.*, 2003) and cholesterol metabolism-related factors such as *APOE*  $\epsilon$ 4 (Tanzi *et al.*, 2001) and statins (Jick *et al.*, 2000; Fassbender *et al.*, 2001). These studies suggest that cholesterol is involved in A $\beta$  generation; high serum cholesterol level is a risk factor for AD. Hartmann and colleagues established a cell model to elucidate the relationship between  $\gamma$ -secretase and lipid metabolism. In this model, cholesterol upregulates  $\gamma$ -secretase activity, A $\beta$ 42 decreases the level of sphingomyelin (SM) by activating the SM degrading enzyme, neutral sphingomyelinase (nSMase), and A $\beta$ 40 downregulates cholesterol *de novo*

synthesis by inhibiting hydroxymethylglutaryl-CoA reductase (HMGR) activity (Grimm *et al.*, 2005; Grösgen *et al.*, 2010). Such a model implies the physiological roles of A $\beta$  in lipid metabolism, in addition to its role in copper homeostasis. APP might work as a Cu (I)-binding neuronal metallochaperone due to its primary N-terminal Cu-binding domain (CuBD) (Bayer *et al.*, 2003).

Enhanced production and/or reduced clearance may elevate the level of A $\beta$  which, as it accumulates, tends to aggregate. Based on assembly states (Figure 1.4 (Ahmed *et al.*, 2010) ), A $\beta$  aggregates contain monomers, oligomers (*e.g.* dimers, trimers, tetramers, pentamers), protofibrils and fibrils (Sandberg *et al.*, 2010). However, not all A $\beta$ 42 conformations are equally toxic and it is still under debate which species are the most toxic. To date, tetramer (Bernstein *et al.*, 2009), dodecamer (Bernstein *et al.*, 2009), protofibril, annular assemblies, A $\beta$ -derived diffusible ligands (ADDLs), A $\beta$ \*56, secreted soluble A $\beta$  dimers and trimers that are formed by 2-50 monomers are considered to be the toxic species in AD (Haass *et al.*, 2007; Demuro *et al.*, 2010); whereas the mature A $\beta$ -amyloid fibers are largely inert (Martins *et al.*, 2008).

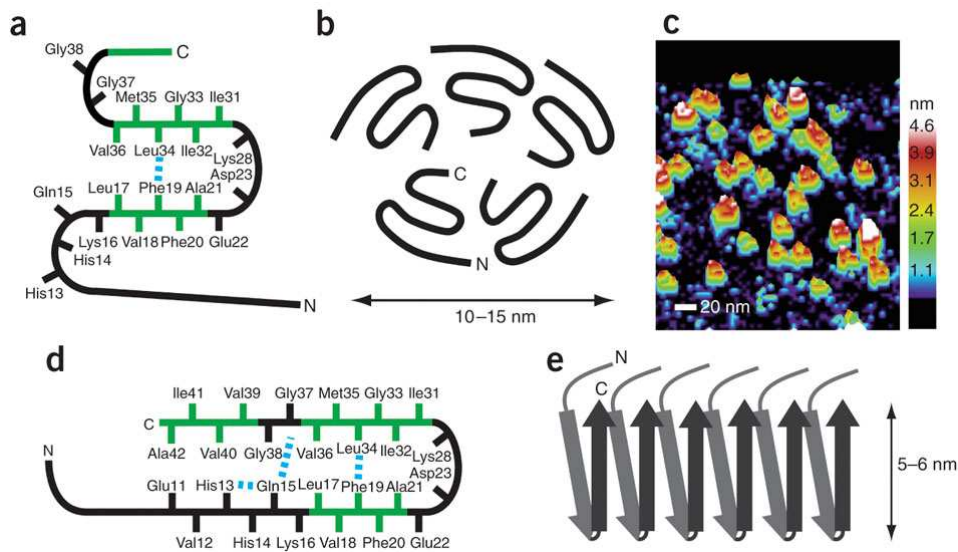


**Figure 1.4. Models of the A $\beta$ 42 oligomers and fibrils (Ahmed *et al.*, 2010).** (a) Schematic of monomer: Solid-state NMR measurements show that Phe19 is in contact with Leu34, and amide exchange measurements indicate solvent-accessible turns at His13-Gln15, Gly25-Gly29 and Gly37-Gly38. (b) Schematic of the A $\beta$ 42 pentamer. The orientation of the C terminus toward the center of the pentamer is based on solvent accessibility. A similar orientation for the hexamer was proposed previously (Bernstein *et al.*, 2009). (c) Three-dimensional image of single-touch AFM measurements of A $\beta$ 42 oligomers. (d-e) Schematic of the monomer within A $\beta$ 42 fibrils (d) and the parallel and in-register packing and staggering of the individual  $\beta$ -strands within A $\beta$ 42 fibrils (e) (Ahmed *et al.*, 2010).

The A $\beta$ -aggregates damage neuron or synaptic integrity (network) both directly and indirectly thereby impairing memory.

A $\beta$  alters neuronal Ca<sup>2+</sup> homeostasis via disruption of the membrane Ca<sup>2+</sup> permeability. Three major mechanisms are proposed (Demuro *et al.*, 2010): i. A $\beta$  interacts with endogenous plasmalemmal Ca<sup>2+</sup>-permeable ion channels, such as voltage-gated Ca<sup>2+</sup> channels (N, P, and Q-VGCC), nicotinic acetylcholine channels ( $\alpha 7$  and  $\alpha 4\beta 2$  nAChRs), glutamate receptors (AMPA and NMDA), dopamine receptors, serotonin receptors (5-hydroxytryptamine type 3), and intracellular inositol trisphosphate receptors (IP3Rs), ii. A $\beta$  disrupts membrane integrity through the interaction with membrane lipids such as phosphoinositides (Decout *et al.*, 1998), phosphatidylglycerol (Terzi *et al.*, 1995), phosphatidylcholine (Avdulov *et al.*, 1997), and gangliosides (McLaurin *et al.*, 1998), and iii. the formation of a Ca<sup>2+</sup>-permeable A $\beta$  pore (Arispe *et al.*, 1993; Quist *et al.*, 2005; Inoue, 2008; Demuro *et al.*, 2010). In synaptic plasticity, A $\beta$ -aggregates alter Ca<sup>2+</sup> concentration in dendrites, either by binding to  $\alpha 7$  nAChRs, or by interacting with L-type VGCC. Increased intracellular Ca<sup>2+</sup> could influence long-term potentiation (LTP) or long-term depression (LTD) directly or, alternatively, by activating extracellular-signal-regulated kinase/mitogen-activated protein kinase (ERK/MAP kinase), which subsequently affects LTP and LTD, and alters dendritic architecture through cytoskeletal remodelling (Small *et al.*, 2001).

A $\beta$  is known to activate glial cells in the brain to release neurotoxic mediators such as pro-inflammatory mediators, Tumor Necrosis Factor- $\alpha$  (TNF- $\alpha$ ), Interleukin-1 $\beta$  (IL-1 $\beta$ ), IL-6, IL-8, prostaglandin E2 (PGE2), reactive oxygen species (ROS), nitric oxide (NO), Cox-2 and chemokines. These mediators trigger neuronal apoptosis or necrosis (Akiyama *et al.*, 2000; Glass *et al.*, 2010; Zotova *et al.*, 2010), as well as synaptic deficits (Medeiros *et al.*, 2007). Although astrocytes were reported to release TNF- $\alpha$ , IL-1 $\beta$ , ROS and NO (Hu *et al.*, 1998; Schubert *et al.*, 2009), microglia are considered to be the main inflammatory effector cells in the central nervous system (CNS).

## 1.2.2 Microglia

Microglia are the resident macrophages in the CNS. A recent study shows that there are  $86.1 \pm 8.1 \times 10^9$  NeuN-positive cells (“neurons”) and  $84.6 \pm 9.8 \times 10^9$  NeuN-negative (“nonneuronal”) cells in the adult human brain (Azevedo *et al.*, 2009). The non-neuronal cells in the CNS include astrocytes, microglia and oligodendrocytes, approximately 20% of which are microglia (Lawson *et al.*, 1990; Santambrogio *et al.*, 2001).

Microglia are non-uniformly distributed in all major regions of the brain, varying in density between different areas (from 5% in the cortex and corpus callosum, to 12% in the substantia nigra). Generally, more microglia are found in the gray matter than in the white

matter. Densely-populated areas include the hippocampus, olfactory telencephalon, basal ganglia and substantia nigra (Walter Lisa *et al.*, 2009). The less densely-populated areas include fibre tracts, cerebellum and most of the brainstem. The cerebral cortex, thalamus and hypothalamus contain average cell-densities (Lawson *et al.*, 1990).

Microglial cells are the first line of defense in the CNS. They serve as sensors and executors of innate immunity within the CNS (Walter Lisa *et al.*, 2009); their morphology varies depending on location and activation states (Lawson *et al.*, 1990). Their activation is non-specific. Even in the healthy condition, microglia are constantly scanning the CNS microenvironment. The wide range of microglial response patterns and the great malleability of the microglial phenotype appear to be the result of the cells' ability to respond in a graded manner to changes around them. Therefore, "resting" microglia are actually constitutively active cells (Nimmerjahn *et al.*, 2005; Wake *et al.*, 2009; Graeber, 2010). Pathogenic stimuli drive the cells to differentiate into active immune complement cells, during which the morphology of microglia transforms from a ramified structure to a hyperramified and finally to an amoeboid morphology (Walter Lisa *et al.*, 2009). They migrate toward the site of injury and release various neuroactive compounds which ultimately result in neuronal injury or neuroprotection (Biber *et al.*, 2007; Wake *et al.*, 2009). Furthermore, microglial cells are capable of proliferating in response to several stimuli. Most immune receptors including the pattern recognition receptors, major histocompatibility complex molecules, and chemokine receptors, which are essential to the initiation and propagation of immune responses, are constitutively expressed at low levels in microglia. During microglial activation, the immunologically relevant molecules are upregulated and inflammatory mediators are produced (Walter Lisa *et al.*, 2009). Microglia express several phagocytic receptors (*e.g.* scavenger receptor A (SR-A), CD36, receptor for advanced glycation endproducts (RAGE), and CD47) and serve as the professional phagocytes of the CNS (Bamberger *et al.*, 2003). Microglia are actively repressed by signals coming from electrically active neurons (Neumann, 2001; Walter Lisa *et al.*, 2009); the removal of this tonic inhibition will lead to microglial activation (Walter Lisa *et al.*, 2009). Microglial responses in the CNS are summarized in Figure 1.5 (Monk *et al.*, 2006).

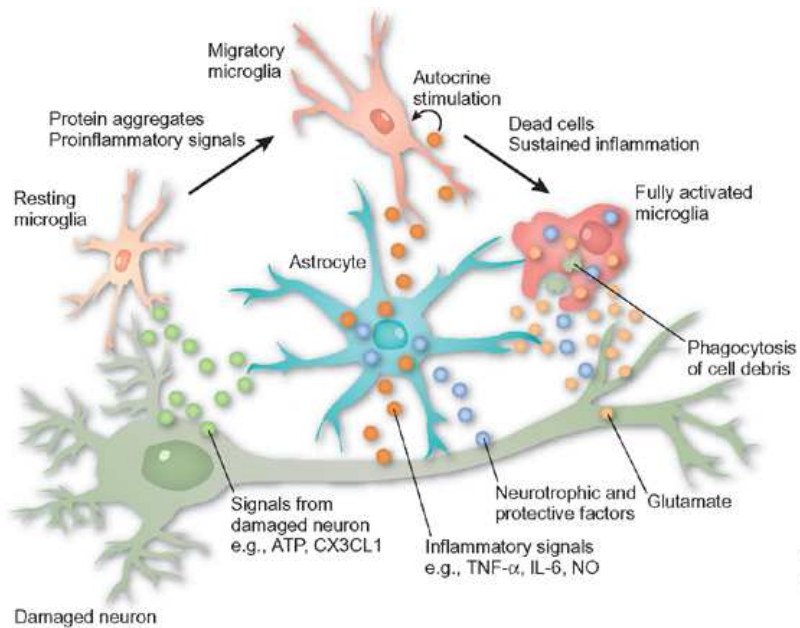


**Figure 1.5. Microglia respond to immunological alarm signals in the CNS (Monk *et al.*, 2006).** In response to factors including cytokines, material from apoptotic cells, viral envelope glycoproteins and aggregated proteins (*e.g.* A $\beta$ ), microglia can undergo several different levels of activation, finally resulting in a fully functioning phagocytic cell. Activated microglia can be friends or foes to neighboring neurons. As friends, they can clear toxic material (apoptotic neurons, protein aggregates), secrete neurotrophic factors such as BDNF and protective factors such as glutathione and increase clearance of excitotoxic glutamate by astrocytes. Microglia can also secrete potentially neurotoxic molecules such as proinflammatory cytokines (TNF- $\alpha$ , IL-1 $\beta$ ), glutamate, free radical species and NO (Monk *et al.*, 2006).

There are some cellular markers to identify microglial cells. Allograft inflammatory factor-1 (AIF1) or ionized calcium-binding adaptor molecule 1 (Iba-1) is expressed specifically in microglia/macrophages (Imai *et al.*, 1996; Ito *et al.*, 1998). CD11b is commonly used as another microglial marker in nervous tissue and is implicated in various adhesive interactions of monocytes, macrophages and granulocytes as well as in mediating the uptake of complement coated particles (Roy *et al.*, 2006). CD11b is the receptor for the fragment of the third complement component (CR3) (Capo *et al.*, 2003) and also for fibrinogen, factor X and ICAM1 (Feng *et al.*, 1998).

The origin and renewal of microglial cells is still under discussion (Davoust *et al.*, 2008). It is believed that microglia are derived from myeloid precursors in the neuroepithelium at an early stage of embryonic development and invade the CNS from the yolk sac during a late stage of embryogenesis (Walter Lisa *et al.*, 2009). It is also demonstrated that ramified microglia are replenished by bone marrow precursor cells, even in adults (Ritter *et al.*, 2006). There is evidence from both patients and animal AD models that bone marrow-derived microglia can be recruited to lesion sites in the brain (Malm *et al.*, 2005; Cartier *et al.*, 2009). It has even been suggested that the bone marrow-derived microglia have a higher capacity to restrict senile plaque formation than their resident counterparts in AD (Simard *et al.*,

2006b). Thus, microglial phenotypes can be modified by changing genetic expression in bone marrow cells, although there are still a number of technical issues needing to be addressed (Graeber, 2010). Recently, adult microglia were shown to be an ontogenically distinct population of mononuclear phagocytes derived from primitive myeloid progenitors that arise before embryonic day 8 (Ginhoux *et al.*, 2010), however, this report does not exclude the possibility of renewal of microglial cells by peripheral precursor cells in pathogenic states.

### 1.2.3 Microglia and A $\beta$ pathogenesis

Microglial activity is a double-edged sword in AD pathogenesis. On one hand they clear A $\beta$  aggregates via phagocytosis and support neuronal survival by releasing neurotrophic molecules; on the other hand, they can be overactivated and release cytotoxic substances including NO or superoxide and pro-inflammatory cytokines, *e.g.* interleukin-1 $\beta$  (IL-1 $\beta$ ) and tumor necrosis factor- $\alpha$  (TNF- $\alpha$ ), thereby killing nearby neurons (Walter Lisa *et al.*, 2009; Fuhrmann *et al.*, 2010; Heneka *et al.*, 2010) (Figure. 1.6 (Monsonogo *et al.*, 2003)).

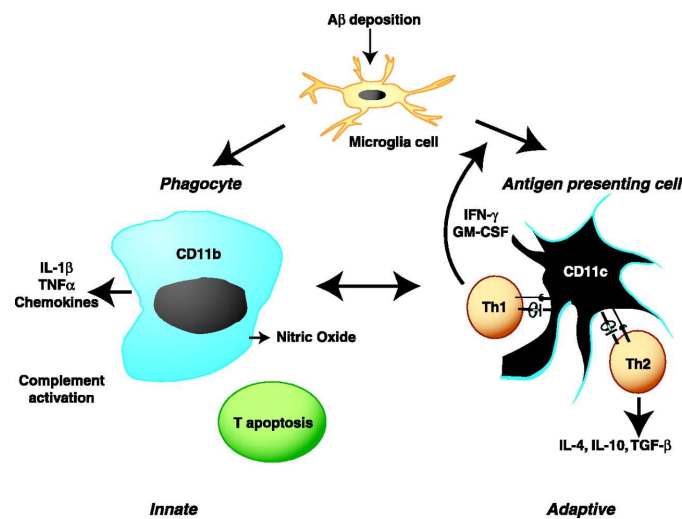


**Figure 1.6. Pathways of microglia activation in Alzheimer's diseases (Monsonogo *et al.*, 2003).** Microglia are ramified morphology in the intact CNS. In response to A $\beta$  deposition in AD, microglial cells are activated and differentiate into phagocytic cells (CD11b+) (left), which induce a proinflammatory environment and secrete IL-1 $\beta$ , TNF- $\gamma$ , NO, free radicals, chemokines, and activate complement. The NO secreted by CD11b+ cells may enhance T cell apoptosis in the CNS. A second pathway for microglial cells is to differentiate into APCs (right), which are induced in the presence of GM-CSF and/or IFN- $\gamma$  secreted by microglia, astrocytes, or other immune cells (T cells, macrophages) that infiltrate the CNS. As a result, microglia cells differentiate to dendritic-like cells that then may function as APCs for both TH1 and TH2 cells (Monsonogo *et al.*, 2003).

The A $\beta$ -initiated microglial phagocytosis and inflammatory activation are reported to be mediated through different but related receptors and signaling pathways.

Schenk and colleagues (Schenk *et al.*, 1999) reported that either active or passive immunization of mice with anti-A $\beta$  antibodies results in the prevention of amyloid deposition as well as the removal of pre-existing plaques. This is the result of immunoglobulin receptor (FcR)-mediated stimulation of phagocytosis of the deposited fibrillar A $\beta$  by microglial cells.

These data clearly demonstrate that microglia have an intrinsic capacity to mount an effective phagocytic response.

To date, RAGE (Yan *et al.*, 1996), SR-A (El Khoury *et al.*, 1996; Paresce *et al.*, 1996), scavenger receptors class B, CD36 (Paresce *et al.*, 1996; El Khoury *et al.*, 2003), scavenger receptors class B1 (SR-BI) (Thanopoulou *et al.*, 2010), CD14 (Liu Y *et al.*, 2005),  $\alpha 6\beta 1$ -integrin (Bamberger *et al.*, 2003), and the integrin associated protein CD47 (Bamberger *et al.*, 2003) have been reported to mediate A $\beta$  phagocytosis (Figure 1.7).

TLR2 (Fassbender *et al.*, 2004; Jana *et al.*, 2008; Udan *et al.*, 2008; Reed-Geaghan *et al.*, 2009) and TLR4 (Walter S *et al.*, 2007; Udan *et al.*, 2008; Reed-Geaghan *et al.*, 2009) have been associated with the A $\beta$ -triggered microglial inflammatory activation. CD14 (Reed-Geaghan *et al.*, 2009; Reed-Geaghan *et al.*, 2010) and CD36 (Coraci *et al.*, 2002) mediate both inflammation and A $\beta$  phagocytosis (Figure 1.7). The *in vivo* findings in those studies were based on either introducing A $\beta$  directly through micro-injection into the cortex of wild-type and *tlr2*-deficient mice (Jana *et al.*, 2008); or by cross-breeding the receptor deficient mouse with APP transgenic mice (Richard *et al.*, 2008; Reed-Geaghan *et al.*, 2009; Reed-Geaghan *et al.*, 2010). However, such models were not feasible enough to address microglia study, because TLR2 itself reduces injury; for example, by injection-induced neuroinflammation (Babcock *et al.*, 2006). Furthermore, TLR2 is expressed in neurons (Rolls *et al.*, 2007), which makes it impossible to distinguish whether the outcome was due to TLR2 deficiency in microglia or non-microglial cells in the cross-breeding model. Moore's group proposed a CD36-TLR4-TLR6 receptor complex for A $\beta$ -triggered inflammation (Stewart *et al.*, 2010) based on their *in vitro* work; however in this study I observed an opposite role of TLR6 when it comes to TLR2, which will be addressed in the following sections.

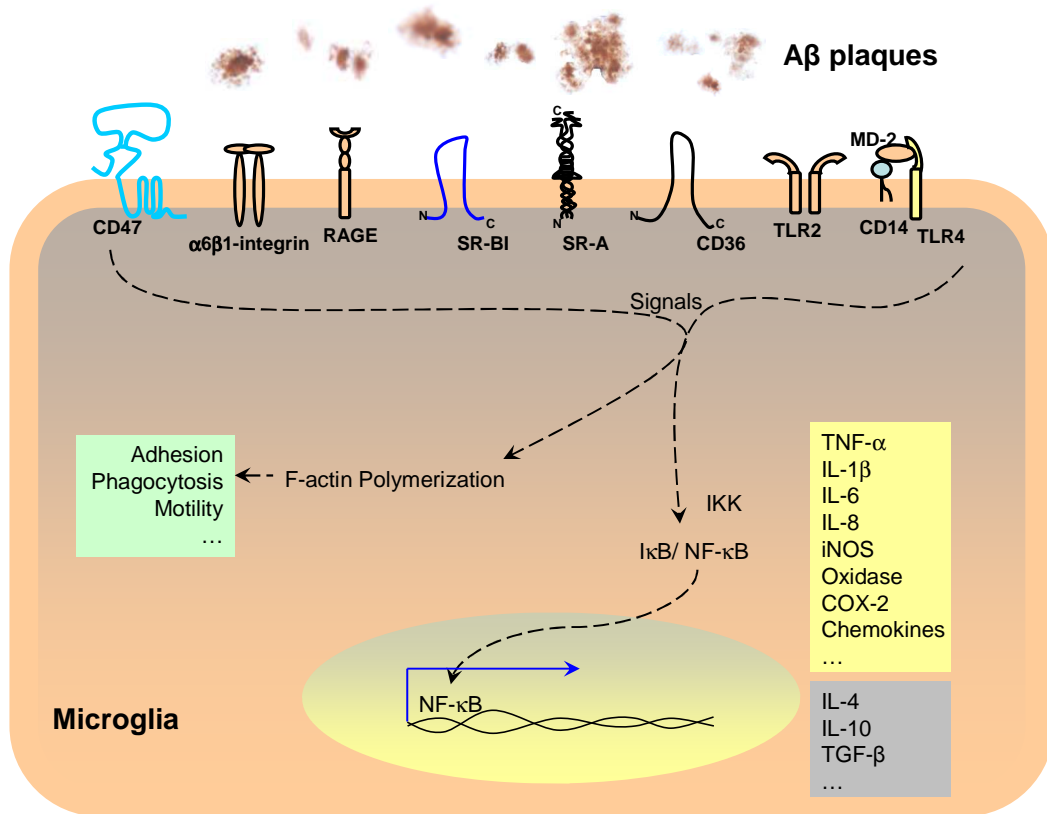


**Figure 1.7. Schematic diagram of receptors involved in A $\beta$  phagocytosis and inflammation triggering.** Microglia-mediated A $\beta$  clearance (phagocytosis) and pro-/anti-inflammatory activation play important roles in AD pathogenesis. Upon interacting with A $\beta$  through receptors such as CD47,  $\alpha$ 6 $\beta$ 1-integrin, receptor for advanced glycation end products (RAGE), scavenger receptor (SR) and CD14, signals were triggered to polymerize actin, which is essential for cell adhesion, migration and phagocytosis; CD36, CD14, TLR2 and TLR4 were reported to be associated with A $\beta$ -triggered microglial inflammatory activation, which results in the activation of NF- $\kappa$ B and the pro-inflammatory cytokines and/or anti-inflammatory cytokines production.

Despite the known knowledge of microglial inflammation and phagocytosis in the pathogenesis of AD, a major unresolved question is whether inhibition of these responses will be a safe and efficient way to reverse or slow the disease progression. To address this question, it will be necessary to learn the detailed molecular mechanisms by which inflammatory responses are induced within the CNS and how these responses ultimately contribute to pathology.

### 1.3 Toll-like receptor 2 and other Toll-like receptors

Toll-like receptors (TLRs) are a family of type I transmembrane pattern recognition receptors (PRR) with leucine-rich repeat (LRR)-contained ectodomains. TLRs mediate the recognition of pathogen-associated molecular patterns (PAMPs) and induce innate immune activation (Takeda *et al.*, 2003).

### 1.3.1 History

#### *“Das war ja toll”*

Although toll-like receptors have only been found for 17 years, they have attracted great study interests. The history of TLR study is well documented in a review by Medzhitov (Medzhitov, 2009); here only summarize some of the milestones in the research.

Between 1983-1986, Christiane Nüsslein-Volhard from the Max Planck Institute of Developmental Biology in Tübingen observed a weird-looking mutated fruit fly larva in which the ventral portion of the body was underdeveloped. She commented “Das war ja toll!”, which means “That was weird!” or “that’s cool/great!”, and named the mutated gene responsible “*Toll*”. The normal function of Toll protein is essential for dorso-ventral polarity in the fly. The *toll* gene was one of the serially discovered genes controlling early embryogenesis for which Nüsslein-Volhard won the Nobel Prize in 1995 (Anderson *et al.*, 1984; Anderson *et al.*, 1985a; Anderson *et al.*, 1985b; Hashimoto *et al.*, 1988; Hansson *et al.*, 2005).

At the annual Cold Spring Harbor Symposium on Quantitative Biology in 1989, Dr. Charles A. Janeway Jr. first presented his ideas on the first line of defense in the host: that pattern recognition receptors on immune cells trigger the response against pathogens (Janeway Jr, 1989; Medzhitov, 2003). This idea was followed by his ground breaking research on the identification of toll-like receptors, which are so named due to their genetic similarity to Toll (Medzhitov *et al.*, 1997b). The first toll-like receptor reported in human is TIL (now known as toll-like receptor 1), which was described as a product of “randomly sequenced cDNA 786” (rsc786) by Nomura and colleagues in 1994 (Nomura *et al.*, 1994). Unfortunately, TIL was not found to activate NF- $\kappa$ B (Mitcham *et al.*, 1996). At the same time, Hoffmann’s group observed that the drosophila Toll have an essential role in drosophila immunity against fungal infection by activating antimicrobial gene expression (Lemaitre *et al.*, 1996). In 1997, Janeway and Medzhitov showed that a human homologue of the drosophila Toll protein, hToll (now known as TLR4), could activate NF- $\kappa$ B and induce expression of IL-1, IL-8, IL-6 and CD80 (Medzhitov *et al.*, 1997b). Because the mammalian immune molecule IL-1 receptor and a tobacco resistant N protein had homology to drosophila Toll, the intracellular domain of Toll-like receptors was named TIR (Toll-IL-1R-Resistance protein) (Gay *et al.*, 1991; Whitham *et al.*, 1994). TLR4, as a LPS sensing receptor, was discovered one year later by Bruce A. Beutler and his colleagues (Poltorak *et al.*, 1998) through positional cloning. Subsequent studies by Shizuo Akira and many others have continuously elucidated the specificities of other TLRs for various microbial ligands (Takeda

*et al.*, 2003; Medzhitov, 2009). So far, 12 murine (TLR1-TLR13, with TLR10 being a pseudo gene because of a retrovirus insertion) and 10 human (TLR1-TLR10. The TLR11, TLR12 and TLR13 have been lost from the human genome) toll-like receptors (TLR1-TLR9 being conserved in both species) have been characterized (Shi Z. *et al.*, 2011). TLR signaling pathways were elucidated in detail after numerous mice with different toll-like receptor knock-outs were generated by Akira and his colleagues (Medzhitov, 2009).

### 1.3.2 Structure

TLRs are expressed not only in innate immune cells, *e.g.* microglia and macrophages, but also in T and B-lymphocytes. They are also expressed in vascular endothelial cells, adipocytes, cardiac myocytes and intestinal epithelial cells, *etc.* (Vandevenne *et al.*, 2010). Human microglial cells were reported to express all of the TLRs (TLR1-TLR9) (Olson *et al.*, 2004).

Each TLR has distinct domains responsible for PAMP recognition and immune signaling transduction. As shown in the table 1.3., TLR1, TLR2, TLR4, TLR5, TLR6, TLR11 and TLR13 are present on the plasma membrane (Takeuchi *et al.*, 2010; Shi Z. *et al.*, 2011), whereas TLR3, TLR7, and TLR9 are compartmentalized in ER. Those TLRs found in the ER could avoid unwanted activation of Toll-like receptors by self-nucleotides acting as potent TLR ligands (Barton *et al.*, 2009; Takeuchi *et al.*, 2010; Shi Z. *et al.*, 2011).

**Table 1.3. Description of the Toll-like receptors family (Summarized from references (Takeuchi *et al.*, 2010; Vandevenne *et al.*, 2010; Shi Z. *et al.*, 2011))**

TLR	Localization	Ligand	Origin of the Ligand	Adaptor
TLR1 (with TLR2)	Plasma membrane	Triacyl lipoprotein	Bacteria	MyD88, TIRAP
TLR2	Plasma membrane	Lipoprotein	Bacteria, viruses, parasites, self	MyD88, TIRAP
TLR3	Endolysosome	dsRNA	Virus	TRIF
TLR4	Plasma membrane	LPS	Bacteria, viruses, self	MyD88, TIRAP, TRAM and TRIF
TLR5	Plasma membrane	Flagellin	Bacteria	MyD88
TLR6 (with TLR2)	Plasma membrane	Diacyl lipoprotein	Bacteria, viruses	MyD88, TIRAP
TLR7 (human TLR8)	Endolysosome	ssRNA	Virus, bacteria, self	MyD88
TLR9	Endolysosome	CpG-DNA	Virus, bacteria, protozoa, self	MyD88
TLR10	Endolysosome	Unknown	Unknown	Unknown
TLR11	Plasma membrane	Uropathogenic bacteria, Profilin-like molecule	Protozoa	MyD88
TLR13	Endolysosome	Unknown	vesicular stomatitis virus	MyD88, TAK1

TLRs are type I transmembrane proteins. All TLRs share some common structural features (Figure 1.8): they are composed of a variable N-terminal extracellular ectodomain containing

16-28 leucine-rich repeats (LRRs) with horseshoe-like shapes that are responsible for the detection and interaction with PAMPs. The individual LRR module is 20-30aas long and is composed of a conserved “LxxLxLxxN” motif and a variable part (Kobe *et al.*, 2001). The hydrophobic core, formed by the conserved leucines and hydrophobic residues in the variable regions, extends throughout the entire protein. The LRRNT and LRRCT modules in the N and C termini do not have LRR motifs but frequently contain clustered cysteines forming disulfide bridges. These modules stabilize the protein by protecting its hydrophobic core from being exposed to solvent. The unique horseshoe-like shape is due to conserved sequence patterns in the LRR modules. The “LxxLxLxxN” motifs are located in the inner concave surfaces of the horseshoe-like structure formed from parallel  $\beta$  strands. The variable parts of the modules form the convex surface generated by helices,  $\beta$  turns, and/or loops (Jin *et al.*, 2008a).

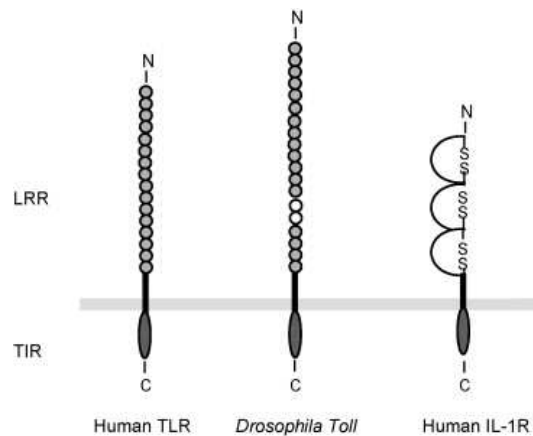


**Figure 1.8. Schematic representation of the protein structure of Toll-Like Receptors (Vandevenne *et al.*, 2010).** The ectodomain consists in 16–28 leucine-rich repeats that are variable among human TLRs and among different species, indicated as grey circle, and involved in the recognition of PAMPs. A cystein-rich domain (depicted as two white circles) is present in *Drosophila Toll* but missing in human TLRs. The ectodomain of the IL-1R consists in three immunoglobulin-like domains. All TLRs share an intracellular domain that is indicated as a dark grey ellipse. This TIR domain is involved in the signal transduction and is highly conserved among human TLRs and among different species (Vandevenne *et al.*, 2010).

The binding of ligands to the extracellular domains of TLRs causes a dimerization of the receptors (Heterodimerization: TLR2-TLR1, TLR2-TLR6, TLR7-TLR8, TLR8-TLR9 and TLR7-TLR9 (Wang *et al.*, 2006); Homodimerization: TLR2 (Strominger, 2007), TLR3, TLR4, TLR5, TLR9 and TLR13 (Ozinsky *et al.*, 2000; O'Neill *et al.*, 2007; Shi Z. *et al.*, 2011) ) and triggers the recruitment of specific adaptor proteins including MyD88, MAL (also known as TIRAP), TRIF, and TRAM to the intracellular TIR domain, thus initiating signaling (Kim *et al.*, 2007). These adaptor proteins also contain TIR domains. TIR-TIR interactions between receptor-receptor, receptor-adaptor, and adaptor-adaptor are critical for activating signaling (O'Neill *et al.*, 2007).

The crystal structures of TLR3-double-stranded RNA (dsRNA) (Bell *et al.*, 2005; Choe *et al.*, 2005), TLR4-MD-2-endotoxin antagonist Eritoran (Kim *et al.*, 2007), TLR1-TLR2-triacylated lipopeptide (Jin *et al.*, 2007) and TLR2-TLR6-diacylated lipopeptide (Kang *et al.*, 2009) have been determined. A typical ligand-induced dimerization is shown in Figure 1.9 (Jin *et al.*, 2007). In these “m”-shaped complexes, the C termini of the extracellular domains of the TLRs converge in the middle. This observation suggests the hypothesis that dimerization of the extracellular domains forces the intracellular TIR domains to dimerize, and this initiates signaling by recruiting intracellular adaptor proteins. Three kinds of ligand-TLR “m”-shape binding examples are shown in Figure 1.10 (Jin *et al.*, 2008a). Hydrophobic ligands of TLR1, TLR2 and TLR4 interact with internal protein pockets of receptors. In contrast, dsRNA, a hydrophilic ligand, interacts with the solvent-exposed surface of TLR3.

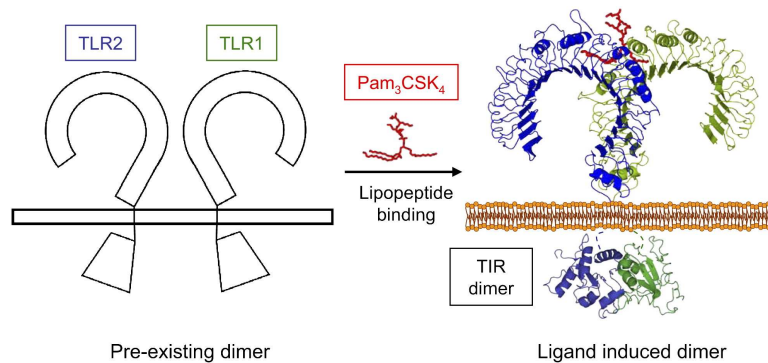


**Figure 1.9. Model of Ligand-Induced Heterodimer of Full-Length TLR1 and TLR2 (Jin *et al.*, 2007).** The cell membrane is shown schematically in orange and connecting linker regions are represented by broken lines. The structure of the heterodimeric TIR domain is drawn as proposed by Gautam *et al.* using PDB coordinates 1FYV and 1FYW (Gautam *et al.*, 2006) and (Xu Yingwu *et al.*, 2000). Distance between the C termini of the TLR1 and 2 ectodomains is approximately 40Å. Diameter of the TIR dimer is estimated to be 50Å (Jin *et al.*, 2007).

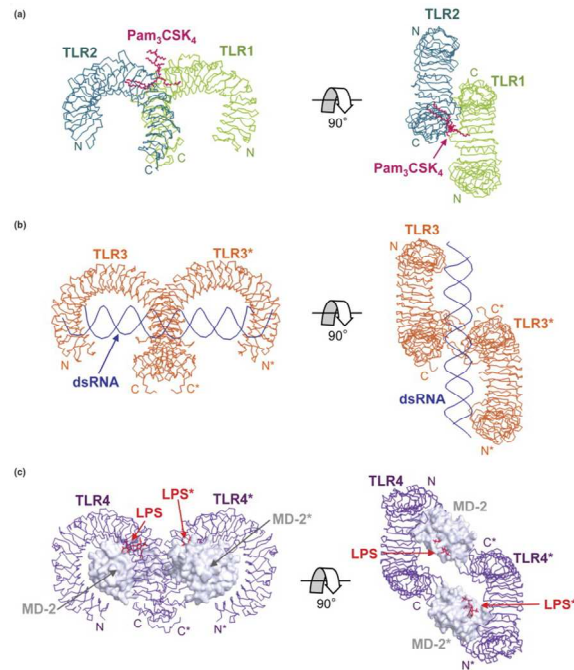


**Figure 1.10. The ‘m’ shaped TLR dimers induced by binding of agonistic ligands (Jin *et al.*, 2008b).** Dimerization may bring the intracellular TIR domains close together to initiate signaling. (a) Structure of the TLR1-TLR2-Pam3CSK4 complex (PDB entry 2Z7X). (b) Structure of the TLR3-dsRNA complex (PDB entry 3CIY). (c) The model of the TLR4-MD-2-LPS complex proposed by Kim (Kim *et al.*, 2007; Jin *et al.*, 2008b).

Contrary to the extracellular LRR, the intracellular C-terminal domain of the TLRs (TIR domain) is highly conserved; the intracellular domain conducts the transduction signal to the nucleus (Vandevenne *et al.*, 2010). The X-ray crystallographic structure of intracellular TIR domains of TLR1, TLR2 (Xu Yingwu *et al.*, 2000) and TLR10 (Nyman *et al.*, 2008) have been determined, revealing the TIR domains to have a common fold containing a 5-stranded  $\beta$  sheet surrounded by 5  $\alpha$  helices. Mutational and modeling studies indicate that the BB loop connecting the second  $\beta$  sheet and the second  $\alpha$ -helix plays an important role in TIR dimerization and/or adaptor recruitment. Mutation Pro681His, in the TLR2 BB loop, abolished signal transduction in response to stimulation by yeast and Gram-positive bacteria (Underhill *et al.*, 1999). The Pro681His mutation did not cause noticeable structural changes but disrupted the physical interaction between the TIR domains of TLR2 and MyD88 (Xu Yingwu *et al.*, 2000). Modeling and docking analyses predict that electrostatic complementarity plays the main role in the interaction between TIR domains (Gautam *et al.*, 2006). Interestingly, a recent crystal structure study showed that the BB loop of the TIR domain of TLR10 was involved in the homodimeric interaction with a neighboring TIR domain in the crystal (Nyman *et al.*, 2008). However, it is not certain whether the homodimeric structure seen in the crystal corresponds to a physiologically relevant dimer of the TLR10 TIR domains because the TIR domain of TLR10 exists as a monomer in solution.

Due to a low affinity between isolated TIR domains in solution, the experimental determination of TIR multimer structure was severely hampered (Xu Yingwu *et al.*, 2000). Several modeling studies have been performed to predict the structures of TIR multimers. The DD loop of TLR2 connecting the fourth  $\beta$  sheet and the fourth  $\alpha$ -helix is proposed to be in a position in close contact with the BB loop of TLR1 (Gautam *et al.*, 2006; Jin *et al.*, 2008a).

### **1.3.3 Toll-like receptor signaling**

Currently, two main toll-like receptor signaling pathways have been described: the MyD88-dependent signaling pathway and the TRIF-dependent signaling pathway (Figure 1.11) (Kawai *et al.*, 2010; Vandevenne *et al.*, 2010). The signaling pathways are cell type-specific, thus define different immunological properties. For instance, plasmacytoid dendritic cells (pDC) and inflammatory monocytes have unique signaling pathways that govern antiviral responses that are probably absent in other cell types such as conventional dendritic cells (cDC) and macrophages (Kawai *et al.*, 2006; Barbalat *et al.*, 2009; Kawai *et al.*, 2010).

#### **1.3.3.1 MyD88-dependent signaling pathway**

Upon ligand recognition, TLR-1, -2, -4, -5, -6, -7 and -9 recruit the adaptor protein MyD88 via their respective TIR domains (Figure 1.11) (Vandevenne *et al.*, 2010). Once activated by the receptor recruitment, MyD88 binds the death domain (DD) of the downstream molecule IL-1 Receptor-Associated Kinase 4 (IRAK4) through homotypic interactions, which results in the activation of the other following IRAKs, such as IRAK1 and IRAK2. Phosphorylated IRAKs are released from MyD88 and can activate the downstream TNF receptor-associated factor 6 (TRAF6), an E3 ligase that catalyzes the synthesis of polyubiquitin linked to Lys63 (K63) on target proteins, including TRAF6 itself and IRAK1, in conjunction with the dimeric E2 ubiquitin-conjugating enzymes Ubc13 and Uev1A (Bhoj *et al.*, 2009; Kawai *et al.*, 2010). The K63-linked polyubiquitin chains then bind to the novel zinc finger-type ubiquitin-binding domain of TAB2 and TAB3, the regulatory components of the kinase TAK1 complex, to activate TAK1 (Kawai *et al.*, 2010). The K63-linked polyubiquitin chains also bind to a regulatory component of the IKK complex, NEMO. A complex of TAK1 and IKK forms; this allows TAK1 to phosphorylate IKK $\beta$  through its close proximity to the IKK complex, which leads to NF- $\kappa$ B nuclear translocation and activation via phosphorylation, polyubiquitination and degradation of I $\kappa$ B $\alpha$  (Bhoj *et al.*, 2009; Kawai *et al.*, 2010; Vandevenne *et al.*, 2010). In the MyD88-dependent pathway, TAK1 simultaneously activates the mitogen-activated protein kinases (MAPKs) such as the extracellular signal-regulated kinase (ERK), the c-jun N-terminal kinase (JNK) and p38 by inducing the phosphorylation (rather than ubiquitination) of

MAPK kinases, which then activate various transcription factors including activating protein (AP)-1 that controls pro-inflammatory gene expression (Vandevenne *et al.*, 2010). In the case of the TLR-1, -2, -4 and -6 activation, besides MyD88, another TIR-containing adaptor, the TIR-associated protein (TIRAP) (also known as MyD88-adaptor-like (MAL)), serves as a linker adaptor to recruit MyD88 to the TLRs (Sheedy *et al.*, 2007; Lin *et al.*, 2010; Vandevenne *et al.*, 2010).

The activation of the MyD88-dependent pathway also induces the transcription of some NF- $\kappa$ B modulating molecules as feedback. These molecules include the I $\kappa$ B protein I $\kappa$ B $\zeta$  that functions as an inducible coactivator for the NF- $\kappa$ B p50 subunit to facilitate IL-6 and IL-12p40 production (Yamamoto *et al.*, 2004); C/EBP $\delta$  that can maximize IL-6 production together with NF- $\kappa$ B (Litvak *et al.*, 2009); I $\kappa$ B-NS that through modulating the DNA-binding capability of the NF- $\kappa$ B p65 subunit suppresses the induction of both IL-6 and TNF- $\alpha$  (Kuwata *et al.*, 2006); and ATF3 that by recruiting histone deacetylase restricts NF- $\kappa$ B activity (Gilchrist *et al.*, 2006; Kawai *et al.*, 2010).

### 1.3.3.2 TRIF-dependent signaling pathway

The TIR-domain-containing adaptor inducing IFN- $\beta$  (TRIF) mediated signaling pathway is important in TLR3 and TLR4 signaling (Figure 1.11) (Vandevenne *et al.*, 2010). TRIF recruits TRAF6 and activates TAK1 for NF- $\kappa$ B activation, probably through ubiquitination-dependent mechanisms similar to those of the MyD88-dependent pathway (Kawai *et al.*, 2010). In addition, the TRIF-dependent pathway leads to the activation of the interferon regulatory factor 3 (IRF3). TRIF-dependent activation of NF- $\kappa$ B, AP-1 and IRF3 triggers the formation of an enhanceosome that permits the expression of IFN- $\beta$  (Sheedy *et al.*, 2007; Vandevenne *et al.*, 2010). Upon LPS stimulation, in addition to TIRAP and MyD88, the TLR4 binds to the TRIF-related adaptor molecule (TRAM) which allows the recruitment of the TRIF and leads to the activation of the IRF3 (Sheedy *et al.*, 2007). In response to dsRNA challenge, TLR3 recruits the adaptor TRIF that interacts with a complex composed of the receptor-interacting protein kinase 1 (RIP1), the tumor necrosis factor receptor type 1-associated death domain protein (TRADD) and the FAS-Associated death domain-containing protein (FADD). RIP1 undergoes K63-linked polyubiquitination that permits the activation of TAK1, which in turn activates NF- $\kappa$ B and AP-1 (Chen Nien-Jung *et al.*, 2008; Vandevenne *et al.*, 2010). TRIF was also reported to recruit a large complex that is comprised of TRAF6/TAB2/TAB3/TAK1. As mentioned above, the activated TAK1 induces the activation

of the downstream IKK complex and MAP kinases leading to nuclear translocation of the NF- $\kappa$ B and AP-1 respectively (Kawai *et al.*, 2010; Vandevenne *et al.*, 2010).

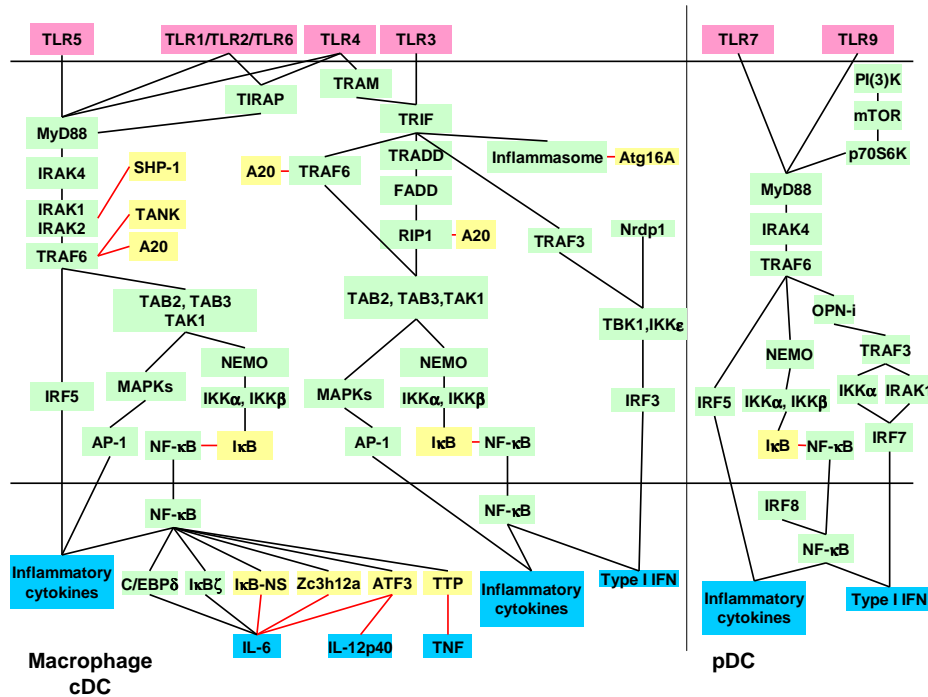


**Figure 1.11. TLR signaling pathways (Kawai *et al.*, 2010; Vandevenne *et al.*, 2010).** TLR-mediated responses are controlled mainly by the MyD88-dependent pathway, which is used by all TLRs except TLR3, and the TRIF-dependent pathway, which is used by TLR3 and TLR4. TRAM and TIRAP are sorting adaptors used by TLR4 and TLR2-TLR4, respectively. In conventional dendritic cell (cDC) and macrophage, MyD88 recruits IRAK4, IRAK1, IRAK2 and TRAF6 and induces inflammatory responses by activating NF- $\kappa$ B, MAPK and IRF5. TRAF6 activates TAK1 in complex with TAB2 and TAB3 and activates the IKK complex consisting of NEMO and IKK $\alpha$ , IKK $\beta$ , which catalyze I $\kappa$ B proteins for phosphorylation. NF- $\kappa$ B induces C/EBP $\delta$ , I $\kappa$ B $\zeta$ , I $\kappa$ B-NS, Zc3h12a, ATF3 and tristetraprolin (TTP), which influence the genes encoding IL-6, IL-12p40 or TNF. TRIF recruits TRAF6, TRADD and TRAF3. TRADD interacts with Pellino-1 and RIP1. RIP1 and TRAF6 cooperatively activate TAK1, which leads to activation of MAPK and NF- $\kappa$ B. TRAF3 activates the kinases TBK1 and IKK $\epsilon$ , which phosphorylate and activate IRF3, the latter of which controls transcription of type I interferon. Nrdp1 is involved in TBK1-IKK $\epsilon$  activation. The TRIF-dependent pathway leads to inflammasome activation during TLR4 signaling. In plasmacytoid dendritic cell (pDC), TLR7 and TLR9 recruit MyD88 along with IRAK4 and TRAF6, which activate IRF5 and NF- $\kappa$ B for inflammatory cytokine induction and IRF7 for type I interferon induction. For IRF7 activation, IRAK1- and IKK $\alpha$ -dependent phosphorylation is required, and TRAF3 is located upstream of these kinases. OPN-i is involved in IRF7 activation, and IRF8 facilitates NF- $\kappa$ B activation. The PI (3) K-mTOR-p70S6K axis enhances the TLR7 and TLR9 signaling pathways. IRF1 is involved in the induction of type I interferon by TLR7 and TLR9 in cDCs rather than pDCs. Among the many negative regulators of TLRs that have been identified, TANK (which suppresses TRAF6), A20 (which suppresses TRAF6 and RIP1), ATG16A (which suppresses inflammasome activation) and SHP-1 (which suppresses IRAK1 and IRAK2) are reported to be indispensable for preventing inflammatory diseases caused by enhanced or prolonged TLR signaling. Pink, TLRs; green, stimulators; yellow, negative regulators; blue, target genes (Kawai *et al.*, 2010; Vandevenne *et al.*, 2010).

### 1.3.4 Toll-like receptor 2: a special TLR

Of all known TLRs, TLR2 is a special member. Unlike other TLRs, which are functionally active as homomers, TLR2 is evolutionary developed to form heteromers with TLR1 or TLR6 to broaden specificity for the diverse ligand repertoire or to induce different immune responses. Comparison of the amino acid sequence reveals that TLR2, TLR1, and TLR6 form

a TLR subfamily, which presumably diverged from one common ancestral gene (Farhat *et al.*, 2008). Among all TLRs, TLR1 and TLR6 have the most sequence identity (66%) of overall amino acid sequence and they are both located in chromosome 4. As described in section 1.3.2 Structure and Figure 1.10., upon ligand binding, unlike other TLRs that typically bind to their ligands on the concave surfaces of horseshoe-like extracellular LRR domain, TLR2, as well as TLR1/TLR6, binds to ligands in the internal pocket and the outside region at the convex region of their horseshoe-like extracellular domain (Brodsky *et al.*, 2007).

## 2 Aim of this work

Microglial activation triggered by extracellularly-deposited A $\beta$  acts as a double-edged sword in the pathogenesis of AD: on one side, it damages neurons by releasing neurotoxic inflammatory mediators, while on the other side it reduces A $\beta$ -induced neuronal injury by internalizing A $\beta$  (Walter Lisa *et al.*, 2009; Fuhrmann *et al.*, 2010; Heneka *et al.*, 2010). Toll-like receptors are associated with A $\beta$ -induced microglial inflammatory activation and A $\beta$  internalization (Fassbender *et al.*, 2004; Tahara *et al.*, 2006; Walter S *et al.*, 2007; Jana *et al.*, 2008; Udan *et al.*, 2008; Reed-Geaghan *et al.*, 2009) but the mechanisms remain unclear. The aim of this study is to investigate the pathogenic role of TLR2 in AD and to identify the detailed molecular mechanisms mediating TLR2-mediated pathology. In detail, this study aims to answer the following questions:

1. How does TLR2 interact with A $\beta$ ?
2. How does TLR2 mediate the cellular responses, upon A $\beta$  challenge, by inflammatory activation and phagocytosis?
3. How does TLR2 transduce signals following A $\beta$  challenge?
4. What are the effects of microglial TLR2 on neuroinflammation, cerebral A $\beta$  load and neuronal function in AD animal model?

The figure 2.1 shows the work flow of the project.

Furthermore, epidemiological studies suggest that diets enriched with omega-3 polyunsaturated fatty acids (PUFAs), *e.g.* docosahexaenoic acid (DHA), reduce risk for AD (Barberger-Gateau *et al.*, 2002). Therefore, as a supplemental study, the effects of omega-3 PUFAs, mainly DHA, on the A $\beta$ -triggered inflammatory and phagocytic responses were investigated. This data will be presented in a separate section (Part II. Omega-3 Fatty Acids Reduce Alzheimer's Amyloid Peptide-induced Proinflammatory Activities in Bone Marrow Derived Macrophages).

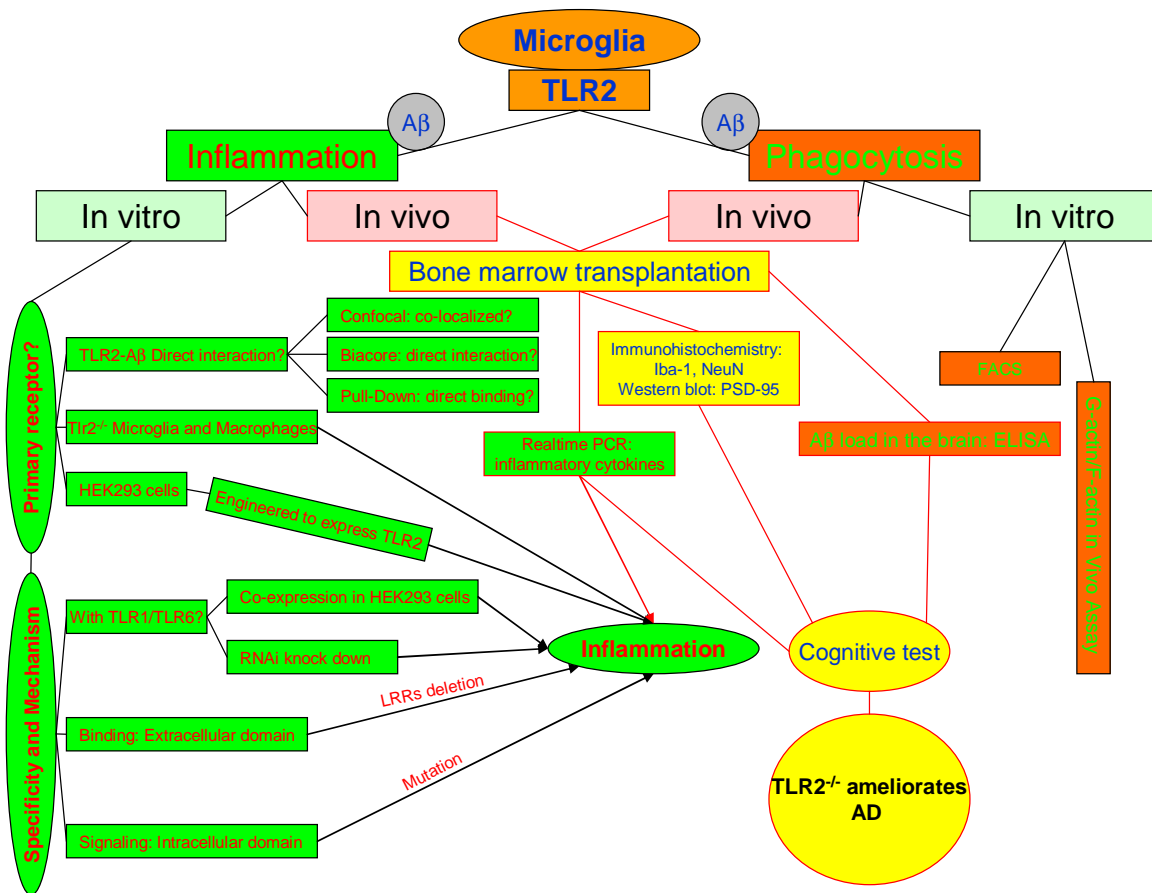


**Figure 2.1. Schematic diagram of the structure of the project (predominantly work Part I).** The pathogenesis role of TLR2 in AD was investigated through *in vivo* and *in vitro* work, from both inflammation and phagocytosis triggered by A $\beta$ . *In vitro*, about inflammation, (1) i. Through testing the response of primary cultured tlr2-deficient microglia to A $\beta$  challenge to tell whether tlr2-deficiency would result in inflammation decrease; ii. Through confocal, Biacore and Pull-Down assays to investigate whether TLR2 colocalizes and directly interacts with A $\beta$ ; iii. Through expressing of TLR2 in endogenously TLR2-deficient HEK-293 cells to investigate whether TLR2 expression can confer A $\beta$ -triggered inflammatory response; these data are to answer whether TLR2 is a primary receptor of A $\beta$  to trigger inflammation. (2) Mechanismly, i. Through over-expressing TLR2/1 and TLR2/6 in HEK-293 cells, and knocking down TLR2, TLR1, and TLR6 via RNA interfering in RAW264.7 cells to determine which one of TLR1 and TLR6 might be co-receptor of TLR2 in mediating A $\beta$ -triggered inflammation; ii. Through testing the responses of domain deleted or motif/point mutated TLRs in HEK-293 cells to identify the critical region/site on TLR2 mediating inflammatory response. About phagocytosis, in a TLR2-deficient/wt cell cultured systems, investigated the effect of TLR2-deficiency on A $\beta$  phagocytosis through FACS and G-actin/F-actin in vivo assay, after co-cultured the cells with A $\beta$ . *In vivo*, through bone marrow transplantation, a tlr2-deficient microglia chimeric AD transgenic mouse model was generated. On these mice, inflammatory cytokine level in the brain was determined via real-time PCR; microglia amount in the brain (hippocampus) was quantified through Iba-1 immunohistochemistry staining, these data tell whether TLR2-deficiency changes the inflammatory pathology in vivo; A $\beta$  load in the brain was determined via ELISA to tell the effect of TLR2-deficiency on the A $\beta$  load in vivo, which reflect the change of phagocytosis. Finally, NeuN immunohistochemistry staining, PSD-95 Western blot and cognitive test were applied to evaluate the outcome of TLR2-deficiency in AD.

## **3 Materials and Methods**

### **3.1 Materials**

#### **3.1.1 Instruments**

Accu-Jet Pipette Controller (BrandTech Scientific, Essex, USA)

Autoclave V-150, V-2540EL (Systec, Wetzlar, Germany)

Axiovert 25 inverted microscope (Carl Zeiss Microscopy, Jena, Germany)

Barnes maze and Ethovision XT, v7.0 system (Noldus Information Technology, Wageningen, The Netherlands)

Biacore® J system (Biacore AB, Uppsala, Sweden)

Biofuge 13 Centrifuge (Heraeus, Hanau, Germany)

Consort E122 Electrophoresis Power supply (Clever Scientific Ltd, Warwickshire, UK)

DNA Engine® Thermal Cycler PTC-200 (Bio-Rad Laboratories, Hercules, USA)

Eclipse TS100 Inverted Microscope (Nikon Instruments Inc., Melville, USA)

Electric Heatable, Forceps for Safer Transfer of Tissue Specimens Leica EG F (Leica Microsystems Nussloch GmbH, Nussloch, Germany)

Eclipse E600 fluorescence microscope (Nikon, Alzenau, Germany)

Epson perfection V700 photo scanner (Epson, Munich, Germany)

FACSCanto™ II Flow Cytometer (BD Biosciences, San Jose, USA)

Fixed-angle rotor for Optima MAX series ultracentrifuge MLA-130, TLA-100.3, TLA-100 (Beckman Coulter, Fullerton, USA)

Forced-air laboratory freezer (Liebherr, Ochsenhausen, Germany)

Forced-air laboratory refrigerator (Liebherr, Ochsenhausen, Germany)

General Rotator, STR4 (Stuart Scientific, Staffordshire, UK)

HERAcell CO<sub>2</sub> incubator (Heraeus, Hanau, Germany)

HERAcell 150i CO<sub>2</sub> Incubator (Thermo Scientific, Langenselbold, Germany)

Heraeus HERAsafe HS 12 biological safety cabinet (Class II) (Heraeus, Hanau, Germany)

Heraeus function line heating and drying ovens (Heraeus, Hanau, Germany)

HERAfreeze -86°C freezer (Heraeus, Hanau, Germany)

Ice machine (Eurfrigor Ice Makers Srl, Lainate, Italy)

Incubation hood TH30 and Universal shaker SM30 (Carl Roth GmbH, Karlsruhe, Germany)

Laboratory balance ALS120-4, EW4200, EW420 (Kern & Sohn, Balingen, Germany)

Laboratory centrifuge SIGMA 4K15C (Sigma Laborzentrifugen GmbH, Osterode am Harz, Germany)

Laboratory pH meter InoLab pH 720 (WTW, Weilheim, Germany)

Leica SM 2000 R Sliding Microtome (Leica Microsystems Nussloch GmbH, Nussloch, Germany)

Leica TP1020 Tissue Processor (Leica Microsystems Nussloch GmbH, Nussloch, Germany)

Leica EG1150C Cold plate (Leica Microsystems Nussloch GmbH, Nussloch, Germany)

Leica EG1150 H Heated Paraffin Embedding Module (Leica Microsystems Nussloch GmbH, Nussloch, Germany)

Leica TCS SP5 Confocal microscope (Leica Microsystems Nussloch GmbH, Nussloch, Germany)

Micro-plate reader (TECAN, Sunrise Remote, Männedorf, Switzerland)

Magnetic stirrer (Ika-Combimag RCO, Namur, Belgium)

Microscope Zeiss Axio Scope (Carl Zeiss, Göttingen, Germany)

Midi agarose chamber, horizontal for gel (Neolab, Heidelberg, Germany)

Mini-PROTEAN® 3 Cell electrophoresis system (Bio-Rad Laboratories, Hercules, USA)

Mini Trans-Blot cell (Bio-Rad Laboratories, Hercules, USA)

MLA-130 Rotor, Fixed Angle, Titanium for Ultracentrifuge (Beckman Coulter, Brea, USA)

Multiband UV table (Peqlab, Karlsruhe, Germany)

Multipette® plus (Eppendorf, Hamburg, Germany)

Nanodrop ND-1000 spectrophotometer (Peqlab, Karlsruhe, Germany)

Nuaire IR AutoFlow NU-2700E Water-Jacketed CO<sub>2</sub> Incubator (Plymouth, MN)

Pipette PIPETMAN P2, P20, P200, P1000 (Gilson, Villiers le Bel, France)

Pipette Single-Channel 2 µl-20 µl, 10 µl-100 µl, 100 µl-1000 µl (Eppendorf, Hamburg, Germany)

Pipette Pipetus (Hirschmann, Eberstadt, Germany)

Platform shaker Duomax 1030 (Heidolph, Schwabach, Germany)

Power supply for electrophoresis system PowerPac 200 (Bio-Rad Laboratories, Hercules, USA)

Precision Balance scale (Sartorius, Goettingen, Germany)

7500 Fast Real-time PCR System (Applied Biosystems, Carlsbad, USA )

Savant DNA 110 SpeedVac System for vacuum centrifuge (Thermo Scientific, Langenselbold, Germany)

Schott KL 750 Illuminator (Schott, Mainz, Germany)

Sigma 4K10 bench top centrifuge (Sigma Laborzentrifugen GmbH, Osterode am Harz, Germany)

SmartSpec™3000 Spectrophotometer (Bio-Rad Laboratories, Hercules, USA)

Stretching Table OTS 40(MEDITE GmbH, Burgdorf, Germany)

Super High pressure Mercury Lamp Power supply (Nikon, Alzenau, Germany)

Thermoblock TDB-120 (BioSan, Riga, Latvia)

Thermomixer Comfort (Eppendorf, Hamburg, Germany)

Ultra-pure water purification system PURELAB Ultra (ELGA, Celle, Germany)

Ultracentrifuge Optima MAX 130,000 rpm (Beckman Coulter, Fullerton, USA)

Ultrasonic bath (Transsonic T780, Elma, Singen, Germany)

Ultrasonic processor UP400S (Hielscher, Teltow, Germany)

UV/visible spectrophotometer Ultrospec3100pro (Amersham Biosciences, Munich, Germany)

Vortex Genie 2 (Scientific Industries, Bohemia, USA)

Vortex-Shaker Reax 2000 (Heidolph, Schwabach, Germany)

Water bath (Köttermann GmbH & Co KG, Hänigsen, Germany)

Wild M3 Stereomikroskop (Wild Heerbrugg, Gais, Switzerland)

XCell SureLock™ Mini-Cell for blotting use Electrophoresis (Invitrogen GmbH, Darmstadt, Germany)

### **3.1.2 Experimental materials**

Amersham Hyperfilm ECL chemiluminescence film (GE Healthcare, Buckinghamshire, UK)

Assistant® 12mmø Microscope cover glasses (Glaswarenfabrik Karl Hecht KG, Sondheim, Germany),

BD Falcon™ FACS tubes (Becton, Dickinson and Company, Heidelberg, Germany)

BD Falcon™ Serological pipet, 5 ml, 10 ml, 25 ml (Becton, Dickinson and Company, Heidelberg, Germany)

BD Plastipak™ syringe, 1 ml (Becton, Dickinson and Company, Heidelberg, Germany)

Biosphere® filter tips 10 µl, 100 µl, 1000 µl (Sarstedt, Nürnberg, Germany)

Bottle Top Filter 500 ml, 0.22 µm (Sarstedt, Nürnberg, Germany)

Cell Scraper 24 cm, sterile (TPP, Trasadingen, Switzerland)

Cell strainer with 70 µm nylon mesh, Sterile (BD Biosciences, San Jose, USA)

Combitips (plus) 5 ml, 10 ml, 12.5 ml (Eppendorf, Hamburg, Germany)

Cover glasses (Assistant, Sondheim, Germany)

Cover slips 10 × 10 mm (Marienfeld, Lauda-Königshofen, Germany)

Cryopure tubes for cell freezing (Sarstedt, Nümbrecht, Germany)  
Falcon round-bottom tubes 14 ml (BD Biosciences, San Jose, USA)  
15 ml, 50 ml, round bottom 50 ml conical centrifuge tubes (Sarstedt, Nümbrecht, Germany)  
Immersion Oil "Immersol" 518 F fluorescence free (Carl Zeiss, Göttingen, Germany)  
Isoflurane (Baxter, Unterschleißheim, Germany)  
Laboratory glassware (Schott, Mainz, Germany)  
Microscope slides 76 × 26 mm (Gerhard Menzel, Braunschweig, Germany)  
Multiwell™ cell culture plate, 6 well, 12 well, 24 well, 48 well, 96 well (Falcon®, Becton Dickinson labware, Franklin Lakes, NJ)  
Needle microlance 21 G, 24 G, 25 G (B.Braun, Melsungen AG)  
96-well microtest plates (Sarstedt, Nümbrecht, Germany)  
NI-NTA Spin Columns (Qiagen, Hilden, Germany)  
Nunc™Black microwell (Thermo Fisher Scientific, Roskilde, Denmark)  
NuPAGE® Novex 4-12% Bis-Tris Gel 1.0 mm, 15 well (Invitrogen, Karlsruhe, Germany)  
Pageruler prestained / unstained protein ladder (Fermentas, St. Leon-Rot, Germany)  
Parafilm M all-purpose laboratory film (Pechiney Plastic Packaging, Chicago, USA)  
Pasteur pipettes plain glass (VWR International, Leicestershire, UK)  
PCR SoftTube, 0.2 ml (Biozym Scientific, Oldendorf, Germany)  
PH-indicator Strips pH 0 - 14 universal indicator (Merck, Darmstadt, Germany)  
Petri Dish Polystyrene 92 × 16 mm with Ventilation Cams (Sarstedt, Nümbrecht, Germany)  
Pipette tip 10 µl, 200 µl, 1000 µl (Sarstedt, Nümbrecht, Germany)  
ProGel-P Tris.Tricine 10-20% gel (Anamed elektrophorese GmbH, Gross-Bieberau, Germany)  
Protran® Nitrocellulose transfer membrane Protran BA83, 0.2 µm (Whatman, Dassel, Germany)  
Safe-Lock micro test tube 2.0 ml (Eppendorf, Hamburg, Germany)  
SafeSeal micro tube 1.5 ml (Sarstedt, Nümbrecht, Germany)  
Sensor chip NTA (Biacore AB, Uppsala, Sweden)  
Sterile insulin syringe 1ml (Becton, Dickinson and Company, Heidelberg, Germany)  
Surgical Blades, sterile (B Braun, Tuttlingen, Germany)  
Syringe filter 0.22 µm Rotilabo (Carl Roth, Karlsruhe, Germany)  
Syringe, 2 ml, 5 ml, 10 ml, 20 ml (B Braun, Tuttlingen, Germany)  
Thickwall Polycarbonate 1ml 11 × 34 mm Tubes for Ultracentrifuge (Beckman Coulter, Brea, CA)  
Tissue culture flask, PE Phenolie style cap, 75 cm<sup>2</sup>, 175 cm<sup>2</sup> (Sarstedt, Nümbrecht, Germany)

Tissue culture dish 100 × 20 mm (Sarstedt, Nürnberg, Germany)

Tissue culture dish 60 × 15 mm (BD Falcon™, BD Biosciences, Durham, USA)

Tube 13 ml for bacteria culture (Sarstedt, Nürnberg, Germany)

UV quartz cuvette 10 mm (Hellma, Müllheim, Germany)

### **3.1.3 Experimental kits and systems**

BD OptEIA™ TMB Substrate Reagent Set (BD Biosciences, San Diego, USA)

BIAMaintenance kit (Biacore AB, Uppsala, Sweden)

DyNAmo™ Flash probe qPCR kit (FINNZYMES, Espoo, Finland)

DyNAmo™ colorflash SYBR® Green qPCR kit (FINNZYMES, Espoo, Finland)

Endo Free Plasmid Maxi Kit (Qiagen, Hilden, Germany)

G-actin/F-actin in Vivo Assay Kit (Cytoskeleton, Inc., Denver, USA)

High pure plasmid isolation kit (Roche, Mannheim, Germany)

Human β Amyloid 1-40 Colorimetric immunoassay kit (Invitrogen, Camarillo, USA)

Human β Amyloid 1-42 Colorimetric immunoassay kit (Invitrogen, Camarillo, USA)

IL-6 DuoSet® ELISA kit (R&D Systems, Minneapolis, USA)

Limulus Amebocyte Lysate (LAL) QCL-1000® kit (CAMBREX Bio Science, Walkersville, USA)

OptEIA Human IL-8 ELISA Set (BD Biosciences, San Diego, USA)

Protein Assay Reagent (Bio-Rad Laboratories, Hercules, USA)

PureLink™ HiPure plasmid maxiprep kit (Invitrogen, Darmstadt, Germany)

QIAprep spin miniprep kit (Qiagen, Hilden, Germany)

QIAquick PCR purification kit (Qiagen, Hilden, Germany)

QIAquick gel extraction kit (Qiagen, Hilden, Germany)

QuantiTect® SYBR® Green PCR Kit (Qiagen, Hilden, Germany)

Rneasy Plus Mini Kit (Qiagen, Hilden, Germany)

RQ1 RNase-Free DNase Kit (Promega, Madison, WI)

SuperScript® II Reverse Transcriptase (Invitrogen, Darmstadt, Germany)

SYBR® Advantage® qPCR Premix (Clontech, Mountain View, USA)

TaKaRa LA Taq™ Hot Start Version (TAKARA BIO INC. Shiga, Japan)

Tetra-His HRP conjugate Kit (Qiagen, Hilden, Germany)

TNF-α/ TNFSF1A DuoSet® ELISA kit (R&D Systems, Minneapolis, MN)

VectaStain Elite ABC kit (Vector Laboratories Inc. Burlingame, USA)

### **3.1.4 Chemicals, reagents and customized services**

**Alexis Biochemicals, Lausen, Switzerland:** Pam3CSK4

**Bachem, Heidelberg, Germany:** FITC-conjugated A $\beta$ 42, A $\beta$ 42-1, Ac-DEVD-AMC

**Biozym Scientific, Oldendorf, Germany:** Biozym LE Agarose

**Carl Roth, Karlsruhe, Germany:** 2-Propanol, Acrylamide/Bisacrylamide Rotiphorese Gel 30, Agar, Agarose, Ammonium chloride, Ampicillin, Antipain, Bis-Tris, Bromophenol blue, Calcium chloride, Chloramphenicol, Coomassie brilliant blue G 250, Coomassie brilliant blue R 250, Di-potassium hydrogen phosphate, Di-sodium hydrogen phosphate, Dithiothreitol (DTT), EDTA, EGTA, Ethanol, Ethidium bromide 1%, Glycerol, Hydrochloric acid, HEPES, Imidazole, Lactose, Magnesium chloride, Methanol, Phosphoric acid, PIPES, Potassium acetate, Potassium chloride, Potassium di-hydrogen phosphate, Potassium hydroxide, Powdered milk, Sodium acetate, Sodium chloride, Sodium di-hydrogen phosphate, Sodium dodecyl sulfate(SDS), Sucrose, Sodium hydroxide, Sodium sulfate, Sulfuric acid, Trichloroacetic acid, Tris, Triton X-100, TWEEN 20

**Fermentas, St. Leon-Rot, Germany:** IPTG, PageRuler™ Prestained Protein Ladder, MassRuler™ Express HR Reverse DNA Ladder, O'GeneRuler™ Express DNA Ladder,

**GE Healthcare, Freiburg, Germany:** Amersham ECL Plus Western blot detection reagents, Surfactant P20 (10% v/v, 0.22  $\mu$ m filtered for biacore use) (Uppsala, Sweden), Glycine 2.0(10 mM Glycine-HCl, pH2.0)

**Hedinger, Stuttgart, Germany:** Aceton, Isopropanol, Xylol

**Invitrogen, Darmstadt, Germany:** Antibiotic-Antimycotic (100X) liquid, Dulbecco's Modified Eagle Medium (DMEM) (High Glucose), Geneticin(G418), Lipofectamine™ LTX Transfection Reagent, Lipofectamine™ 2000 Transfection Reagent, Opti-MEM I Reduced Serum Medium, ProLong® Gold antifade reagent with DAPI, RPMI 1640 Medium, Stealth RNAi™ synthesizing service, 0.05% Trypsin-EDTA, Trizol

**InvivoGen, San Diego, USA:** Pam2CSK4

**Kodak, Rochester, USA:** GBX Developer and Replenisher, GBX Fixer and Replenisher

**Merck, Darmstadt, Germany:** 2-Mercaptoethanol, Ammonium acetate, Ammonium persulfate, Chloroform, Citric acid monohydrate, Entellan® Neu, Magnesium acetate, Magnesium sulfate, Potassium chloride, Sodium carbonate, Sodium cyanoborohydride, Sucrose

**New England Biolabs, Ipswich, USA:** ColorPlus Prestained Protein Marker, Broad Range (7-175 kDa)

**Otto Fishar GmbH, Saarbrueken, Germany:** H<sub>2</sub>O<sub>2</sub> (30%)

**PAN Biotech GmbH, Aidenbach, Germany:** Fetal bovine serum-South America, Ham's F12 Medium (with L-Glutamine, without phenol red, with 25 mM Hepes, with 1.176 g/l NaHCO<sub>3</sub>), Hygromycin B

**Perkin Elmer:** Western lightning™ plus-ECL: Oxidizing reagent plus and Enhanced luminol reagent plus

**Qiagen, Hilden, Germany:** Ni-NTA agarose

**R&D systems, Minneapolis, USA:** Recombinant human IGF-I R, recombinant mouse TLR1, recombinant human TLR2, recombinant human TLR3 ( all 10 × Histidine-tagged at C-terminus)

**Roche, Mannheim, Germany:** dNTP mix (10 mM each), Protease inhibitor cocktail tablets

**Seqlab, Göttingen, Germany:** DNA sequencing service

**Sigma-Aldrich Chemie, Steinheim, Germany:** Albumin from bovine serum (Bovine serum albumin, BSA), bromophenol blue, Dimethyl sulfoxide (DMSO), Ethanol, Formamide, Glutathione, LB Broth, LB Agar, Methyl-β-cyclodextrin, Mowiol, N,N-Dimethylformamide, N,N,N',N'-Tetramethylethylenediamine (TEMED), Kanamycin, Oligonucleotides synthesizing service, 1,1,1,3,3,3-Hexafluoro-2-propanol (Hexafluoroisopropanol, HFIP), Paraformaldehyde (PFA), Phenylmethanesulphonyl fluoride (PMSF), Poly-L-lysine (PLL), Polyethylene glycol 8000 (PEG8000), Sodium citrate, Sodium carbonate, TWEEN 20, 2-Mercaptoethanol, (3-Aminopropyl) triethoxysilane, Triton X-100, HEPES

### 3.1.5 Media

#### 3.1.5.1 Bacterial media and antibiotics

<b>LB-Broth medium</b>	LB Broth	20 g
	Dissolve in 1 l diH <sub>2</sub> O, autoclave.	
<b>LB-Broth-Agar plates</b>	LB Agar	35 g
	Dissolve in 1 l diH <sub>2</sub> O, autoclave. Cool the agar to 50°C. Add 1 ml antibiotic (1:1,000) if applicable and pour into petri dishes. Store at 4°C.	
<b>Ampicillin</b>	Ampicillin	100 mg
100 mg/ml (1,000×)	Dissolve in 1 ml diH <sub>2</sub> O, filter-sterilize. Store at -20°C.	
<b>Kanamycin</b>	Kanamycin	25 mg
25 mg/ml (1,000×)	Dissolve in 1 ml diH <sub>2</sub> O, filter-sterilize. Store at -20°C.	

### 3.1.5.2 Media for cell culture

<b>DMEM</b>	Dulbecco's Modified Eagle	445 ml
	Medium(DMEM)(High Glucose)	
	Fetal bovine serum(56°C water bath, 30 min inactivated)	50 ml
	Antibiotic-antimycotic (100× )	5 ml
	Filter with 0.22 µm bottle Top Filter. Store at 4°C	
<b>RPMI</b>	RPMI 1640 Medium	445 ml
	Fetal bovine serum(56°C water bath, 30 min inactivated)	50 ml
	Antibiotic-antimycotic (100× )	5 ml
	Filter with 0.22 µm bottle Top Filter. Store at 4°C	

### 3.1.6 Enzymes

Klenow enzyme (Roche, Mannheim, Germany)

Restriction enzymes (Fermentas, St. Leon-Rot, Germany; NEB, Frankfurt, Germany and Roche, Mannheim, Germany)

T4 DNA ligase (Roche, Mannheim, Germany)

### 3.1.7 Antibodies

**Table 3.1. Antibodies used in this work**

Antigen	Usage (Dilution)	Species	Type	Source
Alpha Tubulin	1:10,000 for WB	Mouse	Monoclonal	Abcam, Cambridge, UK
Human A $\beta$	1:500 for confocal; 1:2500 for WB	Mouse	Monoclonal WO-2	Millipore, Schwalbach/Ts, Germany
Human beta Amyloid	1:50 for IHC	Mouse	Monoclonal clone 6F/3D	Dako, Hamburg, Germany
Human TLR2	1:1000 for WB	Goat	Polyclonal	R&D systems, Minneapolis, US
Mouse-Iba-1	1:500 FOR IHC	Rabbit	Polyclonal	Wako pure Chemical Industries Ltd, Osaka, Japan
Mouse TLR2	1:500 for confocal	Rabbit	Polyclonal	Abcam, Cambridge, UK
NeuN	1:50 for IHC	Mouse	Monoclonal	Millipore. Temecula, CA
PSD-95	1:2000 for WB	Mouse	Monoclonal	Abcam, Cambridge, UK
Mouse IgG	1:1000	Goat	Peroxidase-conjugated antibody	Sigma-Aldrich Munich, Germany
Rabbit IgG	1:1000	Goat	Peroxidase-conjugated antibody	Sigma-Aldrich Munich, Germany

### 3.1.8 Oligonucleotides

**Table 3.2. Oligonucleotides used for RNAi silence**

Target gene	Stealth RNAi sequences
-------------	------------------------

	Sense	Anti-sense
Mouse Tlr1	GAC AUC CUC UCA UUG UCC AAG CUG A	UCA GCU UGG ACA AUG AGA GGA UGU C
Mouse Tlr2	CCG CUC CAG GUC UUU CAC CUC UAU U	AAU AGA GGU GAA AGA CCU GGA GCG G
Mouse Tlr6	CCA AUA CCA CCG UUC UCC AUU UGG U	ACC AAA UGG AGA ACG GUG GUA UUG G
RNAi control	CCG GAC CUC UGA CUU CUC CUU CAU U	AAU GAA GGA GAA GUC AGA GGU CCG G

**Table 3.3. Primers for human TLRs / mouse CD44 and mutants expression constructs in pIRES vector**

Constr uct name	Forward primer for 5' segment amplification	Reverse primer for 5' segment amplification	Forward primer for 3' segment amplification	Reverse primer for 3' segment amplification
TLR1	CTAGCTAGCTAGCC ACCATGACTAGCAT CTTCCATTT			CCCGACGCGTCGGCTA TTTCTTTGCTTGCTCTG TCAGCTT
TLR2	CTAGTCTAGACTAG GCCACCATGCCACA TACTTTGTGGATG			ATAGTTTAGCGGCCGC ATTCTTATCTAGGACTT TATCGCAGCTCTCAG
TLR6	CTAGCTAGCTAGCC ACCATGACCAAAG ACAAAGAACC			CCCGACGCGTCGGTTA AGATTTACATCATTG TTTTCAG
mCD44	CTAGTCTAGACTAG GCCACCATGGACAA GTTTTGTGGCA			ATAGTTTAGCGGCCGC ATTCTTATCTACACCCC AATCTTCATGTCCAC
TLR2L RR3- 4de	CTAGTCTAGACTAG GCCACCATGCCACA TACTTTGTGGATG	ATTTGTGAGATG AGAAAAAGAAT CTTCTCTAT	GATTCTTTTTCTC ATCTCACAAAAT TGCAAATCC	ATAGTTTAGCGGCCGC ATTCTTATCTAGGACTT TATCGCAGCTCTCAG
TLR1L RR3- 4de	CTAGCTAGCTAGCC ACCATGACTAGCAT CTTCCATTT	TTGAGACATATT TTTGAAAACACT GATATC	AGTGTTCCTCAA AATATGTCTCAA CTAAAAT	CCCGACGCGTCGGCTA TTTCTTTGCTTGCTCTG TCAGCTT
TLR6L RR3- 4de	CTAGCTAGCTAGCC ACCATGACCAAAG ACAAAGAACC	TTGTGATAAGTT CTTGAAAACACT TAAATCA	AGTGTTCCTCAAG AACTTATCACAA CTGAATT	CCCGACGCGTCGGTTA AGATTTACATCATTG TTTTCAG
TLR2L RR7- 9de	CTAGTCTAGACTAG GCCACCATGCCACA TACTTTGTGGATG	TCCAGAAATCTG CTTCAAACTTTT TGGCTCAT	AAAAGTTTGAAG CAGATTTCTGGA TTGTTAG	ATAGTTTAGCGGCCGC ATTCTTATCTAGGACTT TATCGCAGCTCTCAG
TLR1L RR7- 9de	CTAGCTAGCTAGCC ACCATGACTAGCAT CTTCCATTT	AGTTGTATGCCA AAGGCCCTCAG GGTCTTCT	CCTGAGGGCCTT TGGCATACAACT GTATGGT	CCCGACGCGTCGGCTA TTTCTTTGCTTGCTCTG TCAGCTT
TLR6L RR7- 9de	CTAGCTAGCTAGCC ACCATGACCAAAG ACAAAGAACC	AGGTTTGGGCCA TAGACTTTCTGT CTCATTT	ACAGAAAGTCTA TGGCCCAAACCT GTGGAAT	CCCGACGCGTCGGTTA AGATTTACATCATTG TTTTCAG
TLR2L RR10- 11de	CTAGTCTAGACTAG GCCACCATGCCACA TACTTTGTGGATG	TCTTTCTGTAAG ATTCAAAAGTTT CATAACCT	AAACTTTTGAAT CTTACAGAAAGA GTAAAA	ATAGTTTAGCGGCCGC ATTCTTATCTAGGACTT TATCGCAGCTCTCAG
TLR1L RR10- 11de	CTAGCTAGCTAGCC ACCATGACTAGCAT CTTCCATTT	GTTTCATATTCGA AACCAGCTGGA GGATCCTA	CTCCAGCTGGTT TCGAATATGAAC ATCAAAA	CCCGACGCGTCGGCTA TTTCTTTGCTTGCTCTG TCAGCTT
TLR6L RR10- 11de	CTAGCTAGCTAGCC ACCATGACCAAAG ACAAAGAACC	GTTTCATCTCAGA AAGAAATTGAA AGACTCTG	TTCAATTTCTTTC TGAGATGAACAT TATGAT	CCCGACGCGTCGGTTA AGATTTACATCATTG TTTTCAG
TLR2L RR12- 14de	CTAGTCTAGACTAG GCCACCATGCCACA TACTTTGTGGATG	GTTTTTCAGAGT TGAATATAAAGT GCTCAGA	ACTTTATATTCA ACTCTGAAAAAC TTGACTA	ATAGTTTAGCGGCCGC ATTCTTATCTAGGACTT TATCGCAGCTCTCAG
TLR1L RR12- 14de	CTAGCTAGCTAGCC ACCATGACTAGCAT	AGACTTCATCTG AAAGATTCATA	TATGAAATCTTT CAGATGAAGTCT	CCCGACGCGTCGGCTA TTTCTTTGCTTGCTCTG

14de	CTTCCATTT	GATATAAC	CTGCAAC	TCAGCTT
TLR6L RR12- 14de	CTAGCTAGCTAGCC ACCATGACCAAAG ACAAAGAACC	AGAAGGCATAT CAAACACGGTGT ACAAAGCT	TACACCGTGTTT GATATGCCTTCT TTGAAA	CCCGACGCGTCGGTTA AGATTTACATCATTG TTTTCAG
TLR2L RRCTd e	CTAGTCTAGACTAG GCCACCATGCCACA TACTTTGTGGATG	AGACACCAGTG CAATGAAGTTAT TGCCACCAG	AATAACTTCATT GCACTGGTGTCT GGCATGTG	ATAGTTTAGCGGCCGC ATTCTTATCTAGGACTT TATCGCAGCTCTCAG
TLR1L RRCTd e	CTAGCTAGCTAGCC ACCATGACTAGCAT CTTCCATTT	GACGATCAGCA GTTGGAATGGAT TGTCCTCTG	AATCCATTCCAA CTGCTGATCGTC ACCATCG	CCCGACGCGTCGGCTA TTTCTTTGCTTGCTCTG TCAGCTT
TLR6L RRCTd e	CTAGCTAGCTAGCC ACCATGACCAAAG ACAAAGAACC	GACGATCAGCA GTTGGAATGGAT TGTCCTCT	AATCCATTCCAA CTGCTGATCGTC ACCATCG	CCCGACGCGTCGGTTA AGATTTACATCATTG TTTTCAG
TLR1Y 737N	CTAGCTAGCTAGCC ACCATGACTAGCAT CTTCCATTT	CTAGGAATGGA GTTCTGCGGAAT GG	CCATTCCGCAGA ACTCCATTCTA G	CCCGACGCGTCGGCTA TTTCTTTGCTTGCTCTG TCAGCTT
TLR1S S741N K	CTAGCTAGCTAGCC ACCATGACTAGCAT CTTCCATTT	TGAGCTTGTGAT ACTTGTTAGGAA TGGAGT	TACTCCATTCT AACAAGTATCAC AAGCTCA	CCCGACGCGTCGGCTA TTTCTTTGCTTGCTCTG TCAGCTT
TLR6N 742Y	CTAGCTAGCTAGCC ACCATGACCAAAG ACAAAGAACC	GGAATGCTGTAC TGTGGAATGGGT TCC	CCCATTCCACAG TACAGCATTCCC AAC	CCCGACGCGTCGGTTA AGATTTACATCATTG TTTTCAG
TLR2E KKA74 4PQNS	CTAGTCTAGACTAG GCCACCATGCCACA TACTTTGTGGATG	CTGGGGAATGG AATTTTGCAGAA TGGGCTCC	GAGCCCATTCCG CAAAATTCCATT CCCAGC	ATAGTTTAGCGGCCGC ATTCTTATCTAGGACTT TATCGCAGCTCTCAG
TLR2P 631A	CTAGTCTAGACTAG GCCACCATGCCACA TACTTTGTGGATG	GGAGCTTTCCTG GCCTTCCTTTGG C	GCCAAAGGAAG GCCAGGAAAGCT CC	ATAGTTTAGCGGCCGC ATTCTTATCTAGGACTT TATCGCAGCTCTCAG
TLR2S 636QY 641F	CTAGTCTAGACTAG GCCACCATGCCACA TACTTTGTGGATG	TGCATCAAAGCA GATGTCTCTCTG GGGAGCTTTC	GGAAGCTCCCC AGAGGAACATCT GCTTTGATGCA	ATAGTTTAGCGGCCGC ATTCTTATCTAGGACTT TATCGCAGCTCTCAG
TLR6Y 663N	CTAGCTAGCTAGCC ACCATGACCAAAG ACAAAGAACC	CTTTTTCTAGGT TAGGTACCAATT CAC	GAATTGGTACCT AACCTAGAAAA AGAAG	CCCGACGCGTCGGTTA AGATTTACATCATTG TTTTCAG
TLR2S 692C	CTAGTCTAGACTAG GCCACCATGCCACA TACTTTGTGGATG	GGCTCTTTTCAA TGCAGTCAATGA TATTG	CAATATCATTGA CTGCATTGAAAA GAGCC	ATAGTTTAGCGGCCGC ATTCTTATCTAGGACTT TATCGCAGCTCTCAG
TLR2E 741P	CTAGTCTAGACTAG GCCACCATGCCACA TACTTTGTGGATG	AATGGCTTTTTT CGGAATGGGCTC CAG	CTGGAGCCCATT CCGAAAAAAGC CATT	ATAGTTTAGCGGCCGC ATTCTTATCTAGGACTT TATCGCAGCTCTCAG
TLR2K 742Q	CTAGTCTAGACTAG GCCACCATGCCACA TACTTTGTGGATG	GGGAATGGCTTT TTGCTCAATGGG CTC	GAGCCCATTGAG CAAAAAGCCATT CCC	ATAGTTTAGCGGCCGC ATTCTTATCTAGGACTT TATCGCAGCTCTCAG
TLR2K 743N	CTAGTCTAGACTAG GCCACCATGCCACA TACTTTGTGGATG	CTGGGGAATGG CATTTTTCTCAA TG	CATTGAGAAAAA TGCCATTCCCCA G	ATAGTTTAGCGGCCGC ATTCTTATCTAGGACTT TATCGCAGCTCTCAG
TLR2A 744S	CTAGTCTAGACTAG GCCACCATGCCACA TACTTTGTGGATG	GCGCTGGGGAA TGGATTTTTTCT CAAT	ATTGAGAAAAA ATCCATTCCCCA GCGC	ATAGTTTAGCGGCCGC ATTCTTATCTAGGACTT TATCGCAGCTCTCAG

**Table 3.4. Primers for plasmid constructs sequencing**

Primer name	Detect target	Primer sequence 5' to 3'
IRESMCSAforseq	pIRES MCSA insert 5'	AGGTGTCCACTCCCAGTTCA
IRESMCSArevseq	pIRES MCSA insert 3'	GGGGGAGAGGGGCGGAATTGG
IRESMCSBforseq	pIRES MCSB insert 5'	CCGAACCACGGGGACGTGGT
IRESMCSBrevseq	pIRES MCSB insert 3'	AGCATTAACCTCACTAAAGGGAA

**Table 3.5. Primers for Realtime PCR detection (SYBR green method)**

Detector	Primer forward	Primer reverse
mbetaActin	GCAAGCAGGAGTACGATGAG	TAACAGTCCGCTAGAAGCA
mTNF-alpha	ATGAGAAGTTCCCAAATGGC	CTCCACTTGGTGGTTTGCTA
mIL-1beta	GAAGAAGAGCCCATCCTCTG	TCATCTCGGAGCCTGTAGTG
mIL-6	AGTCCGGAGAGGAGACTTCA	ATTTCCACGATTTCCAGAG
mIL-10	AGGGGCTGTCATCGATTTCTC	TGCTCCACTGCCTTGCTCTTA
mPtges1	GAGTTTTACGTTCCGGTGT	GGTAGGCTGTCAGCTCAAGG
mIFN- $\gamma$	AGCTCTTCCTCATGGCTGTT	TTTGCCAGTTCCTCCAGATA
mMCP-1	GAAGGAATGGGTCCAGACAT	ACGGGTCAACTTCACATTCA
mTLR1	CAACAGTCAGCCTCAAGCAT	AACTTTGTACCCGAGAACCG
mTLR2	GTCAGCTCACCGATGAAGAA	GAGCCCATTGAGGGTACAGT
mTLR6	GAGCCTGAGGCATCTAGACC	AGATGCAAGTGAGCAACTGG

Table 3.6. Primers for mutant confirmation via RT-PCR product sequencing

Primer name	Detect target	Primer sequence 5' to 3'
hTLR2mutseqconfPCRfor	Human tlr2	ACT TCA TTC CTG GCA AGT GG
hTLR2mutseqconfPCRrev		CGC AGC TCT CAG ATT TAC CC
hTLR1mut737seqconfor	Human tlr1	GTT CCT GGC AAG AGC ATT GT
hTLR1mut737seqconrev		TGC CCT TAA GTT AGC CCA AA

### 3.1.9 Organisms

#### 3.1.9.1 Escherichia coli strains

Table 3.7. E. coli strains used in this work

	Strain	Genotype	Source
Fusion-Blue™	<i>E. Coli</i> K-12	<i>endA1</i> , <i>hsdR17</i> ( $r_{K12^-}$ , $m_{K12^+}$ ), <i>supE44</i> , <i>thi-1</i> , <i>recA1</i> , <i>gyrA96</i> , <i>relA1</i> , <i>lac F'</i> [ <i>proA</i> <sup>+</sup> <i>B</i> <sup>+</sup> , <i>lacI</i> <sup>q</sup> <i>ZAM15::Tn10</i> ( <i>tet</i> <sup>R</sup> )]	Clontech, Mountain View, CA

#### 3.1.9.2 Cell lines

Table 3.8. Cell lines used in this study

Designations	Growth Properties	Organism	Cell Type	Source
HEK-293	Adherent	Human	Primary embryonal kidney fibroblastoid cells	DSMZ
L-929	Adherent	Mus musculus (mouse)	Subcutaneous connective tissue, areolar and adipose	ATCC
RAW 264.7	Adherent	Mus musculus (mouse)	Macrophage; Abelson murine leukemia virus transformed	ATCC
THP-1	Suspension	Human	Human acute monocytic leukemia	DSMZ

Note:

ATCC: American Type Culture Collection (ATCC), Manassas, USA;

DSMZ: Deutsche Sammlung von Mikroorganismen und Zellkulturen GmbH, Braunschweig, Germany

Culture: HEK-293, L-929, and RAW264.7 cells were cultured in DMEM medium supplemented with 10% fetal bovine serum (FBS) and 1 × Antibiotic-Antimycotic (Invitrogen); THP-1 cells were cultured in RPMI1640 medium supplemented with 10% FBS and 1 × Antibiotic-Antimycotic

### 3.1.9.3 Plasmids

Table 3.9. Vector plasmids used in this work

Plasmid	Marker	Resistance	Source
pCEP4	<i>AMP<sup>r</sup></i>	Hygromycin-B	Invitrogen, Carlsbad, USA
pcDNA3	<i>AMP<sup>r</sup></i>	Neomycin	Invitrogen, Carlsbad, USA
pIRES	<i>AMP<sup>r</sup></i>	Neomycin	Clontech, Palo Alto, USA

**Table 3.10. Plasmids used in this study**

Plasmid	Vect or	Insert and restriction enzyme sites		Source
		MCSA	MCSB	
pcDNA3-TLR1-YFP	pcDNA3	KpnI/hTLR1-YFP/XbaI		Addgene, Cambridge, USA
pcDNA3-TLR6-YFP	pcDNA3	BamHI/hTLR6-YFP/XbaI		Addgene, Cambridge, USA
pcDNA3-TLR2-CFP	pcDNA3	BamHI/hTLR2-CFP/XbaI		Addgene, Cambridge, USA
pCEP4-TLR2	pCEP4	KpnI/hTLR2/NotI		This work
pCEP4-mCD44	pCEP4	KpnI/mCD44/NotI		This work
pIRES-TLR1	pIRES	NheI/hTLR1/MluI		This work
pIRES-TLR2	pIRES		XbaI/hTLR2/NotI	This work
pIRES-TLR6	pIRES	NheI/hTLR6/MluI		This work
pIRES-TLR1-TLR2	pIRES	NheI/hTLR1/MluI	XbaI/hTLR2/NotI	This work
pIRES-TLR6-TLR2	pIRES	NheI/hTLR6/MluI	XbaI/hTLR2/NotI	This work
pIRES-TLR2LRR3-4de	pIRES		XbaI/hTLR2LRR3-4de/NotI	This work
pIRES-TLR1LRR3-4de	pIRES	NheI/hTLR1LRR3-4de/MluI	XbaI/hTLR2/NotI	This work
pIRES-TLR6LRR3-4de	pIRES	NheI/hTLR6LRR3-4de/MluI	XbaI/hTLR2/NotI	This work
pIRES-TLR2LRR7-9de	pIRES		XbaI/hTLR2LRR7-9de/NotI	This work
pIRES-TLR1LRR7-9de	pIRES	NheI/hTLR1LRR7-9de/MluI	XbaI/hTLR2/NotI	This work
pIRES-TLR6LRR7-9de	pIRES	NheI/hTLR6LRR7-9de/MluI	XbaI/hTLR2/NotI	This work
pIRES-TLR2LRR10-11de	pIRES		XbaI/hTLR2LRR10-11de/NotI	This work
pIRES-TLR1LRR10-11de	pIRES	NheI/hTLR1LRR10-11de/MluI	XbaI/hTLR2/NotI	This work
pIRES-TLR6LRR10-11de	pIRES	NheI/hTLR6LRR10-11de/MluI	XbaI/hTLR2/NotI	This work
pIRES-TLR2LRR12-14de	pIRES		XbaI/hTLR2LRR12-14de/NotI	This work
pIRES-TLR1LRR12-14de	pIRES	NheI/hTLR1LRR12-14de/MluI	XbaI/hTLR2/NotI	This work
pIRES-TLR6LRR12-14de	pIRES	NheI/hTLR6LRR12-14de/MluI	XbaI/hTLR2/NotI	This work

pIRES-TLR2LRRCTde	pIRES		XbaI/hTLR2LRRCTde/NotI	This work
pIRES-TLR1LRRCTde	pIRES	NheI/hTLR1LRRCTde/MluI	XbaI/hTLR2/NotI	This work
pIRES-TLR6LRRCTde	pIRES	NheI/hTLR6LRRCTde/MluI	XbaI/hTLR2/NotI	This work
pIRES-TLR1Y737N	pIRES	NheI/hTLR1Y737N/MluI	XbaI/hTLR2/NotI	This work
pIRES-TLR1SS741NK	pIRES	NheI/hTLR1SS741NK/MluI	XbaI/hTLR2/NotI	This work
pIRES-TLR6N742Y	pIRES	NheI/hTLR6N742Y/MluI	XbaI/hTLR2/NotI	This work
pIRES-TLR2EKKA744PQNS	pIRES		XbaI/hTLR2EKKA744PQNS/NotI	This work
pIRES-TLR2EKKA744PQNS-TLR1	pIRES	NheI/hTLR1/MluI	XbaI/hTLR2EKKA744PQNS/NotI	This work
pIRES-TLR2EKKA744PQNS-TLR1Y737N	pIRES	NheI/hTLR1Y737N/MluI	XbaI/hTLR2EKKA744PQNS/NotI	This work
pIRES-TLR2P631A	pIRES		XbaI/hTLR2P631A/NotI	This work
pIRES-TLR2S636QY641F	pIRES		XbaI/hTLR2S636QY641F/NotI	This work
pIRES-TLR6Y663N	pIRES	NheI/hTLR6Y663N/MluI	XbaI/hTLR2/NotI	This work
pIRES-TLR2S692C	pIRES		XbaI/hTLR2S692C/NotI	This work
pIRES-TLR2E741P	pIRES		XbaI/hTLR2E741P/NotI	This work; Made by Lisa Wolf under my supervision
pIRES-TLR2K742Q	pIRES		XbaI/hTLR2K742Q/NotI	This work; Made by Lisa Wolf under my supervision
pIRES-TLR2K743N	pIRES		XbaI/hTLR2K743N/NotI	This work; Made by Lisa Wolf under my supervision
pIRES-TLR2A744S	pIRES		XbaI/hTLR2A744S/NotI	This work; Made by Lisa Wolf under my supervision

### 3.1.10 Mice

APP<sup>swe</sup>/PS1<sup>dE9</sup> mice: Originally generated by D. Borchelt (Johns Hopkins University) (Jankowsky *et al.*, 2001) were bred on C57BL6/J background and genotyped by A. Kiliaan (Radboud University Nijmegen Medical Center). APP<sup>swe</sup>/PS1<sup>dE9</sup> Double transgenic mice express a chimeric mutant mouse/human amyloid precursor protein (Mo/HuAPP695<sup>swe</sup>:

KM594/5NL) and a mutant human presenilin 1 (PS1-dE9: deletion of exon 9) under the control of the mouse prion protein (PrP) promoter, which make the expression of transgene predominantly to CNS neurons (Jankowsky *et al.*, 2001). Both mutations are associated with early-onset Alzheimer's disease. The "humanized" Mo/HuAPP695swe transgene allows the mice to secrete human A $\beta$  peptide (Garcia-Alloza *et al.*, 2006). The transgenic mice start to develop  $\beta$ -amyloid plaques at 4 months of age and by 6 months plaques will be easily detectable (Garcia-Alloza *et al.*, 2006).

TLR2 knockout (TLR2<sup>-/-</sup>) mice in a C57BL6/N background were kindly provided by S. Akira (Osaka University, Osaka, Japan).

Wild-type C57BL6/N mice were purchased from Charles River (Sulzfeld, Germany).

All mice were locally housed in the animal facilities managed by Prof. Dr. M. Freichel and Prof. Dr. M. Menger.

All animal experiments were approved by the ethical committee of the regional council in Saarland, Germany (Versuch Nr. 27/2007).

## 3.2 Methods

### 3.2.1 Primary cell culture

Bone marrow (BM) cells were isolated from 8-week-old TLR2<sup>-/-</sup>, C57BL/6 mice as described previously (Hao *et al.*, 2011). Briefly, Cells were derived from the marrow of medullar cavities of the tibia and femur of the hind limbs. Erythrocytes were removed by lysis with hypotonic erythrocyte lysing solution (EL buffer: 0.156 M ammonium chloride, 0.01 M potassium hydrogen carbonate and 0.1 mM EDTA). For BM transplantation, cells were washed twice with ice-cold phosphate buffered saline (PBS) and suspended in PBS. For BM-derived macrophage (BMDM) culture, cells were cultured in DMEM medium supplemented with 10% FBS, 1  $\times$  Antibiotic-Antimycotic (Invitrogen) and 20% L929 cell-conditioned medium in 75cm<sup>2</sup> flasks. Non-adherent cells were collected 24 hrs later and re-seeded in a new flask. Medium was changed every 3 days until macrophages were used for experiments after 14 days.

Primary microglial cells were isolated from brains of neonatal mice as previously described (Liu Y *et al.*, 2005). Briefly, the meninges from the forebrains of newborn mice were mechanically removed. The cells were seeded into 100 ng/ml poly-lysine-coated flasks and cultured in DMEM medium supplemented with 10% FBS and 1  $\times$  Antibiotic-Antimycotic under a humidified atmosphere of 10% CO<sub>2</sub> at 37°C for at least 14 days (Ishii K,

2000). Microglial cells were then collected from the microglia-astrocyte co-cultures by shaking with a rotary shaker (220 rpm, 2 hrs).

### 3.2.2 Preparation of A $\beta$ peptides and quality control

Human A $\beta$ 42 synthesized and provided by B. Penke (Albert Szent Gyorgyi Medical University, Hungary) (Zarándi *et al.*, 2007). The aggregation of A $\beta$  was sterile prepared according to published protocol (Dahlgren *et al.*, 2002):

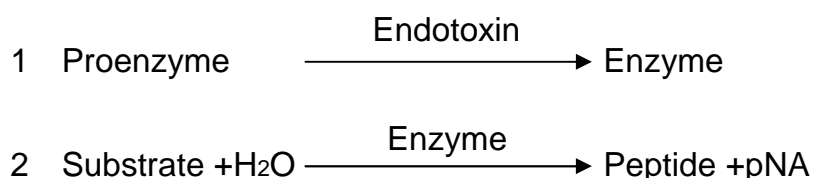
1. Deaggregate by pipetting 1 mg lyophilized A $\beta$ 1-42 in 0.5 ml 1,1,1,3,3,3-Hexafluoro-2-propanol (HFIP, Fluka) until complete dissolved;
2. Lyophilize the dissolved A $\beta$ 1-42 by vacuum centrifugation (by Savant DNA 110 SpeedVac System, Thermo Fisher Scientific), RT, 2.5 hrs;
3. Completely dissolve the lyophilized A $\beta$ 1-42 into 40 $\mu$ l DMSO. Then dilute to a stock concentration of 100  $\mu$ M in Ham's F12 Medium (with L-Glutamine, without phenol red, with 25 mM Hepes, with 1.176 g/l NaHCO<sub>3</sub>) (PAN Biotech GmbH), incubate at 37 °C, 72 hrs.

All A $\beta$  used in this study, for all the assays including cell stimulation, Biacore, Pull-down assay, G-actin/ F-actin assay and confocal assay, if not specifically noted, was aggregated A $\beta$ 42 prepared as described here. In some circumstances the term A $\beta$ 1-42 was used to differentiate the A $\beta$ 42 from A $\beta$ 42-1 control peptide.

The fluorescent A $\beta$  used for FACS analysis of phagocytosis was prepared by mixing FITC-conjugated A $\beta$ 42 (Bachem, Heidelberg, Germany) and unlabeled A $\beta$  at the ratio of 1:4, and incubated the same as with the unlabeled A $\beta$ 42 described above.

The A $\beta$ 42-1(Bachem, Heidelberg, Germany), which has the same amino acids components but a reverse sequence as A $\beta$ 1-42, was treated in a way the same as for A $\beta$ 1-42 and used as A $\beta$ 42 control peptide.

To exclude the possibility of endotoxin contamination in the A $\beta$ , Limulus Amebocyte Lysate (LAL) assay was run with the LAL QCL-1000® kit (CAMBREX Bio Science Walkersville), which is a quantitative test for gram-negative bacterial endotoxin. In LAL test, the test sample is mixed with the LAL (contains proenzyme) and incubated at 37°C for 10 min. A substrate (Ac-Ile-Glu-Ala-Arg-pNA) (pNA: p-nitroaniline) solution is then mixed with the LAL-sample and incubated at 37°C for an additonal 6 min. During this time the activated enzyme catalyzes the splitting of pNA from the colorless substrate. The reaction is stopped with stop reagent:



If endotoxin is present in the sample, the released pNA produces yellow color. The absorbance of the sample can be determined spectrophotometrically at 405-410 nm. The endotoxin concentration can be calculated from a standard curve.

In the case of this study, results show that the A $\beta$ 42 here used contains no detectable endotoxin:

Standard con (EU/ml)	1	0.5	0.25	0.125	0.0625
Standard delta O.D.405	0.169	0.083	0.049	0.044	0.039
A $\beta$ sample delta O.D.405: lot#1:0.034, lot#2: 0.036, both lower than detection limit					

The FITC-conjugated A $\beta$ 42 fluorescent A $\beta$  mixture used for FACS and ordinary A $\beta$  used for other experiments were characterized by Western blot to have a similar oligomeric profile (Figure 3.1):

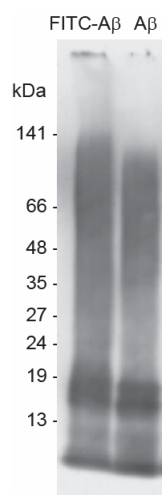


**Figure 3.1. The oligomeric profile of A $\beta$ 42 and FITC-labeled A $\beta$ 42.** The FITC-conjugated A $\beta$ 42 fluorescent A $\beta$  mixture used for FACS and ordinary A $\beta$ 42 used for other experiment were characterized by Western blot to have a similar oligomeric profile.

### 3.2.3 A $\beta$ 42 challenge and sample collection

Microglia, BMDM, RAW264.7 and HEK-293 cells plated in 48-well plates (BD, Heidelberg, Germany) at  $2 \times 10^5$ /well (HEK-293 at  $1 \times 10^5$ /well) were treated with aggregated A $\beta$ 42 at 5  $\mu$ M and 10  $\mu$ M in 200  $\mu$ l DMEM + 10% FBS medium for 24 hrs. For microglia, 10 ng/ml Pam3CSK4 (ALEXIS Biochemicals, Loerrach, Germany) was used as a positive control. For BMDM and HEK-293 cells, a concentration of 100 ng/ml of Pam3CSK4 was used. In some experiments on HEK-293 cells, 100 ng/ml Pam2CSK4 (InvivoGen) was used. The supernatants were collected, stored at -20°C for detection of TNF- $\alpha$ , IL-1 $\beta$  and IL-8 level.

### **3.2.4 TNF- $\alpha$ , IL-1 $\beta$ and IL-8 level detection with ELISA kits**

The TNF- $\alpha$ , IL-1 $\beta$  and IL-8 level in the cell supernatants was determined with commercial ELISA kits (obtained from R&D Systems, Wiesbaden, Germany and from eBioscience, San Diego, USA), according to the manufacturer's protocols. Basic steps are:

1. One day before measurement, dilute the Capture Antibody to the working concentration in PBS without carrier protein. Immediately coat a 96-well microplate with 100  $\mu$ l per well of the diluted Capture Antibody. Seal the plate and incubate overnight at room temperature.
2. Aspirate each well and wash with Wash Buffer (0.05% Tween 20 in PBS), repeating the process two times for a total of three washes. Wash by filling each well with 400  $\mu$ l Wash Buffer. Complete removal of liquid at each wash. After the last wash, remove any remaining Wash Buffer by inverting the plate and blotting it against clean paper towels.
3. Block plates by adding 300  $\mu$ l of Reagent Diluent to each well. Incubate at room temperature for a minimum of 1 hour.
4. Repeat the aspiration /wash as in step 2.
5. Add 100  $\mu$ l of sample or standard in Reagent Diluent, or an appropriate diluent, per well. Cover with an adhesive strip and incubate 2 hrs at room temperature.
6. Repeat the aspiration /wash 3 times as in step 2.
7. Add 100  $\mu$ l of the Detection Antibody, diluted in Reagent Diluent, to each well. Cover with a new adhesive strip and incubate 2 hrs at room temperature.
8. Repeat the aspiration /wash 8 times as in step 2.
9. Add 100  $\mu$ l of the working dilution of Streptavidin-HRP to each well. Cover the plate and incubate for 20 min at room temperature, avoid from direct light.
10. Repeat the aspiration /wash 8 times as in step 2.
11. Add 100  $\mu$ l of Substrate Solution to each well. Incubate for 20 min at room temperature, avoid the plate from direct light.
12. Add 50  $\mu$ l of Stop Solution to each well. Gently tap the plate to ensure thorough mixing.
13. Determine the optical density of each well immediately using a microplate reader; set to 450 nm and wavelength correction to 570 nm. Subtract readings at 570 nm from the readings at 450 nm.

14. Make standard curve according to standard reads and calculate the sample value according to standard equation.

### 3.2.5 Confocal microscopy analysis of TLR2-A $\beta$ 42 co-localization

Unlike conventional microscopy, laser scanning confocal microscopy acquires signals point by point from the whole specimen by an arrangement of diaphragms which, at optically conjugated points of the path of rays, act as a point light source and as a point detector respectively, all structures out of focus are suppressed at image formation by the detection pinhole. The emitted/reflected light passing through the detector pinhole is transformed into electrical signals by a photomultiplier and displayed on a computer monitor screen. Images are reconstructed by computational software. Thus, visualization deep within living and fixed cells and tissues and three-dimensional images can be created. For cell biological use, the high resolution of confocal microscopy is able to differ unrelated molecules.

In this study, to localize A $\beta$  and TLR2 in cells,  $5 \times 10^4$  primary microglia plated on 12 mm $\emptyset$  Assistant<sup>®</sup> microscope cover glasses ( Glaswarenfabrik) in a 24-well cell culture plate (Falcon) were treated with 5  $\mu$ M aggregated A $\beta$ 42 in culture for 30 min and terminated by putting on ice. The cells were immediately washed with ice cold PBS and fixed with 4% PFA. After increasing permeability with 0.1% Triton X-100 and blocking in 1% BSA over 30 min, cells were stained with rabbit anti-mouse TLR2 (1:500, Abcam, Cambridge, UK) and mouse anti-A $\beta$  (1:500, clone WO-2, Millipore, Schwalbach/Ts, Germany), 2 hrs. Cy3-conjugated goat anti-rabbit IgG and Alexa488-conjugated donkey anti-mouse IgG were used as relevant second antibodies. The slides were gently mounted by putting on an object glass with ProLong<sup>®</sup>Gold antifade reagent with DAPI (Invitrogen) to stain the cell nucleus and imaged under Leica TCS SP2 AOBS laser scanning confocal microscope (performed by using the confocal machine in the laboratory of Prof. Dr. P. Lipp, kindly instructed by Mr. Q Tian). Different channels were merged with Image J as described (Hao *et al.*, 2011).

### 3.2.6 Biacore analysis of TLR2-A $\beta$ direct interaction

Surface Plasmon Resonance (SPR) is a physical process that can occur when plane-polarized light hits a metal film under total internal reflection (TIR) conditions. In this condition, although no light is coming out of the prism in TIR, the electrical field of the photons extends about a quarter of a wavelength beyond the reflecting surface. In SPR, the prism is coated with a thin film of gold on the reflection site, which gives a SPR signal at convenient combinations of reflectance angle and wavelength. The binding of biomolecules occurred at

the site results in the change of the refractive index on the sensor surface, which is measured as a change in resonance angle or resonance wavelength. Such signals can be converted to an arbitrary measured value (angle or wavelength). The biacore machine uses the Resonance Unit (RU), which is exactly converted from the actual angle shift in reflected light (Figure 3.2).

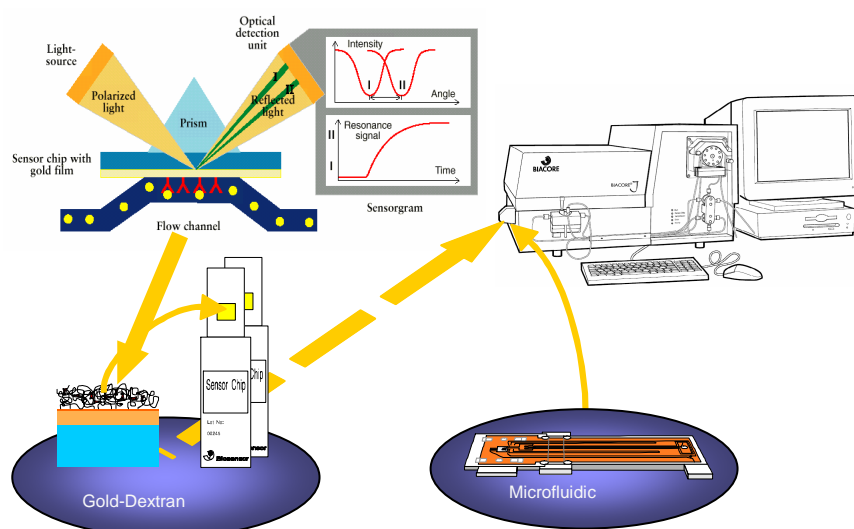


**Figure 3.2. Biacore principle.** Surface Plasmon Resonance (SPR) is a powerful technique to measure biomolecular interactions in real-time in a label free environment. In this experiment, one of the interactants is immobilized to the sensor surface (there are two flow cells on the NTA sensor chip used this work), the other are free in solution and passed over the surface. The binding of the interactants occurred at the site sensor surface is converted to resonance signal and is real-timely record.

In this study, a Biacore® J system (Biacore AB, Uppsala, Sweden) and NTA sensor chips (Biacore AB) was used to investigate whether TLR2 can directly interact with A $\beta$ . In according to the manufacturer's instruction, the C-terminal 10 His-tagged human TLR2 (Glu21-Leu590), or control receptor TLR1 (Ser25-Asp581) and TLR3 (Lys27-Ser711) (all from R&D Systems) was immobilized in the flow cell 1 (FC1) of the NTA chips; insulin-like growth factor-1 receptor (IGF-1R) (Glu31-Asn932) as reference receptor (from R&D Systems) was immobilized in flow cell 2 (FC2) of all the NTA chips. All flow cells were immobilized with an amount to yield 20,000 to 30,000 RU and the basal resonance difference between FC1 and FC2 (FC1-FC2) was around 0 RU. Aggregated A $\beta$ 1-42 or A $\beta$ 42-1, used as a control peptide in the running buffer (0.01 M HEPES, 0.15 M NaCl, 50  $\mu$ M EDTA, 0.005% Surfactant P20, pH=7.4) at the concentration of 5 $\mu$ g/ml, was injected into both flow cells at the rate of 10  $\mu$ l/min for 1 min, followed by another 5 min of running buffer flow at the rate of 10  $\mu$ l/min. The whole binding assay was performed at 25 °C. The difference of basal response between FC1 and FC2 was set to 0 RU. Sensorgrams of FC1-FC2 representing the interactions between ligands and receptors was recorded and analyzed using BIAviewer software (Biacore AB) (The Biacore experiments were performed by using the Biacore® J

system in the laboratory of Prof. Dr. E. Meese and the laboratory of Prof. Dr. J Hemberger (Institut für Biochemische Verfahren und Analysen, Gießen). The laboratory of Prof. Dr. R. Zimmermann kindly provided pre-training).

### **3.2.7 Pull-down analysis of TLR2-A $\beta$ 42 direct interaction**

The pull-down assay is another in vitro method for determination of physical interaction between two or more proteins. It is a form of affinity purification and is useful in confirming the existence of a protein-protein interaction. In a pull-down assay, a bait protein is tagged and captured on an immobilized affinity ligand specific for the tag, thereby generating a “secondary affinity support” for purifying other proteins that interact with the bait protein. The secondary affinity support of immobilized bait is then incubated with a protein source that contains putative “prey” proteins. The potential “prey” would bind to the “bait” and could be eluted together with the bait and be detected with further tools such as Western blot.

Here the pull-down assay was applied to confirm the binding of TLR2 with A $\beta$ . Human TLR2 (Glu21-Leu590) and IGF-1R (Glu31-Asn932) (both are tagged with 10 His on C-terminal) at 50  $\mu$ g/ml, and blank control (PBS without receptor) were incubated with 5  $\mu$ M A $\beta$ 42 aggregates in PBS for 20 hrs and loaded to Ni-NTA spin columns (Qiagen, Hilden, Germany), respectively. After thoroughly washing with a buffer containing 50 mM NaH<sub>2</sub>PO<sub>4</sub>, 300 mM NaCl, 10 mM Imidazole and 0.01% TritonX-100, the columns were eluted with the buffer (50 mM NaH<sub>2</sub>PO<sub>4</sub>, 300 mM NaCl, 500 mM Imidazole and 0.01% TritonX-100, pH 8.0). The A $\beta$  and His-tagged receptors in the eluted buffer was detected by Western blot. Basic procedure was similar to conventional Western blot as will be described below, except using a ProGel-P Tris.Tricine 10-20% (Anamed elektrophorese GmbH, Germany) gel for electrophoresis (Schagger, 2006). A $\beta$  was detected with WO-2 antibody (1  $\mu$ g/ml, Millipore). The TLR2 or IGF-1R on the same blot membrane was detected with a Tetra-His HRP Conjugate Kit (Qiagen) according to the manufacturer's protocol.

### **3.2.8 Construction of plasmids and establishment of TLRs-mutated cell lines**

In general, molecular cloning includes the making of inserts through polymerase chain reaction (PCR), restriction enzyme digestion, ligation and transformation. In addition, to establish protein stable expressing cell lines, further steps of transfection and selection are required (Figure 3.3).

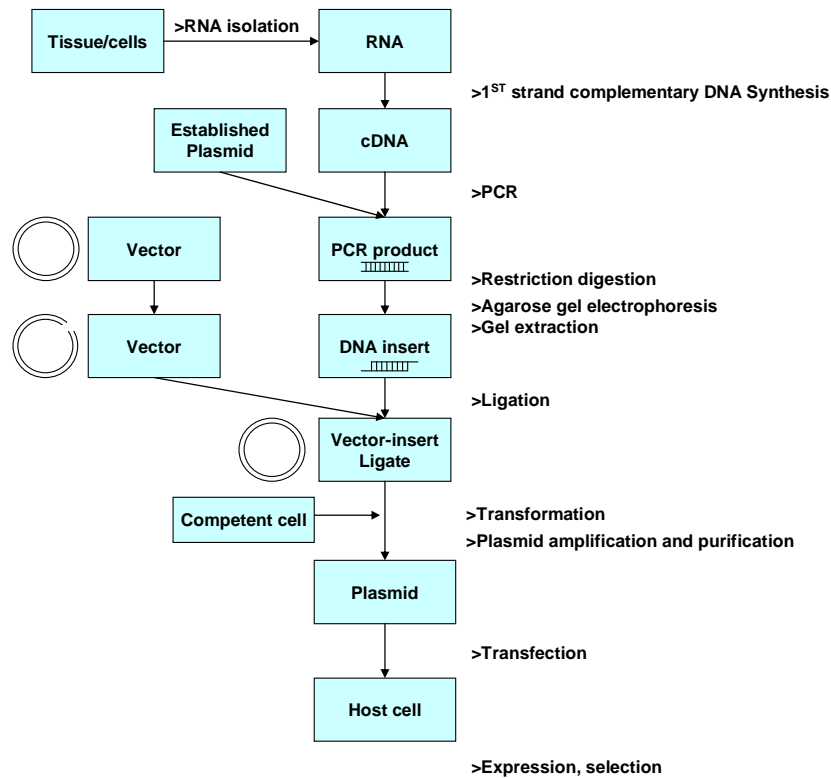


**Figure 3.3. Workflow of molecular cloning.** Molecular cloning includes the making of inserts of interest, restriction enzyme digestion of inserts and vector, ligation and transformation. In addition, to construct protein-of-interest expressing cell line, further steps of transfection and selection are required.

In this study, the templates used for amplifying wild type human TLR2, human TLR1, human TLR6 and mouse CD44 were wild-type hTLR2 plasmid (a gift of Ruslan M. Medzhitov, Yale University) and cDNA derived from human acute monocytic leukemia cell line THP-1 or mouse RAW264.7 cell line. The primers are listed in Table 3.3.

### 3.2.8.1 Total RNA isolation from THP-1 and RAW264.7 cells

Total RNA from human monocytic THP-1 cells and mouse macrophage RAW264.7 cells was isolated with RNeasy® plus kit (Qiagen), which can selectively remove double-stranded DNA without the need for additional DNase digestion. In principle, cells are first lysed and homogenized in a highly denaturing guanidine-isothiocyanate-containing buffer (buffer RLT plus), which immediately inactivates RNases to ensure isolation of intact RNA. The lysate is then passed through a gDNA Eliminator spin column. This column, in combination with the optimized high-salt buffer, allows efficient removal of genomic DNA. Ethanol is added to the flow-through to provide appropriate binding conditions for RNA, and the sample is then applied to an RNeasy spin column, where total RNA binds to the membrane and contaminants are efficiently washed away. High-quality RNA is then eluted in RNase free water:

1. The THP-1 cells or RAW264.7 cells (around  $1 \times 10^7$  cells) were homogenized 10 min, on ice in 600  $\mu$ l buffer RLT plus (supplemented with 10  $\mu$ l  $\beta$ -mercaptoethanol per ml buffer).
2. Transfer the homogenized lysate to a gDNA Eliminator spin column placed in a 2 ml collection tube.
3. Centrifuge for 30 s at  $16,000 \times g$ . Discard the column, and save the flow-through. Add 1 volume (200  $\mu$ l) of 70% ethanol to the flow-through, and mix well by pipetting. Proceed immediately to next step.
4. Transfer the sample, including any precipitate, to an RNeasy spin column placed in a 2 ml collection tube. Close the lid, and centrifuge for 15 s at  $16,000 \times g$ . Discard the flow-through.
5. Add 700  $\mu$ l buffer RW1 solution to the RNeasy mini spin column (in the 2 ml collection tube). Close the lid, and centrifuge for 15 s at  $16,000 \times g$ . Discard the flow-through.
6. Add 500  $\mu$ l buffer RPE to the RNeasy spin column. Close the lid gently, and centrifuge for 15 s at  $16,000 \times g$ . Discard the flow-through.
7. Add 500  $\mu$ l buffer RPE to the RNeasy spin column. Close the lid gently, and centrifuge for 2 min at  $16,000 \times g$ .
8. Place the RNeasy spin column in a new 2 ml collection tube. Centrifuge at full speed for 5 min to further dry the membrane.
9. Place the RNeasy spin column in a new 1.5 ml collection tube. Add 100  $\mu$ l RNase-free water directly to the spin column membrane. Close the lid, and centrifuge for 5 min at  $16,000 \times g$  to elute the RNA.

### 3.2.8.2 First strand cDNA synthesis

First strand cDNA from the above isolated RNA was synthesized using SuperScript™ II Reverse Transcriptase (RT, Invitrogen), which is an engineered version of Moloney Murine Leukemia Virus (MMLV) RT with reduced RNase H activity and increased thermal stability. This enzyme can be used to generate cDNA up to 12.3 kb. The reaction is:

Random primers (250 ng/ $\mu$ l)	1 $\mu$ l
Total RNA	1 ng-5 $\mu$ g
dNTP mix (10 mM each)	1 $\mu$ l
Sterile distilled H <sub>2</sub> O	To 12 $\mu$ l
Heat the mixture to 65°C for 5 min and quick chill on ice. Collect the contents of the tube by brief centrifugation and add:	
5 $\times$ First-strand buffer	4 $\mu$ l

0.1 M DTT	2 $\mu$ l
Mix contents gently. Incubate at 25°C for 2 min	
Add 1 $\mu$ l (200 units) Superscript <sup>TM</sup> II RT and mix by pipetting up and down, incubate at 25 °C for 10 min	
Incubate at 42 °C for 50 min	
Inactivate the reaction by heating at 70 °C for 15 min	
The cDNA can now be used for PCR amplification	

### 3.2.8.3 Polymerase chain reaction (PCR) with TaKaRa LA Taq<sup>TM</sup> DNA polymerase

PCR is a widely used molecular biology method for gene cloning. The TaKaRa LA Taq<sup>TM</sup> DNA polymerase is a thermostable polymerase that possesses a 3' to 5' exonuclease (proofreading) activity, which detects and removes the misincorporated bases that cause slow elongation, making the reaction proceed smoothly, allowing generation of longer and more accurate PCR product. The standard PCR reaction mixture is made as follows:

TaKaRa LA Taq <sup>TM</sup> HS (5 unit/ $\mu$ l)	0.5 $\mu$ l
10 $\times$ LA PCR <sup>TM</sup> Buffer II(Mg <sup>2+</sup> plus)	5 $\mu$ l
dNTP mixture (2.5 mM each)	8 $\mu$ l
Template	<1 $\mu$ g
Primer 1	Final conc.0.2-1.0 $\mu$ M
Primer 2	Final conc.0.2-1.0 $\mu$ M
Sterilized distilled water	Up to 50 $\mu$ l
Thaw all reagents on ice and keep them on ice until reaction set up.	

The standard PCR program is:

step	Temperature	time	Note
1	94 °C	1 min	Initiation
2	98 °C	10 sec	Denaturation
3	52 °C	30 sec	Annealing
4	72 °C	4 min(~1min/ kb)	Elongation
5	Goto step 2	30 cycles	Amplification
6	72 °C	10 min	Final elongation
7	4 °C	For ever	Storage

For mutant TLR1, TLR2 or TLR6 insert generation, site-directed mutagenesis with an overlap extension-PCR using the wild type receptor DNA as templates strategy (Heckman *et al.*, 2007) was applied. That is, as shown in Figure 3.4, for receptor mutagenesis, mutagenic primers b, corresponding to “Reverse primer for 5' segment amplification” in the table 3.3, and c, corresponding to “Forward primer for 3' segment amplification” in the table 3.3 and flanking primers a and d, corresponding to “Forward primer for 5' segment amplification” and “Reverse primer for 3' segment amplification” in the table 3.3, respectively were designed and commercially synthesized in Sigma-Aldrich. Intermediate PCR products AB and CD that are overlapping fragments of the entire product AD but with mutation of interest were first generated. Products AB and CD were then denatured and used as template DNA for the second PCR, in which the flanking primers were used. As strands of each product hybridize at their overlapping, complementary regions that also contain the desired mutation (indicated by

the cross). Thus the amplification of product AD in PCR #2 actually created mutated final products. For wild type receptor insert generation, simply amplifying the product between the flanking primers using wild type plasmids or cDNA as templates was enough. The wild type and mutated TLR1/ TLR6 were inserted into multiple cloning site (MCS) A between NheI and MluI sites of pIRES vector (Clontech Laboratories, Palo Alto, CA). The wild type CD44, TLR2 and mutated TLR2 were inserted into MCS B between XbaI and NotI sites of pIRES vector. In this study, wild type human TLR2 and mouse CD44 were also cloned to pCEP4 vector between KpnI and NotI in the multiple cloning sites.

For receptor domain deletion inserts generation, a strategy similar to the above described site-directed overlap extension-PCR was applied. As shown in figure 3.4, two linking primers b (corresponding to “Reverse primer for 5' segment amplification” in the table 3.3) and c (corresponding to “Forward primer for 3' segment amplification” in the table 3.3), as well as two flanking primers a and d (corresponding to “Forward primer for 5' segment amplification” and “Reverse primer for 3' segment amplification” in the table 3.3, respectively), were designed and used. The linking primer b and c contain sequences on both upstream and downstream side of intested deletion candidate gene fragments. Therefore, primers b and c generate overlapping sequences by including nucleotides that span the junction of upstream and downstream segments in the first PCR. A second PCR using the hybrid gene product would generate products of full sequence including upstream and downstream segments without the deletion sequence. Similarly, the domain deleted TLR1/ TLR6 sequences were inserted into multiple cloning site (MCS) A between NheI and MluI sites of pIRES vector. The domain deleted TLR2 was inserted into MCS B between XbaI and NotI sites of pIRES vector.

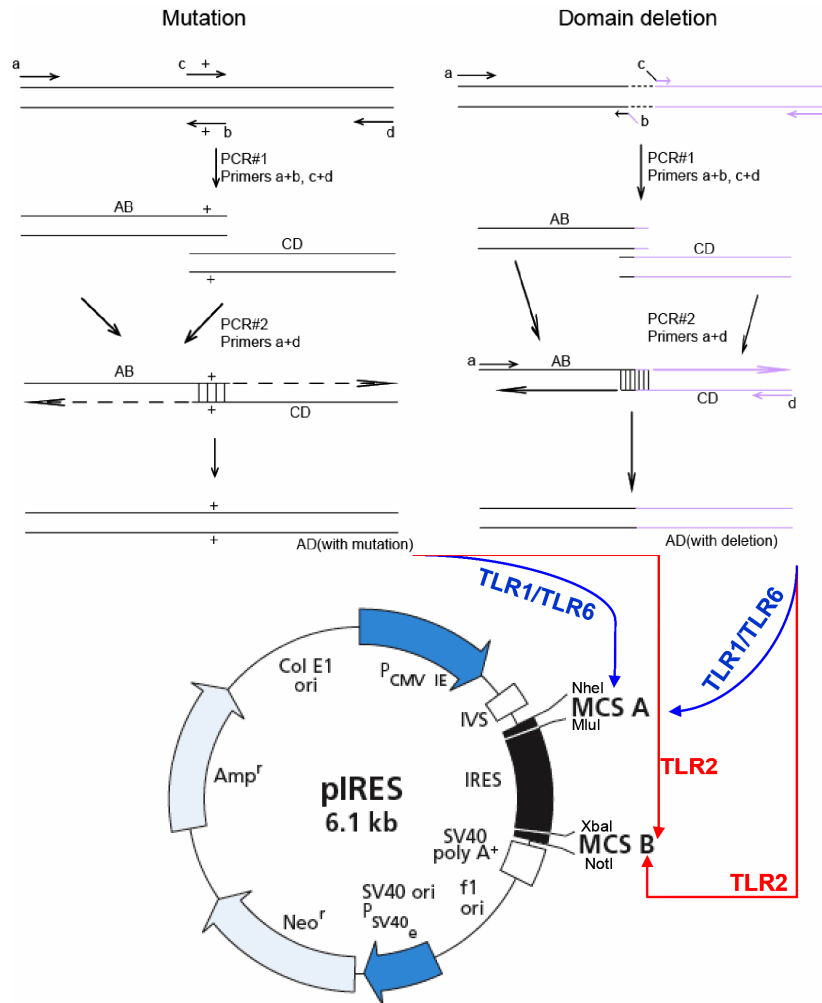


**Figure 3.4. PCR-mediated overlap extension creates specific nucleotide mutations or chimeric domain deletion products of TLR1, 6 or 2.** (Left) Site-directed mutagenesis is accomplished by using mutagenic primers (b and c) and flanking primers (a and d) to generate intermediate PCR products AB and CD that are overlapping fragments of the entire product AD. Products AB and CD are denatured when used as template DNA for the second PCR; strands of each product hybridize at their overlapping, complementary regions that also contain the desired mutation (indicated by the cross). Amplification of product AD in PCR #2 is driven by primers a and d. Final product AD (with mutation) can be inserted into the expression vector, for instance, pIRES, for expression. (Right) Chimeric gene with domain deletion products can be generated by two PCRs, similar to left, except that internal primers b and c are not mutagenic. Instead, because the goal here is to delete an internal segment (shown in dashed line) from a complete gene to get the upstream and downstream side gene segments connected, primers b and c generate overlapping sequences by including nucleotides that span the junction of segments AB (black line) and CD (purple line). The second PCR generates the hybrid gene product AD that is then ready to insert into the expression vector for expression (Adapted from reference (Heckman *et al.*, 2007)).

### 3.2.8.4 Enzymatic restriction digestion

Enzymatic restriction digestion is a widely applied technique that cuts the DNA at specific recognition nucleotide sequences. It produces either sticky or blunt-end terminals and thus facilitates ligating relevant nucleotides. The digestions were carried out in corresponding buffers and incubated at the defined temperature according to the manufacturer's manuals. For analytic digestion confirmation, 0.5 µg DNA was analyzed for each reaction, while 2 µg DNA was used for preparative digestions. The incubation time varied from 30 min to 4 hrs. In

extreme conditions, the incubation time was prolonged up to 12 hrs. The digestion products were analyzed by agarose gel electrophoresis.

In this study, the KpnI, MluI, NheI, NotI and XbaI were used in wild type and mutated TLR1, TLR2 and TLR6 cloning. It was achieved by adding a corresponding restriction enzyme recognition site to the primers for amplification of the inserts.

Specifically for cloning human TLR2 into the pCEP4 vector between KpnI and NotI, there exists a KpnI restriction site within the TLR2 sequence (cut position: 2682), which makes it impossible to apply a KpnI-cut sticky for insert. Thus, blunt-ends after KpnI digestion of the pCEP4 vector and XbaI digestion of engineered pIRES-XbaI-TLR2-NotI plasmid was introduced. The blunt-end was generated by use of Klenow Enzyme (DNA polymerase I, large fragment, Roche). The Klenow enzyme carries the 5'→3' polymerase and the 3'→5' exonuclease activities of intact DNA polymerase I, but lacks the 5'→3' exonuclease activity of the native enzyme; therefore, it catalyzes the addition of mononucleotides from deoxynucleoside-5'-triphosphates to the 3'-hydroxyl terminus of a primer/template DNA. Such a property is used to synthesize DNA complementary to single-stranded DNA templates to generate a blunt terminal for ligation. The klenow reaction is:

Components	Reaction
Template DNA	1 µg DNA
Nucleotides, final concentration	1 mM of desired dNTP each
10 × Filling buffer	2 µl
Klenow	1 U
H <sub>2</sub> O	add up to 20 µl
Incubation	15 min at 37 °C

Further, in order to exchange the intracellular domain of TLR1 with that of TLR6, instead of the above described PCR strategy, a direct restriction enzyme digestion strategy based on the constructed TLR1 and TLR6 plasmids was used, since there is but one *XcmI* site within the transmembrane domain-encoding nucleotide sequence (as suggested by sequence analysis).

### 3.2.8.5 Agarose gel electrophoresis

The agarose gel electrophoresis is a technique to separate DNA or RNA molecules by size difference. The separation is carried out as negatively charged nucleic acid molecules migrate through an agarose matrix at different speeds, due to their sizes, in the electric field. The larger the molecules are, the slower they move. The agarose gel used in this study is either 1% (w/v) for DNA fragments larger than 500 bp or 2% (w/v) for smaller than 500 bp DNA fragments.

### 3.2.8.6 Extraction of DNA from agarose gels

After agarose gel electrophoresis, the DNA bands were checked under UV lamp with 70% UV strength. The DNA band of interest was cut off the gel and extracted with the Gel Extraction Kit (Qiagen). The DNA containing gel slides were dissolved in 3 volumes of high salt QG buffer (100 mg gel = 100 ml) by incubation at 55°C with shaking for 10 min. One gel volume of 2-propanol is added additionally when the DNA fragment is <500 bp or >4 kb. The dissolved gel was then loaded to the QIAquick spin column, which absorbs particular size Nucleic acids to the silica membrane in the spin under high salt condition. The spin was centrifuged at  $25,000 \times g$  for 1 min to let the column membrane bind DNA. After washing away the primers, nucleotides, enzymes, mineral oil, salts, agarose, ethidium bromide, and other impurities from the DNA samples with 0.75 ml PE buffer, the pure interest DNA was eluted with a small volume (10-20  $\mu$ l) of nucleotide free water.

### 3.2.8.7 DNA quantification

DNA quantification was performed by spectrometric measurements at 260 nm because it absorbs UV light with an absorption peak at 260 nm. According to the Beer-Lambert Law, the absorption  $A$  is depending on the path length  $l$ , the concentration  $c$ , and the molar extinction coefficient  $\epsilon$ :  $A = \epsilon \times l \times c$ . dsDNA has an average extinction coefficient of 0.02 ( $\mu$ g/ml)-1cm-1, thus an O.D.260 of 1 corresponds to a concentration of 50  $\mu$ g/ml dsDNA. The O.D.260 value may be interfered with by contaminants such as RNA, proteins, and phenol, *etc.* O.D.260/O.D.280 ratio is an indicator for protein contaminations. The O.D.260/O.D.280 ratio should be in the range between 1.8 and 2.0.

### 3.2.8.8 DNA ligation

Ligation is the process of linking DNA fragments together with the help of a DNA ligase. The ligation reactions were carried out using the T4 DNA ligase kit (Roche) according to the manufacturer's manuals. The relevant purified restriction digested inserts and vectors were added as the following ligation mixture reaction:

10 $\times$ ligation buffer	3 $\mu$ l
Vector DNA	50 - 200 ng
Insert DNA	3 $\times$ excess to vector DNA
T4 DNA ligase	2 U
Nuclease-free H <sub>2</sub> O	Up to 30 $\mu$ l
16 °C, overnight (16 hrs) incubation	

The ligation mixture was stored at 4 °C after ligation. 5  $\mu$ l from the ligation mixture was used for the one transformation reaction.

### 3.2.8.9 Preparation of Fusion-Blue competent E. coli cells

Organisms are, by nature, resistant to extracellular DNA. In order to select and amplify the ligated plasmid of interest, many techniques have been adapted to make the E. coli cells susceptible to uptake bacteriophage DNA. I used a high efficiency competent cell preparation method adapted from Chung et al. (Chung *et al.*, 1989). The recipe of the transformation and storage solution for chemical transformation (TSS) is:

Final concentration	10 ml
10% Polyethyleneglycol (PEG)(w/v, MW8000)	1 g
5% DMSO (vol/vol)	0.5 ml
50 mM MgCl <sub>2</sub> (pH6.5)	MgCl <sub>2</sub> ·6H <sub>2</sub> O, 0.1 g
85% LB Medium	LB up to 10ml
Autoclave or filter to sterilize. Store at 4 °C for < 2weeks	

Procedure:

1. Pick a single, well isolated fusion-blue E. coli clone and inoculate it into LB broth for overnight incubation at 37 °C with shaking at 250 rpm to saturation.
2. Transfer 20 µl of the saturated overnight culture to 100 ml of LB medium, and incubate the cells at 37 °C with the shaking at 220 rpm, until O.D.600 reach 0.5.
3. Chill the flask on the ice for 20 min and then collect the cells by centrifugation at 5,000 rpm for 15 min at +/- 0 °C.
4. Resuspend the cells in 10 ml of ice cold TSS solution; the competent cells are ready to be transformed. The competent cells can be aliquoted and stored at -70 °C for 2 months.

### 3.2.8.10 Transformation of ligates to Fusion-Blue competent E. coli cells

For transformation, 100 µl fusion-blue competent cells were thawed on ice and incubated with 1 µg DNA (*e.g.* 2 µl of miniprep DNA, or 5 µl of ligation mix) on ice for 30 min. This was followed by a heat shock at 42 °C water bath for 45 sec. The heat-shocked cells were then cooled on ice for 2 min. Transformed cells are recovered by adding 500 µl LB medium and incubated at 37 °C with 450 rpm shaking for 60 min. To plate the transformed cells, cells were gently harvested by centrifugation at 1,050 × g for 5 min. Dispose of 500 µl of the supernatant and resuspend the cell pellet in the remaining 100 µl of medium. Resuspended cells are plated on LB plates with the corresponding antibiotics and incubated at 37 °C overnight.

### 3.2.8.11 Plasmid DNA minipreparation

DNA minipreparation is a small-scale DNA preparation that is quick and easy to handle. In this study, a High pure plasmid isolation kit (Roche) was used to isolate high pure plasmid

DNA. The starter culture was inoculated with one colony in 2 ml LB medium with appropriate antibiotics according to the plasmid antibiotic resistance. The bacterial culture was incubated at 37 °C with rolling for more than 8 hours. The cells were harvested by centrifugation at room temperature and  $6,000 \times g$  for 30 sec. The cell pellet was resuspended in 250  $\mu$ l suspension buffers containing RNase and added in 250  $\mu$ l lysis buffer for alkaline lysis and plasmid DNA releasing at room temperature for 5 min. The lysis was terminated by 350  $\mu$ l chilled binding buffer and incubated for 5 min on ice and centrifuged at top speed for 10 min; then transfer the supernatant to the high pure filter tube and centrifuge at top speed for 1 min. The plasmid DNA would bind selectively to glass fiber fleece. After washing the column with 700  $\mu$ l wash buffer, the DNA bound in the filter was eluted in 50  $\mu$ l low salt solution (nuclease free water).

DNA minipreparations were also made using the QIAprep spin miniprep kit (Qiagen) according to the standard protocol.

#### **3.2.8.12 Plasmid DNA maxipreparation**

PureLink™ HiPure plasmid maxiprep kit (Invitrogen) was used to maxiprep the plasmid DNA for transfection use. Briefly, 200 ml of LB cultured cells were harvested by centrifuging at  $4,000 \times g$  for 10 minutes in a bucket. The cell pellet was resuspended in 10 ml Resuspension Buffer with RNase A until homogeneous and then added to 10 ml Lysis Buffer. Mix gently for complete lysis, and then incubate at room temperature for 5 minutes. The lysis process is stopped by 10 ml Precipitation Buffer and the mixture centrifuged at  $>12,000 \times g$  for 10 min at room temperature. The supernatant was loaded onto the column provided by the manufacturer. Plasmid DNA would bind to the column. Allow the solution in the column to drain by gravity flow. After a step of washing with 60 ml Wash Buffer, the DNA component was eluted from the column with 15 ml Elution Buffer, then 10.5 ml isopropanol was added to the elution tube to precipitate the DNA. Centrifuge at  $>15,000 \times g$  for 30 min to get a plasmid DNA pellet. The pellet was washed with 5 ml 70% ethanol and finally resuspended in 500  $\mu$ l nuclease free water.

#### **3.2.8.13 Transfection of plasmid DNA and Stealth RNAi™ to mammalian cells using Lipofectamine™2000**

Transfection of plasmid DNA into cultured mammalian cells allows for analysis of functional mechanisms. It can be achieved with a variety of methods, *e.g.*, retroviruses, electroporation, DEAE dextran, calcium phosphate- and a liposome-based deliveries method. The

Lipofectamine™2000 (Invitrogen) is an adapted proprietary formulation for transfection. In this study, Lipofectamine™2000 was used for both stable introducing TLR1/TLR2/TLR6/CD44 and mutated plasmids DNA to HEK-293 cells and transient transfection of stealth RNAi™ to RAW264.7 cells for RNA silencing. Since both HEK-293 and RAW264.7 cells are adherent cells, one day before transfection the cells were plated in Opti-MEM® I + 10% FBS medium without antibiotics in 24-well plate wells so that cells will be 90-95% confluent at the time of transfection. On the day of transfection, dilute 0.8 µg plasmid DNA (or 20 pmol stealth™RNAi) in 50 µl of Opti-MEM® I Reduced Serum Medium without serum and then dilute the appropriate amount (for plasmid transfection, 2 µl; for stealth™RNAi, 1 µl) of Lipofectamine™2000 in 50 µl of Opti-MEM® I Medium. Incubate for 5 minutes at room temperature, and mix gently. Then combine the diluted DNA with diluted Lipofectamine™ 2000, mix gently and incubate at room temperature for 20 minutes. The complexes were at last added to the cell wells, mix gently and incubate at 37 °C in a CO<sub>2</sub> incubator for 24-48 hrs prior to further experiments. For HEK-293 stable cell lines selection, selective medium (500 µg/ml G418 for plasmid engineered in pIRES vector, 400 µg/ml Hygromycin B for plasmid engineered in pCEP4 vector) was supplied in the following day for selection.

#### **3.2.8.14 Confirm expression of TLRs in HEK-293 cell lines and RNAi knockdown in RAW264.7 cells**

HEK-293 TLRs expression cell lines were screened out with high concentration of G418 or Hygromycin B, the surviving cells should express corresponding TLRs. In order to ensure the findings, TLR2 expression in TLR1, TLR6, TLR2, TLR2-TLR1, TLR2-TLR6, TLR2EKKA741-744PQNS, TLR2E741P, TLR2K742Q, TLR2K743N, TLR2A744S, and TLR2EKKA741-744PQNS-TLR1Y737N co-expressed HEK-293 cell lines was confirmed by Western blot. Briefly,  $5 \times 10^6$  HEK-293 cells per cell line were lysed in 200 µl lysis buffer (10 mM Tris pH8.0, NaCl 150 mM, 1% Triton X-100, plus 1×protein inhibitor cocktail (Roche)). 20 µl of the cell lysates were run in Western blot using goat anti-human TLR2 antibody IgG (AF2616, R&D systems, 1:1,000 in 5% non-fat milk PBS from 0.2 mg/ml stock).  $\alpha$ -tubulin on the same NC membrane was detected as loading control with  $\alpha$ -tubulin antibody (mouse monoclonal, DM1A, abcam). Meanwhile, total mRNA from HEK-293 TLR2wt, TLR2E741P, TLR2K742Q, TLR2K743N, TLR2A744S, TLR2EKKA (741-744) PQNS-TLR1wt and TLR2EKKA (741-744) PQNS-TLR1Y737N cells were isolated with TRIZOL and first strand cDNA was synthesized with a method as will be described in the

following sections (See section 3.2.14.1-3.2.14.3 for procedure). This was followed by an ordinary PCR to generate DNA products containing the interest mutant region for sequencing:

1. Prepare the following 50  $\mu$ l reaction in a 0.5 ml PCR tube on ice:

<b>Component</b>	<b>Volume(<math>\mu</math>l)</b>	<b>Final concentration</b>
10 $\times$ PCR Buffer	2 $\mu$ l	1 $\times$
5 $\times$ Q-solution	4 $\mu$ l	1 $\times$
dNTP Mix (10 mM each)	0.4 $\mu$ l	200 $\mu$ M
Forward tlr1 / tlr2 / tlr6 primer (10 $\mu$ M)	0.5 $\mu$ l	0.25 $\mu$ M
Reverse tlr1 / tlr2 / tlr6 primer (10 $\mu$ M)	0.5 $\mu$ l	0.25 $\mu$ M
DNA template (1 <sup>st</sup> strand cDNA)	2 $\mu$ l	
Taq DNA polymerase	0.1 $\mu$ l	0.5 units/reaction
Nuclease free water	Up to 20 $\mu$ l	

2. Gently mix the reaction and spin down in a microcentrifuge, then run PCR programm in a DNA Engine® Thermal Cycler PTC-200 as below:

Initial denaturation	94 °C	3 min	} 35 Cycles
Denaturation	94 °C	1 min	
Annealing	55 °C	60 sec	
Extension	72 °C	1 min	
Final extension	72 °C	10 min	
Storage	4 °C	For ever	

The PCR products were sequenced to confirm the corresponding mutants (the primers for PCR and sequencing were listed in Table 3.6).

The tlr1, tlr2 and tlr6 RNA silencing knock down effect was confirmed by realtime PCR through SYBR Green method:

1. RNA isolation with RNeasy® plus kit as described in section 3.2.8.1, the RNA was finally eluted in 25  $\mu$ l RNase-free water.
2. First strand cDNA synthesis using the SuperScript™ II Reverse Transcriptase kit as described in section 3.2.8.2.
3. The cDNAs as templates were forward to realtime PCR determination of tlr1, tlr2 and tlr6 RNA level with the DyNAmo™ colorflash SYBR® Green qPCR kit (FINNZYMES):

Reaction setup:

<b>Component</b>	<b>Volume/reaction</b>	<b>Final concentration</b>
2 $\times$ master mix	10 $\mu$ l	1 $\times$
Primer forward (10 $\mu$ M)	0.5 $\mu$ l	0.25 $\mu$ M
Primer reverse (10 $\mu$ M)	0.5 $\mu$ l	0.25 $\mu$ M
cDNA	1 $\mu$ l	$\leq$ 500 ng/reaction
RNase-free water	8 $\mu$ l	
<b>Total reaction volume</b>	<b>20 <math>\mu</math>l</b>	

Note: For Applied Biosystems 7500 use the 0.3  $\times$  ROX final concentration.

Realtime Cyclor conditions:

Step	time	temperature
Initial Denaturation:	7 min	95 °C
Denaturation:	10 s	95 °C
Annealing/extension	30 s	60 °C
Number of cycles	45	
Perform melting curve (dissociation curve) analysis		

### 3.2.9 G-actin/F-actin assay in primary macrophages during A $\beta$ 42 phagocytosis

Primary BMDMs cultured in a 6-well plate (BD) at a density of  $1 \times 10^6$  cells /well were treated with aggregated A $\beta$ 42 (5  $\mu$ M) for 0, 15, 30, and 60 min. The cells were then harvested and analyzed with G-actin/F-actin in Vivo Assay Kit (Cytoskeleton, Inc., Denver, CO) according to the manufacturer's instructions. Briefly, the cells were lysed at the cell culture temperature in a lysis and filamentous actin (F-actin) stabilization buffer, followed by a separation of the globular-actin (G-actin) and F-actin through ultracentrifuge at  $100,000 \times g$  for 1 h at 37 °C. After the G-actin in the supernatant was removed, the F-actin in the pellets was depolymerized to globular form by F-actin depolymerization solution. Finally, both G-form and F-form actin components were detected via Western blot with anti-actin antibody and the ratio of F-actin to G-actin densitometry was determined, which represents the phagocytosis activity (Tu *et al.*, 2003).

### 3.2.10 Flow cytometric analysis of FITC-A $\beta$ 42 phagocytosis in primary macrophages

BMDM cells cultured in a 24-well plate (BD) at a density of  $3 \times 10^5$  cells/well were treated with 5  $\mu$ M FITC-conjugated A $\beta$ 42 for 0, 1, 3, 6, and 24 hrs. Thereafter, macrophages were washed with PBS and detached from the plate with 0.05% Trypsin-EDTA (Invitrogen). The mean fluorescence intensity (mFI) of internalized FITC-labeled A $\beta$ 42 was immediately determined by BD FACSCanto II flow cytometry (Franklin Lakes, NJ) (the use of the FACS machine was based on training by the manufacturer).

### 3.2.11 Bone marrow transplantation

Bone marrow transplantation was performed as described (Hao *et al.*, 2011) and finished together with Dr. Wenlin Hao. Briefly, APP<sup>swe</sup>/PS1<sup>dE9</sup> recipient mice at the age of 6 months were exposed to a 10 Gy whole-body irradiation given as split doses of  $2 \times 5$  Gy with a 4 hrs interval using a linear accelerator ( $\gamma$ -source). Donor BM cells ( $1 \times 10^7$  per mouse) derived from TLR2<sup>-/-</sup> or wild type (wt) C57BL6/N mice were then injected, via the tail vein, into each

recipient. Transplanted mice were housed in autoclaved cages and treated with antibiotics in drinking water (0.2 mg/ml trimethoprim and 1 mg/ml sulfamethoxazole, both from Sigma, Schnellendorf, Germany) for 3 weeks after irradiation.

### 3.2.12 Tissue collection

The mice were euthanized 12 months after BM transplantation by deep anaesthesia with inhalation of isoflurane. They were rapidly perfused transcardially with ice cold PBS. The brain was removed and divided sagittally (Figure 3.5). The left hemi-brain was immediately fixed in 4% paraformaldehyde (PFA) and stored at 4 °C for immunohistochemistry. A 0.5 mm-thick piece of tissue was sagittally cut from the right hemi-brain, homogenized in Trizol and stored at -80 °C for RNA isolation. The rest of the right hemi-brain was snap frozen in liquid nitrogen for biochemical analysis (Figure 3.5).

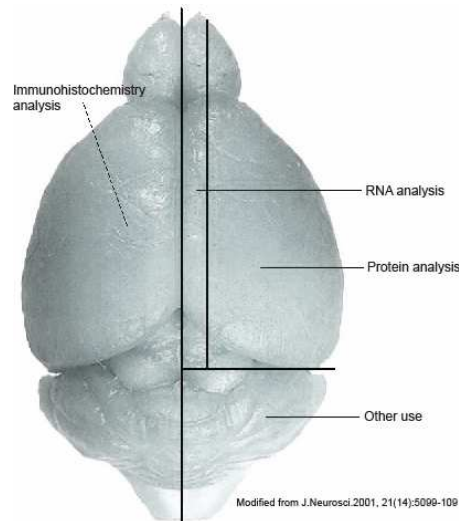


**Figure 3.5. Schematic figure of brain sample sections preparation.** The brain was divided according to the lines into 4 parts. The left hemi-brain was immediately fixed in 4% paraformaldehyde (PFA) and stored at 4 °C for immunohistochemistry process. A 0.5 mm-thick piece of cerebral tissue was sagittally cut from the right hemi-brain, homogenized in Trizol and stored at -80 °C for RNA isolation. The rest of the right hemi-cerebral was snap frozen in liquid nitrogen for biochemical analysis. The remained part was frozen in liquid nitrogen as well.

### 3.2.13 Immunohistochemistry staining of Iba-1

The PFA-fixed brain was embedded in paraffin (Ms. A. Schottek helped with embedding work) and serial 2 µm-thick sagittal sections were cut and mounted on glass slides. Immunohistochemical staining was performed on these sections with the VectaStain *Elite* ABC kit (Vector Laboratories). To demonstrate the inflammatory neuropathological changes, the rabbit anti-Iba-1 (1:500, Wako Chemicals GmbH, Neuss, Germany) was used as a primary antibody, detailed procedures are as follows:

1. The slides were serially deparaffinized in the solutions below:

Xylol	5 min
Xylol	5 min
Ethanol 100%	5 min
Ethanol 100%	5 min
Ethanol 96%	3 min
Ethanol 70%	3 min
Ethanol 50%	3 min
dH <sub>2</sub> O	dip

2. Antigen retrieval by cooking the sections in 1× citrate buffer (10 mM pH6.0) in a microwave oven, 560 watts, 3 min × 5 times. Refill with buffer between each cooking. Cool down slowly by leaving on the bench for >30 min after cook.
3. The endogenous peroxidase of the tissue was inactivated via incubating the slides in the mixture of H<sub>2</sub>O<sub>2</sub> / Methanol/dH<sub>2</sub>O buffer, RT, 30min.
4. Wash slides with TBS, 5 min × 2 times and then with TBS-T, 5 min, once.
5. Block with blocking buffer (Casein + 5% goat serum), RT, 1h.
6. 1<sup>st</sup> Antibody reaction: with 1:500 dilution of the polyclonal rabbit-anti mouse-Iba-1 (Wako) in dilution buffer, incubate at 4 °C, overnight.
7. Wash as step 4.
8. 2<sup>nd</sup> Antibody reaction: with the 1:500 diluted biotin labeled goat-anti-rabbit (Vector Laboratories) in dilution buffer, RT, 1h.
9. Preparation of ABC reagent: Add 10 µl reagent A, 10 µl Reagent B to 1 ml PBS/T. Incubate in dark for at least 30 min before use.
10. Wash the slides as step 4.
11. Incubate the slides with ABC reagent, RT, 30 min
12. Wash as step 4
13. Develop with DAB, 120 sec, and then wash with dH<sub>2</sub>O, 3 times.
14. Counterstaining with Hematoxylin, 10 sec, forward to dH<sub>2</sub>O wash 3 times. Then develop in running tap water for 5 min, and then change back to dH<sub>2</sub>O.
15. Dehydration: serially treat the slides in the following solutions:

50% Ethanol	Dip
70% Ethanol	Dip
96% Ethanol	Dip, 2 times
100% Ethanol	Dip, 2 times
Xylol 1 <sup>st</sup>	2 min
Xylol 2 <sup>nd</sup>	2 min
Then put in Xylol until mount in entellan	

16. Mount the slides with Entellan® Neu (Merck), and then cover the tissue with cover glass.

All slide images were acquired by Zeiss Axiophot microscope (Göttingen, Germany). For microglial quantification, data were reported as the number of Iba-1-labelled cells normalized to the full area (mm<sup>2</sup>) in the total hippocampus. Iba-1-positive cells with clear haematoxylin nucleus staining were counted.

**Buffers recipe:**

Citrate buffer(10× )

Citric acid monohydrate 2.1014 g/l, pH=6.0

H<sub>2</sub>O<sub>2</sub>/Methanol/dH<sub>2</sub>O

10 ml H<sub>2</sub>O<sub>2</sub> (30%) (Otto Fishar GmbH)

17 ml methanol

73 ml dH<sub>2</sub>O

Blocking buffer

0.2% Casein

0.1% Tween-20

0.1% Triton-X

5% Goat serum

In 1× PBS

Diluting buffer

0.02% Casein

0.01% Tween-20

0.01% Triton-X

1% Goat serum

In 1× PBS

DAB

1 mg/ml 3, 3'-Diaminobenzidine tetrahydrochloride (DAB, Sigma) in 1× PBS, Add 1 µl H<sub>2</sub>O<sub>2</sub>/ 3 ml DAB solution right before use (all waistes demand special disposal)

### **3.2.14 Reverse transcription PCR and Real-time PCR analysis of gene transcripts**

Real-time PCR is a quantitative PCR method for the determination of cope number of PCR templates such as DNA or complementary DNA (cDNA) in a PCR reaction. There are two types of real-time PCR: intercalator-based and probe-based. Both methods require a special thermocycler equipped with a sensitive camera that monitors the fluorescence in each well of the 96-well plate at frequent intervals during the PCR Reaction. Intercalator-based method (also known as SYBR Green method) requires a double-stranded DNA dye in the PCR reaction which binds to newly synthesized double-stranded DNA and gives fluorescence.

Probe-based real-time PCR (also known as TaqMan PCR) requires a pair of PCR primers (as regular PCR does), and an additional fluorogenic probe which is an oligonucleotide of 20-26 nucleotides with both a reporter fluorescent dye and a quencher dye attached. The probe is designed to bind only the DNA sequence between the two specific PCR primers. Only a specific PCR product can generate a fluorescent signal in TaqMan PCR. Therefore, the TaqMan method is more accurate and more reliable than SYBR green method. In this study, the TaqMan method was applied to evaluate the relative transcript levels of TNF- $\alpha$ , IL-1 $\beta$ , Chemokine (C-C motif) ligand 2 / monocyte chemoattractant protein-1 (CCL-2 /MCP-1), and iNOS in the TLR2 knockout or wild type bone marrow reconstructed APP mouse brains with the 7500 Fast Real-time PCR System (Applied Biosystems). Ordinarily it includes the isolation of total RNA, first strand cDNA synthesis, and real-time PCR detection:

#### **3.2.14.1 Brain total RNA isolation with Trizol**

Homogenization: The 0.5 mm-thick piece of tissue sagittally cut from the right hemi-brain (see above tissue collection section 3.2.12) was homogenized in 1 ml Trizol (Invitrogen) according to the manufacturer's manuals:

1. Phase separation: Incubate the homogenized samples for 5 min at room temperature to permit complete dissociation of nucleoprotein complexes. Then add 0.2 ml of chloroform and shake vigorously by hand for 15 sec, and then incubate at room temperature for 3 min. Centrifuge the samples at  $12,000 \times g$  for 15 min at 4 °C. The sample mixture was separated into a lower red, phenol-chloroform phase, an interphase and a colorless upper aqueous phase. RNA remains in the aqueous phase.
2. RNA precipitation: Transfer the colorless aqueous phase to a fresh tube; precipitate the RNA from the aqueous phase by mixing with 0.5 ml isopropyl alcohol. Incubate at room temperature for 10 min and then centrifuge at  $12,000 \times g$  for 10 min at 4 °C. The precipitated RNA is the gel-like pellet on the bottom side of the tube.
3. RNA wash: remove the supernatant and wash the RNA once with 1 ml 75% ethanol. Mix by brief vortexing and centrifuge at  $7,500 \times g$  for 5 min at 4 °C.
4. Redissolve the RNA: briefly dry the RNA pellet and then dissolve it in appropriate volume of RNase-free water, incubating for 10 min at 55 °C.

### 3.2.14.2 Genome DNA degradation prior to RT-PCR

To erase trace genomic DNA contamination in the RNA sample, RQ1 (RNA Qualified) RNase-Free DNase (Promega), which is a DNase I that degrades both double-stranded and single-stranded DNA endonucleolytically, was used. The reaction was set up as following:

RNA sample in water	8 $\mu$ l
RQ1 RNase-Free DNase 10 $\times$ Reaction buffer	1 $\mu$ l
RQ1 RNase-Free DNase	1 U/ $\mu$ g RNA
Nuclease-free water	To a final volume of 10 $\mu$ l

Incubate at 37 °C for 30 min, and then add 1  $\mu$ l of RQ1 DNase Stop solution to terminate the reaction. The DNase was then inactivated by incubating at 65 °C for 10 min.

### 3.2.14.3 First strand cDNA synthesis

First-strand cDNA was synthesized by priming total RNA with hexamer random primers (Invitrogen) and using Superscript II reverse transcriptase (Invitrogen) as described in section 3.2.8.2.

### 3.2.14.4 Real-time quantitative PCR

For quantification of *TNF- $\alpha$* , *IL-1 $\beta$* , *iNOS*, *CCL-2* transcription level, real-time quantitative PCR with the Taqman® gene expression assays of mouse *TNF- $\alpha$* , *IL-1 $\beta$* , *iNOS*, *CCL-2* and 18s RNA was performed using the 7500 Fast real-time PCR system with a DyNAmo™Flash probe qPCR kit (FINNZYMES).

Reaction setup for Taqman probe:

Components (in order of addition)	Volume/20 $\mu$ l reaction	Final conc.	Notes
2 $\times$ DyNAmo™ Flash probe	10 $\mu$ l	1 $\times$	
Master mix			
Primer mix (in H <sub>2</sub> O) (including probe)	1 $\mu$ l	500 nM primer, 250 nM TaqMan®probe	
50 $\times$ ROX reference dye (F-401L)	0.4 $\mu$ l	1 $\times$	
Template cDNA(in H <sub>2</sub> O)	1 $\mu$ l		Max 200 ng/20 $\mu$ l reaction
H <sub>2</sub> O	Up to 20 $\mu$ l		

Select FAM-labeled detectors and set up reaction system cycling to run:

step	purpose	temp	time
1	UNG incubation	50 °C	2 min
2	Initial denaturation	95 °C	7 min
3	Denaturation	95 °C	5 s
4	Annealing+extension	60 °C	30 s
5	Data acquisition		
6	Number of cycles	45 cycles, step 3-5	

The amount of double-stranded PCR product synthesized in each cycle was measured by detecting the free FAM dye cleaved from the Taqman® probes. Threshold cycle (Ct) values for each test gene from the replicate PCRs was normalized to the Ct values for the 18s RNA control from the same cDNA preparations. The ratio of transcription of each gene was calculated as  $2^{(\Delta Ct)}$ , where  $\Delta Ct$  is the difference Ct (18s RNA) – Ct (test gene).

### 3.2.15 Brain homogenates

The brain was homogenized according to the published protocol (Figure 3.6)(Mc Donald *et al.*, 2010). Briefly, frozen hemisphere was bounce-homogenized in a Tris-buffered saline (TBS) (500  $\mu$ l/100 mg tissue), supplemented with the Roche Complete Protease Inhibitor Cocktail and centrifuged at  $16,000 \times g$  for 30 min at 4 °C. The supernatant (TBS-soluble fraction) was collected and stored at -80 °C. The pellet was re-suspended (the same volume as shown above) in TBS plus 1% Triton-X 100 (TBS-TX) plus Protease inhibitor, ultrasonicated for 5 min in 4 °C water bath with Transsonic T 780, and centrifuged at  $16,000 \times g$  for another 30 min at 4 °C. The supernatant was collected and stored at -80 °C as the TBS-TX-soluble fraction. The pellet was extracted for a third time using an above described volume of ice-cold guanidine buffer (5 M guanidine-HCl/ 50 mM Tris, pH 8.0, herein referred to as guanidine-soluble fraction) by shaking at room temperature  $\geq 4$ h and then centrifuged as before (at  $16,000 \times g$  and 4 °C, 30 min) (Figure 3.6). The protein concentration of all samples was measured using the Bio-Rad Protein Assay. A $\beta$  concentration in three different fractions of brain homogenates was determined by A $\beta$ 40/42 ELISA kits (see below).

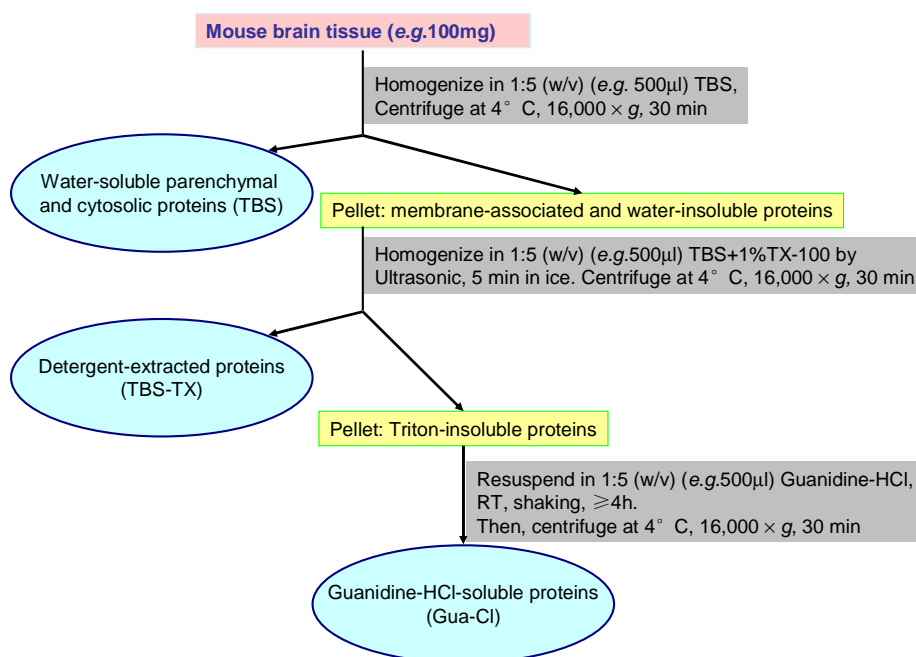


**Figure 3.6. Schematic figure of brain homogenates preparation (Modified from reference (Mc Donald *et al.*, 2010)).** Serial extraction of water-soluble, detergent-soluble and Guanidine-HCl-soluble A $\beta$ . Human brain tissue was homogenized in 5 volumes of Tris-buffered saline (TBS), centrifuged at 16, 000  $\times$ g for 30 min and the supernatant was designated as the TBS extract. The pellet was re-homogenized in 5 volume of Tris-buffered saline containing 1% TX-100 (TBS-TX), centrifuged and the supernatant removed (TBS-TX extract). The remaining pellet was then extracted in 5 volume 5 M guanidine-HCl/ 50 mM Tris, pH 8.0, centrifuged and the supernatant removed (Gua-Cl extract).

### 3.2.16 Bio-Rad Protein Assay

Protein concentration Bio-Rad Assay was completed with Protein Assay Reagent (Bio-Rad), based on the Bradford dye-binding procedure (Bradford, 1976), a simple colorimetric assay for measuring total protein concentration. Protein concentrations between 200  $\mu$ g/ml and 1,400  $\mu$ g/ml (20-140  $\mu$ g totals) can be assayed in a microplate format. Briefly, in high-concentration assay, 10  $\mu$ l sample or serial diluted standards were loaded on a 96-well format microplate, and then 200  $\mu$ l 1 $\times$  assay reagent was added to each well. Absorption at 595 nm was read with a Micro-plate reader and protein concentration was determined according to a standard curve.

### 3.2.17 A $\beta$ ELISA

A $\beta$ 1-40 and A $\beta$ 1-42 concentrations in three different fractions of brain homogenates were determined by A $\beta$ 42/40 ELISA kits (both from Invitrogen). Procedure is as follows:

1. Prepare samples and through serial dilution prepare the following A $\beta$ 1-40/ A $\beta$ 1-42 standards: 250, 125, 62.5, 31.25, 15.63, 7.81, and 0 pg/ml Hu A $\beta$ 40/ A $\beta$ 42.

2. Add 50  $\mu$ l of A $\beta$ 1-40/ A $\beta$ 1-42 peptide standards, controls, and samples to each plate well.
3. Add 50  $\mu$ l of anti-Hu A $\beta$ 40/ A $\beta$ 42 (Detection Antibody) solution to each well. Cover plate with plate cover and incubate for 3 hrs at room temperature with shaking.
4. Thoroughly aspirate solution from wells and discard the liquid. Wash wells 4 times.
5. Add 100  $\mu$ l Anti-rabbit Ig's-HRP Working Solution to each well. Cover plate with the plate cover and incubate for 30 min at room temperature.
6. Thoroughly aspirate solution from wells and discard the liquid. Wash wells 4 times.
7. Add 100  $\mu$ l of Stabilized Chromogen to each well. The liquid in the wells will begin to turn blue. Incubate for 30 min at room temperature and in the dark.
8. Add 100  $\mu$ l of Stop Solution to each well. Tap side of plate gently to mix. The solution in the wells would change from blue to yellow.
9. Read the absorbance of each well at 450 nm having blanked the plate reader against a chromogen blank composed of 100  $\mu$ l each of Stabilized Chromogen and Stop Solution. Read the plate within 30 min after adding the Stop Solution.
10. Use curve fitting software to generate the standard curve. Read the concentrations for test samples and controls from the standard curve. Multiply value(s) obtained for sample(s) by the appropriate factor to correct for the sample dilution.

### **3.2.18 Barnes maze test**

The cognitive function of recipient APP<sup>swe</sup>/PS1<sup>dE9</sup> mice 1 year post bone marrow transplantation was tested with Barnes Maze using the established protocol (O'Leary *et al.*, 2009; Hao *et al.*, 2011). The test involved 5 days of acquisition training with two trials per day. For each trial, the mouse was placed at the center of the maze. After 5-10 sec, the mouse was allowed to run on the platform freely until reaching the escape hole. In order to reduce the stress for mice, no extra aversive stimuli were given. For each trial, latency to enter the escape hole and distance travelled were recorded by EthoVision® XT (V7.0) tracking software. In the end, the latency and total distance were averaged from the two trials per day for statistical analysis.

### **3.2.19 Immunofluorescence staining of NeuN on paraffin brain sections**

The PFA-fixed brain was embedded in paraffin (A. Schottek helped with embedding work) and serial 2  $\mu$ m-thick sagittal sections were cut and mounted on glass slides. In order to investigate the neuronal loss, the slides were stained with NeuN antibody, a neuron-specific

protein restricted to nuclei in most vertebrate CNS and PNS neuronal cell types (Mullen *et al.*, 1992):

1. Deparaffinization:

Xylol	5 min
Xylol	5 min
Ethanol 100%	5 min
Ethanol 100%	5 min
Ethanol 96%	3 min
Ethanol 70%	3 min
Ethanol 50%	3 min
dH <sub>2</sub> O	dip

2. Antigen retrieval by cooking the sections in 1× citrate buffer (10 mM pH6.0) in a microwave oven, 560 watts, 3 min × 7 times. Refill with buffer between each cooking. Cool down slowly by leaving on the bench for >30 min after cook
3. Wash with dH<sub>2</sub>O, dip, 3 times
4. Block with blocking buffer (5% Goat serum, 0.1% Tween-20, 0.1% Triton-X, in 1× PBS), RT, 1 h
5. 1<sup>st</sup> Antibody reaction: with 1:50 dilution of mouse anti-NeuN monoclonal antibody (Millipore), in dilution buffer (1% Goat serum, 0.1% Tween-20, 0.1% Triton-X, in 1× PBS), incubate at 4°C, overnight. Antibody: 1:50 dilution of 1 mg/ml stock, 4 °C, overnight
6. Wash with PBS 5 min, 2 times, then with PBS/TritonX 5 min, 1 time
7. 2<sup>nd</sup> Antibody reaction: with the 1:150 diluted Cy3 conjugated goat-anti-mouse antibody (final concentration 5 µg/ml), 37 °C, 1 h
8. Wash with PBS, 5 min, 3 times
9. Counterstain with DAPI (1:1000) in PBS, RT, 5 min
10. Wash: with aqua dest, 3 times
11. Mount with Mowiol
12. Observe under Eclipse E600 fluorescence microscope. NeuN positive cells in the CA3 region of hippocampus were counted.

### 3.2.20 Western blot analysis of PSD-95

PSD-95 in the brain homogenate (TBS-TX fraction) was detected by Western blot using mouse anti-PSD-95 monoclonal antibody (clone 6G6-1C9, abcam, Cambridge, UK) according to the established protocol (Pham *et al.*, 2010). Mouse α-tubulin was detected as a loading control using the DM1A antibody (Abcam):

### 3.2.20.1 Sodium dodecyl sulfate-polyacrylamide gel electrophoresis

The sodium dodecyl sulfate-polyacrylamide gel electrophoresis (SDS-PAGE) technique separates proteins according to their mobility difference in an electric field. Protein samples treated with SDS show an identical charge per unit mass and migrate in SDS gels only according to their molecular masses.

The SDS-PAGE system used in this study is the Mini-PROTEAN® 3 Cell electrophoresis system (Bio-Rad). One gel is composed of a lower separating gel and an upper stacking gel. The stacking gel is 4%, while the percentage of the separating gel varies from 8% to 15%. Low percentage gels are used for large proteins, while small proteins are separated in high percentage gels. In this study, 12% separating gel was used.

The gel and the electrodes were assembled in the SDS-PAGE chamber. The brain homogenate samples were diluted 1:1 in 2 × SDS-PAGE Sample loading buffer and heated at 95°C for 5min. Then, 20 µl sample per well was loaded to 12% Acrylamide gel for electrophoresis running at 100 V until the Bromophenol blue front runs out of the gel.

Proteins on the gel were transferred to NC membranes and detected by immunoblotting.

Recipe:

Separating gel 12%

ddH <sub>2</sub> O	2	ml
Acrylamide;bisacrylamide 30%	4	ml
Tris-Cl 1 M pH9.2	3.75	ml
SDS 10%	100	µl
Ammonium persulfate (APS) 25%	15	µl
TEMED(N, N, N', N'-tetramethylethylenediamine)	15	µl

Stacking gel 5%

ddH <sub>2</sub> O	3.5	ml
Acrylamide;bisacrylamide 30%	810	µl
Tris-Cl 1M pH6.8	625	µl
SDS 10%	50	µl
Ammonium persulfate 25%	10	µl
TEMED	10	µl

SDS-PAGE electrophoresis buffer 10 × (1Liter):

Chemical	Con. In 10 × buffer	Amount
Tris-base	0.25 M	30.3 g
Glycine	1.92 M	144.1 g

SDS	1%	10 g
ddH <sub>2</sub> O		Until 1 liter
Store at 4 °C. Dilute to 1x for working solution		

2× SDS-PAGE sample Loading Buffer:

1 M Tris-Cl (pH 6.8)	6.25 ml
80% Glycerol	6.25 ml
10% SDS	10 ml
2-Mercaptoethanol	2.5 ml
0.05% (w/v) bromophenol blue	2.5 ml
ddH <sub>2</sub> O	22.5 ml
Total	50 ml

### 3.2.20.2 Protein detection using immunoblotting

Proteins separated by SDS-PAGE were further transferred to a nitrocellulose (NC) transfer membrane (Whatman) with a pore size of 0.20 µm via a Mini Trans-Blot cell (Bio-Rad) system. The SDS gel was loaded into a blotting sandwich, which consists of, starting from Negative charge pole to Positive charge pole: sponge, Whatman paper, SDS gel, NC membrane, Whatman paper, sponge. Sponges and Whatman papers were all rinsed with transfer buffer before assembling. Air bubbles between the SDS gel and the NC membrane were expelled before packing. Proteins were transferred to the NC membrane by running the system at 0.1 mA per cm<sup>2</sup> membrane for 75 min with cooling. The NC membrane was unpacked from the sandwich after running and incubated with the blocking buffer at room temperature for 60 min followed by washing with TBST 5min × 3times. Then, the membrane was incubated with the 1/2000 dilution from stock 1<sup>st</sup> antibody mouse monoclonal [6G6-1C9] IgG2a to PSD-95 (abcam) in blocking buffer at 4 °C overnight. The tracing unbound antibody was rinsed 5 min × 8 times with TBST. The membrane was then incubated with the 1/2000 diluted horseradish peroxidase conjugated 2<sup>nd</sup> goat anti-mouse antibody (Dako) at room temperature for 2 hours. After washing, the same as for the 1<sup>st</sup> antibody, drain washing buffer, add western lightning solution (1:1 mixture of Oxidizing reagent plus and Enhanced luminal reagent plus, Perkin Elmer) and develop for 1 min. Expose the developed NC membrane to a high performance chemiluminescence film (GE healthcare) for 1-30 min. The film was visualized by proceeding with Kodak GBX Developer and Fixer solution.

The same membrane was washed 5 × 5 min with TBST, and blocked in 5% non-fat milk in PBS overnight. The membrane was developed for α-tubulin using α-Tubulin antibody (mouse monoclonal, DM1A) (abcam) (1:10,000 in 5% non-fat milk PBS) at RT for 2 h.

The densitometry of the PSD-95 lanes and the  $\alpha$ -tubulin lanes were quantified with Image J software. The ratio of PSD-95/ $\alpha$ -tubulin density represents the relative PSD-95 level in original samples.

Buffer recipe:

PBST:	NaCl	155	mM
	NaH <sub>2</sub> PO <sub>4</sub>	2.5	mM
	Na <sub>2</sub> HPO <sub>4</sub>	10	mM
	TWEEN 20	0.25	% (v/v)
Dissolve in diH <sub>2</sub> O, pH 7.3, filter-sterilize.			

Blocking buffer:	Milk powder	5	% (w/v)
Resuspend in PBS buffer, pH 7.3.			

10× Membrane transfer buffer stock (4° C)

Tris-base	30.3 g
Glycine	144.1 g
ddH <sub>2</sub> O	Until 1 liter

1× Membrane transfer buffer from 10× stock

10× transfer buffer stock	100 ml
ddH <sub>2</sub> O	500 ml
Ethanol	200 ml
ddH <sub>2</sub> O	Until 1 liter

Blocking buffer:

Nonfatty milk	5 g
PBS	100 ml
Mix until the milk dissolved	

10× TBS (tris-saline) buffer:

Tris base	6.05 g
NaCl	43.9 g
ddH <sub>2</sub> O	Until 500 ml

### 3.2.21 Statistics

Data shown in the result figures are presented as mean  $\pm$  SD (for *in vitro* data) or mean  $\pm$  SEM (for *in vivo* data). For multiple comparisons, one-way or two-way ANOVA followed by Bonferroni's, Tukey's Honestly Significant Difference or Tamhane's T2 post hoc test

(dependent on the result of Levene's test to determine the equality of variances) was applied. Two-independent-samples t-test was used to compare means for two groups of cases. All statistical analysis was performed on Statistical Package for the Social Sciences 15.0 for Windows (SPSS, Chicago). Statistical significance was set at  $p < 0.05$ .

## 4 Results

### 4.1 TLR2 is a primary receptor for A $\beta$ 42 to trigger inflammatory activation

#### 4.1.1 *Tlr2*-deficiency reduces A $\beta$ 42-induced inflammatory activation in microglia and macrophages

Microglia are the resident macrophages in the CNS and play a major role in the neuroinflammatory activation, especially under pathological conditions (Nguyen *et al.*, 2002). TLR2 has been observed to be involved in A $\beta$ -triggered microglial inflammatory activation (Jana *et al.*, 2008; Richard *et al.*, 2008; Reed-Geaghan *et al.*, 2009). Our previous study showed that deficiency of MyD88, the most common signaling adaptor molecule in the toll-like receptor-mediated innate immune response, in macrophages decreased A $\beta$ -triggered inflammatory activation (Hao *et al.*, 2011). Here, in a cell culture system, whether TLR2 deficiency reduces A $\beta$ -triggered inflammatory activation was first tested. Microglia and bone marrow-derived macrophages (may reflect microglial precursor cells (Priller *et al.*, 2001)) were cultured and stimulated with TLR2 ligand Pam3CSK4 or aggregated A $\beta$ 42. Indeed, *tlr2*-deficient microglia (Figure 4.1A-B) or macrophages (Figure 4.1C) secreted significantly less TNF- $\alpha$  (Figure 4.1A,C) or IL-1 $\beta$  (Figure 4.1B) as compared to wild-type control cells after stimulation with 5 or 10  $\mu$ M oligomeric A $\beta$  aggregates, or Pam3CSK4 positive control ligand, suggesting that TLR2 mediates the A $\beta$  inflammatory recognition. This result correlates with the previous observation that TLR2 gene-silencing reduced inflammatory gene transcription in microglia upon A $\beta$  activation (Jana *et al.*, 2008).

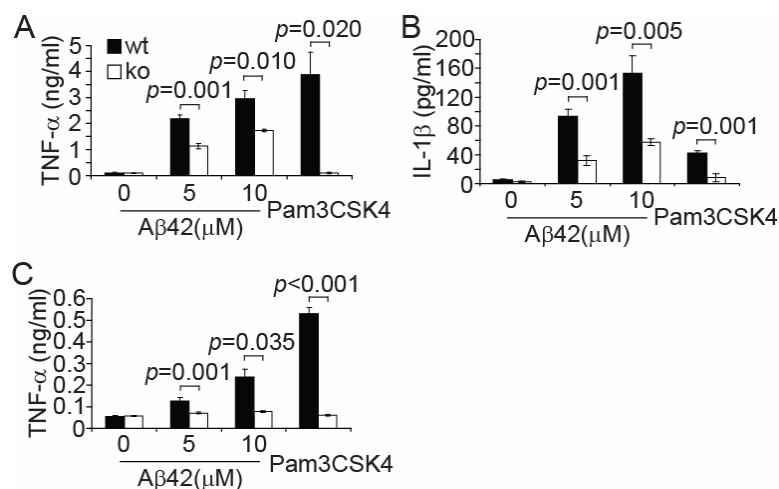


**Figure 4.1. *Tlr2*-deficiency reduces A $\beta$ -induced inflammatory cytokine secretion in microglia and macrophages.** Primary cultured microglia (A-B, n=5) and bone marrow-derived macrophages (BMDMs) (C, n=7) derived from wild-type (wt) or *tlr2*-deficient (ko) mice were challenged with 5 and 10  $\mu$ M A $\beta$ 42 aggregates and 10 ng/ml (for microglia) or 100ng/ml (for BMDMs) Pam3CSK4 for 24 hrs. The supernatants were then collected for the measurements of TNF- $\alpha$  (A, C) and IL-1 $\beta$  (B) with ELISA kits (Data are the means  $\pm$  SD, n $\geq$ 5).

#### 4.1.2 TLR2 co-localizes with A $\beta$ in A $\beta$ -treated microglia

It is hypothesized in this study that TLR2 is a primary receptor of A $\beta$ , thus, the spatial relationship between TLR2 and A $\beta$  on microglia was investigated under confocal microscopy. Thirty minutes after the treatment of aggregated A $\beta$ 42, TLR2 and A $\beta$  were co-stained with corresponding antibodies. The co-localization of TLR2 and A $\beta$  was observed as the overlap between two different fluorophores which were conjugated to TLR2 and A $\beta$ , respectively (Figure 4.2).

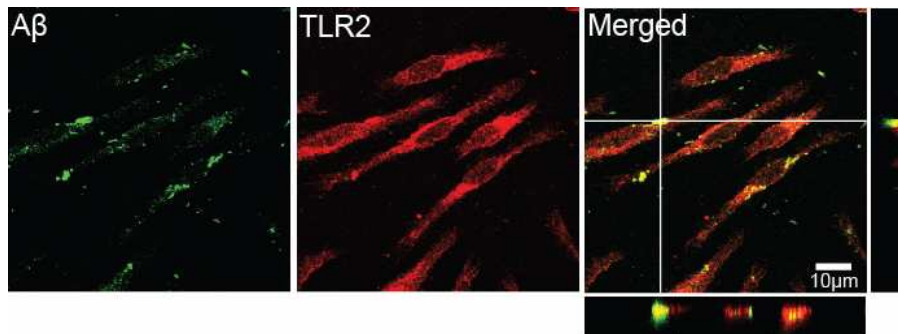


**Figure 4.2. A $\beta$  co-localizes with TLR2 in microglial cells upon incubation with A $\beta$ .** Primary microglia were incubated with aggregated A $\beta$ 42 for 30 min and then fixed for the immunofluorescent staining with antibodies against TLR2 (in red) and A $\beta$  (in green) as described in the methods section. Under confocal microscopy, co-localization of A $\beta$  and TLR2 was shown in yellow colour.

#### 4.1.3 TLR2 directly binds to A $\beta$

In order to study the direct interaction between A $\beta$  and TLR2, real-time surface plasmon resonance spectroscopy (Biacore) was applied. Soluble C-terminus 10  $\times$  His-tagged TLR2, TLR1 or TLR3 and IGF-1R, as a reference receptor, were immobilized in the two paralleled flow cells of the NTA sensor chip. Aggregated A $\beta$ 42 or control peptide A $\beta$ 1-42 was simultaneously injected into these two flow cells. A clear and strong response indicating A $\beta$  binding to the receptor was observed in the TLR2-immobilized flow cell, but not in the TLR control receptors, TLR1 and TLR3 immobilized flow cells. The different response units between TLR2 and IGF-1R flow cells (FC1-FC2) are shown in Figure 4.3 (Figure 4.3 B, D); while no significant response was observed in the TLR1 or TLR3 channel (Figure 4.3 A, C, D). In the control experiment, A $\beta$ 42-1, instead of A $\beta$ 42 was injected to the flow phase. No responsive difference in the two paralleled flow cells was observed (Figure 4.3 A-D).

In order to further study the binding between A $\beta$ 42 and TLR2, a pull-down assay was performed. A $\beta$ 42 aggregates were incubated with TLR2 and IGF-1R tagged with 10  $\times$  His on the C-terminus. Then, the solution was loaded on Ni-NTA spin columns. After thoroughly washing, the complex of A $\beta$ 42 and receptor was eluted and detected with Western blot as described in the method section. As shown in Figure 4.3E and F, the A $\beta$ 42 from the A $\beta$ -

TLR2-loaded column was significantly more than that from the A $\beta$ -IGF-1R-loaded column ( $p < 0.05$ , Figure 4.3 E-F) or from the A $\beta$ 42 aggregates direct load non-receptor blank control column (Figure 4.3E). The blot with anti-His antibody showed that the amount of eluted receptors is comparable. Unfortunately, this assay was not able to tell which species of A $\beta$  does TLR2 bind, since aggregated A $\beta$  eluted from the Ni-NTA spin columns in this assay seems to under go a deaggregation process: the only A $\beta$  species found in the elutes was monomeric. This might be due to the NTA and high imidazole level (500mM) presented in the system, as they may affect the histidine imidazole rings that are important for the formation of A $\beta$  oligomers and fibrils (Dong *et al.*, 2003; Sarell *et al.*, 2009).

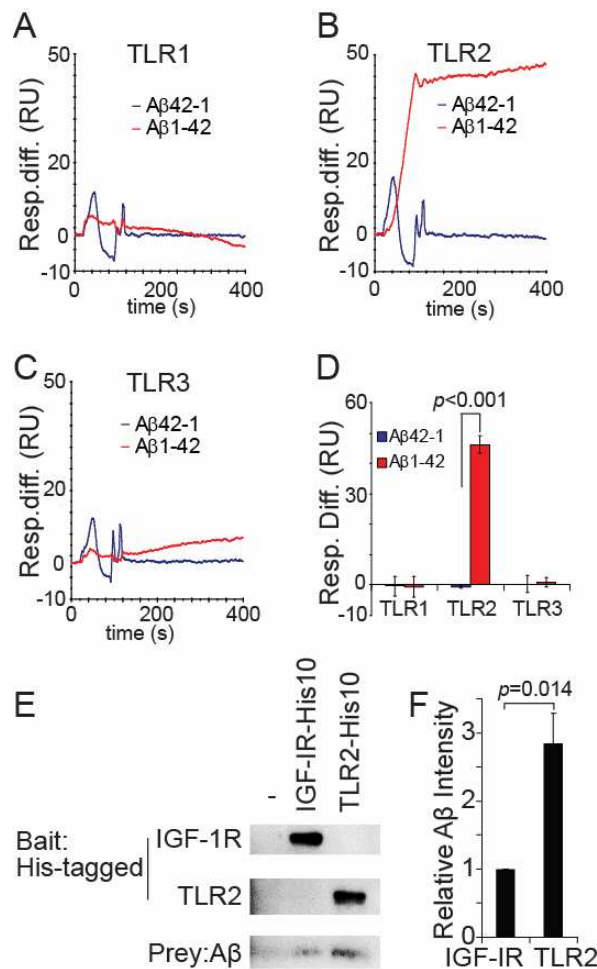


**Figure 4.3. TLR2 directly interacts with A $\beta$ .** (A-D), the interactions between TLR1/TLR2/TLR3 and A $\beta$ 42 aggregates were studied with Biacore J. The response difference (Resp. Diff) between flow cell 1 (FC1) immobilized with TLR1 (A), TLR2 (B) or TLR3 (C) and FC2 immobilized with IGF-1R (FC1-FC2) are shown by sensorgrams (A-C) after loading A $\beta$ 42 or A $\beta$ 42-1 in the flow phase. The “Resp. Diff” at the steady stage is summarized and presented in bars (D). The response due to the interaction between TLR2 and A $\beta$ 42 was markedly larger than that upon interaction of TLR2 and A $\beta$ 42-1 ( $p < 0.001$ ,  $n = 6$ ) (B, D). (E-F), Direct binding of TLR2 and A $\beta$ 42 was further proven by a pull-down assay. Aggregated A $\beta$ 42 was incubated with TLR2 or IGF-1R tagged with His on C-terminal and then loaded onto Ni-NTA spin columns. After washing, A $\beta$ 42 was eluted and detected with immunoblot (E). The amount of A $\beta$  was quantified using densitometric analysis (F). (Data are the means  $\pm$  SD,  $n = 6$ ; A-C and E are representatives of the independent experiments).

#### 4.1.4 TLR2 expression enables HEK-293 cells to respond to A $\beta$ challenge

HEK-293 cells, which do not endogenously express TLR2 (Brightbill *et al.*, 1999; Walter S *et al.*, 2007), do not respond to A $\beta$  (Walter S *et al.*, 2007). Interestingly, after over-expressing TLR2 in HEK-293 cells, it was observed that IL-8 secretion, which indicates a cellular inflammatory response, was induced 24 hours post-treatment with aggregated A $\beta$ 42. Neither mock transfection nor control receptor CD44 over-expression caused IL-8 release ( $p < 0.001$ ) (Figure 4.4).

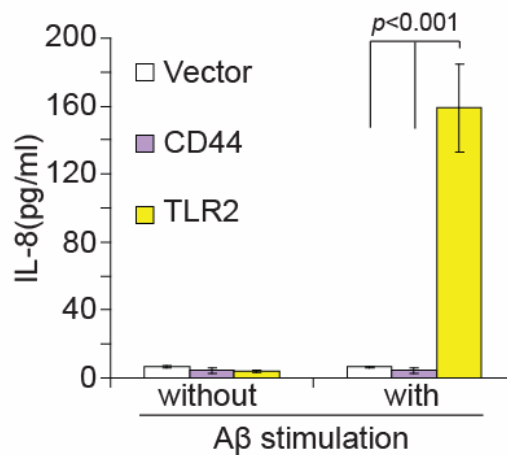


**Figure 4.4. TLR2 expression confers HEK-293 cells to secrete inflammatory cytokine upon A $\beta$  challenge.** HEK-293 cells were engineered to stably express TLR2 or control receptor CD44. The cells were stimulated with 10  $\mu$ M A $\beta$  for 24 hrs, the IL-8 level in the supernatants was determined through ELISA (Data are the means  $\pm$  SD, n=3).

However, the A $\beta$ 42 peptides used in this study were a mixture of monomeric, oligomeric and fibril A $\beta$ 42, although enriched in oligomeric aggregates (see material section 3.2.2 and Figure 3.1). Due to the technical limitation, specific A $\beta$ 42 species was not purified and used in this study. Thus, it is not clear which species of A $\beta$ 42 interacted with TLR2 and activated the inflammatory signaling cascade.

## 4.2 Molecular mechanisms of TLR2 in A $\beta$ -triggered inflammatory signaling

### 4.2.1 TLR1 enhances whereas TLR6 suppresses TLR2-mediated A $\beta$ -triggered inflammatory activation

Typical TLR2 recognition is in co-operation with TLR1 (for triacylated lipopeptides) or TLR6 (for diacylated lipopeptides) (Medzhitov *et al.*, 1997a; Jin *et al.*, 2008a). However, which co-receptor, TLR1 or TLR6, may co-operate with TLR2 in A $\beta$  recognition was not known. To address this, HEK-293 cell lines expressing TLR2 and TLR1, TLR2 and TLR6, TLR2, TLR1 or TLR6 were established. The TLR2 expression level was comparable as

confirmed by TLR2 immunoblot (Figure 4.5A). These cell lines were challenged with aggregated A $\beta$ 42. As shown in Figure 4.5B, HEK-293 cells expressing TLR1 or TLR6 alone did not respond to A $\beta$  as indicated by IL-8 release. IL-8 release in TLR2 and TLR1 co-expressing cells was significantly increased ( $p=0.028$ ); whereas, IL-8 production in TLR2 and TLR6 co-expressing cells was reduced ( $p<0.001$ ) compared to the TLR2 alone expressing cells. In order to further confirm this finding, the *tlr1*, *tlr2* or *tlr6* gene expression in the macrophage cell line, RAW264.7 cells was knocked down using interference RNA (Figure 4.5C). Accordingly, the TNF- $\alpha$  secretion was reduced in the *tlr2*-silenced cells (Figure. 4.5D,  $p=0.018$ ), whereas it was increased in the *tlr6*-silenced macrophages (Figure 4.5D,  $p<0.001$ ).

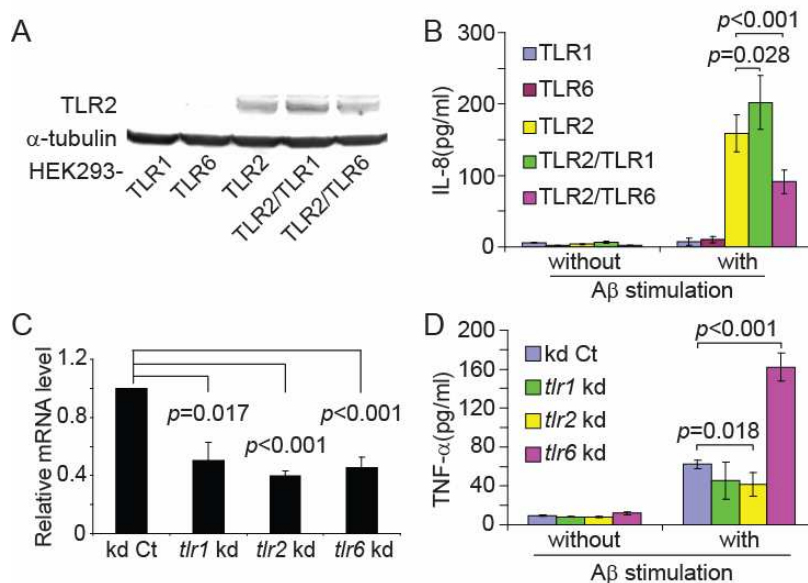


**Figure 4.5. Toll-like receptor 1 enhances whereas Toll-like receptor 6 suppresses the TLR2-mediated A $\beta$ -triggered inflammatory activation.** (A) Western blot confirmed the TLR2 expression in the HEK-293 cell lines constructed to express TLR2, TLR1, or TLR6 alone, or co-expressing TLR2-TLR1 or TLR2-TLR6. (B) The HEK-293 cell lines as shown in (A) were stimulated with 10  $\mu$ M aggregated A $\beta$ 42 for 24 hrs, the inflammatory cytokine IL-8 level in the supernatants was determined through ELISA. (C) In RAW264.7 cells, *tlr1*, *tlr2* and *tlr6* expression were silenced down by introducing stealth siRNA specific for mouse *tlr1*, *tlr2*, *tlr6*. The knock down effect was confirmed through realtime PCR: the *tlr1*, *tlr2*, and *tlr6* mRNA relative level in the corresponding silenced cells were detected. (D) RAW264.7 cells knocking down of *tlr1*, *tlr2* or *tlr6* as shown in (C) were stimulated with 10  $\mu$ M A $\beta$  for 24 hrs; the inflammatory cytokine TNF- $\alpha$  level in the supernatants was determined through ELISA (Data are the means  $\pm$  SD,  $n=4$ ).

#### 4.2.2 Extra cellular LRR domains on TLR2 are essential for ligand recognition

After found that TLR2 mediated A $\beta$ -initiated inflammatory activation in co-operation with TLR1, this study further investigated the detailed mechanisms mediating the A $\beta$  recognition. The precursor of human TLR2 contains 784aa including a signal sequence (aa1-18), an extracellular domain (aa19-588), a transmembrane segment (aa589-609) and a cytoplasmic TIR domain (aa610-784). In the extracellular domains of TLR2, TLR1 and TLR6, as aligned with ClustalW program (Figure 4.7) and reported (Meng *et al.*, 2003; Grabiec *et al.*, 2004;

Omueti *et al.*, 2005; Kang *et al.*, 2009), there are approximately 20 LRR modules, in which LRR7-10 in TLR2, LRR9-12 in TLR1 and LRR11-14 in TLR6 were reported to play crucial roles in the lipopeptide recognition (Figure 4.7). The crystal structures of TLR2-TLR1 and TLR2-TLR6 heterodimers with ligands suggest that the lipopeptide-binding sites of TLR2 are at the convex region formed at the border of central and C-terminal domains opening into a crevice that is connected to a large internal pocket. The heterodimeric interface of TLR1-TLR2 is from H318 to H398 on TLR2 and P315 to Q383 on TLR1 (Figure 4.6) located in the LRR11-14 region for both receptors (Figure 4.7) (Jin *et al.*, 2007). The heterodimeric interface of TLR6-TLR2 is from H318 to K404 on TLR2 and H311 to K390 on TLR6 (Figure 4.6), also locate in the LRR11-14 region for the receptors (Figure 4.7) (Kang *et al.*, 2009). Thus, potential important LRRs in TLR2, TLR1 and TLR6 were screened by constructing expression vectors with deletion of sequences encoding LRR3-4, LRR7-9, LRR10-11, LRR12-14 or LRRCT in TLR2, TLR1 and TLR6. TLR2 mutants were expressed alone or with wild-type TLR1. TLR1 and TLR6 mutants were co-expressed with wild-type TLR2 in HEK-293 cells. As shown in Figure 4.8A, following the treatment with Pam3CSK4 and Pam2CSK4, all of the studied TLR2 LRRs are essential for ligand recognition, as deletion of any studied LRR in TLR2 abolished IL-8 production, either in TLR2-expressed cells or in TLR2-TLR1 co-expressed cells. LRRs of TLR1 and TLR6 were relatively less important. With the exception of the deletion of LRR12-14 or LRRCT on TLR1 resulting in a decreased response upon Pam3CSK4 challenge, deletion of other LRRs in TLR1 and TLR6 did not induce significant changes upon the ligand challenge (Figure 4.8B).

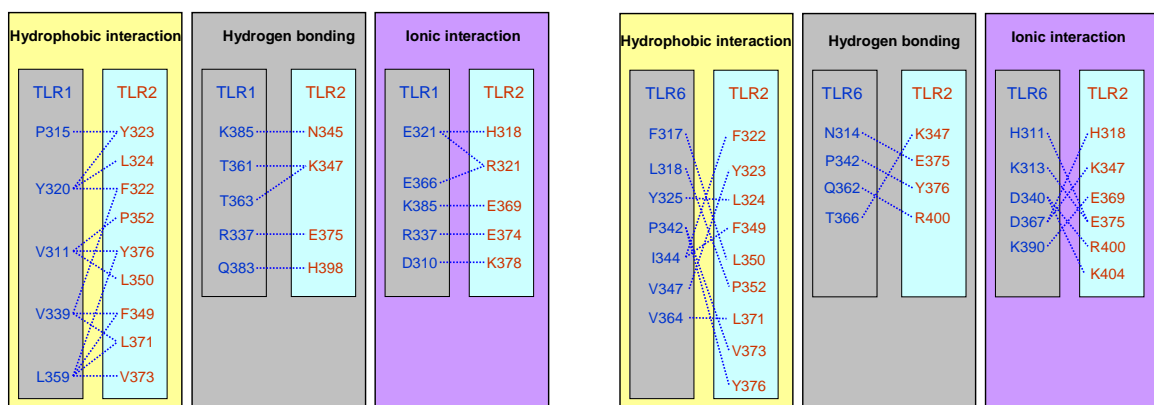


**Figure 4.6. Schematic of the TLR2 and TLR1/TLR6 interaction interface.** The interacting amino acids are sorted according to the interacting force. Interacting Region where interacting residues in the TLR1 and TLR2 (left), TLR6 and TLR2 (right) interface are linked by broken lines, summarized from references (Jin *et al.*, 2007; Kang *et al.*, 2009).

Domain	Receptor	Sequence	Position	Consensus
N-terminal domain	LRRNT			
	hTLR2	QASLSCDRNGICKGSSGSLNSIPSG	49	
	hTLR1	SEFLVDRSKNGLIHVPKD	42	
	hTLR6	RIQFSDGNEFAVDKSKRGLIHVPKD	49	
	LRR1	xLxxLxxLxLxxN		
	hTLR2	LTEAVKSLDLSNNRITYISNSDLQ	73	
	hTLR1	LSQKTTLNISQNYISELWTSIDL	66	
	hTLR6	LPLKTKVLDMSQNYIAELQVSDMS	73	
	LRR2	xLxxLxxLxLxxN		
	hTLR2	RCYNLQALVLTNSGINTIEEDSFS	97	
	hTLR1	SLSKLRILIIHSHNRIQYLDISVFK	90	
	hTLR6	FLSELTVLRSLSHNRIQLDLSVFK	97	
	LRR3	xLxxLxxLxLxxN		
	hTLR2	SLGSLLEHLDSLNYLSNLSVSWFK	121	
	hTLR1	FNQLEYLELDLSHNKLVKISCH	111	
	hTLR6	FNQDLEYLDLSHNQLQKISCH	118	
	LRR4	xLxxLxxLxLxxN		
	hTLR2	PLSSTLFLNLLGNPYKTLGETSLFS	146	
hTLR1	PTYNLKHLDLDFNAFDALPICKEFG	136		
hTLR6	PIVSFRHLDLDFNDFKALPICKEFG	143		
C-terminal domain	LRR5	xLxxLxLx		
	hTLR2	HLTKLQILRVGNMDFTKIQRKDFDA	171	
	hTLR1	NMSQLKFLGLSTTHLEKSSVLP	159	
	hTLR6	NLSQLNFLGLSAMPLQKLDLLPI	166	
	LRR6	xLxxLxLx		
	hTLR2	GLTFLEELIDASDLQSYEPKSLK	195	
	hTLR1	AHLNISKVLLVLGETYGEKEDPEGL	184	
	hTLR6	AHLHLSYILDLRNYIYIKENETESL	191	
	LRR7	xLxxLxLx		
	hTLR2	SIQNVSHLILHMKQHILLLEIFVD	219	
	hTLR1	QDFNTESLHIVFPTNKEFHFDLV	208	
	hTLR6	QILNAKTLHLVHPTSLFAIQVNI	215	
	LRR8	xLxxLxLx		
	hTLR2	VTSSVECLELRDLDLTFHFSELSTGE	246	
	hTLR1	SVKTVANLELSNIKCVLEDNKCSYFLSILAKLQ	241	
	hTLR6	SVNTLGLCQLTNIKLNDNQCQVFIKSELT	246	
	LRR9	xLxxLxLx		
	hTLR2	TNSLIKFKFTFRNVKITDESLEFQVMKLLN	274	
hTLR1	KNLKLNSLTLNNTVETTWNSFINILQLV	268		
hTLR6	RGPTLLNFTLNHIETTWKLCVRVFQFL	273		
LRR10	xLxxLxLx			
hTLR2	QISGLLELEFDDCTLNGVGNFRASDNDRVI	304		
hTLR1	WHTTVWYFISISNVKLGQLDFRDFDY	294		
hTLR6	WPKPVEYLNINYNTIIESIREEDFTY	299		
LRR11	xLxxLxLx			
hTLR2	DPGKVELTIRRLHIPRFYLFYDLSTLYS	333		
hTLR1	SGTSLKALSIHQVSDVFGFPQSYIYEIF	323		
hTLR6	SKTTLKALTEIHTNQVFLFSQTALYTVF	328		
LRR12	xLxxLxLxxN			
hTLR2	LTERVKRITVENS <b>KVFLVPC</b> LLSQ	357		
hTLR1	SNMNIKNFTVSGTR <b>RMV</b> HMLCP5	345		
hTLR6	SEMNIIMLTISDTPFIHMLCPH	350		
LRR13	xLxxLxLxxN			
hTLR2	HLKSLYLDLS <b>ENLMVEEYLK</b> NSACED	384		
hTLR1	KISPFLLHDFSNLL <b>DTVF</b> ENCG	369		
hTLR6	APSTFKFLNFTQNVFTDSIFEKCS	374		
LRR14	xLxxLxLxxN			
hTLR2	AWPSLQTLILRQN <b>HLASLE</b> KTGETLL	410		
hTLR1	HLTELETLILQMN <b>QLKEL</b> SKIAEMTT	395		
hTLR6	TLVKLETILQKNGKLDLKFVGLMTK	400		
LRR15	xLxxLxLxxN			
hTLR2	TLKNTLNDISKNSFHSMPETCQ	433		
hTLR1	OMKSLLOOLDISONSVSVDYDEKKGDCS	420		
hTLR6	DMPSEILDYSWNSLESGRHKENCT	425		
LRR16				
hTLR2	WPEKMKYLNLSSTRIHVSVTGC	454		
hTLR1	WTKSLLLSNMNSNLTDTIFRC	442		
hTLR6	WVESIVVLNLSNMLTDSVFRC	447		
LRR17	xLxxLxLxxN			
hTLR2	IPKTEILDVSNNNLNLFSL	474		
hTLR1	LPPRIKVDLHNSNKIKSIPKQV	465		
hTLR6	LPPRIKVDLHNSNKIKSVPKQV	470		
LRR18	xLxxLxLxxN			
hTLR2	NLPQLKELYISRNKLMTPDAS	496		
hTLR1	KLEALQELNVAFNLSLTDLPGCC	487		
hTLR6	KLEALQELNVAFNLSLTDLPGCC	492		
LRR19	xLxxLxLxxN			
hTLR2	LLPMLLVKISRNAITTFEKEQLD	520		
hTLR1	SFSSLSVLIIHNSVSHPSADFFQ	511		
hTLR6	SFSSLSVLIIHNSVSHPSADFFQ	516		
LRR20	xLxxLxLxxN			
hTLR2	SFHTLKTLEAGGNNFI	536		
hTLR1	SCQKMRSIKAGDNPFFQ	527		
hTLR6	SCQKMRSIKAGDNPFFQ	532		
LRRCT				
hTLR2	CSCEFLSFTQEQAALAKVLIDWPANY	562		
hTLR1	CTCELGEFVKNIQVSSVLEGWPDY	554		
hTLR6	CTCELREFVKNIDQVSSVLEGWPDY	559		
LRRCT				
hTLR2	LCDSPSHVRGQQQVDVRLSVSECHRT	588		
hTLR1	KCDYPESYRGTLLKDFHMSSELSNIT	580		
hTLR6	KCDYPESYRGSPLKDFHMSSELSNIT	585		

x Dimerization  
 x Ligand binding  
 x Ligand binding & dimerization

**Figure 4.7. Sequence alignment of the ectodomains of human TLR1, TLR2, and TLR6.** Human TLR1, TLR2, and TLR6 extracellular sequences are aligned with ClustalW program. The consensus patterns (Kang *et al.*, 2009) are shown above the sequences. Based on crystal structure reports (Jin *et al.*, 2007; Kang *et al.*, 2009), the residues for extracellular TLR2-TLR1/6 dimerization are in red; residues for ligand binding are in green; residues for both receptor dimerization and ligand binding are in bold italic red.

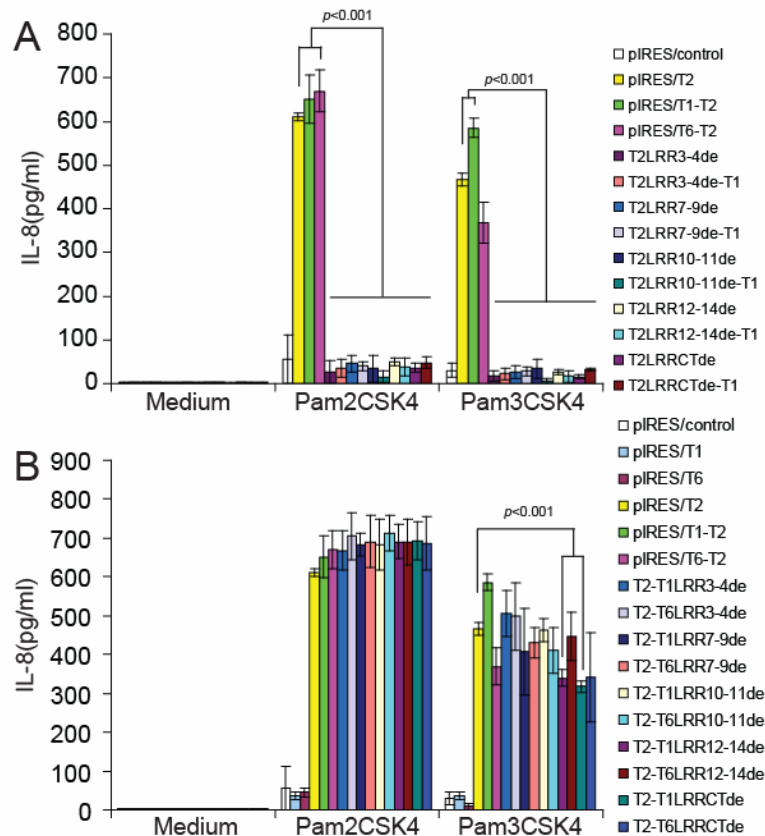


**Figure 4.8. TLR2 extracellular LRRs are essential for ligand recognition and LRRs of TLR1, TLR6 modulate the recognition.** HEK-293 cells were transfected to express TLR2 alone or co-express TLR1 or TLR6 with indicated LRRs deleted. The cells were stimulated with 100 ng/ml Pam2CSK4 or Pam3CSK4 for 24 hrs, IL-8 in the supernatants was determined via ELISA. (A) Any of the TLR2 LRRs deletion resulted in impaired TLR2 response upon ligand stimulation, regardless whether co-expressed with TLR1 or not. (B) Co-expressing with wild type TLR2, TLR1 or TLR6 deletion showed no responsive change, as compared with TLR2-TLR1/6 co-expression cells for Pam2CSK4 stimulation, while for Pam3CSK4 stimulation, the deletion of TLR1 or TLR6 LRR7-14 and extracellular C terminal LRR decreased the response (Data are the means  $\pm$  SD, n=3).

#### 4.2.3 Intracellular domains of TLR1 and TLR6 are involved in the diverse reactions of TLR2/1 and TLR2/6 complexes upon ligand challenge

TLR2 attains specificity for the ligands by forming heteromers with TLR1 or TLR6 (Farhat *et al.*, 2008). And that TLR1 enhanced but TLR6 reduced A $\beta$ -triggered TLR2-mediated inflammatory activation was demonstrated, which is in accordance with the response profile of TLR2/1 complex to its ligand Pam3CSK4. Although different cellular responses might be due to different extracellular ligand-binding interfaces of the receptor complex, in this study, whether the cytoplasmic domains of TLR1, TLR2 and TLR6 also contributes to this diverse reaction was investigated. It is notable that there is but one *XcmI* restriction enzyme cleavage site in the nucleotide sequences encoding both TLR1 and TLR6 transmembrane-domains (Figure 4.9A), which makes it possible to exchange the TLR1 and TLR6 intracellular domains

following *XcmI* cleavage, as shown in Figure 4.9A. The chimeric TLR1-TLR6 receptors alone or together with TLR2 in HEK-293 cells were over-expressed. Following the stimulation with the Pam3CSK4, neither TLR1 nor TLR6-expressing cells released IL-8, whereas TLR2-expressing cells secreted IL-8 and TLR2-TLR1 co-expressing cells produced the highest level of IL-8 (Figure 4.9B). Interestingly, the IL-8 level was significantly reduced in the TLR2-TLR1 co-expressing cells after replacing the TLR1 intracellular domain with the TLR6 intracellular domain (Figure 4.9B). Meanwhile, TLR2-TLR6 co-expressing cells produced the lowest level of IL-8. The replacement of the TLR6 intracellular domain with the one from TLR1 increased the release of IL-8 (Figure 4.9B). Similarly, following the Pam2CSK4 challenge, the replacement of the TLR6 intracellular domain by the TLR1 intracellular domain reduced IL-8 secretion from TLR2-TLR6 co-expressing cells, while the replacement of the TLR1 intracellular domain by the TLR6 relevant domain increased IL-8 secretion from the TLR2-TLR1 co-expressing cells (Figure 4.9C). These results suggest that the intracellular domains of TLR1 and TLR6 have divergent roles in their relationship with TLR2.

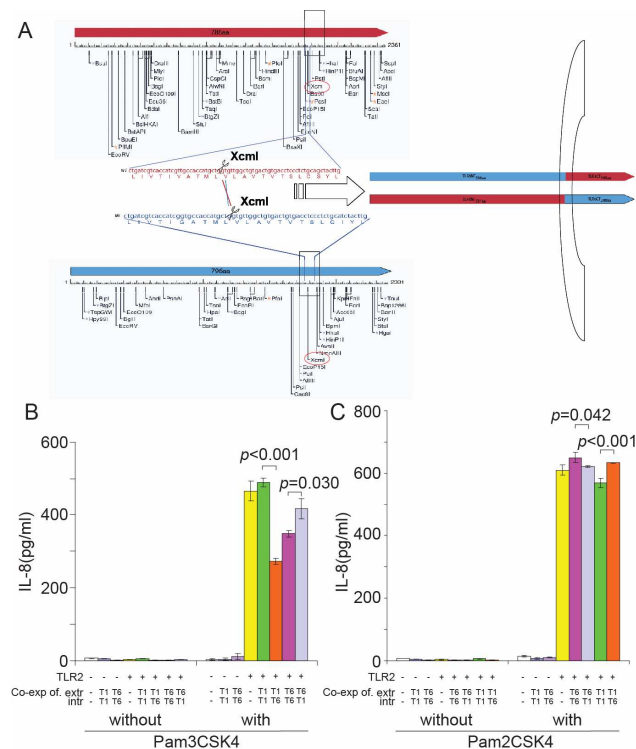


**Figure 4.9. TLR1 and TLR6 intracellular domains are involved in ligand specific signal transduction.** TLR2 and wild type or domain exchanged TLR1 and TLR6 were engineered to be expressed on HEK-293 cells. (A) The intracellular domains of TLR1 and TLR6 were exchanged through *XcmI* restriction digestion based on the restriction sites analysis. (B) Upon Pam3CSK4 stimulation, the TLR2-TLR1 expressing cells respond maximally. The response was minimized by replacing the TLR1 intracellular domain with that of TLR6. Replacement of the TLR6 intracellular domain with that of TLR1 enhanced the response level of TLR2-TLR6 expressing cells (Data are the means  $\pm$  SD, n=3). (C) Upon Pam2CSK4 stimulation, the TLR2-TLR6 expressing cells respond maximally. The response was reduced by replacing the TLR6 intracellular domain with that of TLR1. Replacement of the TLR1 intracellular domain with that of TLR6 enhanced the response level of TLR2-TLR1 expressing cells (Data are the means  $\pm$  SD, n=3).

In order to determine the specific regions in the intracellular fragments responsible for the inflammatory signal transduction, the alignment and functional analysis was performed between the intracellular sequences of TLR1, TLR2 and TLR6 (Figure 4.11). The following facts were also taken into consideration:

1. In eukaryotic cells, the phosphorylation mainly occurs on the three hydroxyl-containing amino acids: serine, threonine, and tyrosine, especially serine. Phosphoserine (pSer), phosphothreonine (pThr), and phosphotyrosine (pTyr) account for 86.4%, 11.8%, and 1.8%, respectively, of the total phosphorylated amino acids (Olsen *et al.*, 2006; Shi Yigong, 2009). The potential phosphorylated sites in TLR2, TLR1 and TLR6 cytoplasmic domains predicted with NetPhos 2.0 programm (<http://www.cbs.dtu.dk/services/NetPhos/>) are shown in Figure 4.10:

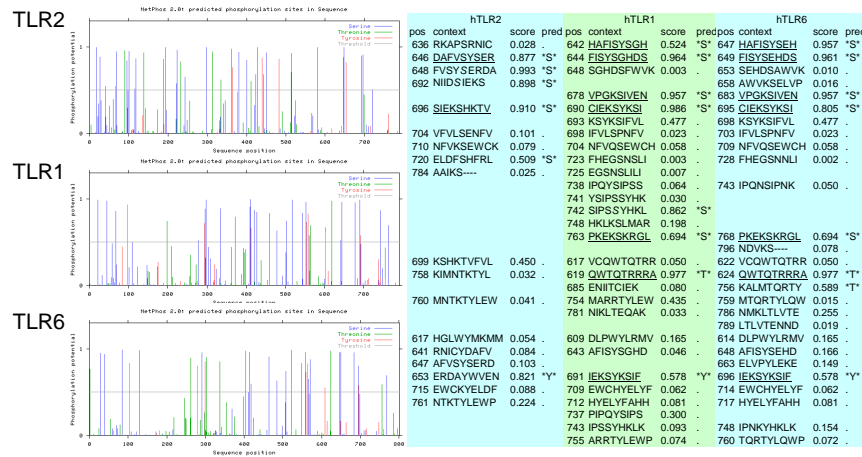


**Figure 4.10. Phosphorylation site prediction for TLR2, TLR1 and TLR6.** The full sequence of TLR2, TLR1 and TLR6 was predicted for potential phosphorylating sites by online NetPhos 2.0 software (<http://www.cbs.dtu.dk/services/NetPhos/>). Score threshold was set to 0.500. The intracellular phosphoserine (S), phosphothreonine (T) and phosphotyrosine (Y) are listed at the right side. The predicted phosphorylating sites conserved in two or more of the three receptors were underlined.

2. Compared with TLR6, TLR1 PQYSIPSS (735-742) is an extra site that might be recognised by GSK3 for Ser/Thr Phosphorylation as predicted with the Eukaryotic Linear Motif (ELM) resource for Functional Sites in Proteins (<http://elm.eu.org>).
3. The secondary structure of DD loop is critical in the TIR-TIR platform formation, which is essential for the dimerization of TLRs (Gautam *et al.*, 2006). The sequences of homologous DD loops of TLR1, TLR2 and TLR6 are compared in Figure 4.11, which shows that only EKKA (741-744) and QR (747-748) in TLR2 are different from the homologous regions of TLR1 and TLR6.
4. Proline (P) is a unique amino acid residue in that the cyclic structure of its side chain locks its  $\phi$  backbone dihedral angle at about  $75^\circ$ , thus, it has an exceptional

conformational rigidity compared to other amino acids and acts as a structural disruptor in secondary structure elements such as  $\alpha$  helices and  $\beta$  sheets. Proline is also commonly found in turns.

5. According to a recent scan on the mouse tissue-specific protein phosphorylation and expression, there are more than 58% of identified phosphorylation sites that are not included in any existing database, such as the Phosphosite database ([www.phosphosite.org](http://www.phosphosite.org)) and the Phospho.ELM database (<http://phospho.elm.eu.org/>) (Huttlin *et al.*, 2010).

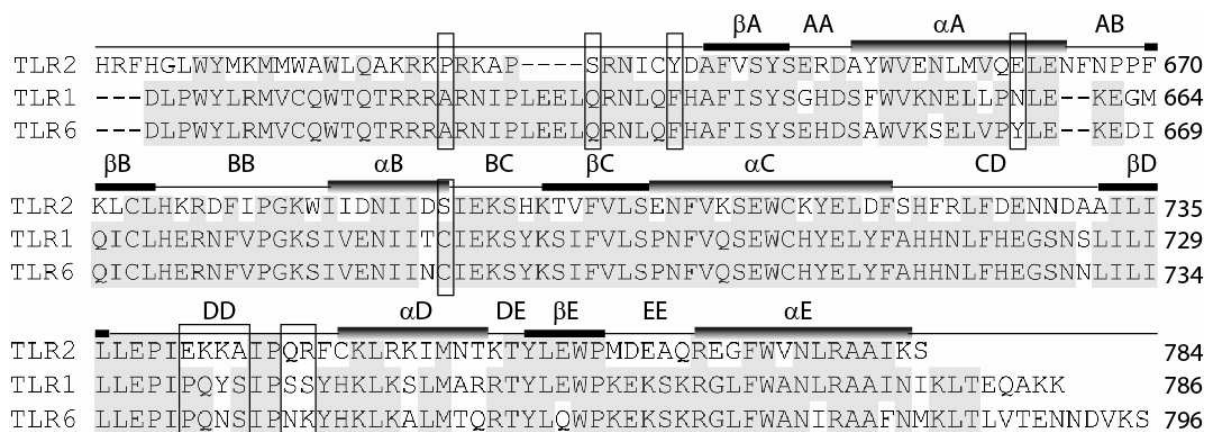


**Figure 4.11. TLR2, TLR1 and TLR6 intracellular domain sequence alignment.** The intracellular sequences of TLR2, TLR1 and TLR6 were aligned with ClustalW program (<http://www.ebi.ac.uk/Tools/msa/clustalw2/>). Identical residues are darkened and the domains of interest investigated in this study are boxed.

Based on the analysis above, the following mutants in TLRs were made and HEK-293 cell lines expressing these mutated receptors were generated to test the functional changes related to these genetic mutations:

- TLR1 Y737N
- TLR1 S741NK
- TLR6 N742Y
- TLR2EKKKA744PQNS
- TLR2P631A
- TLR2S636QY641F
- TLR6Y663N
- TLR2S692C

The cell responses upon Pam3CSK4 and Pam2CSK4 challenge were evaluated and compared to the response of cells expressing TLR2 alone. As shown in Figure 4.12, TLR2EKKKA744PQNS and TLR2P631A mutants almost completely abrogated the cell response to both Pam3CSK4 and Pam2CSK4 stimulation ( $p < 0.001$ ). In addition, TLR1Y737N and TLR1S741NK mutation reduced the cellular response upon Pam3CSK4 stimulation in TLR2-co-expressing cells ( $p < 0.001$ ).

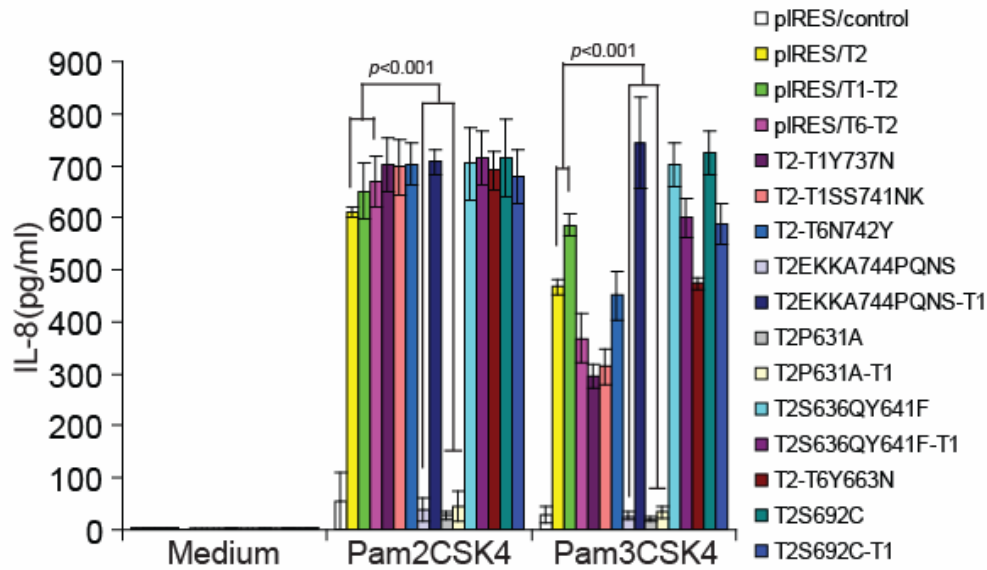


**Figure 4.12. Screen intracellular domain of TLR2, TLR1 and TLR6 for key region essential for signal transduction.** The TLR2, TLR1 and TLR6 intracellular domain as shown in Figure 4.11 were mutated and stably expressed in HEK-293 cells. The cells were stimulated with Pam2CSK4 or Pam3CSK4 at the concentration of 100 ng/ ml for 24 hrs. IL-8 level in the supernatants was determined through ELISA (Data are the means  $\pm$  SD,  $n \geq 3$ ).

#### 4.2.4 EKKA(741-744) motif at DD-loop of TLR2 is essential for A $\beta$ -triggered inflammatory signaling; the signaling defect due to the motif mutation is restored by TLR1 expression in a tyrosine<sup>737</sup>-dependent manner

Based on the findings in the screening experiments above, this study focused on EKKA motif in the DD-loop to investigate its role in A $\beta$ -triggered inflammatory signaling. HEK-293 cell lines were established to express: i, TLR2 or its mutants TLR2EKKA741-744PQNS, ii, TLR2EKKA741-744PQNS and TLR1, iii, TLR2EKKA741-744PQNS and TLR6, and iii, TLR2EKKA741-744PQNS and TLR1Y737N. The TLR2 expression in these cell lines was confirmed by Western blot (Figure 4.13A) and the mutations were confirmed by RT-PCR product sequencing (Figure 4.13B). The cells were activated with aggregated A $\beta$ 42 at the concentrations of 5  $\mu$ M and 10  $\mu$ M for 24 hrs. The IL-8 level in the supernatants was determined. As shown in Figure 4.14, when EKKA (741-744) was replaced by PQNS from TLR6 (Figure 4.14A), the TLR2-mediated inflammatory response was completely abolished (Figure 4.14B,  $p < 0.001$ ). Interestingly, the dysfunction of TLR2 due to this mutation was fully recovered by the co-expression of wild-type TLR1, but not TLR6 or TLR1 with the substitution of Y737N (Figure 4.14B,  $p < 0.001$ ).

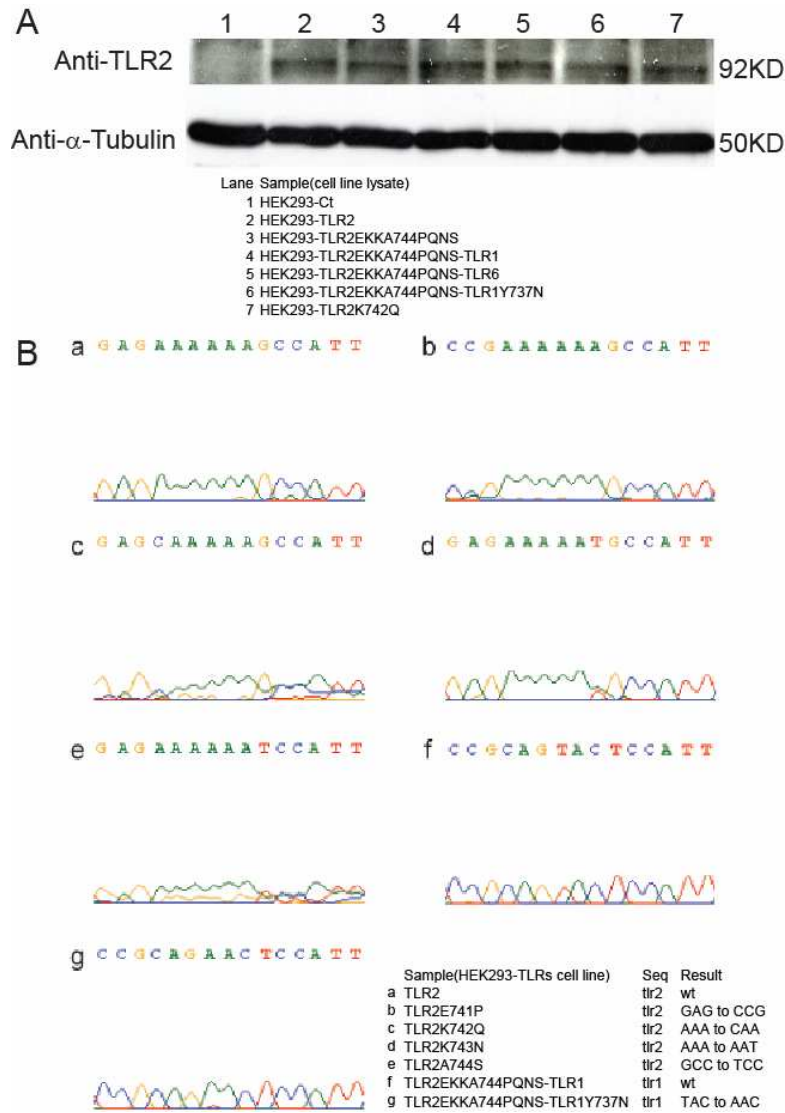


**Figure 4.13 Confirmation of the expression of TLR2 and mutant in the cell lines.** (A) TLR2 expression in the selected TLR2, TLR2EKKKA744PQNS, TLR2EKKKA744PQNS co-expressing TLR1, TLR6 or mutated TLR1 and TLR2K742Q expressing HEK-293 cell lines was confirmed by Western blot. (B) The expression and mutation of TLR2 and TLR1 was confirmed by sequencing the RT-PCR product derived from corresponding cell lines.



type TLR2 expressing cells (Figure 4.15,  $p < 0.001$ ). The mutation of other residues in this motif did not change the cellular response to A $\beta$  challenge.

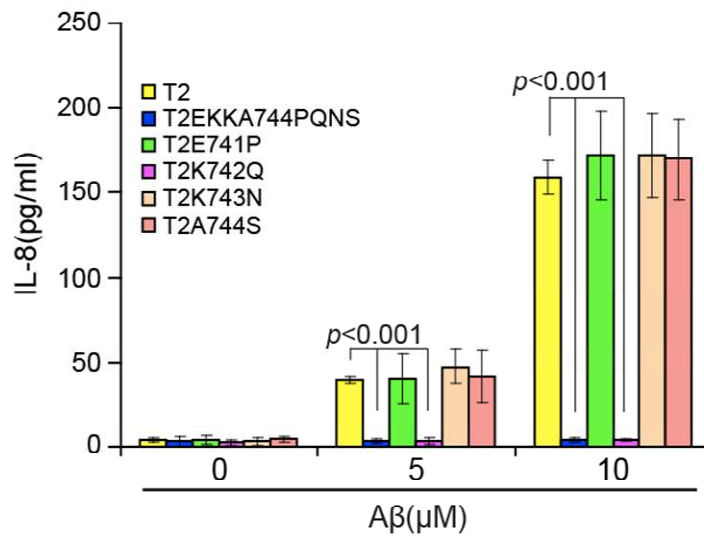


**Figure 4.15. TLR2 lysine<sup>742</sup> in EKKA (741-744) motif is the key residue for signaling.** TLR2, TLR2EKKA744PQNS motif replacement and TLR2E741P, TLR2K742Q, TLR2K743N and TLR2A744S point mutant stably co-expressing HEK-293 cell lines were generated and stimulated with 5  $\mu$ M or 10  $\mu$ M A $\beta$  for 24 hrs, inflammatory release of IL-8 in the supernatants was measured with ELISA (Data are the means  $\pm$  SD,  $n \geq 4$ ).

### 4.3 *Tlr2*-deficiency enhances A $\beta$ phagocytosis in vitro

Recently it was observed that deficiency of MyD88 enhanced A $\beta$  phagocytosis in macrophages (Hao *et al.*, 2011). Here, the effect of TLR2 on A $\beta$  phagocytosis was investigated. As actin polymerization is a prerequisite of phagocytosis and represents the activity of phagocytosis (Tu *et al.*, 2003), the ratio of filamentous actin (F-actin) to globular-actin (G-actin) was measured in aggregated A $\beta$ 42-treated bone marrow-derived macrophages. As shown in Figure 4.16A, after incubation with 5  $\mu$ M A $\beta$ , the polymerization of actin started after 15 min. At time points of 30 min and 60 min, the actin polymerization ratios were significantly higher in *tlr2*-deficient macrophages than in wild-type control cells (Figure 4.16A,  $p = 0.004$  and  $0.023$  at 30 min and 60 min, respectively). No difference of polymerization between these two cell groups was observed in the background or within 15 min after A $\beta$  incubation (Figure 4.16A,  $p > 0.05$ ). In a further measurement, A $\beta$  internalization was directly quantified by measuring fluorescence-conjugated A $\beta$  in macrophages after incubating cells with 5  $\mu$ M aggregated FITC-labeled A $\beta$ 42 for different duration. Similarly, results showed that the internalization of A $\beta$  was significantly increased in *tlr2*-deficient macrophages over a period of 6 hours of incubation as compared to the control cells (Figure

4.16B,  $p=0.029$ ). This difference was more pronounced when A $\beta$ 42 incubation duration was prolonged (Figure 4.16B,  $p<0.001$  at 24 hours post A $\beta$ 42 incubation).

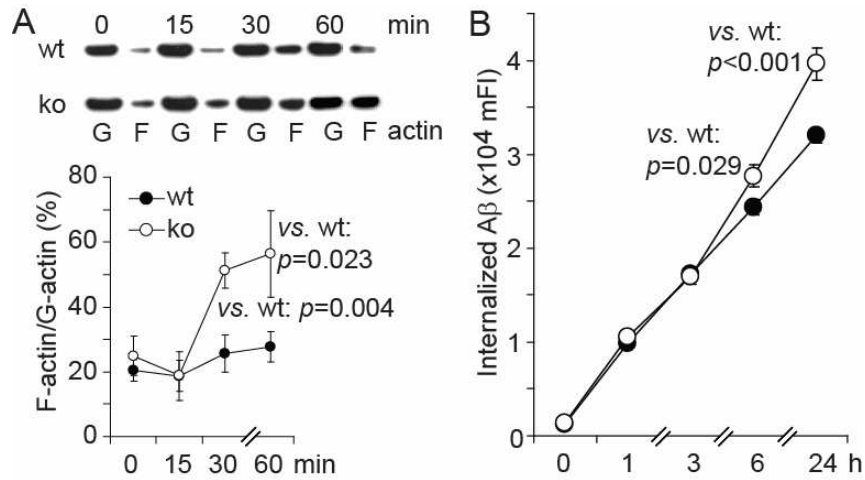


**Figure 4.16. *Tlr2*-deficiency enhances the phagocytosis of A $\beta$ .** (A) Primary bone marrow-derived macrophages from *tlr2* wild type or knockout mice were fed with aggregated A $\beta$ 42 for 0, 15, 30, and 60 min. Actin polymerization was analyzed with G-actin/ F-actin in Vivo Assay Kit, where actin was detected by Western blot; the ratio of filamentous form (F-actin) and globular form actin (G-actin) was quantified through lane density analysis with ImageJ (software download: <http://rsbweb.nih.gov/ij/download.html>) (Data are the means  $\pm$  SD,  $n\geq 4$ ). (B) Primary bone marrow-derived macrophages from *tlr2* wild type or knockout mice were co-cultured with FITC-conjugated A $\beta$ 42 for 0, 1, 3, 6, and 24 hrs. A $\beta$  internalization was analyzed with flow cytometry represented in mean fluorescence intensity (mFI) (Data are the means  $\pm$  SEM,  $n\geq 6$ ).

#### 4.4 *Tlr2*-deficiency ameliorates AD-like pathological changes in AD mouse model

Previous work shows that deficiency of MyD88 in microglia improved cognitive function in APP transgenic mice, which is associated with decreased inflammatory activation and A $\beta$  load in the APP transgenic mouse brain (Hao *et al.*, 2011). Here goes to address whether microglial TLR2 affects AD pathogenesis. Therefore, in this study, *tlr2*-deficient bone marrow chimeric APP transgenic mice were constructed, in which bone marrow cells migrated into the brain and differentiated into microglia, thereby creating a *tlr2*-deficient microglial pool (Khoury *et al.*, 2008). 1 year post bone marrow transplantation, the recipient mice were subjected for analysis.

##### 4.4.1 Deficiency of microglial TLR2 decreases neuroinflammation

A $\beta$  impairs neurons and causes synaptic deficits indirectly via triggering microglial inflammatory activation (Akiyama *et al.*, 2000; Medeiros *et al.*, 2007; Glass *et al.*, 2010; Zotova *et al.*, 2010). Here whether the A $\beta$ -triggered inflammation in *tlr2*-deficient bone marrow reconstructed mice altered was evaluated. The number of microglial cells recruited into the hippocampus was quantified after immunohistochemical staining of Iba-1, a Ca<sup>2+</sup>-binding peptide selectively expressed by microglia in the brain (Leone *et al.*, 2006; Hao *et al.*, 2011). As shown in Figure 4.17, in non-APP recipient mice, there was no significant

difference in the number of Iba-1-positive cells after the *tlr2*-deficient and wild-type bone marrow reconstruction ( $58.51 \pm 5.00$  cells/  $\text{mm}^2$  in *tlr2*-deficient mice and  $63.74 \pm 3.39$  cells/  $\text{mm}^2$  in wild-type controls,  $p=0.412$ ,  $n=5$ ). Interestingly, in the APP transgenic recipient mice, the number of recruited microglia following *tlr2*-deficient bone marrow reconstruction was significantly less than that following wild-type bone marrow reconstruction ( $123.59 \pm 11.03$  cells/  $\text{mm}^2$  versus  $164.88 \pm 10.34$  cells/  $\text{mm}^2$ ,  $p=0.017$ ,  $n \geq 8$ ). However, the morphology of microglia was not markedly different between these two groups of mice.

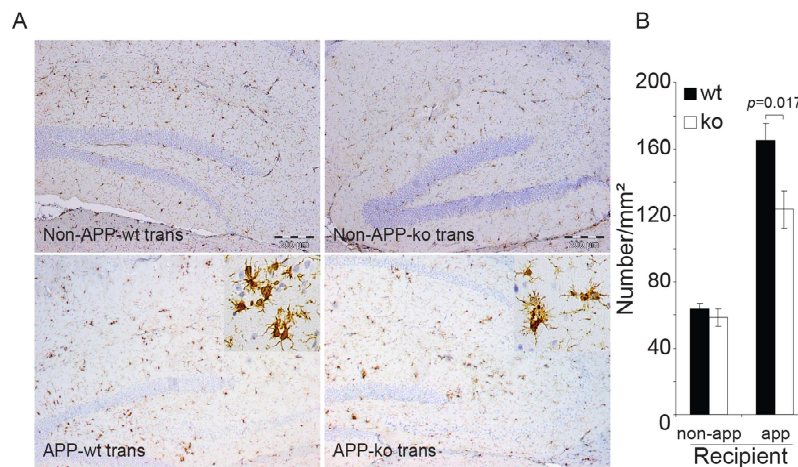


**Figure 4.17. Toll-like receptor 2-deficiency reduces hippocampal microglial cells.** Six-month old APP transgenic mice and their wild-type (non-APP) littermates were transplanted with *tlr2*-deficient or wild-type bone marrows. Microglia in the hippocampus were stained with Iba-1 antibody (A) and were counted and compared. No microglial cell amount difference was found between the TLR2 KO and WT bone marrow reconstructed non-APP mice ( $p=0.412$ ,  $n=5$ ), but the microglia in TLR2KO reconstructed APP mice were much more than those in WT bone marrow reconstructed APP mice ( $n \geq 8$  per group) (B, Data are the means  $\pm$  SEM).

The transcription levels of proinflammatory genes, *e.g.* *TNF- $\alpha$* , *IL-1 $\beta$* , *CCL-2* and *iNOS* in the brain of APP transgenic recipients were further determined. As shown in Figure 4.18, the relative transcription levels of *TNF- $\alpha$* , *IL-1 $\beta$*  and *CCL-2* were significantly reduced in APP transgenic mice after *tlr2*-deficient bone marrow reconstruction compared with wild-type bone marrow reconstruction.

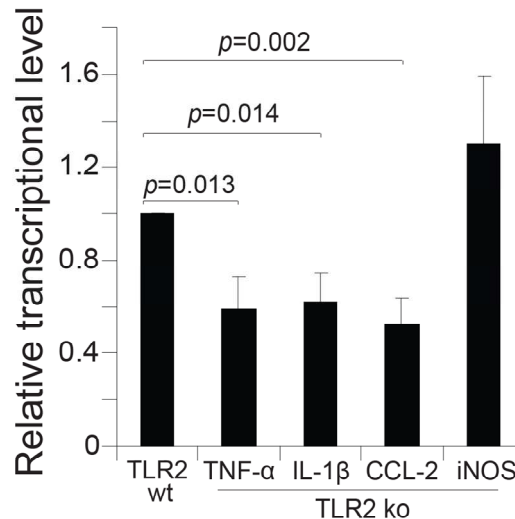


**Figure 4.18. Toll-like receptor 2-deficiency reduces pro-inflammatory gene transcription in the AD mouse brain.** Six-month old APP transgenic mice were transplanted with *tlr2*-deficient or wild-type bone marrow. One year after bone marrow reconstruction, transcription of proinflammatory genes, TNF- $\alpha$ , IL-1 $\beta$ , CCL-2 and iNOS in the brain were determined via real-time PCR. Transcription level of TNF- $\alpha$ , IL-1 $\beta$ , and CCL-2 in *tlr2*-deficient bone marrow reconstructed mouse brain were significantly decreased as compared to wt bone marrow reconstructed mice (Data are the means  $\pm$  SEM,  $n \geq 7$  per group).

#### 4.4.2 *Tlr2*-deficiency in myeloid cells decreases the A $\beta$ load in AD mouse brain

A $\beta$  has been considered a key pathogenic molecule in AD. After the observe of the decreased inflammatory activation in *tlr2*-deficient bone marrow reconstructed mouse brains, the question arise that whether *tlr2*-deficiency would also result in a decrease in the clearance of A $\beta$ , which may increase the A $\beta$  load in the brain. Cerebral A $\beta$  load in the APP mouse brains was evaluated using ELISA 1 year after *tlr2*-deficient and wild-type bone marrow reconstruction. The brains were homogenized and separated into Tris buffer (TBS), Tris plus 1% Triton buffer (TBS-TX) and guanidine chloride buffer (Gua-HCl)-soluble fractions (see Method section 3.2.15). Interestingly, no significant increase of A $\beta$  level was found between the *tlr2*-deficient and wild-type bone marrow chimeric APP transgenic mice (Figure 4.19). On the contrary, A $\beta$  load in the APP transgenic mice reconstructed with *tlr2*-deficient BM showed a slight but significant reduction (around 10%) of A $\beta$ 42 in the guanidine-soluble fraction of brain homogenate compared to wild-type BM reconstructed mice (Figure 4.19).

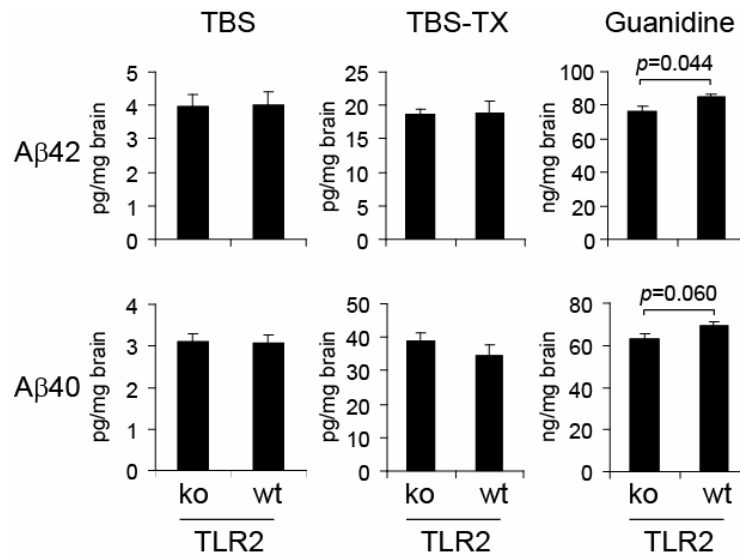


**Figure 4.19. *Tlr2*-deficiency decreases the A $\beta$  load in the brain.** Six-month old APP transgenic mice were transplanted with TLR2-deficient or wild-type bone marrow. One year after bone marrow reconstruction, the A $\beta$ 40 and A $\beta$ 42 level in TBS, TBS-TX and Gua-HCl components (see material and methods for detail) were determined through ELISA. A $\beta$ 42 level in the Guanidine fraction was slightly decreased in *tlr2*-deficient bone marrow reconstructed APP mouse brains (Data are the means  $\pm$  SEM,  $n \geq 8$  per group).

#### 4.4.3 *Tlr2*-deficiency in myeloid cells attenuates neuronal damage in the AD mouse brain

To examine the effects of *tlr2*-deficiency in myeloid cells on neuronal function in APP mice, one year after bone marrow transplantation, the Barnes maze test was performed to assess the cognitive function of the mice. As shown in the Figure 4.20, *tlr2*-deficient bone marrow-reconstructed mice took significantly less time (Figure 4.20A) and traveled a shorter distance (Figure 4.20B) to escape from the open field than their wt bone marrow-reconstructed APP transgenic littermates ( $p=0.044$  and  $0.040$ , respectively,  $n=6$  per group).

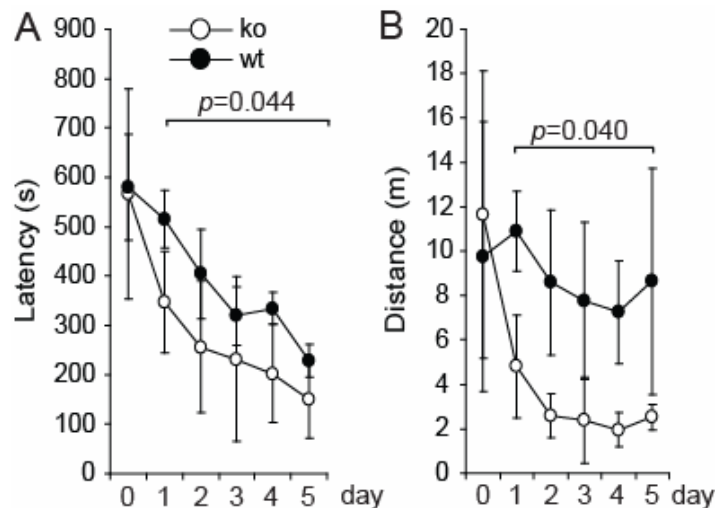


**Figure 4.20. *Tlr2*-deficient bone marrow reconstruction improves the cognitive state of APP transgenic mice.** Six-month old APP transgenic mice were transplanted with *tlr2*-deficient or wild-type bone marrow. One year post bone marrow reconstruction, the cognitive state of the APP transgenic mice was analyzed by Barnes maze test, in which *tlr2*-deficient bone marrow-reconstructed APP transgenic mice spent less time (A) and traveled a shorter distance (B) to escape (A-B, two-way ANOVA, Data are the means  $\pm$  SEM,  $n=6$  per group).

After observing that myeloid *tlr2*-deficiency ameliorated cognitive deficits in APP- transgenic mice, pathological changes of neurons in the mouse brain was investigated. In AD, progressive atrophy and neuronal loss from the entorhinal cortex to the CA1, CA2, CA3 and CA4 hippocampal subfields occurs with disease progression (Bobinski *et al.*, 1997; Apostolova *et al.*, 2006). Hence, neuronal cells in the CA3 area of the hippocampus were counted by staining with a neuron-specific marker (NeuN, neuronal nuclei) (Mullen *et al.*, 1992). However, result showed no significant difference in the number of NeuN-positive cells in the CA3 region between the *tlr2*-deficient and wildtype bone marrow-reconstructed APP transgenic mice (Figure 4.21).

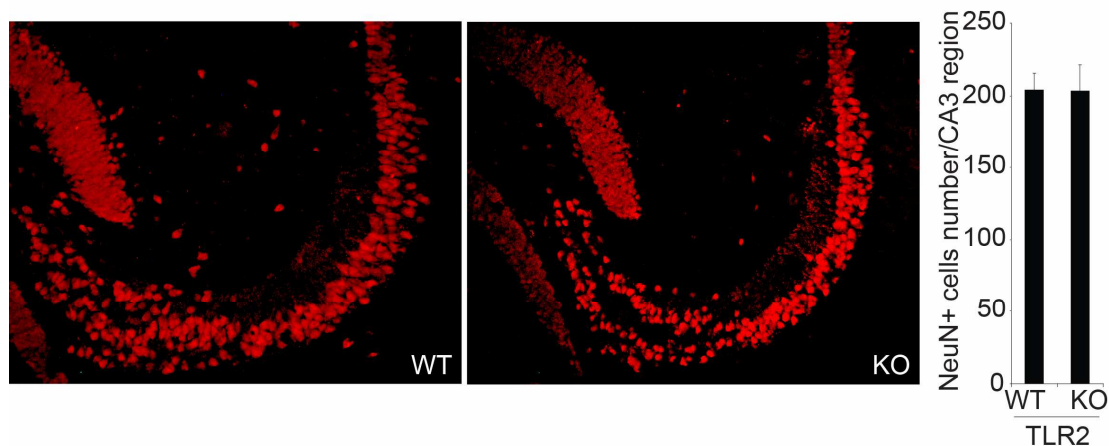


**Figure 4.21. *Tlr2*-deficiency does not protect against neuronal loss in hippocampus CA3 region of AD mice.** Six-month old APP transgenic mice were transplanted with *tlr2*-deficient or wild-type bone marrow. Neuronal cell number, stained with NeuN antibody, in the hippocampal CA3 region was counted and compared between these two mouse groups 1 year post bone marrow reconstruction. No difference was found between *tlr2* wt and ko bone marrow reconstructed APP transgenic mice ( $p > 0.05$ , Data are the means  $\pm$  SEM,  $n \geq 7$  per group)

Decline in synaptic number and synaptic integrity is another key change in AD patients (Hyman *et al.*, 1986; DeKosky *et al.*, 1990) with a decrease of synaptic scaffold protein level also associated (Pham *et al.*, 2010). Thus the protein level of post-synaptic density protein 95 (PSD-95, also known as disks large homolog 4, DLG4), a specialized post-synaptic scaffold protein, in the brain homogenates was evaluated using Western blot. Indeed, PSD-95 level in APP-transgenic mouse brain was lower than that in non-APP mouse brain (Figure 4.22,  $p < 0.005$ ). Furthermore, the relative PSD-95 level in *tlr2*-deficient bone marrow-reconstructed APP-transgenic mouse brains was much higher than that in wild-type bone marrow reconstructed APP-transgenic controls (Figure 4.22,  $p = 0.004$ ), suggesting less synaptic loss after *tlr2*-deficient bone marrow reconstruction. Importantly, in non-APP mice, no PSD-95 level difference was found between the *tlr2*-deficient bone marrow-reconstructed and wild-type bone marrow-reconstructed recipients (Figure 4.22,  $p > 0.05$ ).

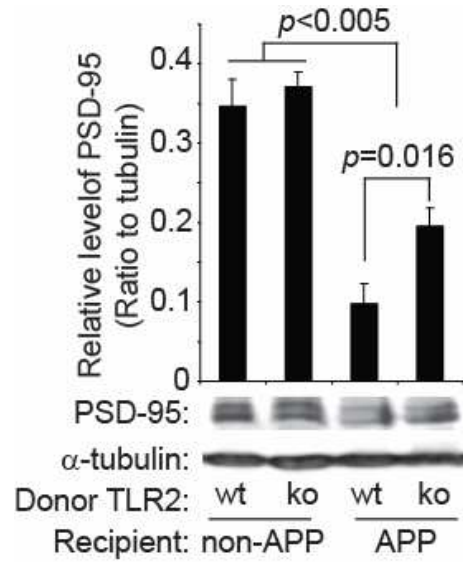


**Figure 4.22. *Tlr2*-deficiency slows synaptic impairment.** Six-month old APP transgenic and non-APP control mice were transplanted with *tlr2*-deficient or wild-type bone marrow. One year after bone marrow reconstruction, the protein level of postsynaptic density protein 95 (PSD-95) in the brain homogenate were evaluated through Western blot with PSD-95 antibody. The amount of PSD-95 was normalized by  $\alpha$ -tubulin. Relative PSD-95 level was higher in *tlr2*-deficient bone marrow reconstructed mice brain than that in wt bone marrow reconstructed APP transgenic mice brain (Data are the means  $\pm$  SEM,  $n \geq 8$  per group)

## 5 Discussion

AD is a progressive neurodegenerative disease pathologically characterized by extracellular A $\beta$  deposits and activated microglia (Citron, 2010; Zotova *et al.*, 2010). Microglia may act as a double-edged sword in AD pathogenesis (Walter Lisa *et al.*, 2009; Fuhrmann *et al.*, 2010). On one side, they injure neurons by releasing neurotoxic inflammatory mediators, and on the other side, they clear A $\beta$  to protect the neuron. Innate immune signaling cascades, *e.g.* TLRs-MyD88 pathway, control the inflammatory profile, and thereby modify AD pathogenesis (Fassbender *et al.*, 2004; Liu Y *et al.*, 2005; Tahara *et al.*, 2006; Jana *et al.*, 2008; Koenigsknecht-Talboo *et al.*, 2008; Richard *et al.*, 2008; Reed-Geaghan *et al.*, 2009; Reed-Geaghan *et al.*, 2010; Hao *et al.*, 2011). Here, the thesis study demonstrated that TLR2 is a primary receptor for A $\beta$ . *Tlr2*-deficiency reduces microglial inflammatory activation but enhances A $\beta$  phagocytosis, which is associated with improved neuronal function in AD mice. Further, this study also show that TLR1 and TLR6, as co-receptors, play opposing roles in modulating TLR2-mediated A $\beta$ -triggered responses. TLR1 enhances, while TLR6 suppresses, the inflammatory response. Furthermore, the amino acid motif EKKA (741-744), especially K742, in the TLR2 cytoplasmic domain was identified to be essential in the A $\beta$ -triggered inflammatory signal transduction and demonstrated a complementary role of TLR1 in the TLR2-mediated inflammatory signaling.

### 5.1 TLR2 is a primary receptor for A $\beta$

Up to now, CD14, CD36, TLR2 and TLR4 have been shown to be involved in the A $\beta$ -triggered inflammatory activation in microglia (Fassbender *et al.*, 2004; Walter S *et al.*, 2007; Jana *et al.*, 2008; Udan *et al.*, 2008; Reed-Geaghan *et al.*, 2009; Reed-Geaghan *et al.*, 2010). These receptors were reported to respond to A $\beta$  and trigger inflammation through a receptor complex, including TLR4/TLR2 (Udan *et al.*, 2008), CD14/TLR2/TLR4 (Reed-Geaghan *et al.*, 2009) or CD36-TLR4-TLR6 (Stewart *et al.*, 2010). However, with the exception of CD14 which was shown to directly bind to A $\beta$  aggregates (Fassbender *et al.*, 2004; Liu Y *et al.*, 2005), no evidence of direct binding between a single immune receptor and A $\beta$  has been reported. Thus, it is unclear whether these are primary receptors for A $\beta$  recognition.

In this study, it was observed that *tlr2*-deficiency reduces proinflammatory responses of the primary cultured microglial cells and bone marrow-derived macrophages upon A $\beta$  challenge, corroborating with a previous report (Jana *et al.*, 2008). Furthermore, this study demonstrated that TLR2 is a primary receptor for A $\beta$  to trigger inflammation with the

following evidence: 1, TLR2 co-localizes with A $\beta$  under confocal microscopy; 2, TLR2 directly binds to A $\beta$  in the biacore and pull-down assay; 3, the transgenic expression of TLR2 is enough to confer inflammatory activation upon A $\beta$  challenge in HEK-293 cells, which do not endogenously express TLR2 (Buwitt-Beckmann *et al.*, 2006) or respond to A $\beta$  via inflammatory signaling.

However, due to the limitation of the Biacore J system, this study was not able to present kinetic binding parameters of TLR2-A $\beta$  interaction.

The TLR2 ectodomain consists of 20 LRRs and it has been shown that LRRs-containing receptors (*e.g.* Nogo-66 receptor) bind to A $\beta$  (Park *et al.*, 2006). Additionally, as reported by our group previously, A $\beta$  also binds to CD14 (Fassbender *et al.*, 2004; Liu Y *et al.*, 2005); however, although the three central LRRs (8–10) of TLR2 are very similar to the LRRs (1–3) in CD14 (Kajava *et al.*, 2010), the interface of the receptor to bind A $\beta$  remains to be identified. Furthermore, the structural requirements of A $\beta$  to bind TLR2 remain to be identified; the aggregated structure seems to be essential for TLR2 recognition as soluble A $\beta$  is not able to activate microglial inflammatory responses (Fassbender *et al.*, 2004).

## **5.2 TLR1 and TLR6 are co-receptors of TLR2 modulating A $\beta$ induced response**

Unlike other TLRs, which are functionally active as homomers, TLR2 has evolutionarily developed a unique ability to form heteromers with TLR1 or TLR6 to attain ligand specificity (Farhat *et al.*, 2008). This study showed that TLR2 alone was able to confer a cellular inflammatory response in HEK-293 cells; the roles of TLR1 and TLR6 in this process were also investigated. Indeed, in TLR2-transgenic HEK-293 cells, which are endogenously deficient of various TLRs (*e.g.* TLR2) and only express low levels of TLR1 and TLR6 (Buwitt-Beckmann *et al.*, 2006), over co-expression of TLR1 with TLR2 enhanced the A $\beta$ <sub>42</sub>-triggered inflammatory response, while over co-expression of TLR6 with TLR2 reduced the response. These results suggest that TLR1 and TLR6 act as co-receptors playing opposing roles in modulating an A $\beta$  triggered inflammatory response. This was confirmed by gene knock down. In RAW264.7 macrophages, the knocking down of *tlr2* gene expression significantly reduced TNF- $\alpha$  production, a proinflammatory cytokine, upon A $\beta$  challenge; while *tlr6* gene silencing increased the cell response. Thus, the TLR2/TLR1 complex is the selected receptor complex for A $\beta$ -induced neuroinflammatory activation. To my knowledge, this is the first to demonstrate that TLR2-mediated A $\beta$ -triggered inflammatory activation is

enhanced by TLR1 and inhibited by TLR6. These findings are important for therapeutic design when using TLR2 as a target.

The selectivity pattern of utilizing the TLR2/TLR1 heterodimer in A $\beta$  recognition is similar to the combination of TLR2/TLR1 in Pam3CSK4 recognition.

### 5.3 TLR2 lysine<sup>742</sup> is essential for signaling

As a primary receptor, the region of TLR2 essential for A $\beta$  recognition is of great interest, since such a region could be a potential therapeutic target. In order to find such a region, while considering the limited A $\beta$  resource and similarity between an A $\beta$ -triggered response and a TLR2/TLR1 ligand-triggered response, this study first screened the domains with TLR2 ligands, and then confirmed the importance of the region with an A $\beta$  challenge.

For TLR2 ligands, through LRR domain deletion, it was observed here that any LRR deletion in TLR2 resulted in no inflammatory response upon ligand challenge, suggesting that an integrated TLR2 extracellular domain is necessary for ligand recognition. As only LRR7-14 and extracellular C terminal LRR deletions in TLR1 and TLR6 decreased the ligand-induced response, the complete integrity of TLR1 and TLR6 might not be as important as TLR2 in ligand recognition. However, because of the current HEK-293 cell model, the lower effects of LRRs deletion in TLR1 and TLR6 on TLR2-mediated inflammatory activation might also be due to compensation by endogenous TLR1 and TLR6.

The roles of intracellular fragments of the receptors were further investigated. Firstly, responses from TLR1 and TLR6 intracellular domain-exchanged cells upon ligand challenge suggest that the intracellular domain of the receptors also participates in determining the ligand response specificity. Secondly, based on bioinformatic analysis and site-directed mutation of TLR2, TLR2EKKA (741-744) motif and TLR2 proline<sup>631</sup> were identified in this study to be essential for the inflammatory signaling of TLR2. Replacement of the TLR2EKKA (741-744) to PQNS or proline<sup>631</sup> to alanine (A) from the homologous region of TLR6 impaired TLR2 signaling. Indeed, although proline<sup>631</sup> is out of the TIR domain, the importance of this residue was indicated by an observation on the association between the TLR2-P631H single nucleotide polymorphisms (SNP) and tuberculosis. The P631H mutation has a dominant negative effect on TLR2 signaling (Etokebe *et al.*, 2010).

The DD loop of TLR2 was observed to be critical for the formation of the TIR-TIR platform (Gautam *et al.*, 2006). Sequence alignment showed that there are only two corresponding regions within the DD loop that are different between TLR2, TLR1 and TLR6: EKKA (741-744) and QR (747-748) for TLR2, PQYS (735-738) and SS (741-742) for TLR1,

and PQNS (740-743) and NK (746-747) for TLR6. Here it was observed that the TLR1SS741NK mutation reduced the cellular response for Pam3CSK4 stimulation in TLR2-co-expressed cells. This corroborates with published results that the corresponding TLR2 R748A mutation reduced NF- $\kappa$ B activity upon Pam3CSK4 stimulation (Gautam *et al.*, 2006). For the first time, in this study, it was found that the TLR2EKKA (741-744) PQNS mutation abolished the inflammatory responses initiated by both Pam3CSK4 and Pam2CSK4. The study thus focused on the effect of this mutation in A $\beta$ -triggered responses.

Indeed, TLR2EKKA (741-744) PQNS mutation abolished the inflammatory activation upon A $\beta$  stimulation. Very interestingly, the abolished response could be recovered by co-expressing wild type TLR1 in a TLR1Y737-dependent manner, which suggests that TLR2 K743, the homologue of TLR1Y737, might be the key residue in the EKKA motif. However, after site-directed mutation of the EKKA motif, one residue after another, it was found out that the key residue was lysine<sup>742</sup>, instead of lysine<sup>743</sup>.

The lysine<sup>742</sup>, in the vertebrate TLR2, is evolutionarily highly conserved (Tschirren *et al.*, 2011). It has been suggested that TLRs are involved in co-evolutionary processes with pathogens. Several studies in humans and livestock have observed that TLRs have been subject to purifying selection (Mukherjee *et al.*, 2009; Seabury *et al.*, 2010). Indeed, Tschirren *et al.* observed that the lysine<sup>742</sup> is conserved in 17 different rodent species, which could be due to the strong purifying selection against functional change (Tschirren *et al.*, 2011).

TLR1 was the first reported toll-like receptor in humans (Nomura *et al.*, 1994). Unfortunately, it was not found to be able to activate NF- $\kappa$ B alone (Mitcham *et al.*, 1996). Later, TLR1, as well as TLR6, was observed to work together with TLR2 to attain specificity for ligand binding (Wyllie *et al.*, 2000; Hajjar *et al.*, 2001; Takeuchi *et al.*, 2001; Takeuchi *et al.*, 2002; Farhat *et al.*, 2008). However, except under certain circumstances, TLR2 does not need TLR1 or TLR6 for the immune reaction (Abplanalp *et al.*, 2009). For example, TLR1<sup>-/-</sup> and TLR6<sup>-/-</sup> mice survive equivalently upon *F. tularensis* infection whereas survival of TLR2<sup>-/-</sup> mice was significantly reduced with increased *F. tularensis* burdens and impaired secretion of TNF- $\alpha$  and other pro-inflammatory cytokines. In addition, human TLR6 and TLR1 are located on the same chromosome 4p14 and have similar genomic structures, which suggests that they are the products of an evolutionary duplication (Takeda *et al.*, 2003). It is also hypothesized, by some investigators, that TLR1 and TLR6 may be redundant in the recognition of ligands in concert with TLR2 (Abplanalp *et al.*, 2009). Here, for the first time, show that TLR1 not only takes part in specific ligand binding, but also is engaged in intracellular signaling. Furthermore, this study revealed that TLR1 can save TLR2 signaling

when TLR2 dysfunctions due to a mutation. The exact mechanism mediating the functions of TLR2 lysine<sup>742</sup> and TLR1 tyrosine<sup>737</sup> in A $\beta$ -triggered signaling remains to be clarified.

## **5.4 A $\beta$ -triggered phagocytosis and inflammatory activation are mediated through relatively independent pathways**

Microglia clear A $\beta$  deposits in the brain to exert beneficial effect in AD pathogenesis. Furthermore, peripherally-recruited microglia have been reported to be more efficient than their endogenous counterparts in A $\beta$  elimination (Simard *et al.*, 2006b; Grathwohl *et al.*, 2009). In this study, the effect of *tlr2*-deficiency on A $\beta$  uptake was tested. It was found out that, similar to *Myd88*-deficiency (Hao *et al.*, 2011), although *tlr2*-deficiency reduced A $\beta$ -induced inflammatory activation, the A $\beta$  phagocytosis was enhanced. Although the mechanism modulating phagocytosis requires further investigation, the signaling pathways controlling A $\beta$ -triggered inflammatory activation and A $\beta$  internalization are likely separate. It is evident that acute TLR-mediated microglial activation of TLR2, TLR4 and TLR9 increase A $\beta$  phagocytosis (Iribarren *et al.*, 2005; Chen Keqiang *et al.*, 2006; Tahara *et al.*, 2006; Scholtzova *et al.*, 2009). However, it should be noted that the increased A $\beta$  phagocytosis in those studies occurred after pre-stimulation of TLRs. Upon A $\beta$  challenge, phagocytosis indeed starts earlier than inflammatory activation (Liu Y *et al.*, 2005), with phagocytosis even serving to trigger inflammatory activation (Halle *et al.*, 2008).

Despite the improved A $\beta$  uptake capability of the *tlr2*-deficient microglia, the A $\beta$  load in the *tlr2*-deficient bone marrow chimeric APP transgenic mice brain was only slightly decreased. The cause(s) of inconsistency between in vitro and in vivo findings will be discussed below.

## **5.5 Pathogenic role of TLR2 in an AD mouse model**

### **5.5.1 *Tlr2*-deficient bone marrow chimeric APP transgenic mice is a feasible model to investigate the pathogenic role of TLR2**

Although the microglial turnover in irradiated bone marrow chimeric rodents was questioned and argued that microglia are not renewed by bone marrow-derived cells under normal conditions (Ajami *et al.*, 2007; Mildner *et al.*, 2007; Davoust *et al.*, 2008), these studies demonstrated that, under specific conditions, bone marrow-derived cells are able to cross the blood-brain barrier and to differentiate into microglia. This implies that (i) the adult bone marrow contains a subpopulation of cells displaying microglial differentiation potential, and

(ii) this subpopulation could be used as vehicle cells for the treatment of CNS disorders, providing an *ad hoc* CNS preconditioning is performed (through irradiation or other means) (Ajami *et al.*, 2007; Davoust *et al.*, 2008). Therefore, this study constructed *tlr2*-deficient/wt chimeric APP mice through BM transplantation, which allow to create a *tlr2*-deficient microglial pool reacting to cerebral A $\beta$  deposits (Keene *et al.*, 2010; Hao *et al.*, 2011).

To construct the animal model, the whole body irradiation was performed before the BM reconstruction. This design was based on three evidences: (i) only  $5.65 \pm 2.66\%$  of microglia in the hippocampus were derived from the BM cells in the TgCRND8 APP transgenic mouse 3 months after head-protected-irradiation based BM-reconstruction (from parallel project performed in our group); (ii) TLR2 did not affect the recruitment of microglia into the brain in the wild-type mice after whole-body irradiation (Figure 4.17) in BM transplantation model; and (iii) TLR2 does not regulate leukocyte recruitment after brain injury (Babcock *et al.*, 2008). The chimeric animal model constructed by cross-breeding the *tlr2*-deficient and APP transgenic mice was not selected because TLR2 expresses in neurons (Rolls *et al.*, 2007), which makes it impossible to distinguish whether the effects are from microglial *tlr2*-deficiency or non-microglial *tlr2*-deficiency. Similarly, injection of A $\beta$  into the *tlr2*-deficient mouse brain could not be a feasible approach because *tlr2*-deficiency reduces brain injury-induced neuroinflammation (Babcock *et al.*, 2006).

### **5.5.2 Reduction of neuroinflammatory activation could improve the cognitive deficits in APP transgenic mice**

Growing evidences suggest that aggregated A $\beta$  damages neurons by triggering microglia to release various neurotoxic inflammatory mediators including cytokines (*e.g.* TNF- $\alpha$  and IL-1 $\beta$ ), chemokines (*e.g.* CCL-2), and reactive oxygen and nitrogen species (Akiyama *et al.*, 2000; Wyss-Coray, 2006). PET analysis has shown that microglial activation correlates with AD progression (Cagnin *et al.*, 2001; Edison *et al.*, 2008; Okello *et al.*, 2009). Some epidemiological studies link the use of non-steroidal anti-inflammatory drugs (NSAIDs) with reduced risk for later AD (in 't Veld *et al.*, 2001). Although the mechanisms for the beneficial effects of NSAIDs are still fully known (Lee Young-Jung *et al.*, 2010). Some studies suggest this anti-AD benefit of NSAIDs is arise from their anti-inflammatory effects, apart from their A $\beta$ 42 lowering effects (Szekely *et al.*, 2008). In AD animal models, which over-express Alzheimer's amyloid precursor protein (APP) in neurons, microglia are observed to be activated and recruited to A $\beta$  deposits, where they subsequently damage neurons (Bard *et al.*,

2000; Liu Y *et al.*, 2005; Meyer-Luehmann *et al.*, 2008). All these studies suggest that suppressing microglial inflammation might be an effective therapeutic strategy for AD.

Indeed, in the bone marrow reconstructed AD mouse model, the amount of microglial cells in the hippocampal region of *tlr2*-deficient BM reconstructed APP mice was significantly less than that in wt BM reconstructed APP mice. Meanwhile, the transcriptional levels of pro-inflammatory cytokines such as TNF- $\alpha$ , IL-1 $\beta$  and CCL-2 were significantly decreased in the brains of *tlr2*-deficient BM transplanted APP mice. Although astrocytes could also be induced to express TLR2 and mediate inflammatory response (Phulwani *et al.*, 2008), as nonhematopoietic original cells they were not likely to play a role in a bone marrow transplantation model (Wagers *et al.*, 2002; Guo *et al.*, 2004). Thus, in this study, the reduced inflammation effect should come from a myeloid source, specifically microglia, which were thought to be at least partially originated from, and can be replenished by, myeloid precursors, especially under pathological states (Walter Lisa *et al.*, 2009; Hao *et al.*, 2011).

Thousands of reports have shown that the inflammatory mediators including IL-1 $\beta$ , IL-6, TNF- $\alpha$ , IL-8, transforming growth factor- $\beta$  (TGF- $\beta$ ), and macrophage inflammatory protein-1 $\alpha$  (MIP-1 $\alpha$ ), are upregulated in AD (Akiyama *et al.*, 2000). Whether this inflammatory response is beneficial or detrimental for the neural environment is under debate. Although low level of cytokines such as TNF- $\alpha$  and IL-1 $\beta$  activate NF- $\kappa$ B-dependent signaling pathways and might promote cellular growth and survival (Piani *et al.*, 1992; Tracey *et al.*, 1994; Chao *et al.*, 1995; Nguyen *et al.*, 2002), high concentration of these cytokines is neurotoxic over a longer term (Strijbos *et al.*, 1995; Simard *et al.*, 2006a). It has been recently established that uncontrolled TNF- $\alpha$  induces neuronal damage and chronic TNF- $\alpha$  infusion in the brain causes neuronal death by apoptosis (Nadeau *et al.*, 2003; Stepanichev *et al.*, 2003; Simard *et al.*, 2006a). In the case of AD, transgenic mice genetically engineered to overexpress APP show less pathology when they are chronically treated with anti-inflammatory agents (Jantzen *et al.*, 2002). Thus, the brain neuronal damage and cognitive changes in the *tlr2*-deficient and wt BM reconstructed APP mice were investigated.

It was found that *tlr2*-deficiency improved the cognitive state of AD mice. Immunohistochemistry showed that neuronal loss was unchanged, whereas the synapse was less impaired in *tlr2*-deficient-reconstructed APP mice, as suggested by a reduction in the loss of the specialized post-synaptic scaffold protein PSD-95 in the brain homogenate.

The reduced neuroinflammatory activation in the *tlr2*-deficient BM chimeric APP mice corroborates our previous observation that *Myd88*-deficient BM cells ameliorate neuroinflammation in AD mice (Hao *et al.*, 2011). Importantly, the synapse loss in the AD

mice used in this study is attenuated after *tlr2*-deficient BM reconstruction although a direct association between this neuronal improvement and reduced neuroinflammation needs further investigation.

### **5.5.3 Reduction of A $\beta$ load could be another mechanism to improve neuronal function in APP transgenic mice**

Pittsburgh compound B-based positron emission tomography (PET) demonstrated that A $\beta$  deposition in the human brain is associated with neuronal dysfunction revealed by both cognitive investigation and functional magnetic resonance imaging even at the pre-dementia stage (Sperling *et al.*, 2009; Ch  telat *et al.*, 2011; Villemagne *et al.*, 2011). The soluble aggregated A $\beta$  in postmortem brain tissue detected with Western blot was closely correlated with AD (Mc Donald *et al.*, 2010). Aggregated A $\beta$  directly injures synaptic junctions in the neocortex and limbic system, thereafter causing neuronal loss (Selkoe, 2002). The soluble A $\beta$  oligomers, especially dimers, were observed to inhibit long-term potentiation (LTP) by increasing activation of extrasynaptic NR2B-containing receptors and cause neuritic degeneration in which Tau hyperphosphorylation is involved (Shankar *et al.*, 2008; Li *et al.*, 2011). Furthermore, aggregated A $\beta$  could decrease adult neurogenesis, thereby interfering with the recovery from neuronal damage in AD pathogenesis (Crews *et al.*, 2010a; Crews *et al.*, 2010b).

Microglia have a beneficial effect in AD pathogenesis by clearing A $\beta$  deposits in the brain. (Simard *et al.*, 2006b; Grathwohl *et al.*, 2009). In accordance with our previous finding on A $\beta$  phagocytosis by *Myd88*-deficient macrophages (Hao *et al.*, 2011), here *tlr2*-deficiency enhances A $\beta$  phagocytosis by BM-derived macrophages was observed. As described above and published (Hao *et al.*, 2011), *tlr2*- or *Myd88*-deficiency increases A $\beta$  phagocytosis but decreases A $\beta$ -triggered inflammatory activation. Indeed, *tlr2*-deficient BM reconstruction reduced the cerebral A $\beta$  of APP mice in this study, especially the highly aggregated A $\beta$  (Figure 4.19).

However, according to the result (Figure 4.19), this A $\beta$  load reduction effect of *tlr2*-deficient BM reconstruction appears to be limited, which could be explained by two dynamic factors regarding the generation and clearance of A $\beta$ : (i) a decrease in the total number of microglia in the brain due to *tlr2*-deficient microglial recruitment (Figure 4.17); (ii) an increase in A $\beta$  production in the brain due to *tlr2*-deficiency; our previous work showed that both TLR2 and its downstream adaptor molecule *Myd88*-deficiency increases  $\beta$ -secretase

activity (*Myd88*-deficiency also increases  $\gamma$ -secretase activity) in the mouse brain (Hao *et al.*, 2011); (iii) the A $\beta$  clearance capability of bone marrow (hematogenous) macrophages in the brain is limited. Although the peripherally-recruited microglia have been assumed to be more efficient than their endogenous counterparts in A $\beta$  elimination (Simard *et al.*, 2006a; Simard *et al.*, 2006b), it is noteworthy that the assumption was deduced from the observation of improved CD11c expression in the bone marrow originated microglia (Simard *et al.*, 2004). This may not be sufficient evidence to draw such a conclusion. Indeed, there is no direct evidence that shows that myeloid microglia are more phagocytic. On the contrary, it was reported that resident microglia are more effective in removal of myelin debris and neuronal cell debris compared to hematogenous macrophages in a bone marrow chimeric experimental autoimmune encephalomyelitis (EAE) rat model (Rinner *et al.*, 1995) and cerebral ischemia mouse model (Schilling *et al.*, 2005). Phagocytosis is a complex process involving receptor binding, internalization, and phagosome biogenesis and maturation. Despite observing an increased A $\beta$  internalization in *tlr2*-deficient BMDMs, this was not sufficient to justify an increase in the clearance of A $\beta$ . It was reported that macrophages from *Myd88*-deficient mice show a range of phagocytosis- and phagosome maturation-associated defects including reduced uptake of particles and killing of pathogens (Henneke *et al.*, 2002; Marr *et al.*, 2003; Liu N *et al.*, 2004). Maturation of bacterium- but not apoptotic cell-containing phagosomes was accelerated or “induced” in a TLR2/4, MyD88 and MAPK p38 signaling-dependent manner (Blander *et al.*, 2004; Blander, 2007, 2008).

In summary, this study demonstrated the molecular mechanisms of TLR2 in A $\beta$ -triggered inflammatory activation. It shows that TLR2, cooperating with TLR1, is the primary receptor for A $\beta$ -triggered inflammation. Inhibition of TLR2 in microglia might reduce the detrimental effect of inflammatory activation, but does not impair the beneficial effect of A $\beta$  clearance. Further more, a (EKKA) motif essential for TLR2 intracellular signaling was discovered; dysfunction due to mutation of this motif can be restored by its co-receptor TLR1. This study contributes to a better understanding of AD pathophysiology and may eventually translate to therapeutic options to prevent and / or treat AD progression.

**Part II. Omega-3 Fatty Acids Reduce Alzheimer's Amyloid  
Peptide-induced Proinflammatory Activities in Macrophages**

## 1 Summary

Epidemiological studies suggest that diets enriched with omega-3 polyunsaturated fatty acids (PUFAs), *e.g.* docosahexaenoic acid (DHA), reduce the risk for AD (Barberger-Gateau *et al.*, 2002; Morris *et al.*, 2003; Schaefer *et al.*, 2006). However, the underlying mechanism remains unclear. In AD, microglia/macrophage-dominated neuroinflammation can be considered a double-edged sword; on one hand, they injure neurons by releasing highly toxic molecules, while on the other hand they protect neurons by clearing pathogenic amyloid  $\beta$  ( $A\beta$ ) (Walter Lisa *et al.*, 2009; Hao *et al.*, 2011). In this part of study, with cultured bone marrow-derived macrophages (BMDMs), It was observed that DHA reduces  $A\beta$  aggregate-induced secretion of pro- (*e.g.* TNF- $\alpha$  and IL-6) but not of anti- (*e.g.* IL-10) inflammatory cytokines. In order to elucidate the mechanisms mediating the anti-inflammatory effects of omega-3 PUFAs, the BMDMs were pre-treated with DHA and then were stimulated with different TLR ligands. Results show that, DHA suppresses TLR2, 3, 4 and 9, as well as interferon- $\gamma$ -mediated inflammatory activation, which has been shown to be directly or indirectly, involved in AD pathogenesis. Interestingly, DHA does not reduce the uptake of  $A\beta$  aggregates by macrophages, which is considered to be a beneficial cellular response in the course of AD. In summary, this study contributes to the understanding of mechanisms mediating preventative effects of omega-3 PUFA-supplemented functional diets in AD patients.

## 2 Introduction

As stated in Part I, AD is the leading cause of dementia and is becoming a major medical challenge (Szekely *et al.*, 2007). Preventative and therapeutic strategies aiming to control the development and progression of AD is of increasing interest. Besides interfering the identified primary innate immune receptor for A $\beta$ -triggered microglial inflammation changes AD pathogenesis in mouse model as shown in Part I work of this thesis, it is notable that studies already demonstrated that non-steroidal anti-inflammatory drugs can delay onset, slow progression, and decrease cognitive deficits of AD (McGeer PL, 1996; in 't Veld *et al.*, 2001). Furthermore, epidemiological studies showed that foods supplemented with omega-3 polyunsaturated fatty acids (PUFAs), *e.g.* docosahexaenoic acid (DHA), can modulate inflammatory profiles in humans (Pischon *et al.*, 2003; Ferrucci *et al.*, 2006; Farooqui *et al.*, 2007), such as reducing proinflammatory cytokines (TNF- $\alpha$  and IL-6) or increasing anti-inflammatory molecules (IL-10 and TGF- $\beta$ ) in circulating monocytes and the serum. Interestingly, omega-3 PUFA-enriched food also reduces the risk for AD, especially when sufficient PUFAs are consumed before the development of clinical dementia (Barberger-Gateau *et al.*, 2002; Morris *et al.*, 2003; Schaefer *et al.*, 2006). In APP transgenic mice, similar “anti-AD” effects of PUFAs have been observed as those resulting from a DHA-supplemented diet, including improved cognitive deficits, reduced A $\beta$  deposition in the brain parenchyma and blood vessels, and decreased phosphorylated tau inside of neurons (Lim *et al.*, 2005; Oksman *et al.*, 2006; Green *et al.*, 2007; Hooijmans *et al.*, 2007). In cultured macrophages, omega-3 PUFAs were observed to inhibit TLR2 and TLR4-induced inflammatory activation (Lee Joo Y. *et al.*, 2003; Lee Joo Y. *et al.*, 2004).

Thus, it is hypothesized in this study that omega-3 PUFAs could suppress A $\beta$ -induced neurotoxic inflammatory activation and that TLRs might be relevant to this modulatory action. In this part of study, bone marrow-derived macrophages (BMDMs) were cultured, pretreated with PUFAs and activated with aggregated A $\beta$ . It was observed that omega-3 PUFAs suppress A $\beta$ -induced pro- but not anti-inflammatory activities. Interestingly, omega-3 PUFAs do not reduce macrophage phagocytosis of A $\beta$ . Confirming the hypothesis that A $\beta$ -triggered microglial inflammation and phagocytosis are mediated through relatively independent pathways.

## **3 Materials and Methods**

### **3.1 Materials**

Instruments, experimental materials and kits, unless otherwise specified, were the same as described in Part I. Polyinosinic-polycytidylic acid (Poly I: C, TLR3 ligand), purified lipopolysaccharides (LPS, TLR4 ligand) and CpG ODN (TLR9 ligand) were from ALEXIS biochemicals (Lörrach, Germany). Imiquimod (R837, TLR7 ligand) was from InvivoGen (Toulouse, France). Docosahexaenoic acid (DHA, C22:6 n-3), Eicosapentaenoic acid (EPA, C20:5 n-3) and Arachidonic acid (AA, C20:4 n-6) were from Sigma-Aldrich (Steinheim, Germany) and dissolved in 95% ethanol at the concentration of 100 mM as stock solutions. The final concentrations of DHA, EPA and AA for cell treatment were decided based on previous publications (Skuladottir *et al.*, 2007; De Smedt-Peyrusse *et al.*, 2008). Vehicle containing the same concentration of ethanol was used as the ligand control. Final ethanol concentration in the medium was below 0.1%.

### **3.2 Methods**

#### **3.2.1 Preparation and characterization of A $\beta$ aggregates**

A $\beta$  aggregates preparation and characterization are same as Part I (Section 3.2.2 and Figure 3.1).

#### **3.2.2 Culture of bone marrow-derived macrophages**

Primary bone marrow-derived macrophages (BMDMs) were isolated from 7 to 9-week-old C57BL/6 (Charles River, Sulzfeld, Germany) and *Myd88*-deficient mice (kindly provided by S. Akira, Osaka University, Osaka, Japan), culture procedure is the same as described in Part I (Section 3.2.1).

#### **3.2.3 Cell challenge and ELISA analysis of cytokine release**

BMDMs, cultured at  $2 \times 10^5$  cells per well in 48-well plate (BD, Heidelberg, Germany), were pretreated with DHA/EPA/AA/Vehicle control (concentrations indicated in the results) for 24 hrs and then challenged with TLR ligands: Pam3CSK4 (100 ng/ml), LPS (100 ng/ml), Poly I:C (30  $\mu$ g/ml), Imiquimod (1  $\mu$ g/ml) and CpG ODN (5  $\mu$ g/ml), as well as IFN- $\gamma$  (200 U/ml) or 10  $\mu$ M A $\beta$ 42 aggregates for 18 hrs in the presence of the pretreated lipids. Supernatants were collected for detection of TNF- $\alpha$ , IL-6, IL-10, interferon-inducible Protein 10 (IP-10) and PGE2 by ELISA kits (R&D Systems, Wiesbaden, Germany) (procedure follows the

manufacturer's manuals and is similar to Part I section 3.2.4). Some of the DHA pretreated cells were lysed for a caspase 3 activity test.

### 3.2.4 Reverse transcription and quantitative PCR for analysis of inflammatory genes and A $\beta$ phagocytosis-related receptors

BMDMs at  $3 \times 10^5$  cells per well in a 24-well plate were treated with 25  $\mu$ M DHA or vehicle for 18 hrs. Total RNA was isolated from BMDMs using the RNeasy Plus mini kit (QIAGEN, Hilden, Germany). First-strand cDNA was synthesized by priming total RNA with hexamer random primers (Roche Molecular Biochemicals, Mannheim, Germany) and using Superscript II reverse transcriptase according to the manufacturer's instructions (Invitrogen). Detailed procedure can be found in Part I (section 3.2.8.1-3.2.8.2).

The quantitative PCR was performed with the Applied Biosystems 7500 Real-Time PCR system (Applied Biosystems, Foster City, CA) using SYBR®Advantage qPCR Premix (Clontech, Mountain View, CA) to determine the amplification products as described previously (Liu et al., 2006). Primer sequences for TNF- $\alpha$ , IL-6, IL-10, PGE2 synthase 1 (ptGES1), CD14, RAGE, CD36, SR-A and GAPDH genes are shown in Table 3.1:

Table 3.1 Primer sequences for real-time quantitative PCR detectors

Product	Forward	Reverse
GAPDH	ACAAC TTTGGCATTGTGGAA	GATGCAGGGATGATGTTCTG
CD14	AGGGTACAGCTGCAAGGACT	CTTCAGCCCAGTGAAAGACA
RAGE	CTGAAGCTTGGAAAGTCCCTC	CCTCATCGACAATCCAGTG
CD36	CCAAGCTATTGCGACATGAT	CCTGCAAATGTCAGAGGAAA
SR-A	CATGGCAACTGACCAAAGAC	AGGACTTGGAGATTGCATCC
TNF- $\alpha$	ATGAGAAGTTCCCAAATGGC	CTCCACTTGGTGGTTTGCTA
IL-6	AGTCCGGAGAGGAGACTTCA	ATTTCCACGATTTCCAGAG
IL-10	AGGGGCTGTCATCGATTTCTC	TGCTCCACTGCCTTGCTCTTA
PTGES1	GAGTTTTACGTTCCGGTGT	GGTAGGCTGTCAGCTCAAGG

The following cycles were performed: initial denaturation cycle at 95 °C for 10 sec, followed by 45 amplification cycles at 95 °C denaturation for 5 sec and annealing/extension at 60°C for 34 sec. In the end, a dissociation curve was performed.

The amount of double-stranded PCR product synthesized in each cycle was measured using SYBR green I dye. Threshold cycle (Ct) values for each detected gene from the replicate PCRs was normalized to the Ct values for the GAPDH control from the same cDNA

preparations. The ratio of transcription of each gene was calculated as  $2^{\Delta\text{Ct}}$ , where  $\Delta\text{Ct}$  is given by:  $\text{Ct (GAPDH)} - \text{Ct (test gene)}$ .

### 3.2.5 Apoptosis caspase 3 assay

BMDMs, cultured at  $2 \times 10^5$  cells per well in 48-well plate (BD, Heidelberg, Germany), were pretreated with 25  $\mu\text{M}$  DHA/vehicle control for 24 hrs, then cells were lysed in 200  $\mu\text{l}$  Caspase lysis buffer [10 mM HEPES, pH 7.4, 42 mM KCl, 5 mM  $\text{MgCl}_2$ , 1 mM phenylmethylsulfonyl fluoride, 0.1 mM EDTA, 0.1 mM EGTA, 1 mM DTT, 1  $\mu\text{g/mL}$  pepstatin A, 1  $\mu\text{g/mL}$  leupeptin, 5  $\mu\text{g/mL}$  aprotinin, 0.5% 3-(3-cholamidopropyl)dimethylammonio-1-propane sulfonate (CHAPS)]. The activity of caspase 3 was determined by use of a fluorescent substrate as described previously (Kögel *et al.*, 2003) with a minor modification: 50  $\mu\text{l}$  of this lysate was added to 150  $\mu\text{l}$  reaction buffer (25 mM HEPES, 1 mM EDTA, 0.1% CHAPS, 10% sucrose, 3 mM DTT, pH 7.5) and 10  $\mu\text{M}$  of the fluorogenic substrate Ac-DEVD-AMC (Ac-DEVD-AMC: Ac-Asp-Glu-Val-Asp-AMC, Bachem, works as a susceptible fluorescent substrate for caspase 3). Accumulation of Acetyl-DEVD-7-amido-4-methylcoumarin (AMC) fluorescence was monitored over 1 h using a Tecan's Safire2™ microplate reader (Tecan, Männedorf, Switzerland) (excitation 380 nm, emission 465 nm). Fluorescence of blanks containing no cell lysate was subtracted from the values. Protein content was determined using the Pierce Coomassie plus Protein Assay reagent (KMF, Cologne, Germany). Caspase activity is expressed as change in fluorescent units per microgram protein and per hour.

### 3.2.6 LDH toxicity assay

BMDM cells were cultured in DMEM medium and treated with DHA/Vehicle for 24 hrs, then cytotoxicity was evaluated through lactate dehydrogenase (LDH) level measurement via the Cytotox 96 Non-Radioactive Cytotoxicity Assay kit (Promega) according to the manufacturer's instructions (Philip J Lee, 2007). Experimental steps are:

- 
1. Transfer 50  $\mu\text{l}$  supernatant to enzymatic assay plate
  2. Reconstitute substrate mix using assay buffer provided in the kit
  3. Add 50  $\mu\text{l}$  reconstituted substrate mix to each well of enzymatic assay plate
  4. Cover plate and incubate 30 min at room temperature, protect from light
  5. Add 50  $\mu\text{l}$  stop solution(1M acetic acid) to each well
  6. Record absorbance 490 nm
-

### **3.2.7 Flow cytometric analysis of A $\beta$ 42 internalization**

BMDMs cultured in a 12-well plate (BD) at a density of  $2 \times 10^5$  cells per well were pretreated with 25  $\mu$ M DHA, EPA, AA or vehicle control for 24 hrs, and then incubated with 0.5  $\mu$ M FITC-conjugated A $\beta$ 42 aggregates in the culture medium containing fatty acids for 0, 3, 6, and 24 hrs. The internalization assay was terminated by placing cells on ice. BMDMs were washed with PBS and detached from the plate with 0.05% Trypsin-EDTA (Invitrogen). The percentage and mean fluorescence intensity (mFI) of macrophages internalizing FITC-labeled A $\beta$ 42 were immediately measured by BD Cytometer FACSCanto II. All experiments were independently replicated at least three times.

### **3.2.8 Statistics**

Data in figures are presented as mean  $\pm$  SD. One-way ANOVA followed by Tukey's HSD or Tamhane's T2 post hoc test (dependent on the result of Levene's test to determine the equality of variances) was used for multiple comparisons. Two-independent-samples t test was used to compare means for two groups of cases. All statistical analysis was performed on SPSS 11.0 for Windows (SPSS, Chicago, IL). Statistical significance was set at  $p < 0.05$ .

## 4 Results

### 4.1 DHA reduces TLR2, 3, 4 and 9-initiated pro- but not anti-inflammatory cytokine secretion in macrophages

Since innate immune receptors, *e.g.* CD14, TLR2 and 4, have been reported to recognize fibrillar A $\beta$  and mediate inflammatory responses in microglia/macrophages (Fassbender *et al.*, 2004; Liu Y *et al.*, 2005; Tahara *et al.*, 2006; Jana *et al.*, 2008; Richard *et al.*, 2008), here how DHA modulates TLR2 and TLR4-initiated inflammatory activation was first investigated. As shown in Figure 4.1A, DHA treatment significantly reduced Pam3CSK4 (TLR2 ligand) and LPS (TLR4 ligand)-induced TNF- $\alpha$  secretion from BMDMs in a concentration-dependent manner ( $p < 0.05$ ). Similarly, the secretion of IL-6 was significantly decreased by DHA (Figure 4.1C,  $p < 0.001$ ). The modulatory effects of DHA on other TLR-initiated inflammatory activation was further investigated. As shown in Figure 4.1B and D, DHA markedly suppressed Poly I: C (TLR3 ligand) and CpG ODN (TLR9 ligand)-induced TNF- $\alpha$  and IL-6 secretion ( $p < 0.001$ ). Imiquimod (R837) (TLR7 ligand) did not induce secretion of the cytokines studied (Figure 4.1B and D). Interestingly, release of the anti-inflammatory cytokine IL-10, following TLR2, 4, 7 and 9, but not TLR3 activation, was not reduced by DHA treatment (Figure 4.1E,  $p > 0.05$ ).

In order to exclude the possibility that DHA suppresses inflammatory activation via inducing cell death, the activity of caspase 3 (a marker for apoptosis) and the release of lactate dehydrogenase (LDH, to detect loss of cell integrity) from macrophages following the DHA treatment was analyzed. No significant cell death caused by DHA was observed (Figure 4.2).

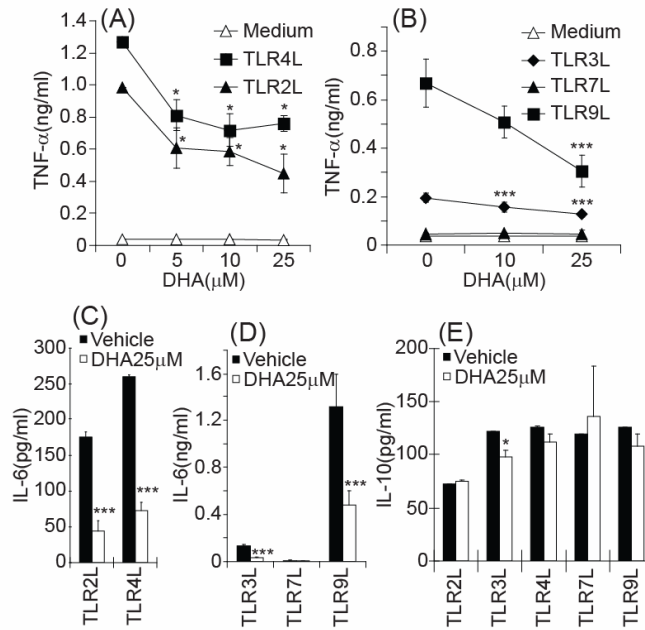


**Figure 4.1, DHA treatment inhibits TLRs-induced inflammatory activation.** BMDMs were pretreated with DHA at the indicated concentrations for 24 hrs and then challenged with TLR2, TLR4 (A, C, E), or TLR3, TLR7, TLR9 (B, D, E) ligands for 18 hrs in the presence of DHA. The media was collected for ELISA analysis of TNF- $\alpha$  (A, B), IL-6 (C, D) and IL-10 (E). \* $p < 0.05$ , \*\*  $p < 0.01$ , \*\*\*  $p < 0.001$ , as compared to vehicle control (one-way ANOVA or t test,  $n \geq 6$  per group).

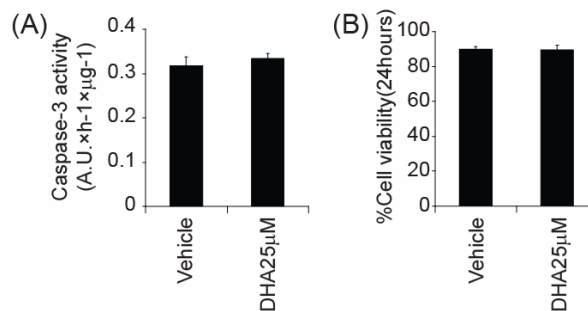


**Figure 4.2, DHA 25  $\mu$ M treatment does not have a significant effect on cell apoptosis and viability.** BMDM cells were cultured in DMEM medium and treated with DHA/Vehicle for 24 hrs; Caspase-3 activity (A) and LDH releasing assay (B) were performed to evaluate the apoptosis and cell death effect caused by DHA treatment. No significant cell apoptosis or death was observed with 25  $\mu$ M DHA treatment (t test,  $n=4$  per group).

## 4.2 DHA suppresses IFN- $\gamma$ -induced IP-10 secretion in macrophages

IFN- $\gamma$  is an important endogenous inflammatory activator and stimulates a different signaling pathway than TLRs. Thus, this study continued to test effects of DHA on IFN- $\gamma$ -initiated inflammatory activation. Secretion of IP-10 was significantly decreased by DHA in a concentration-dependent manner (Figure 4.3A,  $p < 0.05$ ). Interestingly, this suppressive effect

of DHA was independent of MyD88, a common signaling molecule downstream to TLRs. As shown in Figure 4.3B, DHA decreased IP-10 release from *Myd88*-deficient macrophages in a similar manner to wild-type control cells ( $p < 0.05$ ).

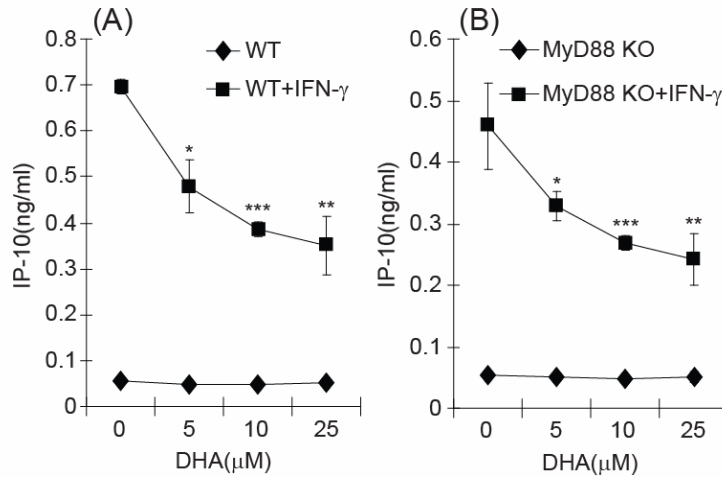


**Figure 4.3, DHA treatment inhibits IFN- $\gamma$ -induced inflammatory activation.** *Myd88*-deficient (A) or wildtype (B) BMDMs were pretreated with DHA at the indicated concentrations for 24 hrs and then challenged with 200 U/ml IFN- $\gamma$  for 18 hrs. The media was collected for ELISA measurement of IP-10. \* $p < 0.05$ , \*\*  $p < 0.01$ , \*\*\*  $p < 0.001$ , as compared to vehicle control (one-way ANOVA,  $n=6$  per group).

### 4.3 DHA reduces aggregated A $\beta$ 42-induced pro-inflammatory cytokine secretion in macrophages

Following the investigation of general anti-inflammatory effects of DHA, the effects of DHA on A $\beta$  aggregate-induced inflammatory activation were examined. It was observed that DHA treatment significantly reduced A $\beta$ 42 aggregate-induced TNF- $\alpha$  secretion from macrophages in a concentration-dependent manner (Figure 4.4A,  $p < 0.05$ ). Similarly, A $\beta$ 42 aggregate-initiated IL-6 secretion was also significantly decreased by DHA (Figure 4.4C,  $p < 0.01$ ). DHA did not reduce A $\beta$ 42 aggregate-initiated IL-10 secretion (Figure 4.4D,  $p > 0.05$ ). Meanwhile, repeated experiments using lipid controls of DHA EPA, another common used omega-3 PUFA, and AA, an omega-6 PUFA in the brain, instead of DHA were used to co-treat macrophages with A $\beta$ 42 aggregates. Upon A $\beta$ 42 activation, EPA, but not AA, significantly reduced the release of TNF- $\alpha$  (Figure 4.4B,  $p < 0.01$ ), whereas AA significantly increased A $\beta$ -initiated IL-6 secretion (Figure 4.4C,  $p < 0.001$ ). In order to determine the mechanisms by which DHA inhibits A $\beta$ 42-induced proinflammatory cytokine secretion, the transcripts of TNF- $\alpha$ , IL-6 and IL-10 were quantified. Interestingly, the transcript of TNF- $\alpha$

was significantly up-regulated and that of IL-6 or IL-10 was not markedly changed by DHA co-treatment upon A $\beta$  activation (Figure 4.4E).

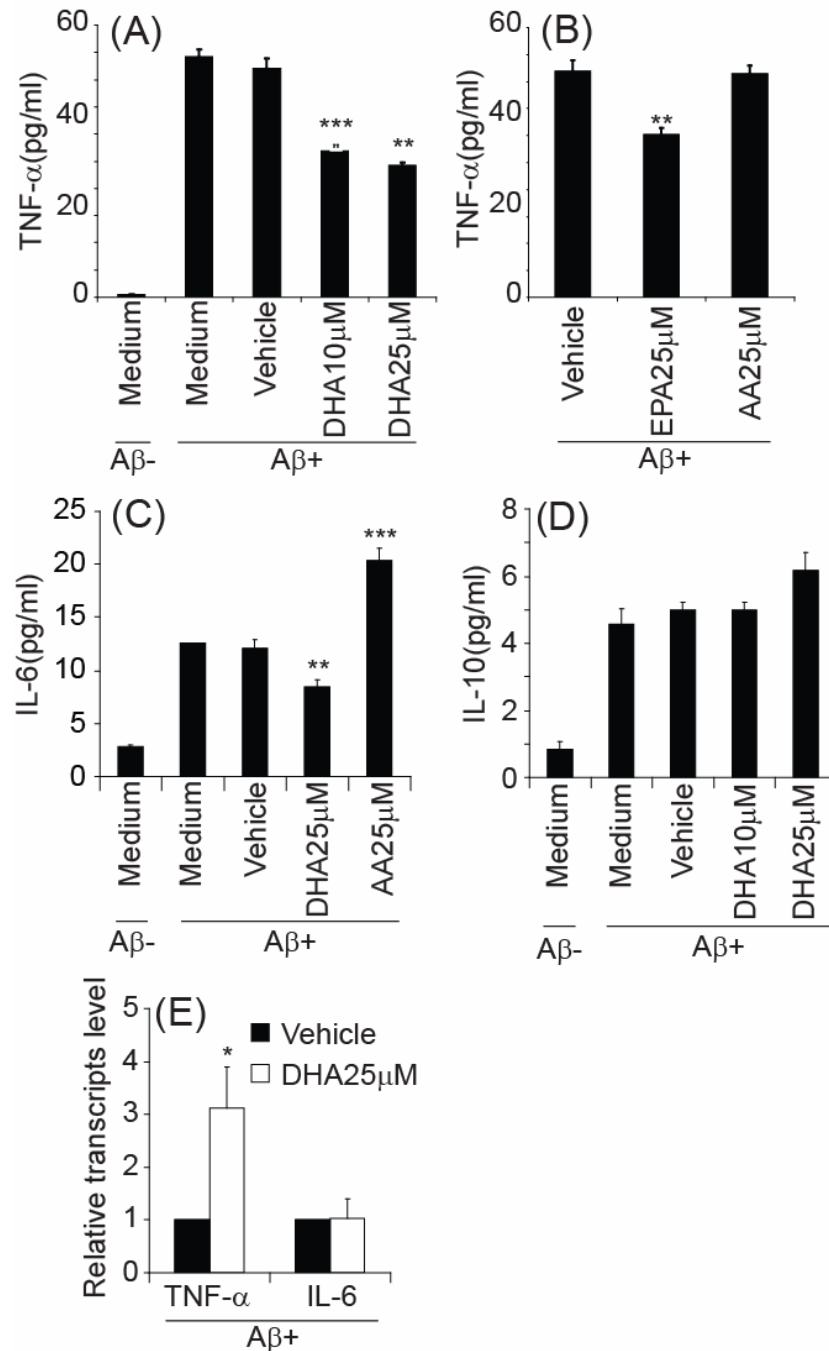


**Figure 4.4, Omega-3 PUFAs inhibit A $\beta$ 42 aggregate-induced inflammatory activation in BMDMs.** BMDMs were pretreated with omega-3 PUFAs DHA and EPA, or omega-6 PUFA AA at the indicated concentrations for 24 hrs and then challenged with 10  $\mu$ M A $\beta$ 42 aggregates for 18 hrs in the presence of relevant PUFAs. The media was collected for ELISA analysis of TNF- $\alpha$  (A, B), IL-6 (C) and IL-10 (D). (E), transcripts of TNF- $\alpha$ , IL-6 in BMDMs treated with or without DHA were quantified by real-time PCR. \*p < 0.05, \*\* p < 0.01, \*\*\* p < 0.001, as compared to vehicle control (one-way ANOVA, n $\geq$ 6 per group).

#### 4.4 DHA suppresses aggregated A $\beta$ -induced PGE2 secretion in macrophages

PGE2 is a primary product of arachidonic metabolism and is synthesized via the cyclooxygenase (COX) and prostaglandin synthase pathways. Postsynaptic PGE2 functions as a retrograde messenger in hippocampal synaptic signaling via a presynaptic EP2 receptor, thereby involving in the pathogenesis of neurodegenerative processes (Sang *et al.*, 2005). Therefore, besides the proinflammatory cytokines level, here the transcription level of PGE2 synthase (PTGES1) and its catalysed product PGE2 level were also investigated after challenge with A $\beta$ 42 for the BMDMs pre-treated with DHA or control lipid AA. As shown in Figure 4.5A, the PGE2 level secreted by the DHA treated BMDMs upon A $\beta$  challenge was lower than vehicle treated cells, while the PGE2 level in arachidonic acid pretreated cells was increased compare with control. Interestingly, however, the PGE2 synthase transcript was also increased in DHA treated cells compared to vehicle treated cells (Figure 4.5B).

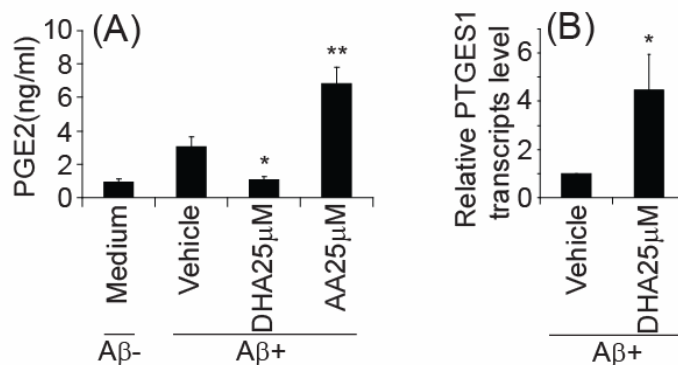


**Figure 4.5, DHA reduces A $\beta$ 42 aggregates induced PGE2 secretion.** BMDMs were pretreated with DHA or AA at the indicated concentrations for 24 hrs and then challenged with 10  $\mu$ M A $\beta$ 42 aggregates for 18 hrs in the presence of relevant PUFAs. The media was collected for ELISA analysis of PGE2 (A). Transcripts of PGE2 synthase 1 (PTGES1) were measured via real-time PCR (B). The \* $p < 0.05$ , \*\* $p < 0.01$ , as compared to vehicle control (one-way ANOVA,  $n=9$  per group).

#### 4.5 DHA does not affect macrophage uptake of A $\beta$ aggregates

Growing evidence has suggested that microglial elimination of A $\beta$  protects neurons against AD-related neurodegeneration (Tahara *et al.*, 2006; Richard *et al.*, 2008). The effect of DHA on A $\beta$  internalization by macrophages was tested. Interestingly, the internalization of A $\beta$ 42 aggregates, as measured by the mFI and percentage of fluorescent cells in flow cytometry, was not altered by DHA treatments (Figure 4.6A,  $p > 0.05$ ). EPA and AA (used as controls for DHA) did not affect A $\beta$  internalization either (Figure 4.6A,  $p > 0.05$ ). In additional

experiments, the transcripts of the known receptors related to A $\beta$  phagocytosis: RAGE, CD36, SR-A and CD14 (El Khoury *et al.*, 1996; Yan *et al.*, 1996; El Khoury *et al.*, 2003; Liu Y *et al.*, 2005) were determined via realtime-PCR. As shown in Figure 4.6B, DHA treatment increased transcription of RAGE and CD36, although the transcription of SR-A and CD14 was decreased in the DHA-treated cells. Thus, DHA did not overall reduce the A $\beta$  phagocytotic capacity.

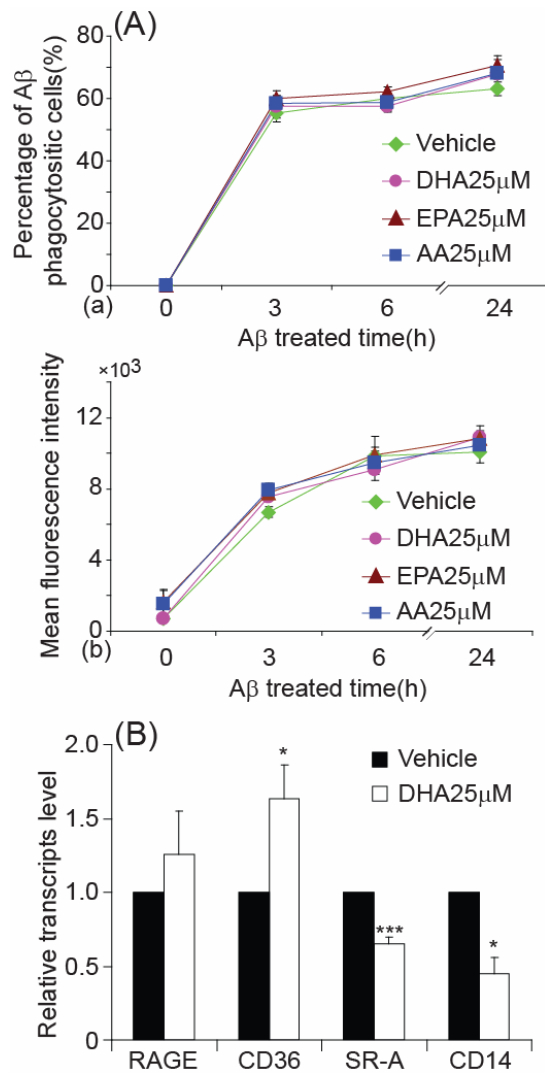


**Figure 4.6, PUFAs do not affect internalization of A $\beta$ 42 aggregates by BMDMs.** BMDMs were pretreated with 25  $\mu$ M DHA, EPA, or AA for 24 h and then incubated with 0.5  $\mu$ M FITC-conjugated A $\beta$ 42 aggregates for 0, 3, 6 or 24 hrs. Cells were detached and the fluorescence was measured with flow cytometry (A). B: transcripts of A $\beta$  phagocytosis-related receptors in DHA-treated cells were measured with real-time PCR. \* $p$  < 0.05, \*\*\*  $p$  < 0.001, as compared to vehicle control (one-way ANOVA,  $n$ =13 per group).

## 5 Discussion

Senile plaques containing A $\beta$  deposits accumulate over decades and induce neuronal death in AD. Microglial activation around A $\beta$  plaques has been demonstrated to make opposing contributions to AD pathophysiology: on one hand, release of neurotoxic inflammatory mediators is considered to be detrimental; on the other hand, phagocytotic A $\beta$  clearance could play a beneficial role. This study using primary cultured macrophages demonstrates that omega-3 fatty acids, *e.g.* DHA and EPA, significantly inhibit A $\beta$ -induced pro-inflammatory activation while leaving uptake of A $\beta$  unchanged.

Higher levels of omega-3 PUFAs in the plasma have been associated with reduced AD risk and anti-inflammatory cytokine profiles in humans (Endres *et al.*, 1989; Barberger-Gateau *et al.*, 2002; Morris *et al.*, 2003; Ferrucci *et al.*, 2006; Schaefer *et al.*, 2006). It is supposed that omega-3 PUFAs, which readily cross the blood-brain barrier, could suppress the inflammatory activation of microglia in the brain, which in turn prevents AD pathogenesis (Edmond, 2001). Indeed, here it was observed that omega-3 PUFAs significantly inhibited A $\beta$ -induced TNF- $\alpha$  and IL-6, but not IL-10, secretion from bone marrow-derived macrophages which, similar to microglia, belong to the mononuclear phagocyte lineage and contribute to AD pathogenesis (Simard *et al.*, 2006b).

However, the mechanisms by which DHA reduced A $\beta$ -induced proinflammatory cytokine release from macrophages are still far from being understood. Innate immune receptors, such as CD14, TLR2 and TLR4, have been demonstrated to recognize A $\beta$  aggregates, thereby triggering microglial inflammatory activation (Fassbender *et al.*, 2004; Liu Y *et al.*, 2005; Walter S *et al.*, 2007; Jana *et al.*, 2008). Interestingly, DHA treatment inhibits TLR2 and TLR4 ligand-induced inflammatory activation in macrophages (Lee Joo Y. *et al.*, 2001; Lee Joo Y. *et al.*, 2003; Lee Joo Y. *et al.*, 2004). Thus, DHA might inhibit A $\beta$ -initiated inflammatory activation by blocking TLRs signaling. However, this study demonstrated that DHA not only targets TLR2 and 4, but also TLR3, 7 and 9; because DHA treatment inhibits the release of all these TLRs-induced proinflammatory cytokines. Moreover, DHA blocked IFN- $\gamma$ -induced inflammatory activation. It was also observed that this anti-inflammatory effect of DHA was independent of MyD88, a common signaling molecule downstream to TLR2, 4 and 9. Since different receptors transduce signals through different pathways, omega-3 PUFAs are thus unlikely targeting one single molecule, *e.g.* receptor or signaling adaptor, in inflammatory activation. Even more interestingly, the transcription level of the

pro-inflammatory cytokines was observed to be not decreased by DHA treatment, suggesting the suppression effect of DHA might be at the post-transcriptional level.

Recently, the beneficial effect of A $\beta$  deposit clearing upon activation of microglia/macrophages has gained great interest (Liu Y *et al.*, 2005; Simard *et al.*, 2006b; Hao *et al.*, 2011). Here in this part of study, it was observed that treatment with omega-3 PUFAs reduces TLR-induced inflammatory activation, but does not reduce the internalization of aggregated A $\beta$ , which clearly argues for the separation of signaling cascades responsible for A $\beta$  uptake and inflammatory responses. Indeed, deficiency of TLR2, TLR4 or MyD88 was first observed to decrease macrophage clearance of bacteria such as *E. coli* (Blander *et al.*, 2004), but a following study did not show this effect upon the uptake of silica particles or *Staphylococcus aureus* (Yates *et al.*, 2005). Moreover, MyD88 was not involved in TLR4-induced phagocytosis of *E. coli* (Kong *et al.*, 2008). Regarding A $\beta$  phagocytosis, previous reports indicated that TLR ligand-induced inflammatory activation facilitates microglial phagocytosis of A $\beta$  (Iribarren *et al.*, 2005; Chen Keqiang *et al.*, 2006; Tahara *et al.*, 2006), whereas previous study of ours (Hao *et al.*, 2011) and the Part I work of this thesis showed that without ligand preactivation, deficiency of TLR2 or MyD88 did not decrease A $\beta$  phagocytosis; instead, deficiency of TLR2 or MyD88 activation increase A $\beta$  internalization (Part I of this thesis and (Hao *et al.*, 2011)). Furthermore, in this study, DHA treatment did not down-regulate the A $\beta$  phagocytosis-related receptors, RAGE and CD36. In some reports, these receptors could even be up-regulated upon treatment with omega-3 PUFAs (Vallvé *et al.*, 2002). Thus, omega-3 PUFAs do not impair the phagocytotic capacity of A $\beta$ .

In summary, this study demonstrated that omega-3 PUFAs prevent neurotoxic pro-inflammatory activation by A $\beta$  aggregates, but do not impair elimination of A $\beta$  by macrophages, showing a beneficial role in AD pathophysiology. This, together with the potential effects of omega-3 PUFAs on APP processing (Lim *et al.*, 2005), neuronal protection (Calon *et al.*, 2004; Akbar *et al.*, 2005) and differentiation (Kan *et al.*, 2007; Liu J-W *et al.*, 2008), suggests that a dietary supplement of omega-3 PUFAs could offer a preventative and therapeutic strategy for AD.

## References

1. Abplanalp AL, Morris IR, Parida BK, Teale JM, Berton MT (2009) TLR-dependent control of francisella tularensis infection and host inflammatory responses. *PLoS One* 4: e7920
2. Adams R, Victor M, Ropper A (1997) Principles of neurology. 6th ed. McGraw-Hill, New York
3. Ahmed M, Davis J, Aucoin D, Sato T, Ahuja S, Aimoto S, Elliott JI, Van Nostrand WE, Smith SO (2010) Structural conversion of neurotoxic amyloid-[beta]1-42 oligomers to fibrils. *Nat Struct Mol Biol* 17: 561-567
4. Ajami B, Bennett JL, Krieger C, Tetzlaff W, Rossi FMV (2007) Local self-renewal can sustain CNS microglia maintenance and function throughout adult life. *Nat Neurosci* 10: 1538-1543
5. Akbar M, Calderon F, Wen Z, Kim H-Y (2005) Docosahexaenoic acid: A positive modulator of Akt signaling in neuronal survival. *Proceedings of the National Academy of Sciences of the United States of America* 102: 10858-10863
6. Akiyama H, Barger S, Barnum S, Bradt B, Bauer J, Cole GM, Cooper NR, Eikelenboom P, Emmerling M, Fiebich BL, Finch CE, Frautschy S, Griffin WST, Hampel H, Hull M, Landreth G, Lue L-F, Mrak R, Mackenzie IR, McGeer PL, O'Banion MK, Pachter J, Pasinetti G, Plata-Salaman C, Rogers J, Rydel R, Shen Y, Streit W, Strommeyer R, Tooyoma I, Van Muiswinkel FL, Veerhuis R, Walker D, Webster S, Wegrzyniak B, Wenk G, Wyss-Coray T (2000) Inflammation and Alzheimer's disease. *Neurobiology of Aging* 21: 383-421
7. Alzheimer's-association (2011) 2011 Alzheimer's disease facts and figures. *Alzheimer's & dementia* 7: 208-244
8. Alzheimer A (1911) Über eigenartige Krankheitsfälle des späteren Alters. *Zeitschrift für die Gesamte Neurologie und Psychiatrie* 4: 356-85
9. Anderson KV, Nüsslein-Volhard C (1984) Information for the dorsal-ventral pattern of the Drosophila embryo is stored as maternal mRNA. *Nature* 311: 223-227
10. Anderson KV, Bokla L, Nüsslein-Volhard C (1985a) Establishment of dorsal-ventral polarity in the drosophila embryo: The induction of polarity by the Toll gene product. *Cell* 42: 791-798
11. Anderson KV, Jürgens G, Nüsslein-Volhard C (1985b) Establishment of dorsal-ventral polarity in the Drosophila embryo: Genetic studies on the role of the Toll gene product. *Cell* 42: 779-789
12. Apostolova LG, Dinov ID, Dutton RA, Hayashi KM, Toga AW, Cummings JL, Thompson PM (2006) 3D comparison of hippocampal atrophy in amnesic mild cognitive impairment and Alzheimer's disease. *Brain* 129: 2867-2873
13. Arispe N, Pollard HB, Rojas E (1993) Giant multilevel cation channels formed by Alzheimer disease amyloid beta-protein [A beta P-(1-40)] in bilayer membranes. *Proceedings of the National Academy of Sciences of the United States of America* 90: 10573-10577
14. Avdulov NA, Chochina SV, Igbavboa U, Warden CS, Vassiliev AV, Wood WG (1997) Lipid binding to Amyloid  $\beta$ -peptide aggregates: preferential binding of

- cholesterol as compared with phosphatidylcholine and fatty acids. *Journal of Neurochemistry* 69: 1746-1752
15. Azevedo FAC, Carvalho LRB, Grinberg LT, Farfel JM, Ferretti REL, Leite REP, Filho WJ, Lent R, Herculano-Houzel S (2009) Equal numbers of neuronal and nonneuronal cells make the human brain an isometrically scaled-up primate brain. *The Journal of Comparative Neurology* 513: 532-541
  16. Babcock AA, Wirenfeldt M, Holm T, Nielsen HH, Dissing-Olesen L, Toft-Hansen H, Millward JM, Landmann R, Rivest S, Finsen B, Owens T (2006) Toll-Like Receptor 2 Signaling in Response to Brain Injury: An Innate Bridge to Neuroinflammation. *The Journal of Neuroscience* 26: 12826-12837
  17. Babcock AA, Toft-Hansen H, Owens T (2008) Signaling through MyD88 regulates leukocyte recruitment after brain injury. *The Journal of Immunology* 181: 6481-6490
  18. Bamberger ME, Harris ME, McDonald DR, Husemann J, Landreth GE (2003) A cell surface receptor complex for fibrillar beta -amyloid mediates microglial activation. *J. Neurosci.* 23: 2665-2674
  19. Barbalat R, Lau L, Locksley RM, Barton GM (2009) Toll-like receptor 2 on inflammatory monocytes induces type I interferon in response to viral but not bacterial ligands. *Nat Immunol* 10: 1200-1207
  20. Barberger-Gateau P, Letenneur L, Deschamps V, Pérès K, Dartigues J-F, Renaud S (2002) Fish, meat, and risk of dementia: cohort study. *BMJ* 325: 932-933
  21. Bard F, Cannon C, Barbour R, Burke R-L, Games D, Grajeda H, Guido T, Hu K, Huang J, Johnson-Wood K, Khan K, Kholodenko D, Lee M, Lieberburg I, Motter R, Nguyen M, Soriano F, Vasquez N, Weiss K, Welch B, Seubert P, Schenk D, Yednock T (2000) Peripherally administered antibodies against amyloid [beta]-peptide enter the central nervous system and reduce pathology in a mouse model of Alzheimer disease. *Nat Med* 6: 916-919
  22. Barton GM, Kagan JC (2009) A cell biological view of Toll-like receptor function: regulation through compartmentalization. *Nat Rev Immunol* 9: 535-542
  23. Bayer TA, Schäfer S, Simons A, Kemmling A, Kamer T, Tepests R, Eckert A, Schlüssel K, Eikenberg O, Sturchler-Pierrat C, Abramowski D, Staufenbiel M, Multhaup G (2003) Dietary Cu stabilizes brain superoxide dismutase 1 activity and reduces amyloid A $\beta$  production in APP23 transgenic mice. *Proceedings of the National Academy of Sciences of the United States of America* 100: 14187-14192
  24. Bell JK, Botos I, Hall PR, Askins J, Shiloach J, Segal DM, Davies DR (2005) The molecular structure of the Toll-like receptor 3 ligand-binding domain. *Proceedings of the National Academy of Sciences of the United States of America* 102: 10976-10980
  25. Bernstein SL, Dupuis NF, Lazo ND, Wytttenbach T, Condrón MM, Bitan G, Teplow DB, Shea J-E, Ruotolo BT, Robinson CV, Bowers MT (2009) Amyloid- $\beta$  protein oligomerization and the importance of tetramers and dodecamers in the aetiology of Alzheimer's disease. *Nat Chem* 1: 326-331
  26. Bhoj VG, Chen ZJ (2009) Ubiquitylation in innate and adaptive immunity. *Nature* 458: 430-437
  27. Biber K, Neumann H, Inoue K, Boddeke HWGM (2007) Neuronal "On" and "Off" signals control microglia. *Trends in Neurosciences* 30: 596-602

28. Blander J, Medzhitov R (2004) Regulation of Phagosome Maturation by Signals from Toll-Like Receptors. *Science* 304: 1014-1018
29. Blander J (2007) Coupling Toll-like receptor signaling with phagocytosis: potentiation of antigen presentation. *Trends in Immunology* 28: 19-25
30. Blander J (2008) Phagocytosis and antigen presentation: a partnership initiated by Toll-like receptors. *Annals of the Rheumatic Diseases* 67: iii44-iii49
31. Bobinski M, Wegiel J, Tarnawski M, Reisberg B, deLeon MJ, Miller DC, Wisniewski HM (1997) Relationships between regional neuronal loss and neurofibrillary changes in the hippocampal formation and duration and severity of Alzheimer disease. *Journal of Neuropathology and Experimental Neurology* 56: 414-420
32. Bradford MM (1976) A rapid and sensitive method for the quantitation of microgram quantities of protein utilizing the principle of protein-dye binding. *Analytical Biochemistry* 72: 248-254
33. Brightbill HD, Libraty DH, Krutzik SR, Yang R-B, Belisle JT, Bleharski JR, Maitland M, Norgard MV, Plevy SE, Smale ST, Brennan PJ, Bloom BR, Godowski PJ, Modlin RL (1999) Host defense mechanisms triggered by microbial lipoproteins through Toll-like receptors. *Science* 285: 732-736
34. Brodsky I, Medzhitov R (2007) Two modes of ligand recognition by TLRs. *Cell* 130: 979-981
35. Buwitt-Beckmann U, Heine H, Wiesmüller K-H, Jung G, Brock R, Akira S, Ulmer AJ (2006) TLR1- and TLR6-independent recognition of bacterial lipopeptides. *Journal of Biological Chemistry* 281: 9049-9057
36. Cagnin A, Brooks DJ, Kennedy AM, Gunn RN, Myers R, Turkheimer FE, Jones T, Banati RB (2001) In-vivo measurement of activated microglia in dementia. *The Lancet* 358: 461-467
37. Calon F, Lim GP, Yang F, Morihara T, Teter B, Ubeda O, Rostaing P, Triller A, Salem Jr N, Ashe KH, Frautschy SA, Cole GM (2004) Docosahexaenoic Acid Protects from Dendritic Pathology in an Alzheimer's Disease Mouse Model. *Neuron* 43: 633-645
38. Capo C, Moynault A, Collette Y, Olive D, Brown EJ, Raoult D, Mege J-L (2003) *Coxiella burnetii* Avoids Macrophage Phagocytosis by Interfering with Spatial Distribution of Complement Receptor 3. *The Journal of Immunology* 170: 4217-4225
39. Cartier N, Hacein-Bey-Abina S, Bartholomae CC, Veres G, Schmidt M, Kutschera I, Vidaud M, Abel U, Dal-Cortivo L, Caccavelli L, Mahlaoui N, Kiermer V, Mittelstaedt D, Bellesme C, Lahlou N, Lefrere F, Blanche S, Audit M, Payen E, Leboulch P, l'Homme B, Bougneres P, Von Kalle C, Fischer A, Cavazzana-Calvo M, Aubourg P (2009) Hematopoietic stem cell gene therapy with a lentiviral vector in X-Linked adrenoleukodystrophy. *Science* 326: 818-823
40. Chao CC, Hu SX, Ehrlich L, Peterson PK (1995) Interleukin-1 and tumor necrosis factor- $\alpha$  synergistically mediate neurotoxicity: involvement of nitric oxide and of N-methyl-D-aspartate receptors. *Brain, Behavior, and Immunity* 9: 355-365
41. Chen K, Iribarren P, Hu J, Chen J, Gong W, Cho EH, Lockett S, Dunlop NM, Wang JM (2006) Activation of Toll-like receptor 2 on microglia promotes cell uptake of Alzheimer disease-associated amyloid  $\beta$  peptide. *Journal of Biological Chemistry* 281: 3651-3659

42. Chen N-J, Chio IIC, Lin W-J, Duncan G, Chau H, Katz D, Huang H-L, Pike KA, Hao Z, Su Y-W, Yamamoto K, de Pooter RF, Zúñiga-Pflücker JC, Wakeham A, Yeh W-C, Mak TW (2008) Beyond tumor necrosis factor receptor: TRADD signaling in toll-like receptors. *Proceedings of the National Academy of Sciences* 105: 12429-12434
43. Chételat G, Villemagne VL, Pike KE, Ellis KA, Bourgeat P, Jones G, O'Keefe GJ, Salvado O, Szoëke C, Martins RN, Ames D, Masters CL, Rowe CC, Biomarkers tAI, Group LSoaR (2011) Independent contribution of temporal  $\beta$ -amyloid deposition to memory decline in the pre-dementia phase of Alzheimer's disease. *Brain* 134: 798-807
44. Choe J, Kelker MS, Wilson IA (2005) Crystal structure of human Toll-like receptor 3 (TLR3) ectodomain. *Science* 309: 581-585
45. Chung CT, Niemela SL, Miller RH (1989) One-step preparation of competent *Escherichia coli*: transformation and storage of bacterial cells in the same solution. *Proceedings of the National Academy of Sciences of the United States of America* 86: 2172-2175
46. Citron M (2010) Alzheimer's disease: strategies for disease modification. *Nat Rev Drug Discov* 9: 387-398
47. Coraci IS, Husemann J, Berman JW, Hulette C, Dufour JH, Campanella GK, Luster AD, Silverstein SC, El Khoury JB (2002) CD36, a Class B Scavenger Receptor, Is Expressed on Microglia in Alzheimer's Disease Brains and Can Mediate Production of Reactive Oxygen Species in Response to  $\beta$ -Amyloid Fibrils. *Am J Pathol* 160: 101-112
48. Crews L, Masliah E (2010a) Molecular mechanisms of neurodegeneration in Alzheimer's disease. *Human Molecular Genetics* 19: R12-R20
49. Crews L, Rockenstein E, Masliah E (2010b) APP transgenic modeling of Alzheimer's disease: mechanisms of neurodegeneration and aberrant neurogenesis. *Brain Structure and Function* 214: 111-126
50. Dahlgren KN, Manelli AM, Stine WB, Baker LK, Krafft GA, LaDu MJ (2002) Oligomeric and fibrillar species of amyloid- $\beta$  peptides differentially affect neuronal viability. *Journal of Biological Chemistry* 277: 32046-32053
51. Davoust N, Vuillat C, Androdias G, Nataf S (2008) From bone marrow to microglia: barriers and avenues. *Trends in Immunology* 29: 227-234
52. De Smedt-Peyrusse V, Sargueil F, Moranis A, Harizi H, Mongrand S, Layé S (2008) Docosahexaenoic acid prevents lipopolysaccharide-induced cytokine production in microglial cells by inhibiting lipopolysaccharide receptor presentation but not its membrane subdomain localization. *Journal of Neurochemistry* 105: 296-307
53. Decout A, Labeur C, Goethals M, Brasseur R, Vandekerckhove J, Rosseneu M (1998) Enhanced efficiency of a targeted fusogenic peptide. *Biochimica et Biophysica Acta (BBA) - Biomembranes* 1372: 102-116
54. DeKosky ST, Scheff SW (1990) Synapse loss in frontal cortex biopsies in Alzheimer's disease: Correlation with cognitive severity. *Annals of Neurology* 27: 457-464
55. Demuro A, Parker I, Stutzmann GE (2010) Calcium signaling and amyloid toxicity in Alzheimer disease. *Journal of Biological Chemistry* 285: 12463-12468
56. Dong J, Atwood CS, Anderson VE, Siedlak SL, Smith MA, Perry G, Carey PR (2003) Metal binding and oxidation of Amyloid- $\beta$  within isolated senile plaque cores: Raman microscopic evidence. *Biochemistry* 42: 2768-2773

57. Edison P, Archer HA, Gerhard A, Hinz R, Pavese N, Turkheimer FE, Hammers A, Tai YF, Fox N, Kennedy A, Rossor M, Brooks DJ (2008) Microglia, amyloid, and cognition in Alzheimer's disease: An [11C](R)PK11195-PET and [11C]PIB-PET study. *Neurobiology of Disease* 32: 412-419
58. Edmond J (2001) Essential polyunsaturated fatty acids and the barrier to the brain. *Journal of Molecular Neuroscience* 16: 181-193
59. El Khoury J, Hickman S, CA T, Cao L, Silverstein S, JD L (1996) Scavenger receptor-mediated adhesion of microglia to [beta]-amyloid fibrils. *Nature* 382: 716-719
60. El Khoury J, Moore KJ, Means TK, Leung J, Terada K, Toft M, Freeman MW, Luster AD (2003) CD36 mediates the innate host response to  $\beta$ -Amyloid. *The Journal of Experimental Medicine* 197: 1657-1666
61. Endres S, Ghorbani R, Kelley VE, Georgilis K, Lonnemann G, van der Meer JWM, Cannon JG, Rogers TS, Klempner MS, Weber PC, Schaefer EJ, Wolff SM, Dinarello CA (1989) The effect of dietary supplementation with n—3 polyunsaturated fatty acids on the synthesis of interleukin-1 and tumor necrosis factor by mononuclear cells. *New England Journal of Medicine* 320: 265-271
62. Etokebe GE, Skjeldal F, Nilsen N, Rodionov D, Knezevic J, Bulat-Kardum L, Espevik T, Bakke O, Dembic Z (2010) Toll-like receptor 2 (P631H) mutant impairs membrane internalization and is a dominant negative allele. *Scandinavian Journal of Immunology* 71: 369-381
63. Evans DA, Funkenstein HH, Albert MS, Scherr PA, Cook NR, Chown MJ, Hebert LE, Hennekens CH, Taylor JO (1989) Prevalence of Alzheimer's Disease in a Community Population of Older Persons. *JAMA: The Journal of the American Medical Association* 262: 2551-2556
64. Farhat K, Riekenberg S, Heine H, Debarry J, Lang R, Mages J, Buwitt-Beckmann U, Röschmann K, Jung G, Wiesmüller K-H, Ulmer AJ (2008) Heterodimerization of TLR2 with TLR1 or TLR6 expands the ligand spectrum but does not lead to differential signaling. *Journal of Leukocyte Biology* 83: 692-701
65. Farooqui AA, Horrocks LA, Farooqui T (2007) Modulation of inflammation in brain: a matter of fat. *Journal of Neurochemistry* 101: 577-599
66. Fassbender K, Simons M, Bergmann C, Stroick M, Lütjohann D, Keller P, Runz H, Kühl S, Bertsch T, von Bergmann K, Hennerici M, Beyreuther K, Hartmann T (2001) Simvastatin strongly reduces levels of Alzheimer's disease  $\beta$ -amyloid peptides A $\beta$ 42 and A $\beta$ 40 in vitro and in vivo. *Proceedings of the National Academy of Sciences of the United States of America* 98: 5856-5861
67. Fassbender K, Walter S, Kühl S, Landmann R, Ishii K, Bertsch T, Stalder A, Muehlhauser F, Liu Y, Ulmer A, Rivest S, Lentschat A, Gulbins E, Jucker M, Staufenbiel M, Brechtel K, Walter J, Multhaup G, Penke B, Adachi Y, Hartmann T, Beyreuther K (2004) The LPS receptor (CD14) links innate immunity with Alzheimer's disease. *FASEB J.* 18: 203-205
68. Feng Y, Chung D, Garrard L, McEnroe G, Lim D, Scardina J, McFadden K, Guzzetta A, Lam A, Abraham J, Liu D, Endemann G (1998) Peptides derived from the complementarity-determining regions of anti-Mac-1 antibodies block intercellular adhesion molecule-1 Interaction with Mac-1. *Journal of Biological Chemistry* 273: 5625-5630

69. Ferrucci L, Cherubini A, Bandinelli S, Bartali B, Corsi A, Lauretani F, Martin A, Andres-Lacueva C, Senin U, Guralnik JM (2006) Relationship of plasma polyunsaturated fatty acids to circulating inflammatory markers. *J Clin Endocrinol Metab* 91: 439-446
70. Fuhrmann M, Bittner T, Jung CKE, Burgold S, Page RM, Mitteregger G, Haass C, LaFerla FM, Kretzschmar H, Herms J (2010) Microglial Cx3cr1 knockout prevents neuron loss in a mouse model of Alzheimer's disease. *Nat Neurosci* 13: 411-413
71. Garcia-Alloza M, Robbins EM, Zhang-Nunes SX, Purcell SM, Betensky RA, Raju S, Prada C, Greenberg SM, Bacskai BJ, Frosch MP (2006) Characterization of amyloid deposition in the APP<sup>swe</sup>/PS1<sup>dE9</sup> mouse model of Alzheimer disease. *Neurobiology of Disease* 24: 516-524
72. Gautam JK, Ashish, Comeau LD, Krueger JK, Smith MF (2006) Structural and Functional Evidence for the Role of the TLR2 DD Loop in TLR1/TLR2 Heterodimerization and Signaling. *Journal of Biological Chemistry* 281: 30132-30142
73. Gay NJ, Keith FJ (1991) Drosophila Toll and IL-1 receptor. *Nature* 351: 355-356
74. Gilchrist M, Thorsson V, Li B, Rust AG, Korb M, Kennedy K, Hai T, Bolouri H, Aderem A (2006) Systems biology approaches identify ATF3 as a negative regulator of Toll-like receptor 4. *Nature* 441: 173-178
75. Ginhoux F, Greter M, Leboeuf M, Nandi S, See P, Gokhan S, Mehler MF, Conway SJ, Ng LG, Stanley ER, Samokhvalov IM, Merad M (2010) Fate mapping analysis reveals that adult microglia derive from primitive macrophages. *Science* 330: 841-845
76. Glass CK, Saijo K, Winner B, Marchetto MC, Gage FH (2010) Mechanisms underlying inflammation in neurodegeneration. *Cell* 140: 918-934
77. Goedert M, Spillantini M (2006) A century of Alzheimer's disease. *Science* 314: 777-781
78. Grabiec A, Meng G, Fichte S, Bessler W, Wagner H, Kirschning CJ (2004) Human but not murine toll-like receptor 2 discriminates between tri-palmitoylated and tri-lauroylated peptides. *Journal of Biological Chemistry* 279: 48004-48012
79. Graeber MB (2010) Changing face of microglia. *Science* 330: 783-788
80. Grathwohl SA, Kalin RE, Bolmont T, Prokop S, Winkelmann G, Kaeser SA, Odenthal J, Radde R, Eldh T, Gandy S, Aguzzi A, Staufenbiel M, Mathews PM, Wolburg H, Heppner FL, Jucker M (2009) Formation and maintenance of Alzheimer's disease [beta]-amyloid plaques in the absence of microglia. *Nat Neurosci* 12: 1361-1363
81. Green KN, Martinez-Coria H, Khashwji H, Hall EB, Yurko-Mauro KA, Ellis L, LaFerla FM (2007) Dietary docosahexaenoic acid and docosapentaenoic acid ameliorate Amyloid- $\beta$  and Tau pathology via a mechanism involving presenilin 1 levels. *J. Neurosci.* 27: 4385-4395
82. Grimm MOW, Grimm HS, Patzold AJ, Zinser EG, Halonen R, Duering M, Tschape J-A, Strooper BD, Muller U, Shen J, Hartmann T (2005) Regulation of cholesterol and sphingomyelin metabolism by amyloid- $\beta$  and presenilin. *Nat Cell Biol* 7: 1118-1123
83. Grösgen S, Grimm MOW, Frieß P, Hartmann T (2010) Role of amyloid beta in lipid homeostasis. *Biochimica et Biophysica Acta (BBA) - Molecular and Cell Biology of Lipids* 1801: 966-974

84. Guo Z, Iyun T, Fu W, Zhang P, Mattson M (2004) Bone marrow transplantation reveals roles for brain macrophage/microglia TNF signaling and nitric oxide production in excitotoxic neuronal death. *NeuroMolecular Medicine* 5: 219-234
85. Haass C, Selkoe DJ (2007) Soluble protein oligomers in neurodegeneration: lessons from the Alzheimer's amyloid [beta]-peptide. *Nat Rev Mol Cell Biol* 8: 101-112
86. Hajjar AM, O'Mahony DS, Ozinsky A, Underhill DM, Aderem A, Klebanoff SJ, Wilson CB (2001) Cutting Edge: Functional interactions between Toll-like receptor (TLR) 2 and TLR1 or TLR6 in response to phenol-soluble modulin. *The Journal of Immunology* 166: 15-19
87. Halle A, Hornung V, Petzold GC, Stewart CR, Monks BG, Reinheckel T, Fitzgerald KA, Latz E, Moore KJ, Golenbock DT (2008) The NALP3 inflammasome is involved in the innate immune response to amyloid-[beta]. *Nat Immunol* 9: 857-865
88. Hansson GK, Edfeldt K (2005) Toll to be paid at the gateway to the vessel wall. *Arterioscler Thromb Vasc Biol* 25: 1085-1087
89. Hao W, Liu Y, Liu S, Walter S, Grimm MO, Kiliaan AJ, Penke B, Hartmann T, Rube CE, Menger MD, Fassbender K (2011) Myeloid differentiation factor 88-deficient bone marrow cells improve Alzheimer's disease-related symptoms and pathology. *Brain* 134: 278-92
90. Hartmann T, Bieger SC, Bruhl B, Tienari PJ, Ida N, Allsop D, Roberts GW, Masters CL, Dotti CG, Unsicker K, Beyreuther K (1997) Distinct sites of intracellular production for Alzheimer's disease A[beta]40/42 amyloid peptides. *Nat Med* 3: 1016-1020
91. Hashimoto C, Hudson KL, Anderson KV (1988) The Toll gene of drosophila, required for dorsal-ventral embryonic polarity, appears to encode a transmembrane protein. *Cell* 52: 269-279
92. Heckman KL, Pease LR (2007) Gene splicing and mutagenesis by PCR-driven overlap extension. *Nat. Protocols* 2: 924-932
93. Heneka MT, Nadrigny F, Regen T, Martinez-Hernandez A, Dumitrescu-Ozimek L, Terwel D, Jardanhazi-Kurutz D, Walter J, Kirchhoff F, Hanisch U-K, Kummer MP (2010) Locus ceruleus controls Alzheimer's disease pathology by modulating microglial functions through norepinephrine. *Proceedings of the National Academy of Sciences* 107: 6058-6063
94. Henneke P, Takeuchi O, Malley R, Lien E, Ingalls RR, Freeman MW, Mayadas T, Nizet V, Akira S, Kasper DL, Golenbock DT (2002) Cellular activation, phagocytosis, and bactericidal activity against group B streptococcus involve parallel myeloid differentiation factor 88-dependent and independent signaling Pathways. *The Journal of Immunology* 169: 3970-3977
95. Hooijmans CR, Rutters F, Dederen PJ, Gambarota G, Veltien A, van Groen T, Broersen LM, Lütjohann D, Heerschap A, Tanila H, Kiliaan AJ (2007) Changes in cerebral blood volume and amyloid pathology in aged Alzheimer APP/PS1 mice on a docosahexaenoic acid (DHA) diet or cholesterol enriched Typical Western Diet (TWD). *Neurobiology of Disease* 28: 16-29
96. Hu J, Akama KT, Krafft GA, Chromy BA, Van Eldik LJ (1998) Amyloid-[beta] peptide activates cultured astrocytes: morphological alterations, cytokine induction and nitric oxide release. *Brain Research* 785: 195-206

97. Huttlin EL, Jedrychowski MP, Elias JE, Goswami T, Rad R, Beausoleil SA, Villén J, Haas W, Sowa ME, Gygi SP (2010) A tissue-specific Atlas of mouse protein phosphorylation and expression. *Cell* 143: 1174-1189
98. Hyman BT, Van Hoesen GW, Kromer LJ, Damasio AR (1986) Perforant pathway changes and the memory impairment of Alzheimer's disease. *Annals of Neurology* 20: 472-481
99. Imai Y, Iбата I, Ito D, Ohsawa K, Kohsaka S (1996) A novel gene in the major histocompatibility complex class III region encoding an EF hand protein expressed in a monocytic lineage. *Biochemical and Biophysical Research Communications* 224: 855-862
100. in 't Veld BA, Ruitenberг A, Hofman A, Launer LJ, van Duijn CM, Stijnen T, Breteler MMB, Stricker BHC (2001) Nonsteroidal antiinflammatory drugs and the risk of Alzheimer's disease. *New England Journal of Medicine* 345: 1515-1521
101. Inoue S (2008) In situ Aβ pores in AD brain are cylindrical assembly of Aβ protofilaments. *Amyloid* 15: 223-233
102. Iribarren P, Chen K, Hu J, Gong W, Cho EH, Lockett S, Uranchimeg B, Wang JM (2005) CpG-containing oligodeoxynucleotide promotes microglial cell uptake of amyloid β 1-42 peptide by up-regulating the expression of the G-protein-coupled receptor mFPR2. *The FASEB Journal* 19: 2032-2034
103. Ishii K MF, Liebl U, Picard M, Kühl S, Penke B, Bayer T, Wiessler M, Hennerici M, Beyreuther K, Hartmann T, Fassbender K. (2000) Subacute NO generation induced by Alzheimer's {beta}-amyloid in the living brain: reversal by inhibition of the inducible NO synthase. *FASEB J.* 14: 1485-1489
104. Ito D, Imai Y, Ohsawa K, Nakajima K, Fukuuchi Y, Kohsaka S (1998) Microglia-specific localisation of a novel calcium binding protein, Iba1. *Molecular Brain Research* 57: 1-9
105. Iwatsubo T, Odaka A, Suzuki N, Mizusawa H, Nukina N, Ihara Y (1994) Visualization of A[β]42(43) and A[β]40 in senile plaques with end-specific A[β] monoclonals: Evidence that an initially deposited species is A[β]42(43). *Neuron* 13: 45-53
106. Jana M, Palencia CA, Pahan K (2008) Fibrillar Amyloid-β peptides activate microglia via TLR2: implications for Alzheimer's disease. *J Immunol* 181: 7254-7262
107. Janeway Jr CA (1989) Approaching the asymptote? Evolution and revolution in immunology. *Cold Spring Harbor Symposia on Quantitative Biology* 54: 1-13
108. Jankowsky JL, Slunt HH, Ratovitski T, Jenkins NA, Copeland NG, Borchelt DR (2001) Co-expression of multiple transgenes in mouse CNS: a comparison of strategies. *Biomolecular Engineering* 17: 157-165
109. Jantzen PT, Connor KE, DiCarlo G, Wenk GL, Wallace JL, Rojiani AM, Coppola D, Morgan D, Gordon MN (2002) Microglial activation and β-Amyloid deposit reduction caused by a nitric oxide-releasing nonsteroidal anti-inflammatory drug in Amyloid precursor protein plus presenilin-1 transgenic mice. *The Journal of Neuroscience* 22: 2246-2254
110. Jick H, Zornberg GL, Jick SS, Seshadri S, Drachman DA (2000) Statins and the risk of dementia. *Lancet* 356: 1627

111. Jin MS, Kim SE, Heo JY, Lee ME, Kim HM, Paik S-G, Lee H, Lee J-O (2007) Crystal structure of the TLR1-TLR2 heterodimer induced by binding of a Tri-acylated lipopeptide. *Cell* 130: 1071-1082
112. Jin MS, Lee J-O (2008a) Structures of the Toll-like Receptor family and its ligand complexes. *Immunity* 29: 182-191
113. Jin MS, Lee J-O (2008b) Structures of TLR-ligand complexes. *Current Opinion in Immunology* 20: 414-419
114. Kajava AV, Vasselon T (2010) A network of hydrogen bonds on the surface of TLR2 controls ligand positioning and cell signaling. *Journal of Biological Chemistry* 285: 6227-6234
115. Kan I, Melamed E, Offen D, Green P (2007) Docosahexaenoic acid and arachidonic acid are fundamental supplements for the induction of neuronal differentiation. *Journal of Lipid Research* 48: 513-517
116. Kang JY, Nan X, Jin MS, Youn S-J, Ryu YH, Mah S, Han SH, Lee H, Paik S-G, Lee J-O (2009) Recognition of lipopeptide patterns by Toll-like receptor 2-Toll-like receptor 6 heterodimer. *Immunity* 31: 873-884
117. Kawai T, Akira S (2006) Innate immune recognition of viral infection. *Nat Immunol* 7: 131-137
118. Kawai T, Akira S (2010) The role of pattern-recognition receptors in innate immunity: update on Toll-like receptors. *Nat Immunol* 11: 373-384
119. Keene CD, Chang RC, Lopez-Yglesias AH, Shalloway BR, Sokal I, Li X, Reed PJ, Keene LM, Montine KS, Breyer RM, Rockhill JK, Montine TJ (2010) Suppressed accumulation of cerebral Amyloid {beta} peptides in aged transgenic Alzheimer's disease mice by transplantation with wild-type or prostaglandin E2 receptor subtype 2-null bone marrow. *Am J Pathol* 177: 346-354
120. Khoury JE, Luster AD (2008) Mechanisms of microglia accumulation in Alzheimer's disease: therapeutic implications. *Trends in Pharmacological Sciences* 29: 626-632
121. Kim HM, Park BS, Kim J-I, Kim SE, Lee J, Oh SC, Enkhbayar P, Matsushima N, Lee H, Yoo OJ, Lee J-O (2007) Crystal structure of the TLR4-MD-2 complex with bound endotoxin antagonist eritoran. *Cell* 130: 906-917
122. Kobe B, Kajava AV (2001) The leucine-rich repeat as a protein recognition motif. *Current Opinion in Structural Biology* 11: 725-732
123. Koenigsknecht-Talboo J, Meyer-Luehmann M, Parsadanian M, Garcia-Alloza M, Finn MB, Hyman BT, Bacskai BJ, Holtzman DM (2008) Rapid microglial response around amyloid pathology after systemic anti-A{beta} antibody administration in PDAPP mice. *J. Neurosci.* 28: 14156-14164
124. Kögel D, Schomburg R, Schürmann T, Reimertz C, König H-G, Poppe M, Eckert A, Müller WE, Prehn JHM (2003) The amyloid precursor protein protects PC12 cells against endoplasmic reticulum stress-induced apoptosis. *Journal of Neurochemistry* 87: 248-256
125. Kong L, Ge B-X (2008) MyD88-independent activation of a novel actin-Cdc42/Rac pathway is required for Toll-like receptor-stimulated phagocytosis. *Cell Res* 18: 745-755

126. Kuwata H, Matsumoto M, Atarashi K, Morishita H, Hirotsu T, Koga R, Takeda K (2006) I[math>\kappa]BNS inhibits induction of a subset of Toll-like receptor-dependent genes and limits inflammation. *Immunity* 24: 41-51
127. Lawson LJ, Perry VH, Dri P, Gordon S (1990) Heterogeneity in the distribution and morphology of microglia in the normal adult mouse brain. *Neuroscience* 39: 151-170
128. Lee JY, Sohn KH, Rhee SH, Hwang D (2001) Saturated Fatty Acids, but Not Unsaturated Fatty Acids, Induce the Expression of Cyclooxygenase-2 Mediated through Toll-like Receptor 4. *Journal of Biological Chemistry* 276: 16683-16689
129. Lee JY, Plakidas A, Lee WH, Heikkinen A, Chanmugam P, Bray G, Hwang DH (2003) Differential modulation of Toll-like receptors by fatty acids. *Journal of Lipid Research* 44: 479-486
130. Lee JY, Zhao L, Youn HS, Weatherill AR, Tapping R, Feng L, Lee WH, Fitzgerald KA, Hwang DH (2004) Saturated fatty acid activates but polyunsaturated fatty acid inhibits Toll-like receptor 2 dimerized with Toll-like receptor 6 or 1. *Journal of Biological Chemistry* 279: 16971-16979
131. Lee Y-J, Han S, Nam S-Y, Oh K-W, Hong J (2010) Inflammation and Alzheimer's disease. *Archives of Pharmacal Research* 33: 1539-1556
132. Lemaitre B, Nicolas E, Michaut L, Reichhart J-M, Hoffmann JA (1996) The dorsoventral regulatory gene cassette *spätzle/Toll/cactus* controls the potent antifungal response in *Drosophila* adults. *Cell* 86: 973-983
133. Leone C, Le Pavec G, Mème W, Porcheray F, Samah B, Dormont D, Gras G (2006) Characterization of human monocyte-derived microglia-like cells. *Glia* 54: 183-192
134. Li S, Jin M, Koeglsperger T, Shepardson NE, Shankar GM, Selkoe DJ (2011) Soluble A $\beta$  oligomers inhibit long-term potentiation through a mechanism involving excessive activation of extrasynaptic NR2B-containing NMDA receptors. *J. Neurosci* 31: 6627-6638
135. Lim GP, Calon F, Morihara T, Yang F, Teter B, Ubeda O, Salem N, Jr, Frautschy SA, Cole GM (2005) A diet enriched with the Omega-3 fatty acid docosahexaenoic acid reduces Amyloid burden in an aged Alzheimer mouse model. *J. Neurosci.* 25: 3032-3040
136. Lin S-C, Lo Y-C, Wu H (2010) Helical assembly in the MyD88-IRAK4-IRAK2 complex in TLR/IL-1R signalling. *Nature* 465: 885-890
137. Litvak V, Ramsey SA, Rust AG, Zak DE, Kennedy KA, Lampano AE, Nykter M, Shmulevich I, Aderem A (2009) Function of C/EBP[math>\delta] in a regulatory circuit that discriminates between transient and persistent TLR4-induced signals. *Nat Immunol* 10: 437-443
138. Liu J-W, Almaguel FG, Bu L, De Leon DD, De Leon M (2008) Expression of E-FABP in PC12 cells increases neurite extension during differentiation: involvement of n-3 and n-6 fatty acids. *Journal of Neurochemistry* 106: 2015-2029
139. Liu N, Montgomery RR, Barthold SW, Bockenstedt LK (2004) Myeloid differentiation antigen 88 deficiency impairs pathogen clearance but does not alter inflammation in *Borrelia burgdorferi*-infected mice. *Infect. Immun.* 72: 3195-3203
140. Liu Y, Walter S, Stagi M, Cherny D, Letiembre M, Schulz-Schaeffer W, Heine H, Penke B, Neumann H, Fassbender K (2005) LPS receptor (CD14): a receptor for phagocytosis of Alzheimer's amyloid peptide. *Brain* 128: 1778-1789

141. Malm TM, Koistinaho M, Pärepallo M, Vatanen T, Ooka A, Karlsson S, Koistinaho J (2005) Bone-marrow-derived cells contribute to the recruitment of microglial cells in response to [beta]-amyloid deposition in APP/PS1 double transgenic Alzheimer mice. *Neurobiology of Disease* 18: 134-142
142. Marr KA, Arunmozhi Balajee S, Hawn TR, Ozinsky A, Pham U, Akira S, Aderem A, Conrad Liles W (2003) Differential role of MyD88 in macrophage-mediated responses to opportunistic fungal pathogens. *Infect. Immun.* 71: 5280-5286
143. Martins IC, Kuperstein I, Wilkinson H, Maes E, Vanbrabant M, Jonckheere W, Van Gelder P, Hartmann D, D'Hooge R, De Strooper B, Schymkowitz J, Rousseau F (2008) Lipids revert inert A[beta] amyloid fibrils to neurotoxic protofibrils that affect learning in mice. *EMBO J* 27: 224-233
144. Maurer K, Volk S, Gerbaldo H (1997) Auguste D and Alzheimer's disease. *The Lancet* 349: 1546-1549
145. Mc Donald JM, Savva GM, Brayne C, Welzel AT, Forster G, Shankar GM, Selkoe DJ, Ince PG, Walsh DM (2010) The presence of sodium dodecyl sulphate-stable A $\beta$  dimers is strongly associated with Alzheimer-type dementia. *Brain* 133: 1328-1341
146. McGeer PL SM, McGeer EG. (1996) Arthritis and anti-inflammatory agents as possible protective factors for Alzheimer's disease: a review of 17 epidemiologic studies. *Neurology* 47: 425-32
147. McLaurin J, Franklin T, Chakrabartty A, Fraser PE (1998) Phosphatidylinositol and inositol involvement in alzheimer amyloid-[beta] fibril growth and arrest. *Journal of Molecular Biology* 278: 183-194
148. Medeiros R, Prediger RDS, Passos GF, Pandolfo P, Duarte FS, Franco JL, Dafre AL, Di Giunta G, Figueiredo CP, Takahashi RN, Campos MM, Calixto JB (2007) Connecting TNF- $\alpha$  signaling pathways to iNOS expression in a mouse model of Alzheimer's disease: relevance for the behavioral and synaptic deficits induced by Amyloid  $\beta$  protein. *J. Neurosci.* 27: 5394-5404
149. Medzhitov R, Janeway CA (1997a) Innate Immunity: the virtues of a nonclonal system of recognition. *Cell* 91: 295-298
150. Medzhitov R, Preston-Hurlburt P, Janeway CA (1997b) A human homologue of the Drosophila Toll protein signals activation of adaptive immunity. *Nature* 388: 394-397
151. Medzhitov R (2003) Charles A. Janeway, Jr. 1943-2003. *Nat Immunol* 4: 502-502
152. Medzhitov R (2009) Approaching the Asymptote: 20 Years Later. *Immunity* 30: 766-775
153. Meng G, Grabiec A, Vallon M, Ebe B, Hampel S, Bessler W, Wagner H, Kirschning CJ (2003) Cellular recognition of tri-/di-palmitoylated peptides is independent from a domain encompassing the N-terminal seven leucine-rich repeat (LRR)/LRR-like motifs of TLR2. *Journal of Biological Chemistry* 278: 39822-39829
154. Meyer-Luehmann M, Spiess-Jones TL, Prada C, Garcia-Alloza M, de Calignon A, Rozkalne A, Koenigsknecht-Talboo J, Holtzman DM, Bacskai BJ, Hyman BT (2008) Rapid appearance and local toxicity of amyloid-[bgr] plaques in a mouse model of Alzheimer's disease. *Nature* 451: 720-724
155. Mildner A, Schmidt H, Nitsche M, Merkler D, Hanisch U-K, Mack M, Heikenwalder M, Bruck W, Priller J, Prinz M (2007) Microglia in the adult brain arise from Ly-

- 6ChiCCR2+ monocytes only under defined host conditions. *Nat Neurosci* 10: 1544-1553
156. Mitcham JL, Parnet P, Bonnert TP, Garka KE, Gerhart MJ, Slack JL, Gayle MA, Dower SK, Sims JE (1996) T1/ST2 Signaling Establishes It as a Member of an Expanding Interleukin-1 Receptor Family. *Journal of Biological Chemistry* 271: 5777-5783
157. Monk PN, Shaw PJ (2006) ALS: life and death in a bad neighborhood. *Nat Med* 12: 885-887
158. Monsonogo A, Weiner HL (2003) Immunotherapeutic Approaches to Alzheimer's Disease. *Science* 302: 834-838
159. Morris MC, Evans DA, Bienias JL, Tangney CC, Bennett DA, Wilson RS, Aggarwal N, Schneider J (2003) Consumption of fish and n-3 fatty acids and risk of incident Alzheimer disease. *Arch Neurol* 60: 940-946
160. Mukherjee S, Sarkar-Roy N, Wagener DK, Majumder PP (2009) Signatures of natural selection are not uniform across genes of innate immune system, but purifying selection is the dominant signature. *Proceedings of the National Academy of Sciences* 106: 7073-7078
161. Mullen RJ, Buck CR, Smith AM (1992) NeuN, a neuronal specific nuclear protein in vertebrates. *Development* 116: 201-211
162. Nadeau S, Rivest S (2003) Glucocorticoids play a fundamental role in protecting the brain during innate immune response. *The Journal of Neuroscience* 23: 5536-5544
163. Neumann H (2001) Control of glial immune function by neurons. *Glia* 36: 191-199
164. Nguyen MD, Julien J-P, Rivest S (2002) Innate immunity: the missing link in neuroprotection and neurodegeneration? *Nat Rev Neurosci* 3: 216-227
165. Nimmerjahn A, Kirchhoff F, Helmchen F (2005) Resting microglial cells are highly dynamic surveillants of brain parenchyma in vivo. *Science* 308: 1314-1318
166. Nomura N, Miyajima N, Sazuka T, Tanaka A, Kawarabayasi Y, Sato S, Nagase T, Seki N, Ishikawa K-i, Tabata S (1994) Prediction of the coding sequences of unidentified human genes. I. the coding sequences of 40 new genes (KIAA0001-KIAA0040) deduced by analysis of randomly sampled cDNA clones from human immature myeloid cell line KG-1. *DNA Research* 1: 27-35
167. Nyman T, Stenmark P, Flodin S, Johansson I, Hammarström M, Nordlund P (2008) The crystal structure of the human Toll-like receptor 10 cytoplasmic domain reveals a putative signaling dimer. *Journal of Biological Chemistry* 283: 11861-11865
168. O'Brien C (1996) Science History: Auguste D. and Alzheimer's Disease. *Science* 273: 28
169. O'Leary TP, Brown RE (2009) Visuo-spatial learning and memory deficits on the Barnes maze in the 16-month-old APP<sup>swe</sup>/PS1<sup>dE9</sup> mouse model of Alzheimer's disease. *Behavioural Brain Research* 201: 120-127
170. O'Neill LAJ, Bowie AG (2007) The family of five: TIR-domain-containing adaptors in Toll-like receptor signalling. *Nat Rev Immunol* 7: 353-364
171. Okello A, Edison P, Archer H, Turkheimer F, Kennedy J, Bullock R, Walker Z, Kennedy A, Fox N, Rossor M, DJ B (2009) Microglial activation and amyloid deposition in mild cognitive impairment: a PET study. *Neurology* 72.: 56-62

172. Oksman M, Iivonen H, Hogyes E, Amtul Z, Penke B, Leenders I, Broersen L, Lütjohann D, Hartmann T, Tanila H (2006) Impact of different saturated fatty acid, polyunsaturated fatty acid and cholesterol containing diets on beta-amyloid accumulation in APP/PS1 transgenic mice. *Neurobiology of Disease* 23: 563-572
173. Olsen JV, Blagoev B, Gnad F, Macek B, Kumar C, Mortensen P, Mann M (2006) Global, in vivo, and site-specific phosphorylation dynamics in signaling networks. *Cell* 127: 635-648
174. Olson JK, Miller SD (2004) Microglia initiate central nervous system innate and adaptive immune responses through multiple TLRs. *The Journal of Immunology* 173: 3916-3924
175. Omueti KO, Beyer JM, Johnson CM, Lyle EA, Tapping RI (2005) Domain exchange between human Toll-like receptors 1 and 6 reveals a region required for lipopeptide discrimination. *Journal of Biological Chemistry* 280: 36616-36625
176. Ozinsky A, Underhill DM, Fontenot JD, Hajjar AM, Smith KD, Wilson CB, Schroeder L, Aderem A (2000) The repertoire for pattern recognition of pathogens by the innate immune system is defined by cooperation between Toll-like receptors. *Proceedings of the National Academy of Sciences of the United States of America* 97: 13766-13771
177. Paresce DM, Ghosh RN, Maxfield FR (1996) Microglial cells internalize aggregates of the Alzheimer's disease Amyloid [beta]-protein via a scavenger receptor. *Neuron* 17: 553-565
178. Park JH, Widi GA, Gimbel DA, Harel NY, Lee DHS, Strittmatter SM (2006) Subcutaneous nogo receptor removes brain Amyloid- $\beta$  and improves spatial memory in Alzheimer's transgenic mice. *J. Neurosci.* 26: 13279-13286
179. Pham E, Crews L, Ubhi K, Hansen L, Adame A, Cartier A, Salmon D, Galasko D, Michael S, Savas JN, Yates JR, Glabe C, Masliah E (2010) Progressive accumulation of amyloid- $\beta$  oligomers in Alzheimer's disease and in amyloid precursor protein transgenic mice is accompanied by selective alterations in synaptic scaffold proteins. *FEBS Journal* 277: 3051-3067
180. Philip J Lee NG, Terry A Gaige, and Paul J Hung (2007) Microfluidic System for Automated Cell-based Assays. *JALA Charlottesville Va* 12: 363-367
181. Phulwani NK, Esen N, Syed MM, Kielian T (2008) TLR2 expression in astrocytes is induced by TNF- $\alpha$ - and NF- $\kappa$ B-dependent pathways. *The Journal of Immunology* 181: 3841-3849
182. Piani D, Spranger M, Frei K, Schaffner A, Fontana A (1992) Macrophage-induced cytotoxicity of N-methyl-D-aspartate receptor positive neurons involves excitatory amino acids rather than reactive oxygen intermediates and cytokines. *European Journal of Immunology* 22: 2429-2436
183. Pischon T, Hankinson SE, Hotamisligil GS, Rifai N, Willett WC, Rimm EB (2003) Habitual dietary intake of n-3 and n-6 fatty acids in relation to inflammatory markers among US men and women. *Circulation* 108: 155-160
184. Poltorak A, He X, Smirnova I, Liu M-Y, Huffel CV, Du X, Birdwell D, Alejos E, Silva M, Galanos C, Freudenberg M, Ricciardi-Castagnoli P, Layton B, Beutler B (1998) Defective LPS signaling in C3H/HeJ and C57BL/10ScCr mice: mutations in *tlr4* gene. *Science* 282: 2085-2088

185. Priller J, Flugel A, Wehner T, Boentert M, Haas CA, Prinz M, Fernandez-Klett F, Prass K, Bechmann I, de Boer BA, Frotscher M, Kreutzberg GW, Persons DA, Dirnagl U (2001) Targeting gene-modified hematopoietic cells to the central nervous system: Use of green fluorescent protein uncovers microglial engraftment. *Nat Med* 7: 1356-1361
186. Puglielli L, Tanzi RE, Kovacs DM (2003) Alzheimer's disease: the cholesterol connection. *Nat Neurosci* 6: 345-351
187. Quist A, Doudevski I, Lin H, Azimova R, Ng D, Frangione B, Kagan B, Ghiso J, Lal R (2005) Amyloid ion channels: A common structural link for protein-misfolding disease. *Proceedings of the National Academy of Sciences of the United States of America* 102: 10427-10432
188. Reed-Geaghan EG, Savage JC, Hise AG, Landreth GE (2009) CD14 and Toll-like receptors 2 and 4 are required for fibrillar A $\beta$ -stimulated microglial activation. *J. Neurosci.* 29: 11982-11992
189. Reed-Geaghan EG, Reed QW, Cramer PE, Landreth GE (2010) Deletion of CD14 Attenuates Alzheimer's Disease Pathology by Influencing the Brain's Inflammatory Milieu. *J. Neurosci.* 30: 15369-15373
190. Richard KL, Filali M, Prefontaine P, Rivest S (2008) Toll-like receptor 2 acts as a natural innate immune receptor to clear Amyloid  $\beta$ 1-42 and delay the cognitive decline in a mouse model of Alzheimer's disease. *J. Neurosci.* 28: 5784-5793
191. Rinner WA, Bauer J, Schmidts M, Lassmann H, Hickey WF (1995) Resident microglia and hematogenous macrophages as phagocytes in adoptively transferred experimental autoimmune transferred experimental autoimmune encephalomyelitis: An investigation using rat radiation bone marrow chimeras. *Glia* 14: 257-266
192. Ritter MR, Banin E, Moreno SK, Aguilar E, Dorrell MI, Friedlander M (2006) Myeloid progenitors differentiate into microglia and promote vascular repair in a model of ischemic retinopathy. *The Journal of Clinical Investigation* 116: 3266-3276
193. Rolls A, Shechter R, London A, Ziv Y, Ronen A, Levy R, Schwartz M (2007) Toll-like receptors modulate adult hippocampal neurogenesis. *Nat Cell Biol* 9: 1081-1088
194. Roy A, Fung YK, Liu X, Pahan K (2006) Up-regulation of microglial CD11b expression by nitric oxide. *Journal of Biological Chemistry* 281: 14971-14980
195. Sandberg A, Luheshi LM, Söllvander S, Pereira de Barros T, Macao B, Knowles TPJ, Biverstål H, Lendel C, Ekholm-Petterson F, Dubnovitsky A, Lannfelt L, Dobson CM, Härd T (2010) Stabilization of neurotoxic Alzheimer amyloid- $\beta$  oligomers by protein engineering. *Proceedings of the National Academy of Sciences* 107: 15595-15600
196. Sang N, Zhang J, Marcheselli V, Bazan NG, Chen C (2005) Postsynaptically synthesized prostaglandin E2 (PGE2) modulates hippocampal synaptic transmission via a presynaptic PGE2 EP2 receptor. *J. Neurosci* 25: 9858-9870
197. Santambrogio L, Belyanskaya SL, Fischer FR, Cipriani B, Brosnan CF, Ricciardi-Castagnoli P, Stern LJ, Strominger JL, Riese R (2001) Developmental plasticity of CNS microglia. *Proceedings of the National Academy of Sciences of the United States of America* 98: 6295-6300
198. Sarell CJ, Syme CD, Rigby SEJ, Viles JH (2009) Copper(II) binding to Amyloid- $\beta$  fibrils of Alzheimer's disease reveals a picomolar affinity: stoichiometry and coordination geometry are independent of A $\beta$  oligomeric form. *Biochemistry* 48: 4388-4402

199. Schaefer EJ, Bongard V, Beiser AS, Lamon-Fava S, Robins SJ, Au R, Tucker KL, Kyle DJ, Wilson PWF, Wolf PA (2006) Plasma phosphatidylcholine docosahexaenoic acid content and risk of dementia and Alzheimer disease: the Framingham heart study. *Arch Neurol* 63: 1545-1550
200. Schagger H (2006) Tricine-SDS-PAGE. *Nat. Protocols* 1: 16-22
201. Schenk D, Barbour R, Dunn W, Gordon G, Grajeda H, Guido T, Hu K, Huang J, Johnson-Wood K, Khan K, Kholodenko D, Lee M, Liao Z, Lieberburg I, Motter R, Mutter L, Soriano F, Shopp G, Vasquez N, Vandeventer C, Walker S, Wogulis M, Yednock T, Games D, Seubert P (1999) Immunization with amyloid- $\beta$  attenuates Alzheimer-disease-like pathology in the PDAPP mouse. *Nature* 400: 173-177
202. Schilling M, Besselmann M, Müller M, Strecker JK, Ringelstein EB, Kiefer R (2005) Predominant phagocytic activity of resident microglia over hematogenous macrophages following transient focal cerebral ischemia: An investigation using green fluorescent protein transgenic bone marrow chimeric mice. *Experimental Neurology* 196: 290-297
203. Scholtzova H, Kascsak RJ, Bates KA, Boutajangout A, Kerr DJ, Meeker HC, Mehta PD, Spinner DS, Wisniewski T (2009) Induction of Toll-Like Receptor 9 Signaling as a Method for Ameliorating Alzheimer's Disease-Related Pathology. *J. Neurosci.* 29: 1846-1854
204. Schubert D, Soucek T, Blouw B (2009) The induction of HIF-1 reduces astrocyte activation by amyloid beta peptide. *European Journal of Neuroscience* 29: 1323-1334
205. Seabury CM, Seabury PM, Decker JE, Schnabel RD, Taylor JF, Womack JE (2010) Diversity and evolution of 11 innate immune genes in *Bos taurus taurus* and *Bos taurus indicus* cattle. *Proceedings of the National Academy of Sciences* 107: 151-156
206. Selkoe DJ (2002) Alzheimer's Disease is a synaptic failure. *Science* 298: 789-791
207. Shankar GM, Li S, Mehta TH, Garcia-Munoz A, Shepardson NE, Smith I, Brett FM, Farrell MA, Rowan MJ, Lemere CA, Regan CM, Walsh DM, Sabatini BL, Selkoe DJ (2008) Amyloid- $\beta$  protein dimers isolated directly from Alzheimer's brains impair synaptic plasticity and memory. *Nat Med* 14: 837-842
208. Sheedy FJ, O'Neill LAJ (2007) The Troll in Toll: Mal and Tram as bridges for TLR2 and TLR4 signaling. *Journal of Leukocyte Biology* 82: 196-203
209. Shi Y (2009) Serine/Threonine phosphatases: mechanism through structure. *Cell* 139: 468-484
210. Shi Z, Cai Z, Sanchez A, Zhang T, Wen S, Wang J, Yang J, Fu S, Zhang D (2011) A novel Toll-like receptor that recognizes vesicular stomatitis virus. *J Biol Chem* 286: 4517-24
211. Simard A, Rivest S (2004) Bone marrow stem cells have the ability to populate the entire central nervous system into fully differentiated parenchymal microglia. *FASEB Journal* 18: 998-1000
212. Simard A, Rivest S (2006a) Neuroprotective properties of the innate immune system and bone marrow stem cells in Alzheimer's disease. *Mol Psychiatry* 11: 327-335
213. Simard A, Soulet D, Gowing G, Julien J-P, Rivest S (2006b) Bone marrow-derived microglia play a critical role in restricting senile plaque formation in Alzheimer's disease. *Neuron* 49: 489-502

214. Skuladottir I, Petursdottir D, Hardardottir I (2007) The effects of Omega-3 polyunsaturated fatty acids on TNF- $\alpha$  and IL-10 secretion by murine peritoneal cells In vitro. *Lipids* 42: 699-706
215. Small DH, Mok SS, Bornstein JC (2001) Alzheimer's disease and A[ $\beta$ ] toxicity: from top to bottom. *Nat Rev Neurosci* 2: 595-598
216. Sperling RA, LaViolette PS, O'Keefe K, O'Brien J, Rentz DM, Pihlajamaki M, Marshall G, Hyman BT, Selkoe DJ, Hedden T, Buckner RL, Becker JA, Johnson KA (2009) Amyloid deposition is associated with impaired default network function in older persons without dementia. *Neuron* 63: 178-188
217. Stepanichev MY, Zdobnova IM, Yakovlev AA, Onufriev MV, Lazareva NA, Zarubenko II, Gulyaeva NV (2003) Effects of tumor necrosis factor- $\alpha$  central administration on hippocampal damage in rat induced by amyloid beta-peptide (25–35). *Journal of Neuroscience Research* 71: 110-120
218. Stewart CR, Stuart LM, Wilkinson K, van Gils JM, Deng J, Halle A, Rayner KJ, Boyer L, Zhong R, Frazier WA, Lacy-Hulbert A, Khoury JE, Golenbock DT, Moore KJ (2010) CD36 ligands promote sterile inflammation through assembly of a Toll-like receptor 4 and 6 heterodimer. *Nat Immunol* 11: 155-161
219. Strijbos P, Rothwell N (1995) Interleukin-1 beta attenuates excitatory amino acid-induced neurodegeneration in vitro: involvement of nerve growth factor. *The Journal of Neuroscience* 15: 3468-3474
220. Strominger JL (2007) Bacterial cell walls, innate immunity and immunoadjuvants. *Nat Immunol* 8: 1269-1271
221. Szekely CA, Breitner JCS, Zandi PP (2007) Prevention of Alzheimer's disease. *International Review of Psychiatry* 19: 693-706
222. Szekely CA, Green RC, Breitner JCS, Østbye T, Beiser AS, Corrada MM, Dodge HH, Ganguli M, Kawas CH, Kuller LH, Psaty BM, Resnick SM, Wolf PA, Zonderman AB, Welsh-Bohmer KA, Zandi PP (2008) No advantage of A $\beta$ 42-lowering NSAIDs for prevention of Alzheimer dementia in six pooled cohort studies. *Neurology* 70: 2291-2298
223. Tahara K, Kim H-D, Jin J-J, Maxwell JA, Li L, Fukuchi K-i (2006) Role of toll-like receptor signalling in A $\beta$  uptake and clearance. *Brain* 129: 3006-3019
224. Takeda K, Kaisho T, Akira S (2003) Toll-like receptors. *Annual Review of Immunology* 21: 335-376
225. Takeuchi O, Kawai T, Mühlradt PF, Morr M, Radolf JD, Zychlinsky A, Takeda K, Akira S (2001) Discrimination of bacterial lipoproteins by Toll-like receptor 6. *International Immunology* 13: 933-940
226. Takeuchi O, Sato S, Horiuchi T, Hoshino K, Takeda K, Dong Z, Modlin RL, Akira S (2002) Cutting Edge: Role of toll-like receptor 1 in mediating immune response to microbial lipoproteins. *J Immunol* 169: 10-14
227. Takeuchi O, Akira S (2010) Pattern recognition receptors and inflammation. *Cell* 140: 805-820
228. Tanzi RE, Bertram L (2001) New frontiers in Alzheimer's disease genetics. *Neuron* 32: 181-184

229. Terzi E, Hölzemann G, Seelig J (1995) Self-association of [beta]-Amyloid Peptide (1-40) in solution and binding to lipid membranes. *Journal of Molecular Biology* 252: 633-642
230. Thanopoulou K, Fragkouli A, Stylianopoulou F, Georgopoulos S (2010) Scavenger receptor class B type I (SR-BI) regulates perivascular macrophages and modifies amyloid pathology in an Alzheimer mouse model. *Proceedings of the National Academy of Sciences* 107: 20816-20821
231. The Lancet N (2010) Alzheimer's disease prevention: a reality check. *The Lancet Neurology* 9: 643-643
232. Tracey MD, Kevin J., Cerami PD, Anthony (1994) Tumor necrosis factor: a pleiotropic cytokine and therapeutic target. *Annual Review of Medicine* 45: 491-503
233. Tschirren B, RÅBerg L, Westerdahl H (2011) Signatures of selection acting on the innate immunity gene Toll-like receptor 2 (TLR2) during the evolutionary history of rodents. *Journal of Evolutionary Biology* 24: 1232-1240
234. Tu Y, Wu S, Shi X, Chen K, Wu C (2003) Migfilin and Mig-2 link focal adhesions to filamin and the actin cytoskeleton and function in cell shape modulation. *Cell* 113: 37-47
235. Udan MLD, Ajit D, Crouse NR, Nichols MR (2008) Toll-like receptors 2 and 4 mediate A $\beta$ (1-42) activation of the innate immune response in a human monocytic cell line. *Journal of Neurochemistry* 104: 524-533
236. Underhill DM, Ozinsky A, Hajjar AM, Stevens A, Wilson CB, Bassetti M, Aderem A (1999) The Toll-like receptor 2 is recruited to macrophage phagosomes and discriminates between pathogens. *Nature* 401: 811-815
237. Vallvé J-C, Uliaque K, Girona J, Cabré A, Ribalta J, Heras M, Masana L (2002) Unsaturated fatty acids and their oxidation products stimulate CD36 gene expression in human macrophages. *Atherosclerosis* 164: 45-56
238. Vandevenne P, Sadzot-Delvaux C, Piette J (2010) Innate immune response and viral interference strategies developed by Human Herpesviruses. *Biochemical Pharmacology* 80: 1955-1972
239. Villemagne VL, Pike KE, Chételat G, Ellis KA, Mulligan RS, Bourgeat P, Ackermann U, Jones G, Szoeke C, Salvado O, Martins R, O'Keefe G, Mathis CA, Klunk WE, Ames D, Masters CL, Rowe CC (2011) Longitudinal assessment of A $\beta$  and cognition in aging and Alzheimer disease. *Annals of Neurology* 69: 181-192
240. Wagers AJ, Sherwood RI, Christensen JL, Weissman IL (2002) Little evidence for developmental plasticity of adult hematopoietic stem cells. *Science* 297: 2256-2259
241. Wake H, Moorhouse AJ, Jinno S, Kohsaka S, Nabekura J (2009) Resting microglia directly monitor the functional state of synapses in vivo and determine the fate of ischemic terminals. *J. Neurosci.* 29: 3974-3980
242. Walter L, Neumann H (2009) Role of microglia in neuronal degeneration and regeneration. *Seminars in Immunopathology* 31: 513-525
243. Walter S, Letiembre M, Liu Y, Heine H, Penke B, Hao W, Bode B, Manietta N, Walter J, Schulz-Schuffer W, Fassbender K (2007) Role of the toll-like receptor 4 in neuroinflammation in Alzheimer's disease. *Cell Physiol Biochem* 20: 947-56

244. Wang J, Shao Y, Bennett TA, Shankar RA, Wightman PD, Reddy LG (2006) The functional effects of physical interactions among Toll-like receptors 7, 8, and 9. *Journal of Biological Chemistry* 281: 37427-37434
245. Whitham S, Dinesh-Kumar SP, Choi D, Hehl R, Corr C, Baker B (1994) The product of the tobacco mosaic virus resistance gene N: Similarity to toll and the interleukin-1 receptor. *Cell* 78: 1101-1115
246. Wyllie DH, Kiss-Toth E, Visintin A, Smith SC, Boussouf S, Segal DM, Duff GW, Dower SK (2000) Evidence for an accessory protein function for Toll-like receptor 1 in anti-bacterial responses. *The Journal of Immunology* 165: 7125-7132
247. Wyss-Coray T (2006) Inflammation in Alzheimer disease: driving force, bystander or beneficial response? *Nat Med* 12: 1005-1015
248. Xu J, Kochanek K, Murphy S, Tejada-Vera B (2010) Deaths: Final Data for 2007. *National Vital Statistics Reports* 58: Hyattsville, MD: National Center For Health Statistics. 2010
249. Xu Y, Tao X, Shen B, Horng T, Medzhitov R, Manley JL, Tong L (2000) Structural basis for signal transduction by the Toll/interleukin-1 receptor domains. *Nature* 408: 111-115
250. Yamamoto M, Yamazaki S, Uematsu S, Sato S, Hemmi H, Hoshino K, Kaisho T, Kuwata H, Takeuchi O, Takeshige K, Saitoh T, Yamaoka S, Yamamoto N, Yamamoto S, Muta T, Takeda K, Akira S (2004) Regulation of Toll/IL-1-receptor-mediated gene expression by the inducible nuclear protein I[ $\kappa$ ]B[ $\zeta$ ]. *Nature* 430: 218-222
251. Yan SD, Chen X, Fu J, Chen M, Zhu H, Roher A, Slattery T, Zhao L, Nagashima M, Morser J, Migheli A, Nawroth P, Stern D, Schmidt AM (1996) RAGE and amyloid-[ $\beta$ ] peptide neurotoxicity in Alzheimer's disease. *Nature* 382: 685-691
252. Yates RM, Russell DG (2005) Phagosome Maturation Proceeds Independently of Stimulation of Toll-like Receptors 2 and 4. *Immunity* 23: 409-417
253. Younkin SG (1995) Evidence that A $\beta$ 42 is the real culprit in alzheimer's disease. *Annals of Neurology* 37: 287-288
254. Zarándi M, Soós K, Fülöp L, Bozsó Z, Datki Z, Tóth GK, Penke B (2007) Synthesis of A $\beta$ [1-42] and its derivatives with improved efficiency. *Journal of Peptide Science* 13: 94-99
255. Zotova E, Nicoll J, Kalaria R, Holmes C, Boche D (2010) Inflammation in Alzheimer's disease: relevance to pathogenesis and therapy. *Alzheimers Res Ther* 2: 1

## Publications

Based on the PhD study, the following papers were published or planned to be published:

1. Liu S, Liu Y, Hao W, Wolf L, Kiliaan AJ, Penke B, Rube CE, Hartmann T, Menger MD, Fassbender K. Toll-like receptor 2 is a primary receptor for Alzheimer's amyloid  $\beta$  peptide to trigger neuroinflammatory activation. *J Immunol.* 2011, *submitted, in revision.*
2. Liu S, Liu Y, Hao W, Penke B, Hartmann T, Fassbender K. Omega-3 fatty acids reduce Alzheimer's amyloid  $\beta$  peptide-induced proinflammatory activities in macrophages. *Manuscript prepared.*
3. Hao W, Liu Y, Liu S, Walter S, Grimm MO, Kiliaan AJ, Penke B, Hartmann T, Rube CE, Menger MD, Fassbender K. Myeloid differentiation factor 88-deficient bone marrow cells improve Alzheimer's disease-related symptoms and pathology. *Brain.* 2011, 134(1):278-92.
4. Liu Y, Hao W, Dawson A, Liu S, Fassbender K. Expression of amyotrophic lateral sclerosis-linked SOD1 mutant increases the neurotoxic potential of microglia via TLR2. *J Biol Chem.* 2009, 284(6):3691-9.

## **Acknowledgements**

First and foremost I place my sincerest gratitude and respect to my advisors Dr. Yang Liu, Prof. Dr. Klaus Fassbender and Prof. Dr. Tobias Hartmann for their outstanding guidance in accomplishing this work. I express my thanks to Dr. Yang Liu for his intelligence, motivation and patience in supporting my scientific career as well as personal life. I would also like to acknowledge Prof. Dr. Klaus Fassbender, who inspired the projects with his enthusiasm and immense knowledge. I am grateful to both of them for their time and valuable discussions throughout the development of the projects and this dissertation.

I am heartily thankful to Prof. Dr. Tobias Hartmann for his encouragement, comments, critical questions and help throughout the course of these projects.

I would like to credit my friendly and cheerful AG Fassbender colleagues for making the last four years a joyful experience. Special thanks must go to Dr. Wenlin Hao, who assisted me in initiating my thesis work and provided daily supportive guidance with her knowledge and experience. Andrea Schottek and Nadine Commercon provided skillful technical support for the progress of the projects. Kan Xie and Manuela Gries are my best neighbors in the lab; they helped me to translate the abstract of this thesis into German. Rober Schomburg provided apoptosis caspase 3 assay instructions. Lisa Wolf did excellent research for her Bachelor thesis under my supervision. Xu Liu took over the animal work and is very motivated for the projects. I am in debt to Miss Laura Davies who gave the English language edition and correction suggestions on my manuscript. I express my thanks to all my lab mates as well as all members from AG Hartmann for their supportive discussions and suggestions.

I would also like to appreciate Prof. Drs. Amanda J. Kiliaan (Radboud University Nijmegen Medical Center, Nijmegen, The Netherlands), who provided and genotyped the APP<sup>swe</sup>/PS1<sup>dE9</sup> mice; Prof. Dr. Botond Penke (Albert Szent Gyorgyi Medical University, Szeged, Hungary), who provided high quality A $\beta$ ; Prof. Dr. Eckart Meese and Prof. Dr. Jürgen Hemberger (Institut für Biochemische Verfahren und Analysen, Gießen), who provided the Biacore J system and very kindly let me perform the experiments in their laboratory; Prof. Dr. Richard Zimmermann, who provided Biacore training in his laboratory; Prof. Dr. Claudia E. Rube, who helped to irradiate the recipient mice for my bone marrow transplantation work; Prof. Dr. Michael D. Menger and Prof. Dr. Marc Freichel housed all the experimental animals for us; Prof. Dr. Peter Lipp provided confocal microscope use in his laboratory and Prof. Dr. Gunther Wennemuth allowed Zeiss Axiophot microscope use for

high quality immunohistochemistry slides imaging. I would appreciate all of them and their their lab members, without their help my thesis project would be impossible.

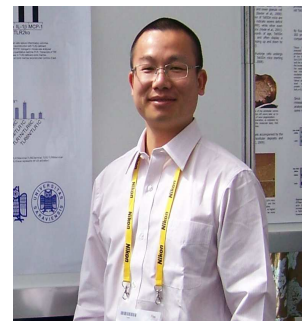
I want to gratefully acknowledge the sufficient financial support on my thesis projects from the Fritz Thyssen Stiftung, the Alzheimer Forschung Initiative e.V., the Medical Faculty of University of the Saarland through HOMFOR, the EU FP7 project LipiDiDiet and the stipend award from Deutscher Akademischer Austausch Dienst (DAAD).

Lastly, and most importantly, I offer my regards and gratitude to my parents, who bore me, raised me, supported me, taught me, and loved me. To them I dedicate this dissertation.

## Curriculum Vitae

### Personal Information

**Name** Shirong LIU  
**Current Address** Semmelweisstr.16  
D-66424, Homburg/Saar  
Germany  
**Lab Address** AG Fassbender, Geb 90  
Department of Neurology  
University of the Saarland  
D-66421, Homburg/Saar  
Germany  
**Tel(Lab)** +49-6841-1624169  
**Fax** +49-6841-1624175  
**Email** [shirong.liu@uniklinikum-saarland.de](mailto:shirong.liu@uniklinikum-saarland.de)  
**Date and Place of Birth** 12 Nov 1976, Jiangxi  
**Nationality** China



### Education

**Date (from-to)** Sep 2007 - now  
**University** University of the Saarland, Germany  
**Department** Department of Neurology  
**Expect Degree** Ph.D (*Dr. rer. nat*)  
**Advisor** Dr. Yang Liu, Prof. Dr. Klaus Fassbender and Prof. Dr. Tobias Hartmann  
**Dissertation** Toll-Like Receptor 2 and Partner Receptors in Alzheimer's disease

**Date (from-to)** Sep 2003 - Jul 2006  
**University** Peking Union Medical College & Chinese Academy of Medical Sciences, China  
**Department** Department of Immunology  
**Degree** M.Sc.  
**Major Field** Immunology  
**Advisor** Prof. Dr. Wei He and Prof. Dr. Lianxian Cui  
**Thesis** Functional Study of a Novel Thymus Atrophy Associated Gene ih1

**Date (from-to)** Sep 1996 - Jul 2001  
**University** Jiangxi Medical College (Nanchang University), China  
**Department** Department of Clinical Medicine  
**Degree** Bachelor of Medicine  
**Major Field** Clinical Medicine

### Work Experience

**Date (from-to)** Aug 2001 - Aug 2003  
**Role, Affiliation** Resident doctor (licensed), Zongrui (Beilun)Hospital, Ningbo, China

**Date (from-to)** Jul 2000 - Jul 2001  
**Role, Affiliation** Clinical Internship, People's Hospital of Jiangxi Province, Nanchang, China

## Publications

1. **LIU S**, Liu Y, Hao W, Wolf L, Kiliaan AJ, Penke B, Rube CE, Hartmann T, Menger MD, Fassbender K. Toll-like receptor 2 is a primary receptor for Alzheimer's amyloid  $\beta$  peptide to trigger neuroinflammatory activation. *J Immunol.* 2011, *submitted, in revision.*
2. **LIU S**, Liu Y, Hao W, Penke B, Hartmann T, Fassbender K. Omega-3 fatty acids reduce Alzheimer's amyloid  $\beta$  peptide-induced proinflammatory activities in macrophages. *Manuscript.*
3. Hao W, Liu Y, **LIU S**, Walter S, Grimm MO, Kiliaan AJ, Penke B, Hartmann T, Rube CE, Menger MD, Fassbender K. Myeloid differentiation factor 88-deficient bone marrow cells improve Alzheimer's disease-related symptoms and pathology. *Brain.* 2011, 134(1):278-92.
4. Liu Y, Hao W, Dawson A, **LIU S**, Fassbender K. Expression of amyotrophic lateral sclerosis-linked SOD1 mutant increases the neurotoxic potential of microglia via TLR2. *J Biol Chem.* 2009, 284(6):3691-9.
5. Kang N, Chen D, Wang L, Duan L, **LIU S**, Tang L, Liu Q, Cui L, He W. Rwdd1, a thymus aging related molecule, is a new member of the intrinsically unstructured protein family. *Cell Mol Immunol.* 2008, 5(5):333-9.
6. Kang N, Duan L, Tang L, **LIU S**, Li C, Li Y, Liu Q, Hu Y, Cui L, He W. Identification and characterization of a novel thymus aging related protein Rwdd1. *Cell Mol Immunol.* 2008,5(4):279-85.
7. [**LIU S**, He W. Sumoylation-a Multifunctional Post-translational Protein modification]. *J Med Mol Biol.* 2006,3(3):212-5. Chinese.

## Conferences

1. **LIU S**, Liu Y, Hao W, Hartmann T, Fassbender K. A Robust Complementary Mechanism in TLR2/TLR1 Signaling. *Toll2011 Meeting-Decoding Innate Immunity.* Riva del Garda, Italy, 2011.05 (Poster presentation)
2. **LIU S**, Liu Y, Hao W, Penke B, Fassbender K. Toll like receptor 2 (TLR2) and its partner receptors in Alzheimer's disease. *7th FENS Forum of Neuroscience 2010.* Amsterdam, the Netherlands, 2010. 07. FENS Abstr.,vol.5, 078.52, 2010 (Poster presentation)
3. **LIU S**. Omega-3 fatty acids reduce Abeta initiated inflammatory cytokines level in macrophage. *Forschertreffen 2009 der Neurologischen Klinik.* Homburg, Germany, 2009.10 (Oral presentation)
4. **LIU S**, Liu Y, Hao W, Penke B, Hartmann T, Fassbender K. The polyunsaturated fatty acid docosahexaenoic acid reduces  $\beta$ -amyloid induced pro-inflammatory cytokines expression while maintains the clearance capability of  $\beta$ -amyloid in BMDMs. *The international conference AD/PD 2009 conference.* Prague, Czech Republic, 2009.03 (Poster presentation)
5. **LIU S**, Duan L, Kang N, Cui L, He W. IH1 effects on NF- $\kappa$ B signal transduction. *The Annual Conference of Chinese Society of Immunology (CSI).* Beijing, China, 2006.11 (Abstract)

## Honors/Awards

DAAD geförderten Doktorandenprogramm (STIBET) stipendium, 2010